UNIVERSIDADE ESTADUAL DE CAMPINAS

FACULDADE DE ENGENHARIA QUÍMICA

DANIELA DA SILVA DAMACENO

EQUILÍBRIO LÍQUIDO-VAPOR DE MISTURAS BINÁRIAS ENVOLVENDO COMPOSTOS GRAXOS COM GRUPO OH À PRESSÕES SUBATMOSFÉRICAS

VAPOR-LIQUID EQUILIBRIUM OF BINARY MIXTURES INVOLVING FATTY COMPOUNDS WITH GROUP OH AT SUBATMOSPHERIC PRESSURE

CAMPINAS

2018

DANIELA DA SILVA DAMACENO

Equilíbrio líquido-vapor de misturas binárias envolvendo compostos graxos com grupo OH à pressões subatmosféricas

Vapor-liquid equilibrium of binary mixtures involving fatty compounds with group OH at subatmospheric pressure

Tese de doutorado apresentada à Faculdade de Engenharia Química da Universidade Estadual de Campinas como parte dos requisitos exigidos para obtenção do título de Doutora em Engenharia Química.

Dissertation presented to the School of Chemical Engineering of the University of Campinas in partial fulfillment of the requirements for the degree of Doctor in the area of Chemical Engineering.

ESTE EXEMPLAR CORRESPONDE À VERSÃO FINAL DA TESE DEFENDIDA PELA ALUNA DANIELA DA SILVA DAMACENO E ORIENTADA PELA PROFA. DRA. ROBERTA CERIANI

CAMPINAS

2018

Ficha catalográfica
Universidade Estadual de Campinas
Biblioteca da Área de Engenharia e Arquitetura
Luciana Pietrosanto Milla - CRB 8/8129

Informações para Biblioteca Digital

Dissertação de Doutorado defendida por Daniela da Silva Damaceno e aprovada em 04 de abril de 2018 pela banca examinadora constituída pelos doutores:

_____
Profa. Dra. Roberta Ceriani – Orientadora – FEQ/UNICAMP
Membro titular

_____
Profa. Dra. Christianne Elisabete da Costa Rodrigues – FZEA/USP
Membro titular

_____
Prof. Dr. Pedro de Alcântara Pessoa Filho – NAPAN/USP
Membro titular

_____
Profa. Dra. Maria Regina Wolf Maciel – FEQ/UNICAMP
Membro titular

_____
Prof. Dr. Leonardo Vasconcelos Fregolente – FEQ/UNICAMP
Membro titular

A Ata da Defesa, assinada pelos membros da Comissão Examinadora, consta no processo de vida acadêmica da aluna.

DEDICATÓRIA

Dedico a todos aqueles que acreditam que o
impossível é possível!

AGRADECIMENTOS

RESUMO

Nos últimos anos, a indústria de óleos e gorduras vem crescendo em larga escala, principalmente por causa do aumento de produção de biocombustíveis (biodiesel). Dentre as operações unitárias, as que envolvem a transferência de massa, como a destilação e o esgotamento, estão entre as mais importantes nas etapas de separação e purificação de produtos. Nessas, a descrição do equilíbrio líquido-vapor da mistura multicomponente é fundamental. Como consequência, a demanda por dados experimentais de equilíbrio de fases e modelagem termodinâmica envolvendo compostos da tecnologia de lipídios estão se tornando cada vez mais temas de pesquisa. Avaliando esse cenário, esse trabalho de doutorado teve como principal objetivo mapear a interação entre os diferentes grupos funcionais que constituem as classes de compostos de interesse. Esse mapeamento foi feito a partir da determinação da pressão de vapor da monononanoina, monolaurina e dinonanoina a pressões subatmosféricas, além de dados de equilíbrio líquido-vapor das seguintes misturas: monocaprilina + ácido láurico (3,42 kPa), monononanoina + monolaurina (2,06 kPa), monononanoina + hexadecanol (2,02 kPa), monolaurina + octadecanol (2,05 kPa), hexadecanol + octadecanol (1,73 kPa), hexadecanol + metil miristato (1,72 kPa) monononanina + tributirina (1,69 kPa), dinonanoina + octacosano (1,70 kPa), pela técnica da calorimetria diferencial exploratória (DSC), e o próprio aprimoramento da técnica em si. Também foram obtidas as temperaturas normais de ebulição dos seguintes compostos: monobutirina, monocaprina, monolaurina, monopalmitina, monoestearina, dicaprilina, dinonanoina e dicaprina, pela técnica da termogravimetria (TGA). Em conjunto, foram feitos a avaliação e o aprimoramento da capacidade preditiva do método UNIFAC em suas diferentes versões. A relevância de ferramentas preditivas de elevada acurácia e de amplo espectro de aplicação em projetos de engenharia na área de óleos, gorduras e biodiesel é evidente, uma vez que na grande maioria das vezes, o engenheiro tem que fazer uso da termodinâmica aplicada para estimar o comportamento de misturas multicomponentes cujas informações específicas nas condições desejadas (temperatura, pressão e/ou composição) não estão disponíveis, recorrendo-se muitas vezes à informações obtidas à partir de misturas binárias.

ABSTRACT

In recent years, the oil and fat industry has been growing on a large scale, primarily because of the increase in the production of biofuels (biodiesel). Among the unit operations, those that involve mass transfer, such as distillation and stripping, figure as the most important steps for separation and purification of products. In these processes, the description of the vapor-liquid equilibria of the multicomponent mixture is crucial. Consequently, the demand for experimental data of phase equilibria and thermodynamic modeling involving compounds of the lipid technology are increasingly becoming areas of research. Evaluating this scenario, the developed doctoral project had as main objective to map the interaction between the different functional groups that constitute the classes of compounds of interest. This mapping was made from the determination of vapor-liquid equilibrium data of the following mixtures: monocaprylin + lauric acid (3.42 kPa), monononanoin + monolaurin (2.06 kPa), monononanoin + hexadecanol (2.02 kPa), monolaurin + octadecanol (2.05 kPa), hexadecanol + octadecanol (1.73 kPa), hexadecanol + methyl myristate (1.72 kPa) monononanin + tributyrin (1.69 kPa), dinonanoin + octacosane (1.70 kPa), by the differential scanning calorimetry (DSC) technique, together with the improvement of the technique itself. Normal boiling points for the following compounds were also measured using the thermogravimetric analysis (TGA): monobutyrin, monocaprin, monolaurin, monopalmitin, monoestearin, dicaprylin, dinonanoin and dicaprin. In conjunction, an evaluation and improvement of predictive capacity of the UNIFAC method in its different versions were performed. The relevance of these predictive tools of high accuracy and vast application for engineering design of oil/fat and biodiesel processes is evident, i.e., an engineer frequently relies on applied thermodynamics and binary mixture data for estimating the behavior of multicomponent mixtures for which specific information at desired conditions in terms of temperature, pressure and/or composition are not available.

LISTA DE FIGURAS

LISTA DE TABELAS

SUMÁRIO

CAPÍTULO 1

INTRODUÇÃO E OBJETIVOS

Óleos e gorduras são uma relevante fonte nutricional, de ácidos graxos essenciais, de vitaminas e de antioxidantes naturais, além da demanda recente como matéria-prima para produção de biodiesel. Em sua grande maioria, passam por algum tipo de processamento antes de serem destinados ao consumo humano. Além disso, derivados de óleos vegetais como ácidos graxos, ésteres graxos, triacilgliceróis, diacilgliceróis e monoacilgliceróis são importantes produtos oleoquímicos, de aplicação nas indústrias de alimentos e química. A produção mundial de óleos vegetais aumentou aproximadamente 7,3 vezes entre 1974/75 e 2016/17, passando de 25,7 milhões de toneladas para 186,8 milhões de toneladas (USDA, 2017). Além disso, as estatísticas mostram que este número só tende a aumentar, para suprir as demandas decorrentes do aumento populacional e da produção de biodiesel.

Devido a este crescimento populacional, a necessidade do consumo energético vem aumentando a cada dia, e tornando a sociedade cada vez mais dependente dos combustíveis fósseis. Entretanto, esse tipo de fonte energética, além de não ser renovável pode causar diversos impactos ambientais, tanto de forma local como global. Em virtude desse esgotamento, o biodiesel está cada vez mais em destaque tanto para pesquisas quanto para a área industrial. No Brasil, em 2018, é obrigatória a sua adição em 9% no diesel, sendo que em 2019 esse percentual passará para 10% (ANP, 2018).

Avaliando esta alta demanda de produção de biodiesel e, consequentemente, o aumento na escala de produção de óleos e gorduras, a procura por dados experimentais referentes ao equilíbrio de fases tem se tornado cada vez maior. No entanto, ainda há uma evidente escassez desses dados, principalmente quando envolve compostos minoritários, como mono- e diacilgliceróis (DAMACENO et al. 2014). Além disso, a descrição do equilíbrio líquido-vapor (ELV) de misturas multicomponentes é fundamental para mapear o comportamento dos diferentes compostos nas condições de processo. Como consequência, a demanda por dados experimentais e métodos preditivos para descrever o equilíbrio de fases envolvendo compostos da tecnologia de lipídios estão se tornando cada vez mais relevantes em recentes temas de pesquisa. Conforme Kang et al. (2015), ainda há uma escassez e baixa qualidade de dados experimentais disponíveis na literatura, ou seja, um extenso, robusto e acurado banco de dados é essencial para melhor estimar propriedades termofísicas e de

equilíbrio de fases de compostos graxos. Visando sanar essa carência, este estudo tem como objetivo mapear a interação entre os diferentes grupos funcionais que constituem as classes de compostos de interesse provenientes da reação de transesterificação de óleos/gorduras e, consequentemente, presentes nas etapas de separação e purificação do biodiesel. Dessa forma foram determinados dados inéditos de equilíbrio líquido-vapor envolvendo compostos graxos, são eles: monocaprilina + ácido láurico (3,42 kPa), monononanoina + monolaurina (2,06 kPa), monononanoina + hexadecanol (2,02 kPa), monolaurina + octadecanol (2,05 kPa), hexadecanol + octadecanol (1,73 kPa), hexadecanol + metil miristato (1,72 kPa) monononanina + tributirina (1,69 kPa), dinonanoina + octacosano (1,70 kPa), pela técnica da calorimetria diferencial exploratória (DSC), além do aprimoramento da técnica em si. A modelagem termodinâmica aplicada aos dados experimentais foi a abordagem *gamma-phi* (Wilson, NRTL e UNIQUAC). Testes de consistência termodinâmica adequados aos dados do tipo PTx (obtidos via DSC) foram realizados (KANG et al., 2010). Além disso, considerando os diferentes sistemas obtidos, foi possível testar a capacidade preditiva do método de contribuição de grupos UNIFAC, em suas diferentes versões (FREDENSLUND et al., 1977; LARSEN et al., 1987; WEIDLICH e GMEHLING 1987; HANSEN et al., 1992). Também foram obtidas as temperaturas normais de ebulição dos seguintes compostos: monobutirina, monocaprina, monolaurina, monopalmitina, monoestearina, dicaprilina, dinonanoina e dicaprina, pela técnica do TGA, e com esses dados foi testada a acurácia na predição de diferentes métodos de contribuição de grupos para a obtenção de temperatura normal de ebulição. Por fim, foi desenvolvido na Universidade Técnica da Dinamarca (DTU), sob supervisão do professor Rafiqul Gani, o aprimoramento do método UNIFAC (LARSEN et al., 1987; WEIDLICH e GMEHLING 1987; HANSEN et al., 1992), a partir do ajuste de parâmetros de interação da parte residual (a_{mn}) dos grupos funcionais característicos dos compostos de interesse da tecnologia de lipídeos.

Essa tese de doutorado será dividida em sete capítulos, sendo eles: Introdução (**Capítulo 1**), Revisão Bibliográfica (**Capítulo 2**), Artigo 1 (**Capítulo 3**), Artigo 2 (**Capítulo 4**), Artigo 3 (**Capítulo 5**), Artigo 4 (**Capítulo 6**), Artigo 5 (**Capítulo 7**), Conclusões (**Capítulo 8**) e Trabalhos Futuros (**Capítulo 9**).

A Revisão Bibliográfica (**Capítulo 2**) apresenta o estado da arte deste estudo de doutorado.

O **Capítulo 3** apresenta o aprimoramento da técnica do DSC no artigo intitulado: "Effect of heating rates on the accuracy of DSC technique for determining boiling points at subatmospherical pressure". A técnica do DSC, assim como qualquer outro método analítico, apresenta diversos fatores que influenciam sua acurácia, como faixa de pressão/temperatura,

tamanho da amostra e sua pureza, configuração do cadinho e taxa de aquecimento. Visando o melhoramento da técnica para obtenção de dados de temperatura de ebulição, foi avaliada a taxa de aquecimento de 5 a 25 K/min em um intervalo de 5 K/min, a (4,85 ± 0,05) kPa. O tamanho da amostra foi fixado em 4 – 5 mg para cadinho hermeticamente selado com *pinhole* de 0,8 mm na tampa e uma esfera de carboneto de tungstênio com 1,0 mm colocada sobre a tampa. Três classes diferentes de compostos foram utilizadas neste estudo: n-parafina (n-eicosano), álcool graxo (1-octadecanol) e ácido graxo (ácido palmítico). Como resultado, a melhor taxa foi a de 25 K/min.

A primeira parte de dados experimentais de equilíbrio líquido-vapor encontra-se no **Capítulo 4**, intitulado: "Vapor-liquid equilibria of monoacylglicerol + monoacylglicerol or alcohol or fatty acid at subatmospheric pressures". Os sistemas monocaprilina + ácido láurico (3,42 kPa), monononanoina + monolaurina (2,06 kPa), monononanoina + hexadecanol (2,02 kPa), monolaurina + octadecanol (2,05 kPa) foram determinados pela técnica do DSC. Todos os sistemas foram ajustados com sucesso pelos modelos moleculares Wilson, NRTL e UNIQUAC. Também foi testada a capacidade preditiva dos métodos de contribuição de grupos, UNIFAC em suas diferentes versões (FREDENSLUND et a. 1975; LARSEN et al., 1987; GMEHLING et al., 1993), sendo que, de forma geral, o UNIFAC original apresentou o melhor desempenho.

O **Capítulo 5** apresenta a segunda parte experimental de equilíbrio líquido-vapor dessa tese intitulado: "Vapor-liquid equilibria of binary systems with long-chain organic compounds (fatty alcohol, fatty ester, acylglycerol and n-paraffin) at subatmospheric pressures". Os sistemas binários obtidos pela técnica do DSC foram hexadecanol + octadecanol (1,73 kPa), hexadecanol + metil miristato (1,72 kPa) monononanina + tributirina (1,69 kPa), dinonanoina + octacosano (1,70 kPa), além de dados de pressão de vapor da dinonanoina à pressões subatmosféricas. Todas todos os dados experimentais foram ajustados com sucesso pelo modelo UNIQUAC. A capacidade preditiva dos métodos UNIFAC Linear, UNIFAC Modificado, UNIFAC Dortmund e UNIFAC NIST foi avaliada com os seus parâmetros originais publicados e os com os novos parâmetros a_{mn} ajustados especialmente para compostos lipídicos por DAMACENO et al., 2017. De forma geral, o UNIFAC Modificado com os parâmetros ajustados por Damaceno et al. (2017) apresentou os menores desvios para os sistemas hexadecanol + octadecanol e dinonanoina + octacosano e com os seus parâmetros originais para o sistema hexadecanol + metil miristato. Já para o sistema tributirina + monononanoina, o método UNIFAC Linear com os parâmetros originais mostrou-se ser o mais adequado.

O trabalho desenvolvido na Denmark Technical University encontra-se no **Capítulo 6**, intitulado: "Improvement of predictive tools for vapor-liquid equilibrium based on group contribution methods applied to lipid technology". Considerando que o UNIFAC apresenta certas limitações para compostos complexos, tais como lipídios, esse estudo teve como objetivo propor um novo conjunto de valores os parâmetros de interação energética dos grupos funcionais encontrados na indústria de lipídios, como também, a criação de dois novos grupos (OHacyl e GLY). Além disso, foi testada a capacidade preditiva tanto dos métodos com seus valores originais como com os novos valores ajustados para os compostos lipídicos. Os métodos avaliados foram o UNIFAC Linear, UNIFAC Modificado e o UNIFAC Dortmund. Todos exibiram uma melhora significativa no seu desempenho, tanto quantitativamente quanto qualitativamente. O UNIFAC Linear foi o método que apresentou menor desvio médio relativo para todos os sistemas avaliados.

O **Capítulo 7** apresenta os dados de temperatura normal de ebulição obtidos pela técnica do TGA. Intitula-se: "Experimental data and prediction of normal boiling point of partial acylglycerols". Neste capítulo estão apresentados dados experimentais de temperatura normal de ebulição de monoacilgliceróis e diacilgliceróis, sendo eles: monobutirina, monocaprina, monolaurina, monopalmitina, monoestearina, dicaprilina, dinonanoina e dicaprina, obtidos pela técnica do TGA. Os resultados foram comparados com os métodos preditivos de Ceriani et al. (2013), Zong et al. (2010), Marrero e Gani (2001) e Joback e Reid (1987) para obtenção de temperatura normal de ebulição. Os métodos desenvolvidos por Ceriani et al. (2013) e Marrero e Gani (2001) apresentaram os menores desvios médios absolutos e relativos.

O **Capítulo 8** apresenta a conclusão geral do trabalho desenvolvido. E o **Capítulo 9** os trabalhos futuros.

De forma geral, a primeira etapa da tese foi o aprimoramento da técnica do DSC, com isso foi possível determinar dados inéditos de pressão de vapor e temperatura normal de ebulição de mono- e diacilgliceróis, e de equilíbrio líquido-vapor de sistemas graxos. Além disso, foram feitas a análise da capacidade preditiva bem como o aprimoramento do método UNIFAC visando melhor predizer o equilíbrio de fases de sistemas lipídicos. Foram também determinados dados inéditos de temperatura normal de ebulição para diversos acilgliceróis parciais. Assim conclui-se que, esta tese de doutorado contribui no preenchimento de lacunas relacionadas à tecnologia de lipídeos no que tange processos de separação que envolvem o equilíbrio líquido-vapor a pressões subatmosféricas, na purificação do biodiesel e da bioglicerina, e no refino de óleos e gorduras, bem como no seu estoque e armazenamento.

CAPÍTULO 2

REVISÃO BIBLIOGRÁFICA

Nesse Capítulo 2 será abordada a revisão bibliográfica estudada para o desenvolvimento desta tese de doutorado.

2.1 ÓLEOS E GORDURAS

Óleos e gorduras são substâncias muito pouco solúveis em água, e que em seu estado bruto consistem predominantemente de triacilglicerois e ácidos graxos livres (SWERN, 1964). Seu valor nutricional está relacionado à presença de ácidos graxos essenciais e de vitaminas lipossolúveis A, D, E e K (KITTS, 1996). Quase a totalidade dos óleos vegetais e gorduras passam por algum tipo de processamento (refino) antes de ser destinado ao consumo humano. Os objetivos do refino são diversos, como a remoção de odor e acidez livre, alteração na cor (O'BRIEN, 1998), podendo ser definido como a purificação do óleo ou gordura brutos. De forma simplificada, as etapas que compõem o processamento de óleos e gorduras são: preparação, extração mecânica e/ou com solvente, degomagem, branqueamento, desacidificação (física ou química) e desodorização.

De acordo com Cahoon e Schmid (2008), a composição em ácidos graxos determina as características físicas de um determinado óleo ou gordura. Por exemplo, uma proporção suficiente de ácidos graxos saturados que não tem ligações duplas carbono-carbono, pode elevar o ponto de fusão do óleo até que este seja sólido à temperatura ambiente, tal como é exigido em alguns produtos de panificação. O ácido palmítico, com 16 átomos de carbono e nenhuma ligação dupla, é o mais abundante dos ácidos graxos saturados em plantas. Já o ácido oleico, de dezoito carbonos e uma dupla ligação, pode compreender de 65-85% do azeite de oliva, mas está presente em apenas 20% dos óleos comuns, como de girassol ou de soja (GUNSTONE *et al.*,1994). Os óleos vegetais são também uma importante fonte de ácidos graxos poli-insaturados, incluindo o ácido linoleico (C18:2) e linolênico (C18:3), essenciais para a dieta humana.

As etapas de desacidificação física e de desodorização de óleos e gorduras, que são responsáveis, respectivamente, pela remoção de ácidos graxos livres e de odores indesejados são configuradas como processos de esgotamento sob elevadas temperaturas e baixas pressões, com injeção de vapor de arraste. De acordo com De Greyt (2013), a desacidificação por via física/ desodorização tem como desafios a busca por maior eficiência, ou seja, com menor perda de óleo neutro no destilado e uma melhor valoração das correntes laterais (*side-streams*) e condições de processamento mais brandas (*mild deodorization*), em termos de temperaturas e pressões. Mais uma vez, as ferramentas geradas nesse trabalho podem nortear a escolha de melhores condições de processamento em termos da qualidade e valor do produto final, bem como a implementação de ações corretivas e controladores numa planta real de processamento, que visam ao aumento das receitas anuais. Um estudo dessa natureza, realizado diretamente em planta industrial, impactaria os processos envolvidos na geração dos produtos finais. Portanto, o emprego da simulação computacional pode, deste modo, representar uma ferramenta adequada e menos invasiva para a investigação e otimização de processos industriais.

Monoacilgliceróis (MAG) e diacilgliceróis (DAG), encontrados na massa reacional do biodiesel e também nas etapas de refino de óleos e gorduras (hidrólise de triacilgliceróis), são excelentes emulsionantes. Estima-se que 75 % da produção mundial de emulsionantes é proveniente de acilgliceróis parciais, o que corresponde a aproximadamente 250 mil toneladas por ano. A popularidade de acilgliceróis parciais como emulsionantes, especialmente monoacilgliceróis destilados (90 % m/m) é devido à sua segurança alimentar, juntamente com a sua estrutura molecular, que combina uma porção hidrofílica e hidrofóbica. A etapa de purificação por destilação molecular de monoacilgliceróis (FREGOLENTE et al., 2009) é mais um processo que pode se beneficiar das ferramentas geradas nesse projeto de pesquisa.

É importante ressaltar que os MAGs são normalmente uma mistura dos seus isômeros (1-MAG ou 2-MAG) e a relação entre os isômeros pode variar dependendo da temperatura, composição de ácidos graxos, forma do cristal e tempo de armazenamento (KROG e SPARSO, 1990; CAMPTON et al., 2007; LAZLO et al., 2008).

Atualmente, há uma alta demanda de óleos e gorduras para a produção de biodiesel, pois este combustível utiliza como matéria-prima principal uma oleaginosa (grão ou fruto ou farelo) e/ou gordura animal.

2.2 BIODIESEL

O biodiesel é um combustível comumente produzido na reação de transesterificação a partir de triacilgliceróis, que provém de fontes renováveis (óleo/gordura vegetal ou animal), com um álcool na presença de um catalisador. Em 2008, a fração de biodiesel no diesel era de 2% e sua produção era de, aproximadamente, 1.000 mil m³. Em 2014, a sua participação na mistura aumentou para 7 %, e a sua produção triplicou (ANP, 2015). Em 2015, o país produziu 3,9 bilhões de litros de biodiesel, representando um aumento de 15% em relação a 2014 (OLIVEIRA, 2016). Além disso, uma autorização da normativa n° 3/2015 (BRASIL, 2015) (comercialização de biodiesel) prevê a comercialização de uso voluntário de misturas, aplicando-se até o B20 (20 %) para frotas cativas e até o B30 (30 %) para uso agrícola, industrial e ferroviário. É devido à essa crescente demanda que pesquisas voltadas a biocombustíveis têm se destacado.

A forma de obtenção de biodiesel pode-se dar por craqueamento térmico, microemulsificação e transesterificação, sendo que o terceiro método é de longe o mais utilizado na indústria para produção de biodiesel (ARANSIOLA *et al.*, 2014; KNOTHE *et al.* 2005). A transesterificação consiste em uma série de reações consecutivas e reversíveis, na qual primeiramente os triacilgliceróis na presença do álcool e catalisador são convertidos em diacilgliceróis e ésteres graxos. Os diacilgliceróis são convertidos em monoacilgliceróis e ésteres graxos. Por fim, os monoacilgliceróis são convertidos em glicerol e ésteres graxos. Os ésteres graxos são os compostos que perfazem o biodiesel. A reação de transesterificação alcalina está ilustrada na Figura 2.1. (ATABANI et al., 2012).

Figura 2.1. Reação de transesterificação. FONTE: Adaptado Altabani et al., 2012
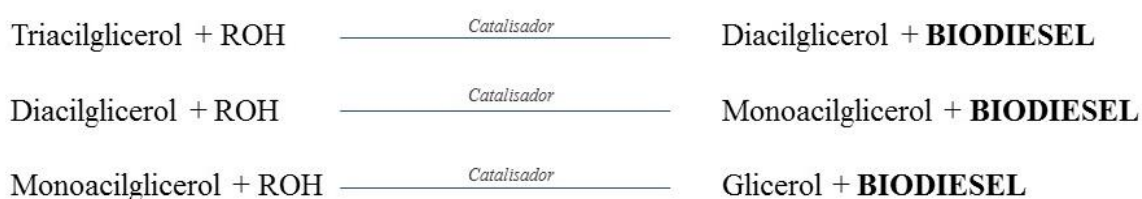
Os reagentes da reação de transesterificação são óleos e/ou gorduras, álcool e catalisador. Há diversas oleaginosas que podem ser utilizadas na produção de biodiesel, entre elas destacam-se: soja, palma, girassol, pinhão-manso, mamona e canola. Além das oleaginosas, a gordura animal e o óleo de fritura também fazem parte das matérias-primas. Já os álcoois mais utilizados são: metanol, etanol, 1-propanol, 2-propanol, 1-butanol, 2-butanol, 2-metil 1-propanol e 2-metil 2propanol, sendo o metanol o de maior destaque (KNOTHE et al. 2005). No entanto, como o Brasil é o maior produtor de etanol de cana-de-açúcar do mundo, a utilização do mesmo para produção de biodiesel é bastante interessante, o que torna os ésteres

etílicos uma classe importante de pesquisa. Quanto ao catalisador, ele pode ser alcalino ou ácido, sendo que a reação por via alcalina é mais rápida e a mais comumente utilizada pela indústria.

Vale ressaltar ainda que MAG e DAG estão também presentes na massa reacional após a reação de transesterificação na produção de biodiesel. De fato, a especificação brasileira para o biodiesel (ANP, 2012) estabelece os limites máximos para compostos provenientes da reação de transesterificação (glicerina total: glicerol + tri-, di- e monoacilgliceróis = 0,25 % m/m, máx; glicerina livre: glicerol = 0,02 % m/m, máx) e uma faixa de valores para a viscosidade cinemática a 40°C (2,0 a 5,0 cSt). Isso porque a presença destes compostos exerce influência nas propriedades físicas do biodiesel. Os acilgliceróis parciais (MAG e DAG), por exemplo, podem afetar de forma significativa a viscosidade do combustível, sobretudo a temperaturas próximas à ambiente (CERIANI et al., 2011), mesmo em baixas concentrações (< 1,5 %, m/m), um exemplo de óleo que apresenta alta viscosidade é a mamona (OLIVEIRA, 2016). Yu et al. (1998) demostraram que o ponto de névoa do biodiesel de soja é afetado pela presença de MAG e DAG saturados, mesmo em baixas concentrações (0,1 % a 0,4 %). Por outro lado, MAG tem excelente lubricidade e são, de fato, apontados como largamente responsáveis pela boa lubricidade do diesel com baixo teor de enxofre aditivado com até 1 a 2 % de biodiesel (KNOTHE e STEIDLEY, 2005). Segundo Oliveira (2016), o óleo de macaúba, novo propulsor de diversas pesquisas na produção de biodiesel, é muito estável, e apresenta ácido láurico, importante composto da indústria de cosméticos, contudo ele se acidifica muito rápido, em torno de dois dias. Além dos acilgliceróis parciais, triacilgliceróis não reagidos, glicerol, excesso de álcool e o catalisador podem contaminar o produto final, o que pode gerar diversos problemas operacionais, como, formação de depósitos, entupimento de filtro e deterioração do combustível (KNOTHE et al., 2005).

Para atender as diversas especificações de qualidade do biodiesel (ANP, 2012), o produto obtido na reação de transesterificação deve passar por etapas de separação e purificação, que se tornam essenciais para a comercialização do biocombustível. De acordo com Miranda (2011), o processo de produção de biodiesel pode ser dividido em três etapas: a reação de transesterificação, a recuperação de etanol e a purificação/ reciclo. Assim, após a reação, e a recuperação do etanol por destilação, ocorre a separação das fases leve (rica em biodiesel) e pesada (rica em glicerol) por diferença de densidade (decantação ou centrifugação). Ambas as fases estão contaminadas com os demais compostos da massa reacional e passam por processos subsequentes de purificação (PARENTE, 2003). A fase leve é lavada com água a 60 ºC para remoção do catalisador e de glicerol. A destilação dos ésteres pode ser feita a 170 ºC a

pressão atmosférica (MIRANDA, 2011). Da fase pesada, pode-se obter glicerina por processos de separação que envolvem destilação a vácuo e a desodorização. O projeto das etapas de purificação do biodiesel é, portanto, totalmente dependente da modelagem do equilíbrio líquido-vapor envolvido. Além disso, recentemente, biocombustíveis sem glicerina, como Ecodiesel®, foram relatados na literatura, em que o glicerol permanece na forma de MAGs evitando a produção de bioglicerol (subproduto) (CABALLERO et al., 2009; VERDUGO et al., 2010; CALERO et al., 2015).

Considerando o que foi descrito, o conhecimento das propriedades termofísicas e do equilíbrio de fases de tais compostos é essencial para desacidificação/desodorização de óleo/gorduras e purificação de biodiesel e bioglicerina, a fim de evitar perda de óleo neutro e melhorar a qualidade dos produtos.

2.3 COMPOSTOS PUROS E SISTEMAS BINÁRIOS

Levando em conta o que foi exposto nos itens 2.1 e 2.2 fica clara a importância de se conhecer as propriedades termofísicas de compostos puros e do equilíbrio fases de misturas graxas, especialmente os acilgliceróis parciais.

Considerando o conceito de contribuição de grupos, sabe-se que um banco de dados diversificado e de qualidade é essencial para testar e/ou melhorar a capacidade preditiva desses métodos. Os acilgliceróis parciais apresentam diferentes grupos funcionais num mesmo composto, os quais são: CH_2 (subgrupos CH_3, CH_2), CCOO (subgrupo CH_2COO) e OH, ou seja, quatro diferentes grupos, além da interação do grupo OH proveniente de um lipídio e não de um álcool (por exemplo o etanol): CH_2 (subgrupos CH_3, CH_2) e OH. Outro exemplo seria um sistema binário de monoacilglicerol + ácido graxo, no qual além dos grupos CH_2 (subgrupos CH_3, CH_2), CCOO (subgrupo CH_2COO) e OH também encontra-se o grupo COOH (proveniente do ácido graxo). A Figura 2.2 apresenta um exemplo dos grupos funcionais encontrados em um monoacilglicerol (monocaprilina) mais um ácido graxo (ácido láurico). Para testar a capacidade preditiva do UNIFAC é importante ter sistemas binários com diversos grupos funcionais, assim como é apresentado neste trabalho.

Figura 2.2 Representação dos grupos funcionais do sistema binário de monocaprilina + ácido láurico conforme UNIFAC original
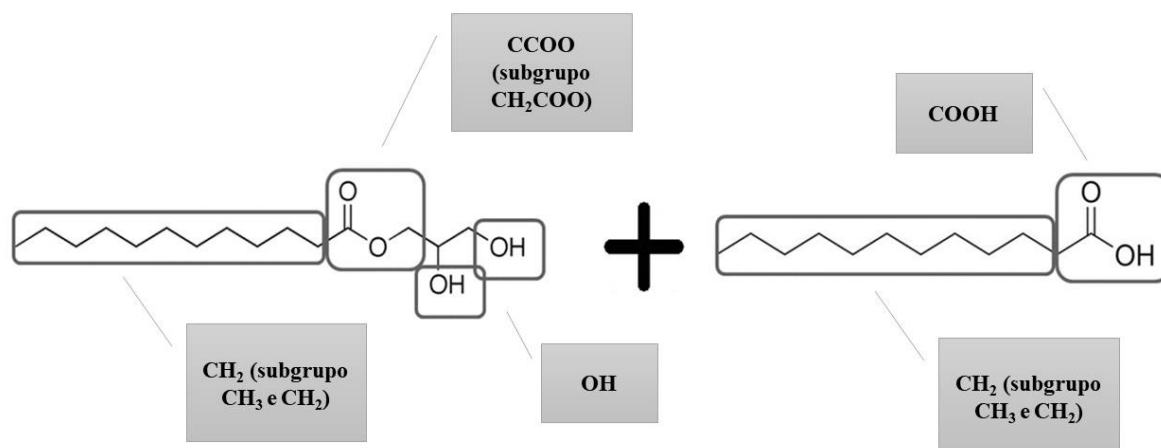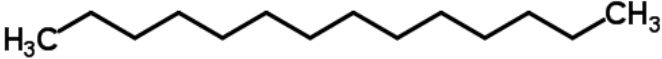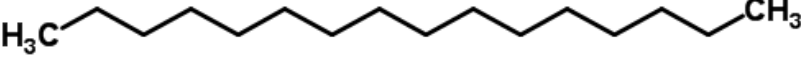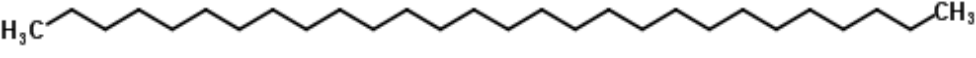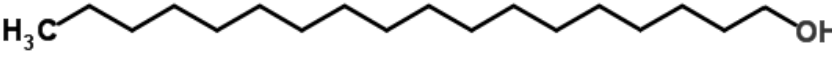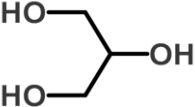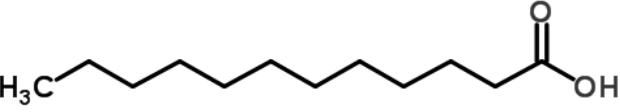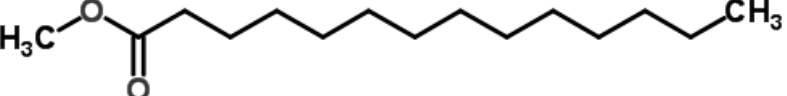
Nessa tese foram determinados dados inéditos de temperatura normal de ebulição para oito monoacilgliceróis e três diacilgliceróis, de pressão de vapor para dois monoacilgliceróis e um diacilglicerol, e de equilíbrio líquido-vapor para oito sistemas binários. Na Tabela 2.1, encontram-se todos os compostos estudados e seus grupos funcionais de acordo com o método de contribuição de grupos UNIFAC. E nas Tabela 2.2a, Tabela 2.2b e Tabela 2.2c apresentam-se os compostos, a estrutura molecular, o fornecedor, o número CAS e a pureza.

Tabela 2.1. Compostos utilizados na tese e seus diferentes grupos funcionais de acordo com o método UNIFAC original
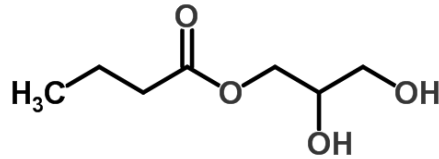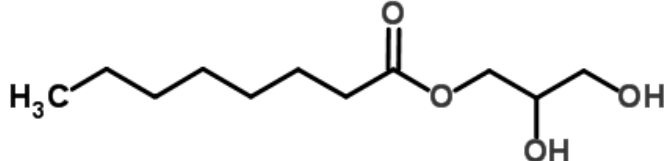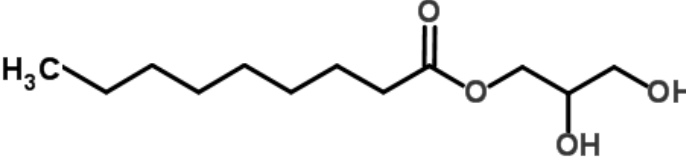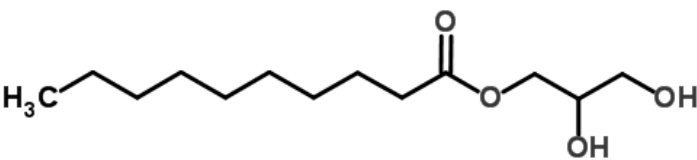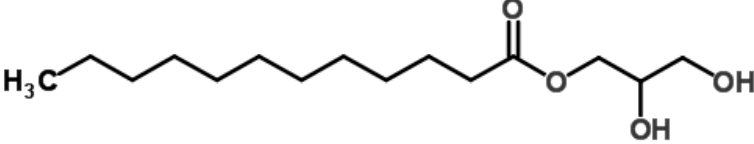
Composto	Grupos funcionais principais	Subgrupos
tetradecano	CH_2 e CH_2	1 CH_3 e 13 CH_2
hexadecano	CH_3 e CH_2	1 CH_3 e 15 CH_2
octacosano	CH_2 e CH_2	1 CH_3 e 27 CH_2
hexadecanol	CH_2 e OH	1 CH_3, 15 CH_2 e 1 OH
octadecanol	CH_2 e OH	1 CH_3, 17 CH_2 e 1 OH
ácido laúrico	CH_2 e COOH	1 CH_3, 10 CH_2 e COOH
metil miristato	CH_2 e CCOO	2 CH_3, 11 CH_2 e 1 CH_2COO
glicerol	CH_2 e OH	1 CH, 2 CH_2 e 3 OH
monobutirina	CH_2, CCOO e OH	1 CH_3, 2 CH_2, 1 CH, 1 CH_2COO e 2 OH
monocaprilina	CH_2, CCOO e OH	1 CH_3, 7 CH_2, 1 CH, 1 CH_2COO e 2 OH
monononanoina	CH_2, CCOO e OH	1 CH_3, 8 CH_2, 1 CH, 1 CH_2COO e 2 OH
monocaprina	CH_2, CCOO e OH	1 CH_3, 9 CH_2, 1 CH, 1 CH_2COO e 2 OH
monolaurina	CH_2, CCOO e OH	1 CH_3, 11 CH_2, 1 CH, 1 CH_2COO e 2 OH
monopalmitina	CH_2, CCOO e OH	1 CH_3, 15 CH_2, 1 CH, 1 CH_2COO e 2 OH
monoestearina	CH_2, CCOO e OH	1 CH_3, 17 CH_2, 1 CH, 1 CH_2COO e 2 OH
dicaprilina	CH_2, CCOO e OH	2 CH_3, 12 CH_2, 1 CH, 2 CH_2COO e 1 OH
dinonanoina	CH_2, CCOO e OH	2 CH_3, 14 CH_2, 1 CH, 2 CH_2COO e 1 OH
dicaprina	CH_2, CCOO e OH	2 CH_3, 16 CH_2, 1 CH, 2 CH_2COO e 1 OH
tributirina	CH_2 e CCOO	3 CH_3, 5 CH_2, 1 CH e 3 CH_2COO

Tabela 2.2a. Compostos utilizados nesta tese de doutorado, número CAS, fornecedor, estrutura molecular e pureza[*].

Composto	Número CAS	Fornecedor	Estrutura molecular
tetradecano	629-59-4	Sigma-Aldrich	
hexadecano	544-76-3	Sigma-Aldrich	
octacosano	630-02-4	Sigma-Aldrich	
hexadecanol	36653-82-4	Sigma-Aldrich	
octadecanol	112-92-5	Sigma-Aldrich	
glicerol	56-81-5	Sigma-Aldrich	
ácido láurico	143-07-7	Sigma-Aldrich	
miristato de metila	124-10-7	Sigma-Aldrich	
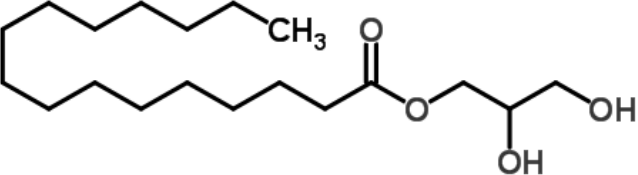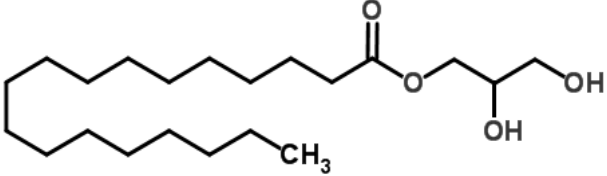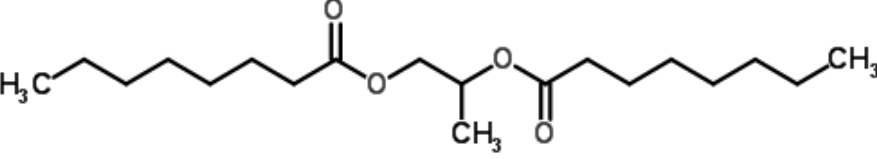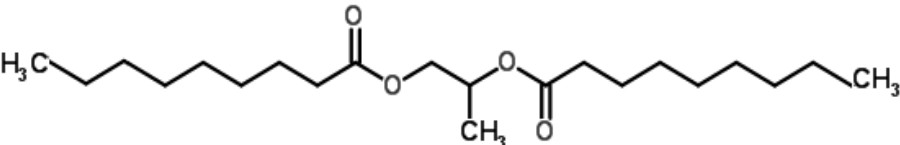
[*]Todos os compostos utilizados nesta tese de doutorado apresentam pureza de 99% de massa

Tabela 2.2b. Compostos utilizados nesta tese de doutorado, número CAS, fornecedor, estrutura molecular e pureza[*].

Composto	Número CAS	Fornecedor	Estrutura molecular
monobutirina	557-25-5	Sigma-Aldrich	
monocaprilina	26402-26-6	Nu-Chek prep.	
monononanoina	3065-51-8	Nu-Chek prep.	
monocaprina	26402-22-2	Nu-Chek prep.	
monolaurina	27215-38-9	Nu-Chek prep.	
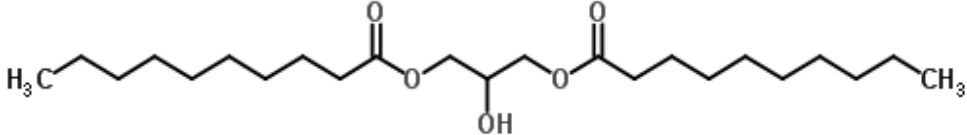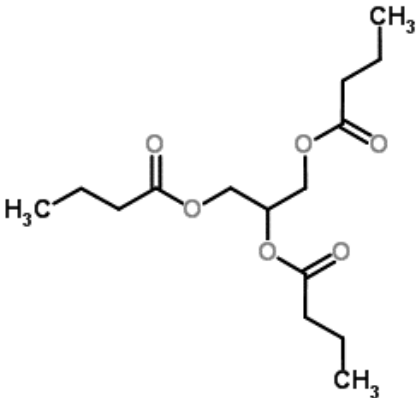
[*]Todos os compostos utilizados nesta tese de doutorado apresentam pureza de 99% de massa

Tabela 2.2b. Compostos utilizados nesta tese de doutorado, número CAS, fornecedor, estrutura molecular e pureza[*].

Composto	Número CAS	Fornecedor	Estrutura molecular
monopalmitina	542-44-9	Nu-Chek prep.	
monoestearina	123-94-4	Nu-Chek prep.	
dicaprilina	36354-80-0	Nu-Chek prep.	
dinonanoina	-	Nu-Chek prep.	

[*]Todos os compostos utilizados nesta tese de doutorado apresentam pureza de 99% de massa

Tabela 2.2c. Compostos utilizados nesta tese de doutorado, número CAS, fornecedor, estrutura molecular e pureza[*].

Composto	Número CAS	Fornecedor	Estrutura molecular
dicaprina	53988-07-01	Nu-Chek prep.	
tributirina	60-01-5	Sigma-Aldrich	

[*]Todos os compostos utilizados nesta tese de doutorado apresentam pureza de 99% de massa

2.4 DETERMINAÇÃO EXPERIMENTAL DE TEMPERATURA DE EBULIÇÃO

Propriedades físicas, juntamente com os dados de equilíbrio de fases binários são cruciais para expressar o comportamento termodinâmico e estudar os mecanismos dos processos de separação (REDDY et al., 2014). Dessa forma, a escolha de uma técnica apropriada para a determinação experimental de dados de equilíbrio líquido-vapor deve levar em conta, além de outros aspectos, a natureza química dos elementos constituintes e a rapidez com que se deseja obter os resultados (MATRICARDE FALLEIRO, 2012). A princípio, há três formas de determinação de dados de ELV: o método dinâmico, o estático e o de recirculação (HALA, 1958; NDIAYE, 2004).

Os métodos dinâmicos, extrativo ou contínuo, caracterizam-se por ter, pelo menos, uma das fases do sistema sujeita a um deslocamento em relação à outra. Os dois tipos de métodos dinâmicos distinguem-se quanto ao modo pelo qual o contato entre as fases envolvidas no equilíbrio é estabelecido. Já os métodos estáticos apresentam como característica fundamental o fato do sistema ser fechado, podendo as composições das fases coexistentes serem determinadas indiretamente (sintético) ou ocorrer a retirada de amostras das fases em equilíbrio para posterior análise (analítico). O método de recirculação pode ser considerado ao mesmo tempo como dinâmico (já que ocorre um fluxo de uma fase em relação à outra), ou como estático, devido às semelhanças na etapa de retirada das amostras das fases em equilíbrio (NDIAYE, 2004).

Dentre as inúmeras técnicas, o estudo do equilíbrio líquido-vapor é normalmente realizado em equipamentos mantidos à pressão ou temperatura constante nos quais se verifica o ponto de ebulição do líquido (puro ou mistura). Esta técnica é a ebuliometria (MATRICARDE FALLEIRO, 2012), a qual data desde o início de século passado, e teve vários métodos e equipamentos desenvolvidos, cada qual com suas vantagens e desvantagens. Os ebuliômetros podem ser de recirculação ou de fluxo. Os de circulação são aqueles nos quais pelo menos uma das fases recircula pelo sistema. Já nos ebuliômetros de fluxo, o equilíbrio ocorre durante o escoamento da mistura líquido-vapor sendo que, na sequência, as fases são coletadas separadamente em frascos anexos ao equipamento (COELHO, 2011). Os métodos tradicionais de determinação de dados de pressão de vapor e de equilíbrio líquido-vapor (ebuliometria, por exemplo) requerem volume considerável de amostra (dezenas de mililitros) e um considerável tempo de operação. Já com a utilização da técnica do DSC a quantidade da amostra é

significativamente menor (miligramas) e o tempo de trabalho é reduzido (minutos) (TRONI et al., 2016; CASSERINO, et al., 1996).

Pensando no emprego de novas tecnologias, aliado à acurácia, ao tempo dos ensaios e, principalmente, à reduzida quantidade de amostra, este estudo visou à utilização da técnica da calorimetria diferencial exploratória (DSC), a qual permite determinar dados de equilíbrio líquido-vapor com precisão, conforme foi evidenciado nos trabalhos de Siitsman e Oja (2016), Cunico et al. (2015), Matricarde Falleiro et al. (2010) e Silva et al. (2011) utilizando sistemas binários graxos. E também para compostos puros por Troni et al. (2016), Damaceno et al. (2014), Brozena (2013), Siistman et al. (2014), Matricarde Falleiro et al. (2011) e Seyler (1976).

Goodrum e Siesel (1996) reportaram o uso do TGA (Análise termogravimétrica) para a determinação de temperatura de ebulição de compostos orgânicos. A técnica do TGA acompanha a perda ou ganho de massa de uma amostra em função do tempo ou da temperatura. Outros trabalhos como o de Goodrum et al. (1998), Goodrum e Geller (2002) e Santander et al. (2010), Raslavičius et al. (2018) utilizaram essa técnica para a obtenção de dados de temperatura de ebulição ou temperatura normal de ebulição para compostos graxos e misturas.

Assim, como a técnica do DSC, o TGA também requer quantidades ínfimas de amostra para sua análise. No DSC é utilizado em torno de 4 – 5 mg de massa de amostra e no TGA em torno de 7 mg de massa de amostra, o que viabiliza este estudo, uma vez que os acilgliceróis parciais (MAG e DAG), triacilgliceróis e ésteres graxos de elevada pureza (> 99 % m/m) são compostos de acusto muito elevado. Os subitens 2.4.1 e 2.4.2 a seguir apresentam, de forma mais detalhada, essas duas técnicas.

2.4.1 Calorimetria Diferencial Exploratória (DSC)

A calorimetria diferencial exploratória (DSC) é uma técnica térmica capaz de quantificar a energia envolvida nas reações e transições de fases de modo que as diferenças no fluxo de calor de uma substância e a referência são medidas como uma função da temperatura da amostra, enquanto ambas estão sujeitas a um programa de temperatura controlada. Atualmente, a técnica do DSC tem se tornado a mais utilizada dentre todos os métodos térmicos na determinação da transição vítrea, cristalização, fusão, estabilidade de produtos, cinética de cura e estabilidade oxidativa. Pode ser empregada também no estudo da mudança de fases líquido→vapor, sólido→vapor, sólido→sólido e sólido→líquido, além de medir as entalpias de vaporização, sublimação e fusão (MATRICARDE FALLEIRO, 2009; SKOOG *et al.*, 1992).

Dois tipos de métodos são utilizados para obter dados na calorimetria diferencial exploratória. Na técnica do DSC com compensação de potência, a amostra e o material de referência são aquecidos através de aquecedores separados, de tal maneira que as suas temperaturas são mantidas iguais enquanto estas temperaturas são aumentadas (ou diminuídas) linearmente. Já na técnica do DSC com fluxo de calor, a diferença no fluxo de calor da amostra e da referência é medida quando a temperatura da amostra é aumentada ou diminuída linearmente (SKOOG et al., 1992). Neste trabalho foi utilizado o DSC com fluxo de calor, conforme Figura 2.3.

Figura 2.3. Esquema de célula de DSC. FONTE: TA Instruments (2000)
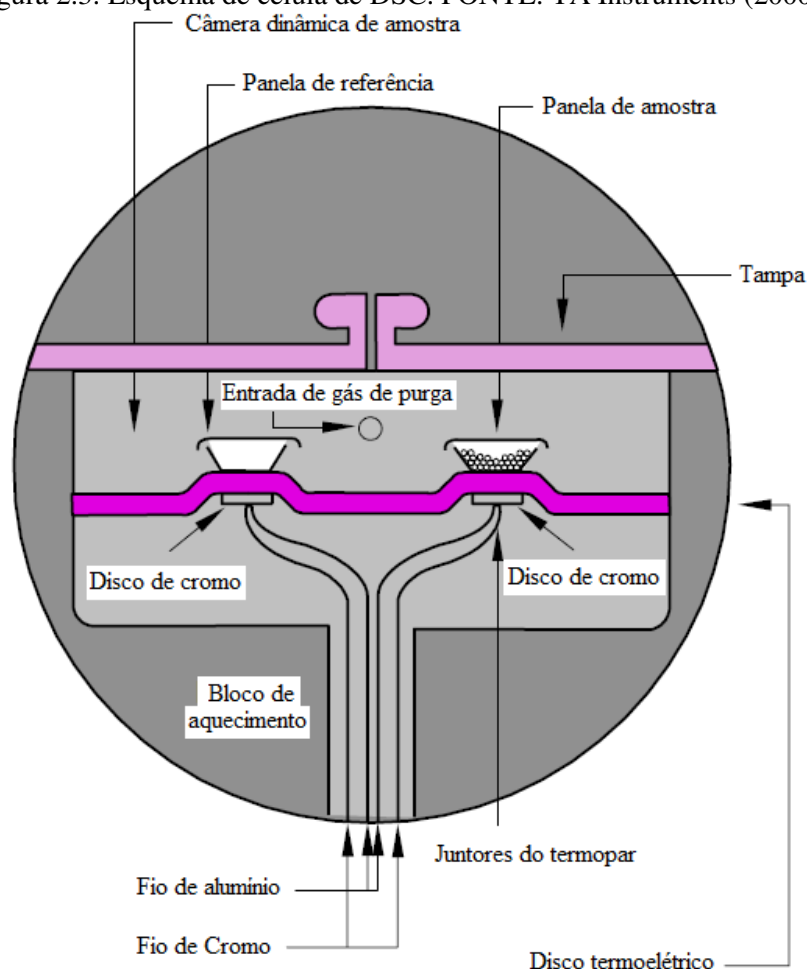
Para análises nas quais há necessidade de se medir dados em determinadas pressões, como dados de equilíbrio líquido-vapor, é indispensável usar uma célula de pressão no DSC que é conhecida como PDSC (*Pressure Differential Scanning Calorimetry*). O PDSC é uma análise de calorimetria diferencial exploratória conduzida sob pressão, com a capacidade adicional de operar a pressões de até 7 MPa e pode atingir um vácuo de até 1 Pa com um bom

sistema de bombeamento (SILVA, 2010). Esta análise apresenta duas vantagens sobre o DSC, as quais são: diminuição das reações sensíveis à pressão (incluindo a volatilização), e tempo de operação (BELINADO, 2010). A Figura 2.4 apresenta o sistema de uma célula de PDSC.

Figura 2.4. Esquema de uma célula de PDSC. FONTE: Adaptado do TA Instruments (2000)
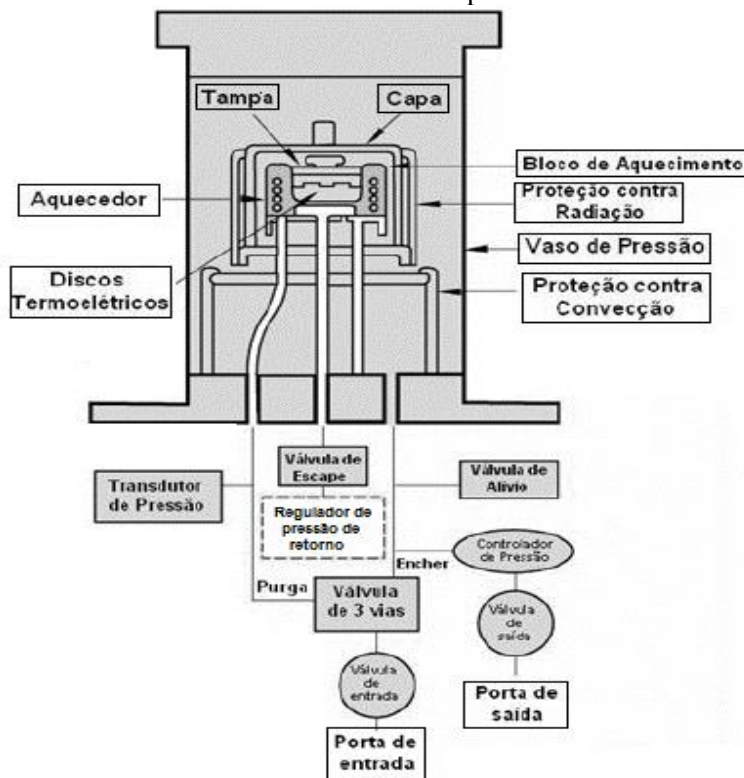
As amostras a serem analisadas no PDSC são adicionadas num conjunto cadinho e tampa. Na tampa é confeccionado um *pinhole* (orifício na tampa do cadinho), e junto a esse conjunto pode ser utilizado ou não uma esfera de carboneto de tungstênio, dependendo do diâmetro do orifício. Diâmetros de 0,8 mm necessitam da esfera, já sobre os menores, como mencionados na ASTM E1782, não é utilizada a esfera de carboneto de tungstênio. A Figura 2.5. apresenta um exemplo de tampa e cadinho hermeticamente fechados, com um *pinhole* de 0,8 mm e uma esfera de carboneto de tungstênio (retirada da caneta Bic Cristal).

Figura 2.5. Conjunto cadinho, tampa (com *pinhole*) e esfera de carboneto de tungstênio.

O registro gráfico da técnica do DSC é expresso em temperatura (ºC, K) ou tempo (min) no eixo das abscissas e em fluxo de calor (mW/mg ou W/g) no eixo das ordenadas. Transições de primeira ordem (endotérmicas ou exotérmicas) são caracterizadas como picos. A área do pico diretamente sob a curva W/g é proporcional à entalpia envolvida no processo de liberação ou absorção de energia, expressa em Joule por grama (J/g) (MATRICARDE FALLEIRO, 2012).

A Figura 2.6 é um exemplo de endoterma de ebulição obtida por DSC a uma dada pressão para determinação de dados de temperatura de ebulição. A temperatura de *onset* é a intersecção das tangentes da linha base e do pico do evento térmico. Segundo a literatura (ASTM E1782, 2008; MATRICARDE FALLEIRO et al., 2012; SILVA, 2010), é a temperatura de *onset* que origina a temperatura de ebulição, pois neste ponto de extrapolação das tangentes é possível estimar a mudança de fluxo de calor que ocorre com a transição de fase pela inclinação sofrida pela linha base da curva térmica diferencial (MATRICARDE FALLEIRO, 2012).

Figura 2.6. Endoterma DSC
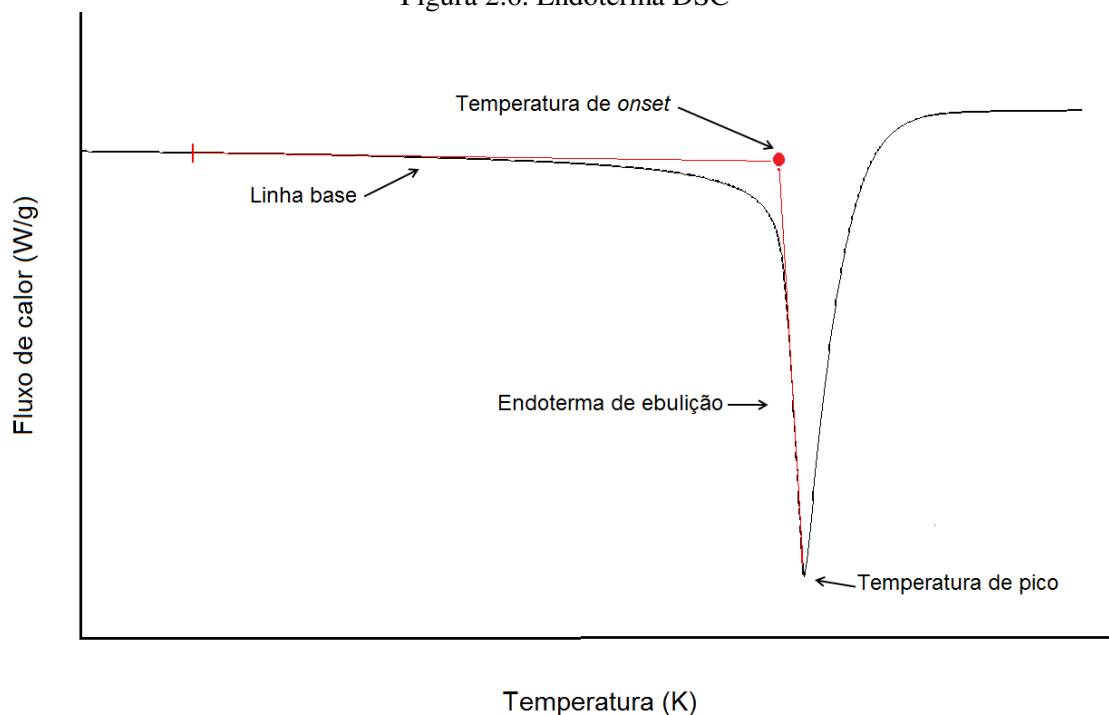
Como em qualquer técnica analítica, há alguns fatores que podem afetar o desempenho da técnica do DSC na medida de dados de temperatura de ebulição, como impurezas, controle e precisão da medida da pressão, configurações do equipamento, configuração do cadinho, taxa de aquecimento, faixa de temperatura e pressão, e interferências termodinâmicas (SEYLER, 1976; CONTRERAS et al., 1993; BROZENA, 2013; SIITSMAN et al., 2015; SIITSMAN e OJA, 2016; TRONI et al., 2016). Nesta tese de doutorado, foi feita uma investigação para determinar a melhor taxa de aquecimento a uma determinada pressão a ser utilizada na determinação dos dados de ELV de sistemas graxos, para uma massa de amostra de 4 – 5 mg, com cadinho hermético da TA Instruments com *pinhole* de 0,8 mm e esfera de tungstênio de 1 mm. De fato, Matricarde Falleiro et al. (2011) avaliaram a influência de diferentes taxas de aquecimento (10, 15, 20, 25, 35, 50 e 100 ℃/min) na temperatura de ebulição medida para uma mistura binária tetradecano/ 1-hexadeceno a 20 mmHg, para concentrações molares do composto mais volátil de 0,1, 0,5 e 0,9. Os autores verificaram que a taxa de aquecimento de 25℃/min foi a que minimizou os desvios absolutos da temperatura de ebulição medida pela técnica do DSC com os dados experimentais da literatura medidos com técnica convencional. Além disso, Troni (2017) fez um extenso levantamento bibliográfico sobre os fatores que podem afetar os resultados de temperatura de ebulição para compostos puros e sistemas binários. A autora também realizou um aprimoramento da técnica do DSC com o uso de uma esfera de carboneto de tungstênio sobre o *pinhole* da tampa do cadinho. Neste

aprimoramento, foram avaliados os efeitos individuais e combinados da quantidade de amostra e da taxa de aquecimento utilizando a ferramenta do planejamento fatorial. Como resultado, a condição otimizada para compostos puros foi uma taxa de aquecimento de 24,52 K/min e para uma massa de amostra de $(4,6 \pm 0,5)$ mg.

De acordo com Matricarde Falleiro (2012), outro fator que se reflete na acurácia dos dados de ELV via técnica do DSC é a diferença na temperatura de ebulição dos compostos puros da mistura binária a uma dada pressão. De uma forma geral, seu trabalho mostra que, no caso de misturas binárias mais próximas do comportamento ideal, quando a diferença na temperatura de ebulição dos compostos puros é elevada (acima de ≥ 30 °C) pode ocorrer a vaporização prévia do componente mais volátil, formando um pico ou deformação da endoterma antes do pico da temperatura *onset* (intersecção das tangentes da linha base e do pico do evento térmico). Por outro lado, se essa diferença for menor (inferior a ≤ 10 ºC), a metodologia também passa a ser inviável, uma vez que as curvas térmicas diferenciais ficam sobrepostas, independentemente da composição, gerando, assim, temperaturas praticamente iguais para cada ponto do diagrama de fases, levando a uma interpretação errônea de não-idealidade do sistema. Cunico et al. (2014) também observaram essa limitação de utilização da técnica do DSC na determinação de dados de ELV de misturas binárias graxas de comportamento não-ideal. Algumas misturas que foram descartadas a posteriori foram monocaprilina + miristato de metila e monoestearina + tricaprilina. A primeira apresenta 25,6 ºC de diferença entre as temperaturas de ebulição a 1,2 kPa, estando dentro da faixa apontada por Matricarde Falleiro (2012). Já para a segunda, esse valor é de 40,6 ºC, sendo superior à essa faixa. Mais recentemente, algumas limitações da técnica referentes à misturas binárias foram mapeadas por Troni (2016), que trabalharam com 17 combinações de n-parafinas (C_{11} a C_{13}) e/ou álcoois graxos saturados (C_8OH a $C_{11}OH$), variando-se entre elas a diferença da temperatura de ebulição dos puros entre 7 e 63 K a 4,97 kPa. Corroborando com os achados de Matricarde Falleiro (2012), também foi demostrado que a diferença entre a temperatura de ebulição dos puros exerce influência na precisão da técnica. No entanto, esse não foi o único fator identificado, uma vez que para algumas das misturas estudadas houve também a influência da fração molar do composto mais volátil tanto na precisão da técnica como na formação de dois picos endotérmicos durante o processo de vaporização.

Ressalta-se aqui que, para selecionar as misturas binárias contempladas nesse projeto, primeiramente foi necessário fazer uma predição da temperatura de ebulição de compostos dentro das classes de interesse dessa pesquisa a uma dada pressão (5 kPa) utilizando-se informações e metodologias preditivas da literatura (CERIANI et al., 2013; DAMACENO

et al., 2014). Posteriormente, selecionou-se uma faixa para as diferenças entre as temperaturas ebulição dos compostos das misturas binárias como sugere a literatura, levando-se ainda em consideração a preferência por compostos mais voláteis numa tentativa de evitar a degradação térmica previamente à volatilização. Considerou-se também as limitações da técnica do DSC identificadas até o momento em relação à diferença na temperatura de ebulição dos compostos, além da disponibilidade e custo dos reagentes de elevada pureza.

Por fim, Siitsman e Oja (2015) realizaram um levantamento de artigos publicados na literatura desde 1972 que aplicaram a técnica do DSC para medir dados de equilíbrio líquido-vapor e/ou dados de pressão de vapor de diferentes classes de compostos. Os autores observaram que antes do método ser padronizado pela ASTM E1782-96 (ASTM, 1996), os estudos eram dirigidos para determinar as melhores condições de análise para obtenção de resultados confiáveis. Após a normatização, os estudos concentraram-se na extensão do método para aplicações específicas, sendo que o método padronizado raramente tem sido aplicado em sua totalidade, existindo sempre uma variação da metodologia, indicando uma preocupação em relação ao melhor desenvolvimento da própria técnica, ou seja, a melhor combinação de condições operacionais de análise que produzirá resultados de elevada acurácia para uma aplicação escolhida (TRONI, 2016).

2.4.1.1   *DSC utilizado na obtenção de propriedades termodinâmicas*

As medidas de pressão de vapor são necessárias para uma ampla gama de aplicações na indústria química. Os métodos tradicionais requerem 10 mililitros a 30 mililitros de amostra e 6 horas a 8 horas de tempo de operação. Já com a utilização da DSC, a quantidade da amostra é menor e o tempo de trabalho é reduzido (CASSERINO et al., 1996). No entanto, a técnica do DSC é pouco utilizada na determinação de dados de equilíbrio líquido-vapor, sendo largamente utilizada na determinação de dados de equilíbrio sólido-líquido (MATSUOKA e OZAWA, 1989; YOUNG e SCHALL, 2001; COSTA et al., 2010; CARARETO et al., 2011; GHOSH et al., 2014). Devido à acurácia da DSC para análises térmicas em geral, em 1996 foi proposta a ASTM (American Society for Testing and Materials) E1782, que é uma metodologia para obtenção de dados de pressão de vapor em análises térmicas (DTA e DSC). Anteriormente, Krawetz e Tovrog (1962) determinaram a pressão de vapor de tolueno utilizando análise térmica diferencial (DTA), que é uma técnica semelhante à DSC. Já Seyler (1976), apresentou um artigo sobre os parâmetros que afetam as medidas da DSC para a obtenção dos dados de

pressão de vapor. Contreras *et al.* (1993) investigaram a influência de diversos fatores na utilização da DSC para análises térmicas e pressão de vapor, como a quantidade de amostra, diâmetro do *pinhole* (orifício localizado no centro da tampa do cadinho), taxa de aquecimento, entre outros, para a futura aplicação de propriedades de álcoois e ésteres lipídicos de alto peso molecular.

Mais recentemente, Butrow e Seyler (2003) realizaram testes para aumentar a faixa de pressão utilizada na ASTM E1782 para a baixo de 5 kPa e com o uso de pinholes com diâmetros maiores 125 μm que é o indicado na norma, e obtiveram uma boa aplicabilidade. Matricarde Falleiro et al. (2010) obtiveram dados de ELV para ácido mirístico (C14: 0) + ácido palmítico (C16:0), ácido mirístico (C14:0) + ácido esteárico (C18:0), e o ácido palmítico (C16:0) + ácido esteárico (C18:0), medidos a 50 mmHg e com frações molares entre 0,0 e 1,0 pela técnica do DSC. Foram determinados dados de equilíbrio líquido-vapor por DSC para os sistemas de palmitato de etila/estearato de etila a 5,3 kPa, palmitato de etila/oleato de etila a 5,3 kPa e a 9,3 kPa, e palmitato de etila/linoleato de etila a 9,3 kPa. Os ésteres utilizados são os principais componentes de biodiesel obtidos a partir da transesterificação de óleo de soja com etanol (SILVA et al., 2011).

A técnica do DSC foi usada para determinar a pressão de vapor dos seguintes ésteres etílicos: laurato de etila, miristato de etila, palmitato de etila, estearato de etila, oleato de etila e linoleato de etila no intervalo de 1,33-9,33 kPa (SILVA et al., 2011).

Dados de pressão de vapor de ácido láurico (C12:0), mirístico (C14:0), palmítico (C16:0), esteárico (C18:0) e oléico (C18:1) foram determinados por meio da DSC, com alguns ajustes no procedimento, que incluem o uso de uma pequena (carboneto de tungstênio) colocada sobre o orifício do cadinho (diâmetro de 800 μm), o que tornou possível a utilização de uma taxa de aquecimento mais rápida do que a do método padrão e reduziu o tempo experimental, sendo essa taxa de 25 ^{0}C/min. As medidas foram feitas numa faixa de pressão de 1,3 kPa a 9,3 kPa, utilizando amostras 3 mg a 5 mg de cada ácido graxo (MATRICARDE FALLEIRO et al., 2012). Damaceno et al. (2014) e Damaceno (2014) também empregaram condições semelhantes na determinação da pressão de vapor de acilglicerois parciais de cadeia curta.

Siitsman et al. (2014) determinaram dados de pressão de vapor para nicotina, anabasina e cotinina pela técnica do DSC. Eles utilizaram uma taxa de 5K/min e cadinhos de alumínio hermeticamente selados com pinhole de 50 μm confeccionados a laser. Este mesmo grupo de pesquisa em 2015 determinou dados de pressão de vapor de frações de petróleo pela técnica do DSC (SIITSMAN et al., 2015). E por fim, em 2016 ele trabalharam com misturas de óleos para testar a idealidade desses compostos (SIITSMAN et al., 2016).

Cunico et al. (2015) determinaram dados de ELV de sistemas binários com monoacilgliceróis pela técnica do DSC. De 1,2 kPa – 2,50 kPa, utilizando a mesma configuração de cadinho utilizada nesse trabalho de doutorado. Troni et al. (2016), como foi abordado anteriormente (seção 2.3.1) realizou um trabalho de aprimoramento da técnica do DSC para essa configuração de cadinho, sendo a condição ótima de taxa de aquecimento de 24,52 K/min e de massa da amostra de (4,6 ± 0,5).

2.4.2 Análise termogravimétrica (TGA)

A técnica do TGA é uma forma rápida de quantificar a temperatura de ebulição de compostos orgânicos.

O equipamento de TGA é composto basicamente de uma termobalança, que é um instrumento que permite a pesagem contínua de uma determinada amostra em função da temperatura a medida que a mesma é aquecida. De forma geral, os principais itens de um TGA são: balança registradora, forno, suporte de amostra e sensor de temperatura, programador de temperatura de forno, sistema registrador e controle da atmosfera do forno (DENARI, 2012). A Figura 2.7 representa, de forma simplificada, um equipamento TGA.

Figura 2.7 Diagrama simplificado de um TGA. FONTE: Denari, 2012
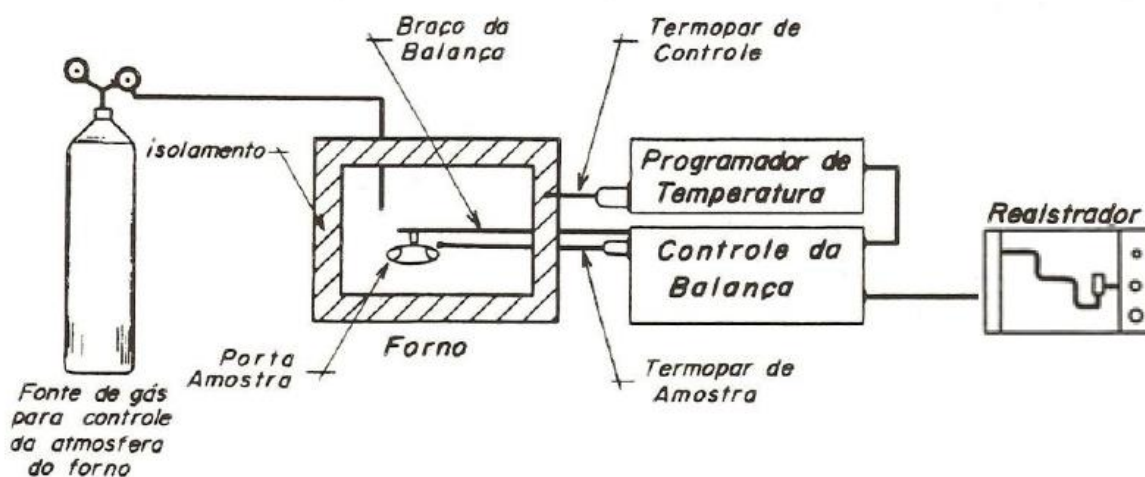
Santander et al. (2012) fizeram um estudo para determinar a temperatura normal de ebulição de ésteres graxos e triacilgliceróis pela técnica do TGA, baseado no trabalho de Goodrum e Siesel (1996). A metodologia experimental consiste em primeiramente medir uma

massa de amostra de 7 mg (± 2 mg) e adiciona-la em um cadinho de volume 40 µL de fabricação da Mettler Toledo (Brasil) com a adição de 1 mg de α-alumina (± 0,2 mg), que serve para evitar altas taxas de vaporização ou superaquecimento da amostra (GOODRUM e GELLER, 2002). O conjunto cadinho/tampa é hermeticamente selado, com um *pinhole* de (0,25 – 0,31) mm na tampa. Após isso, a amostra é inserida no equipamento TGA. As condições de análise são constantes e todas as medidas são tomadas em atmosfera de gás nitrogênio (N_2) com vazão de 50 mL/min a uma taxa de aquecimento de 10 °C/min sob pressão atmosférica. Recentemente, Raslavičius et al. (2018) realizaram um estudo para determinar a temperatura de ebulição de misturas de diesel com biodiesel, ou com óleo de *P. moriformis* por termogravimetria utilizando mesma metodologia de Goodrum e Seisel (1996) e Santander et al (2012). Esta técnica de determinação de temperatura de ebulição se adequa perfeitamente com os compostos utilizados nesta tese, pelos seguintes fatores:

a. Compostos graxos – Santander et al. (2012) e Raslavičius et al. (2018) utilizaram esta técnica com sucesso para compostos graxos;

b. Alto custo – baixa quantidade de massa de amostra e semelhante ao DSC (TGA = 7 mg e DSC = 5 mg);

c. Misturas – a termogravimetria se mostrou eficar para determinar temperatura de ebulição de misturas graxas,

d. Compostos termosensíveis – a utilização de 1 mg de alumina evita a termodegração das amostras.

A temperatura normal de ebulição é obtida pela temperatura *onset*, que é calculada pelo software do próprio equipamento de TGA (Mettler Toledo - TGA) traçando-se tangentes a linha base e à curva de perda de massa. A Figura 2.8 ilustra como é obtida a temperatura *onset*, que é a temperatura de ebulição da amostra.

Figura 2.8 Exemplo de diagrama gerado pelo TGA. Legenda: Linha preta (—) é a curva termogravimétrica; Linhas vermelha (—) é a tangente da perda de massa e as linhas azuis (—) são as linhas tangentes a linha base para o cálculo de temperatura *onset*
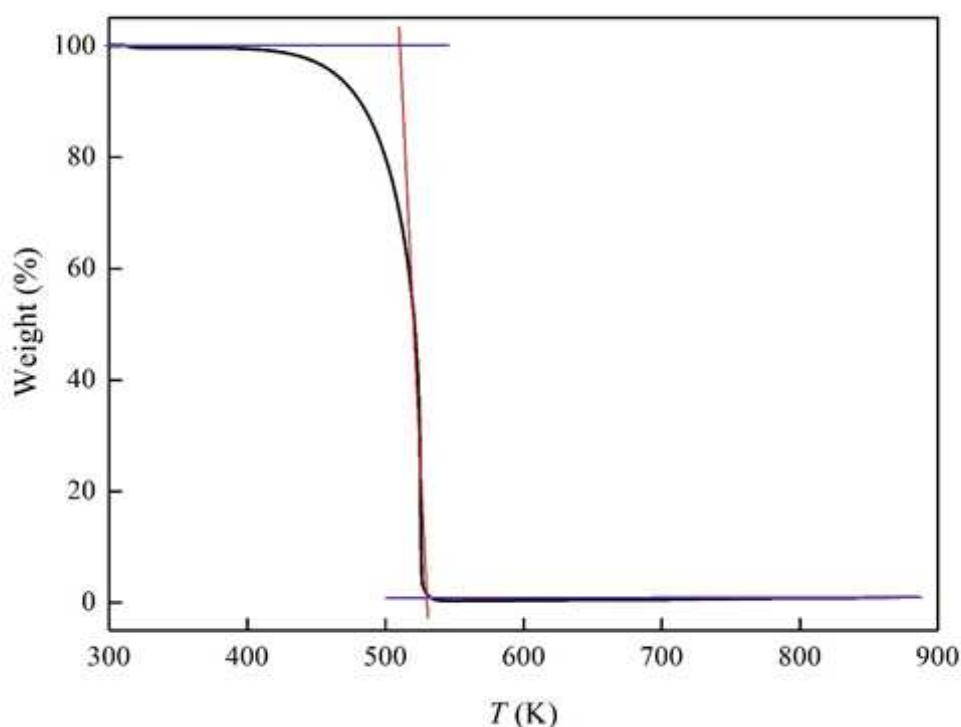
2.5 PROPRIEDADES FÍSICAS E DADOS DE EQUILÍBRIO LÍQUIDO-VAPOR

De uma forma geral, há uma escassez de dados experimentais de propriedades de compostos graxos puros e de suas misturas, os quais são de grande importância para o projeto, simulação computacional e otimização de processos da indústria de óleos, gorduras e biodiesel (CORRÊA et al., 2014; CUNICO et al., 2013).

Dados experimentais de propriedades termofísicas de acilgliceróis na literatura aberta são bastante escassos, principalmente com relação aos acilgliceróis parciais. Por exemplo, no caso da temperatura de ebulição, até recentemente encontravam-se na literatura aberta apenas 6 dados experimentais a 0,13 kPa para 6 diferentes monoacilgliceróis (MAG) e nenhum dado para diacilgliceróis (DAG). Já para os triacilgliceróis (TAG), há em torno de 226 dados reportados (CERIANI et al. 2013; DAMACENO et al., 2014). Devido a essa carência, Damaceno et al. (2014) desenvolveram um trabalho experimental para determinação de dados de temperatura de ebulição a baixas pressões (1,0 kPa a 13,2 kPa) para quatro acilgliceróis

parciais de cadeia curta, denominados monocaprilina (MM = 218,2 g/mol), monocaprina (MM = 246, 3 g/mol), dicaprilina (MM = 344,5 g/mol) e dicaprina (MM = 400,6 g/mol).

Corrêa et al. (2014) fizeram um levantamento bibliográfico de dados experimentais de equilíbrio líquido-vapor de sistemas graxos e biodiesel a pressão subatmosférica, envolvendo pelo menos um composto graxo, sendo esse ácido graxo, éster graxo metílico ou etílico, biodiesel, acilglicerol parcial, triacilglicerol ou óleo/gordura, além de glicerol e álcoois de cadeia curta. Desse total, 93 são misturas binárias ou pseudobinárias, 21 são ternárias ou pseudoternárias e 8 são multicomponentes. No caso das misturas pseudobinárias e pseudoternárias, o pseudocomposto é biodiesel ou óleo/gordura. Das 122 misturas, 55 % trazem dados PTx, sendo os demais PTxy. Em mais de 90 % das misturas, os dados de ELV são isobáricos. A Tabela 2.3 mostra de forma genérica os tipos de sistemas encontrados. E para compreender melhor a demanda por dados experimentais, conforme o **Capítulo 5**, foi realizada uma pesquisa bibliográfica de 2014 – 2017 de sistemas EVL com pelo menos um composto graxo (binário, ternário ou quaternário) e foram encontrados 1522 dados experimentais, o que representa praticamente um terço de todos os dados experimentais publicados de 1900 – 2013 para sistemas EVL, o que indica claramente o interesse da comunidade científica neste assunto.

Tabela 2.3 Equilíbrio líquido-vapor de sistemas de interesse de acordo com o tipo de mistura: binária/ pseudobinária. FONTE: Corrêa et al. (2014)

Classe dos compostos	Tipo de mistura	Número de misturas	Número de dados experimentais
Ácido graxo/ ácido graxo		16	195
Ácido graxo/ álcool		1	28
Ácido graxo/ éster graxo		1	9
Éster graxo/ álcool		36	1682
Éster graxo/ éster graxo	Binária	9	163
Éster graxo/ hidrocarboneto		8	344
Acilglicerol/Acilglicerol		2	4
Glicerol/água		5	276
Glicerol/ álcool		10	543
Biodiesel/ álcool	Pseudobinária	4	553
Biodiesel/ hidrocarboneto		1	187
Total		93	4050
Éster graxo/ álcool/ água		4	100
Éster graxo/ álcool/ glicerol	Ternária	4	110
Glicerol/ álcool/ água		3	63
Biodiesel/óleo vegetal/ álcool	Pseudoternária	7	48
Biodiesel/ álcool/ glicerol		3	24
Total		21	345
Ésteres graxos	Multicomponente	4	12
Monoacilgliceróis		4	12
Total		8	24

2.6 MODELAGEM TERMODINÂMICA

Para o desenvolvimento e o planejamento de um processo industrial, envolvendo processos de contato líquido-vapor, é essencial o conhecimento do equilíbrio de fases do sistema de interesse e a escolha de métodos e/ou equações de predição das propriedades físicas das misturas envolvidas (CERIANI, 2005).

Equilíbrio é uma condição na qual não ocorrem variações das propriedades macroscópicas de um sistema com o tempo. Isso implica uma igualdade de todos os potenciais que causam mudanças. Na prática da engenharia, a hipótese de equilíbrio é justificada quando ela leva a resultados com precisão satisfatória (SMITH et al., 2007).

2.6.1 Relações fundamentais

Cada substância tem uma tendência a mudar, isto é: para reagir com outras substâncias, para mudança de estado e migrar para outro lugar. Esta tendência pode ser descrita por uma grandeza física, o potencial químico (Equação 1) que é uma grandeza que relaciona a energia de Gibbs e a variação da quantidade de matéria de um sistema a pressão e temperatura constantes.

$$\mu_i = \left(\frac{\partial G}{\partial n_i} \right)_{T,P,n_j} \tag{1}$$

onde, μ_i é o potencial químico, G é a energia de Gibbs, n_i refere-se a todos os números de moles e n_j a todos os números de moles com exceção do i-ésimo e tempetatura (T) e pressão (P).

Então considerando o equilíbrio químico entre misturas:

$$\mu_i^{\alpha} = \mu_i^{\beta} \tag{2}$$

O potencial químico fornece o critério fundamental para o equilíbrio de fases. Entretanto, ele exibe características que desencorajam a sua utilização. A energia de Gibbs, e consequentemente o μ_i, é definida em relação à energia interna e à entropia. Como valores

absolutos de energia interna são desconhecidos, o mesmo é verdadeiro para o μ_i. Embora essas características não impeçam o uso do potencial químico, a aplicação de critérios de equilíbrio é facilitada pela introdução da fugacidade, uma propriedade que toma o lugar o μ_i.

$$f_i^\alpha = f_i^\beta \tag{3}$$

Assim, a Equação 3 diz que a condição de equilíbrio em termos de potenciais químicos pode ser substituída, sem perda de generalidade, por uma relação idêntica em termos de fugacidades, sendo que esta equação é análoga à Equação 2, e, de um ponto de vista estritamente termodinâmico, tanto faz usar uma quanto a outra; entretanto, de um ponto de vista prático, uma equação com fugacidades é preferível a uma contendo potenciais químicos.

Considerando a distribuição de equilíbrio de um componente numa mistura entre as fases líquida e vapor, a relação simples que descreve a relação da fração molar na fase líquida com a fase vapor encontra-se na Equação 4.

$$f_i^V = f_i^L \tag{4}$$

A Equação 4 pode ser reescrita em termos de coeficientes de fugacidade da fase vapor (ϕ_i), coeficientes de atividade da fase líquida (γ_i) e da fugacidade no estado padrão (f_i^0):

$$\phi_i\, y_i\, P = \gamma_i\, x_i\, f_i^0 \tag{5}$$

A fugacidade do composto i no estado padrão (componente puro a T e P do sistema) está definido pela Equação 6, em função da pressão de vapor do composto puro (P_i^{sat}), do coeficiente de fugacidade na saturação (ϕ_i^{sat}) e do fator de Poynting (POY, termo exponencial):

$$f_i^0 = P_i^{sat} \phi_i^{sat} \exp \int_{P_i^{sat}}^{P} \left(\frac{v_i\, dP}{RT} \right) \tag{6}$$

Combinando as equações 5 e 6, tem-se o critério de equilíbrio, conforme Equação 7.

$$\phi_i \, y_i \, P = \gamma_i \, x_i \, P_i^{sat} \phi_i^{sat} POY \tag{7}$$

Esta é a equação chave para o cálculo do equilíbrio líquido-vapor que pode ser aplicada a uma ampla variedade de misturas pela abordagem *gamma-phi*. Para sistemas ideais considera-se o fator de Poynting (*POY*), as fugacidades ϕ_i e ϕ_i^{sat} e o coeficiente de atividade iguais à unidade (PRAUSNITZ et al., 1999; SMITH et al., 2007; MATRICARDE FALLEIRO, 2012). Para sistemas à baixas pressões, as fugacidades ϕ_i e ϕ_i^{sat} são igualadas à unidade (Equação 8), na qual a não-idealidade do sistema está na fase líquida e é expressa pelo coeficiente de atividade:

$$y_i \, P = \gamma_i \, x_i \, P_i^{sat} \tag{8}$$

2.6.2 Funções em Excesso

As forças intermoleculares causam um arranjo não-aleatório de moléculas na mistura, sendo que o arranjo das moléculas e a sua orientação preferencial em equilíbrio na interface são considerados no cálculo da energia de Gibbs em excesso (G^E). Funções em excesso são as propriedades termodinâmicas das soluções que excedem aquelas da solução ideal nas mesmas condições de pressão, temperatura e composição da fase líquida. Para uma solução ideal, todas as propriedades em excesso são nulas. As Equações 9 e 10 representam a energia de Gibbs em excesso (PRAUSNITZ et al., 1999).

$$G^E \equiv G_{(\text{solução real a T, P, x})} - G_{(\text{solução ideal a T, P, x})} \tag{9}$$

$$G^E = RT \sum_i x_i \ln \gamma_i \tag{10}$$

onde, G^E é a energia em Gibbs de excesso, G é a energia de Gibbs, R é a constantes dos gases, T é a temperatura, x_i é a composição da fase líquida e γ_i é o coeficiente de atividade.

Diversos modelos termodinâmicos se baseiam na energia de Gibbs em excesso, tais como, Wilson, NRTL (*Non-Random Two-Liquid*), UNIQUAC (*Universal Quasichemical*) e o método UNIFAC (UNIQUAC *Functional-group Activity Coefficients*).

2.6.2.1   Modelo de Wilson

Wilson apresentou em 1964 um modelo (Equação 11) relacionando G^E com as frações molares, baseado parcialmente em considerações moleculares, usando o conceito de composição local, onde a composição local estabelece que a composição do sistema nas vizinhanças de uma dada molécula não é igual à composição global, por causa das forças intermoleculares.

$$\frac{G^E}{RT} = -x_1 \ln(x_1 + \Lambda_{12} x_2) - x_2 \ln(x_2 + \Lambda_{21} x_1) \tag{11}$$

onde x1 e x2 são as frações molares da fase líquida dos compostos 1 e 2, e Λ_{12} (Equação 12) e Λ_{21} (Equação 13) são parâmetros ajustáveis, relacionados aos volumes molares dos líquidos puros e às diferenças de energia características.

$$\Lambda_{12} \equiv \frac{v_1}{v_2} \exp\left(-\frac{\lambda_{12} - \lambda_{11}}{RT} \right) \tag{12}$$

$$\Lambda_{21} \equiv \frac{v_2}{v_1} \exp\left(-\frac{\lambda_{12} - \lambda_{22}}{RT} \right) \tag{13}$$

onde os λ são energias de interação entre as moléculas designadas nos subscritos. Num sentido estrito, as diferenças entre as energias devem ser consideradas como dependentes da temperatura, mas em muitos casos esta dependência pode ser desprezada sem introduzir erros muito significativos. Se essas diferenças são consideradas independentes da temperatura, pelo menos ao longo de pequenos intervalos, a equação de Wilson proporciona não apenas uma expressão para os coeficientes de atividade em função da composição, mas também uma estimativa da variação dos coeficientes de atividade com a temperatura. Isto é uma grande vantagem em cálculos isobáricos, onde a temperatura varia com a composição.

Os coeficientes de atividade podem ser calculados pelas Equações 14 e 15.

$$\ln \gamma_1 = -\ln(x_1 + \Lambda_{12}x_2) + x_2\left[\frac{\Lambda_{12}}{x_1 + \Lambda_{12}x_2} - \frac{\Lambda_{21}}{\Lambda_{21}x_1 + x_2}\right] \tag{14}$$

$$\ln \gamma_2 = -\ln(x_2 + \Lambda_{21}x_1) - x_1\left[\frac{\Lambda_{12}}{x_1 + \Lambda_{12}x_2} - \frac{\Lambda_{21}}{\Lambda_{21}x_1 + x_2}\right] \tag{15}$$

Na Equação 11, G^E é definida em relação a uma solução ideal de Lewis-Randall; portanto, esta equação obedece a condição limite de $G^E = 0$ quando x_1 ou x_2 são iguais a zero.

A equação de Wilson fornece uma boa representação da energia de Gibbs em excesso para uma variedade de misturas, e é particularmente útil para soluções de compostos polares ou com tendência à associação em solventes não polares, onde equações como Van Laar ou Margules não são suficientes. A equação de Wilson apresenta também como vantagem o fato de ser facilmente estendida para soluções multicomponentes, mas apresenta uma séria desvantagem: o modelo não é capaz de predizer miscibilidade parcial, ou seja, não é aplicável para cálculos de equilíbrio líquido-líquido (PRAUSNITZ et al., 1999).

2.6.2.2 Modelo NRTL

Renon e Prausnitz (1968) desenvolveram a equação NRTL (*non-random, two-liquid*) baseada também no conceito de composição local, mas, à diferença do modelo de Wilson, o modelo NRTL é aplicável a sistemas de miscibilidade parcial, conforme Equação 16.

$$\frac{G^E}{RT} = x_1 x_2\left[\frac{\tau_{21}G_{21}}{x_1 + x_2 G_{21}} + \frac{\tau_{12}G_{12}}{x_2 + x_1 G_{12}}\right] \tag{16}$$

onde:

$$\tau_{12} = \frac{g_{12} - g_{22}}{RT} \tag{17}$$

$$\tau_{21} = \frac{g_{21} - g_{11}}{RT} \tag{18}$$

$$G_{12} = \exp(-\alpha_{12}\tau_{12}) \tag{19}$$

$$G_{21} = \exp(-\alpha_{12}\tau_{21}) \tag{20}$$

O significado dos g_{ij} é similar aos λ_{ij} da equação de Wilson, ou seja, são parâmetros de energia característicos das interações *i-j*. O parâmetro α_{12} está relacionado com a não-aleatoriedade da mistura, quer dizer, que os componentes na mistura não se distribuem uniformemente, mas que seguem um padrão ditado pela composição local. Quando α_{12} é zero, a mistura é completamente aleatória, e a equação se reduz à equação de Margules dois sufixos.

Os coeficientes de atividade se apresentam conforme as Equações 21 e 22.

$$\ln\gamma_1 = x_2^2\left[\tau_{21}\left(\frac{G_{21}}{x_1 + x_2 G_{21}}\right)^2 + \frac{\tau_{12}G_{12}}{(x_2 + x_1 G_{12})^2}\right] \tag{21}$$

$$\ln\gamma_2 = x_1^2\left[\tau_{12}\left(\frac{G_{12}}{x_2 + x_1 G_{12}}\right)^2 + \frac{\tau_{21}G_{21}}{(x_1 + x_2 G_{21})^2}\right] \tag{22}$$

Para sistemas ideais ou moderadamente ideais, o modelo NRTL não oferece muita vantagem sobre Van Laar ou Margules-três sufixos, mas, para sistemas fortemente não ideais, esta equação pode fornecer uma boa representação dos dados experimentais, embora sejam necessários dados de boa qualidade para estimar os três parâmetros. O modelo NRTL também pode ser facilmente estendido para misturas multicomponentes (PRAUSNITZ et al., 1999).

2.6.2.3   *Modelo UNIQUAC*

Abrams e Prausnitz (1975) desenvolveram o modelo conhecido como *Universal Quasichemical* (UNIQUAC). A equação UNIQUAC para G^E consiste em duas partes: uma parte combinatorial, que descreve as contribuições entrópicas dos componentes, e uma parte residual, que expressa as forças intermoleculares que são responsáveis pela entalpia de mistura. A parte combinatorial depende apenas da composição, do tamanho e forma das moléculas, pelo que necessita apenas de dados do componente puro; no entanto, a parte residual depende das

forças intermoleculares, de onde aparecem os dois parâmetros ajustáveis. A equação tem o seguinte princípio:

$$G^E = G^E_{(combinatorial)} + G^E_{(residual)} \qquad (23)$$

Para uma mistura binária:

$$\frac{G^E_{comb}}{RT} = x_1 \ln \frac{\Phi_1^*}{x_1} + x_2 \ln \frac{\Phi_2^*}{x_2} + \frac{z}{2}\left(q_1 x_1 \ln \frac{\theta_1}{\Phi_1^*} + q_2 x_2 \ln \frac{\theta_2}{\Phi_2^*}\right) \qquad (24)$$

$$\frac{G^E_{res}}{RT} = -q'_1 x_1 \ln(\theta'_1 + \theta'_2 \tau_{21}) - q'_2 x_2 \ln(\theta'_2 + \theta'_1 \tau_{12}) \qquad (25)$$

onde o número de coordenação z é igual a 10. As frações de segmentos, Φ_i^*, e as frações de área, θ_i e θ'_i estão dadas por:

$$\Phi_1^* = \frac{x_1 r_1}{x_1 r_1 + x_2 r_2} \qquad (26)$$

$$\Phi_2^* = \frac{x_2 r_2}{x_1 r_1 + x_2 r_2} \qquad (27)$$

$$\theta_1 = \frac{x_1 q_1}{x_1 q_1 + x_2 q_2} \qquad (28)$$

$$\theta_2 = \frac{x_2 q_2}{x_1 q_1 + x_2 q_2} \qquad (29)$$

$$\theta'_1 = \frac{x_1 q'_1}{x_1 q'_1 + x_2 q'_2} \qquad (30)$$

$$\theta'_2 = \frac{x_2 q'_2}{x_1 q'_1 + x_2 q'_2} \qquad (31)$$

Os parâmetros r, q e q' são constantes da estrutura molecular dos componentes puros, e dependem do tamanho da molécula e da área superficial externa da mesma.

Para cada mistura binária existem dois parâmetros ajustáveis τ_{12} e τ_{21}, que, pela sua vez, estão dados por:

$$\tau_{12} = \exp\left(-\frac{\Delta u_{12}}{RT}\right) \equiv \exp\left(-\frac{a_{12}}{T}\right) \tag{32}$$

$$\tau_{21} = \exp\left(-\frac{\Delta u_{21}}{RT}\right) \equiv \exp\left(-\frac{a_{21}}{T}\right) \tag{33}$$

onde Δu_{12} e Δu_{21} são as energias características de interação, que são fracamente dependentes da temperatura.

Os coeficientes de atividade são:

$$\ln\gamma_1 = \ln\frac{\Phi_1^*}{x_1} + \frac{z}{2}q_1\ln\frac{\theta_1}{\Phi_1^*} + \Phi_2^*\left(l_1 - \frac{r_1}{r_2}l_2\right) - q'_1\ln(\theta'_1 + \theta'_2\,\tau_{21}) + \theta'_2\,q'_1\left(\frac{\tau_{21}}{\theta'_1 + \theta'_2\,\tau_{21}} - \frac{\tau_{12}}{\theta'_2 + \theta'_1\,\tau_{12}}\right) \tag{34}$$

$$\ln\gamma_2 = \ln\frac{\Phi_2^*}{x_2} + \frac{z}{2}q_2\ln\frac{\theta_2}{\Phi_2^*} + \Phi_2^*\left(l_2 - \frac{r_2}{r_1}l_1\right) - q'_2\ln(\theta'_2 + \theta'_2\,\tau_{12}) + \theta'_1\,q'_2\left(\frac{\tau_{12}}{\theta'_2 + \theta'_1\,\tau_{12}} - \frac{\tau_{21}}{\theta'_1 + \theta'_2\,\tau_{21}}\right) \tag{35}$$

onde:

$$l_1 = \frac{z}{2}(r_1 - q_1) - (r_1 - 1) \tag{36}$$

$$l_2 = \frac{z}{2}(r_2 - q_2) - (r_2 - 1) \tag{37}$$

O modelo UNIQUAC é aplicável a uma ampla variedade de misturas líquidas não-eletrolíticas, contendo componentes polares e não polares, incluindo sistemas de miscibilidade parcial (PRAUSNITZ et al., 1999).

2.7 MÉTODO DE CONTRIBUIÇÃO DE GRUPOS

Métodos preditivos baseados no conceito de contribuição de grupos consistem em considerar uma mistura ou substância qualquer como um agregado de grupos funcionais presentes nas moléculas que a constituem. Desta forma, suas propriedades são resultantes do somatório de cada uma destas contribuições, representadas através de parâmetros de contribuição de grupos, ajustados com base nos dados experimentais de interesse. A vantagem deste tipo de metodologia é permitir calcular propriedades termofísicas de misturas multicomponentes tão complexas como as envolvidas nesse trabalho, mas que são compostas de moléculas formadas, em geral, pelos mesmos grupos funcionais: CH_2, CCOO, COOH e OH (REID et al., 1987). Dessa forma, a utilização de metodologias preditivas baseadas no conceito de contribuição de grupos no projeto, análise e otimização de processos de separação da indústria de óleos, gorduras e biodiesel é bastante conveniente. Em especial, àquelas associadas ao equilíbrio de fases figuram entre as mais importantes.

Os coeficientes de atividade, γ_i, podem ser calculados utilizando-se a metodologia de contribuição de grupos UNIFAC (UNIQUAC Functional-group Activity Coefficients) original (FREDENSLUND et al., 1977) e suas diferentes versões subsequentes (KIKIC et al., 1980; LARSEN et al., 1987; WEIDLICH e GMEHLING 1987; HANSEN et al., 1992). No caso da lei de Raoult (mistura ideal), os coeficientes de atividade γ_i na Equação 8 são iguais à unidade.

No modelo UNIFAC original proposto por Fredenslund et al. (1977), o coeficiente de atividade é calculado considerando-se uma contribuição entrópica, relacionada à diferença de tamanho e forma das moléculas e uma contribuição residual, devido às interações intermoleculares (Equação 38).

$$ln\gamma_i = ln\gamma_i^C + ln\gamma_i^R \tag{38}$$

A Equação 39 apresenta a forma geral da parte combinatorial para todos os seguintes modelos UNIFAC: Original, Linear, Modificado e o Dortmund. Os UNIFAC Original e Linear apresentam o mesmo equacionamento. Já os modelos Modificado e Dortmund apresentam diferentes frações de volume na parte combinatorial, que estão descritos na Tabela 2.2. O UNIFAC Modificado utiliza a fração de volume de $r^{2/3}$, assim como foi sugerido por Kikic et al. (1980), enquanto o UNIFAC Dortmund a porção combinatorial foi modificada de uma forma empírica, com o objetivo de se trabalhar com misturas de compostos com tamanhos bem

diferentes. O UNIFAC Modificado é o único que não apresenta o termo de correção de Staverman-Guggenhe (LARSEN et al., 1987). Os parâmetros de área e de volume para os modelos Original, Linear e Modificados foram determinados pelo método de Bondi (BONDI, 1968), entretanto o Dortmund apresentou novos valores para esses parâmetros, o quais foram ajustados a partir de dados experimentais.

$$\ln \gamma_i^C = \ln \frac{r_i^{C_0}}{\sum_j x_j r_j^{C_0}} + 1 - \frac{r_i^{C_0}}{\sum_j x_j r_j^{C_0}} - C_1 \left(\ln\left(\frac{\Phi_i}{\theta_i} \right) + 1 - \frac{\Phi_i}{\theta_i} \right) \tag{39}$$

$$\Phi_i = \frac{r_i}{\sum_j x_j r_j} \tag{40}$$

$$\theta_i = \frac{q_i}{\sum_j x_j q_j} \tag{41}$$

Tabela 2.4 C_0 e C_1 da Equação 39

Modelo	C_0	C_1
Original	1	$5q_i$
Linear	1	$5 q_i$
Modificado	$^2/_3$	0
Dortmund	¾	$5 q_i$

O termo residual é descrito na Equação 42 e na Tabela 2.4 Entre todos os modelos UNIFAC a diferença encontra-se no parâmetro de interação de grupos (a_{mn}). O UNIFAC Original é o único modelo que não apresenta dependência de temperatura. Já o UNIFAC Linear, como o nome mesmo fala, apresenta um termo de linearidade na temperatura. O UNIFAC Mofificado tem um termo logaritimo e o UNIFAC Dortmund uma função quadrática na temperatura.

$$\ln \gamma_i^R = \sum_K^{groups} v_k^{(i)} \left[\ln \Gamma_k - \ln \Gamma_k^{(i)} \right] \tag{42}$$

$$ln\Gamma_k = Q_k \cdot \left[1 - ln\left(\sum_m \Theta_m \Psi_{mk} \right) - \sum_m \left(\theta_m \Psi_{mk} \Big/ \sum_n \Theta_n \Psi_{nm} \right) \right] \tag{43}$$

$$\Theta_m = \frac{Q_m X_m}{\sum_n Q_n X_n} \tag{44}$$

$$X_m = \frac{\sum_i^M v_m^{(i)} x_i}{\sum_i^M \sum_j^N v_j^{(i)} x_i} \tag{45}$$

$$\Psi_{mn} = \exp\left(\frac{-a_{m,n}}{T}\right) \tag{46}$$

$$a_{m,n} = A_0 a_{mn,0} + A_1 a_{mn,1} + A_2 a_{mn,2} \tag{47}$$

Tabela 2.5 A_0, A_1 e A_2 da Equação 47

Modelo	A_0	A_1	A_2
Original	1	0	0
Linear	1	$T-T_0$	0
Modificado	1	$T-T_0$	$T\ln(T_0/T) + T - T_0$
Dortmund	1	T	T^2

T_0 é a temperatura de referência ($T_0 = 298.15$ K)

O método UNIFAC apresenta limitações que são intrínsecas a sua generalidade, como qualquer outro método baseado no conceito de contribuição de grupos, que considera que as propriedades de uma mistura ou substância qualquer são resultantes do somatório da contribuição de cada grupo funcional presente nas moléculas que a constituem. Esses efeitos de aproximação ocorrem quando dois ou mais grupos estão situados em posições iguais ou adjacentes do átomo de carbono. No caso particular de sistemas graxos, trabalhos recentes na literatura têm mapeado limitações do método UNIFAC. Cunico et al. (2015) e Belting et al. (2014, 2015), avaliando o UNIFAC original e/ou UNIFAC Dortmund, observaram que esses não foram capazes de predizer de forma adequada a não idealidade da fase líquida de sistemas graxos, sendo então propostas alterações na divisão e/ou parâmetros de interação dos grupos funcionais.

Ressalta-se que Hirata et al. (2013) reajustaram os parâmetros de interação do método UNIFAC para sistemas contendo diferentes óleos vegetais, diferentes ácidos graxos (principalmente oleico e linoleico) e diferentes solventes (principalmente etanol), sendo

possível predizer, assim, o equilíbrio líquido-líquido desses sistemas, uma vez que os parâmetros de Magnussen et al. (1981), reajustados considerando apenas dados do equilíbrio líquido-líquido, não predisseram de forma satisfatória o comportamento desses sistemas. Mais recentemente, Bessa et al (2016) parametrizaram o UNIFAC para a predição do equilíbrio líquido-líquido de sistemas de biodiesel. Esses trabalhos indicam uma tendência no sentido de um esforço de diferentes grupos de pesquisadores com forte atuação nas áreas da tecnologia de lipídeos e da termodinâmica aplicada no aprimoramento de métodos preditivos de menor amplitude de aplicação, mas de maior capacidade preditiva dentro de um determinado nicho de classes de compostos. É claro que, visando melhorar a capacidade preditiva do método UNIFAC, faz-se necessária à coleta de um extenso banco de dados experimentais que contemple os grupos funcionais característicos das classes de compostos encontradas em sistemas graxos, porém não restritos à elas. No capítulo referente à reparametrização do UNIFAC Linear, Dortmund e Modificado realizada nessa tese de doutorado foi utilizado o banco de dados *SPEED Lipids database*, que pertence ao grupo de pesquisa *KT consortium* da DTU. No **Capítulo 5** há mais detalhes sobre o banco de dados.

2.8 CONSISTÊNCIA TERMODINÂMICA

As medidas experimentais de equilíbrio líquido-vapor, por mais precisas que sejam sempre estão sujeitas a desvios, isto é, erros inerentes ao equipamento, à precisão dos instrumentos, a técnicas de medidas, entre outros. Felizmente a termodinâmica oferece relações exatas que podem ser empregadas em testes para se verificar a consistência dos dados. Basicamente, todos os testes originam-se da equação de Gibbs-Duhen (Equação 48) e suas mais diversas formas derivadas (ULTCHAK, 2000).

$$-\frac{H^E}{RT^2}dT + \frac{V^E}{RT^2}dP - \sum_i x_i d\ln\gamma_i = 0 \tag{48}$$

Em geral, os volumes de excesso V^E variam pouco com a pressão, e o segundo termo pode ser negligenciado. No entanto, a variação da entalpia de excesso H^E com a temperatura nem sempre pode ser desprezada. Note que, no caso de dados isobáricos, o segundo termo é necessariamente nulo; já no caso isotérmico, o primeiro termo é necessariamente nulo. Adotando as duas simplificações, a equação de Gibbs-Duhen isotérmica-isobárica é dada por:

$$\sum_i x_i \, d\ln\gamma_i = 0 \tag{49}$$

Os diversos testes de consistência termodinâmica apresentados na literatura consistem em verificar a validade da Equação 49. Contudo poucos podem ser aplicados à dados de ELV do tipo PTx. Kang et al. (2010) abordam sobre quatro diferentes testes de consistência para dados PTxy: teste de área ou de Herington, teste de van Ness, teste diferencial e o teste da diluição infinita. Em adição à esses testes, os autores também apresentam o chamado teste de consistência termodinâmica do composto puro, ou *pure component consistency test* (Equação 50) que pode ser aplicado a dados de ELV tanto do tipo PTxy quanto do tipo PTx. A consistência é checada entre os pontos finais da curva de equilíbrio líquido-vapor, ou seja, frações molares se aproximando de 0 e 1 e os valores das pressões de vapor dos compostos puros. Assim, para dados PTx isobáricos, a equação aplicada tem a forma:

$$p_{bolha}(x_1 \to 1) = P_1^{sat}; \; p_{bolha}(x_1 \to 0) = P_2^{sat} \tag{50}$$

onde, p_{bolha} é a pressão do ponto de bolha da mistura, e P_1^{sat} e P_2^{sat} são as pressões de vapor dos compostos puros calculadas na temperatura do ponto de bolha.

O parâmetro de qualidade associado ao teste (F_{puro}) pode ser calculado pela Equação 51, sendo os valores de Δp_1^0 e Δp_2^0 calculados pela Equação 52.

$$F_{puro} = \frac{2}{100\left(\Delta p_1^0 + \Delta p_2^0\right)}, \; 1 \ge \Delta p_1^0 \; e \; \Delta p_2^0 \tag{51}$$

$$\Delta p_1^0 = \left| \frac{p_{bolha}(x_1 \to 1) - P_1^{sat}}{P_1^{sat}} \right|, \Delta p_2^0 = \left| \frac{p_{bolha}(x_1 \to 0) - P_2^{sat}}{P_2^{sat}} \right| \tag{52}$$

Se a pressão do ponto de bolha da mistura diferir em até 1 % da pressão de vapor para ambos os componentes puros, o valor de $F_{puro} = 1$. Caso contrário, o fator é menor, com o limite inferior de 0,1.

2.9 CONSIDERAÇÕES FINAIS

No **Capítulo 2** foi abordado o referencial teórico dessa tese de doutorado. Todo o embasamento teórico discutido se faz essencial para elucidar a relevância do trabalho desenvolvido: (i) obtenção dos dados de pressão vapor da monononanoina, monolaurina e dinonanoina pela técnica da DSC, (ii) obtenção de dados de equilíbrio liquido-vapor da monocaprilina + ácido láurico (3,42 kPa), monononanoina + monolaurina (2,06 kPa), monononanoina + hexadecanol (2,02 kPa), monolaurina + octadecanol (2,05 kPa), hexadecanol + octadecanol (1,73 kPa), hexadecanol + metil miristato (1,72 kPa) monononanina + tributirina (1,69 kPa), dinonanoina + octacosano (1,70 kPa) pela técnica da DSC, (iii) obtenção de dados de temperatura normal de ebulição da monobutirina, monocaprina, monolaurina, monopalmitina, monoestearina, dicaprilina, dinonanoina e dicaprina pela técnica do TGA, e finalmente, (iv): aprimoramento do parâmetro a_{mn} da parte residual do UNIFAC Linear, Modificado e Dortmund aplicados a tecnologia de lipídios.

Considerando que dados experimentais são a base para etapas de modelagem e simulações de processos, pode-se concluir que o trabalho desenvolvido nessa tese tem aplicabilidade direta nos processos de refino e purificação de biodiesel e bioglicerol, e nas etapas de desacidificação e desodorização de óleos. Além disso, o conhecimento da temperatura normal de ebulição é também crucial para estoque, transporte de produtos e controle de qualidade do biodiesel.

2.10 REFERÊNCIAS

ABRAMS, D. S.; PRAUSNITZ, J. M. Statistical thermodynamics of liquid mixtures: A new expression for the excess Gibbs energy of partly or completely miscible systems. **American Institute of Chemical Engineers Journal**, v. 21, p. 116–128, 1975.

AGÊNCIA NACIONAL DO PETRÓLEO, GÁS NATURAL E BICOMBUSTÍVEIS. RESOLUÇÃO ANP Nº 14, DE 11.5.2012. <www.anp.gov.br/SITE/acao/download/?id=70934>. Acesso em: 27 fev. 2018.

AGÊNCIA NACIONAL DO PETRÓLEO, GÁS NATURAL E BICOMBUSTÍVEIS. ANP. <www.anp.gov.br/?dw=8740>Acesso em: 15 maio 2017.

AGÊNCIA NACIONAL DO PETRÓLEO, GÁS NATURAL E BICOMBUSTÍVEIS. ANP. Agência Nacional de Petróleo, Gás Natural e Biocombustíveis. Disponível em: <http://www.anp.gov.br/?id=472>. Acesso em: 6 maio 2017.

ARANSIOLA, E.F.; OJUMU, T.V.; OYEKOLA, O.O.; MADZIMBAMUTO, T.F.; IKHU-OMOREGBE, D.I.O. A review of current technology for biodiesel production: State of the art. **Biomass and Bioenergy**, v. 61, p.276-297, 2014.

ATABANI, A. E.; SILITONGA, A. S.; BADRUDDIN, I. A.; MAHLIA, T. M. I.; MASJUKI, H. H.; MEKHILEF, S. A comprehensive review on biodiesel as an alternative energy resource and its characteristics. **Renewable and Sustainable Energy Reviews**, v. 16, n. 4, p. 2070-2093, 2012.

AMERICAN SOCIETY FOR TESTING AND MATERIALS. **ASTM E1782**. Standard test method for determining vapor pressure by thermal analysis. Annual Book of ASTM Standards, v. 1402, 2008.

_____. **ASTM E967**. Standard Practice for Temperature Calibration of Differential Scanning Calorimeters and Differential Thermal Analyzers. Annual Book of ASTM Standards, v. 1402, 2008.

BELINATO, G. Estudo da oxidação dos óleos de soja e dendê aditivados com antioxidantes para uso em tratamentos térmicos de têmpera. Campinas, 2010. Dissertação em Ciência e Engenharia de Materiais – USP. 2010.

BELTING, P. C.; GMEHLING, J.; BÖLTS, R.; RAREY, J.; CERIANI, R.; CHIAVONE-FILHO, O.; MEIRELLES, A. J. A. Measurement, correlation and prediction of isothermal vapor–liquid equilibria of different systems containing vegetable oils. **Fluid Phase Equilibria**, v. 395, p.15-25, 2015.

BELTING, P. C.; RAREY, J.; GMEHLING, J.; CERIANI, R.; CHIAVONE-FILHO, O.; MEIRELLES, A. J. A. Measurements of activity coefficients at infinite dilution in vegetable oils and capric acid using the dilutor technique. **Fluid Phase Equilibria**, v. 361, p. 215-222, 2014.

BESSA, L.C.B.A; FERREIRA, M.C.; ABREU, C.R.A.; BATISTA, E.A.C.; MEIRELLES, A.J.A. A new UNIFAC parameterization for the prediction of liquid-liquid equilibrium of biodiesel systems. **Fluid Phase Equilibria**, v. 425, p. 98-107, 2016.

BUTROW, A. B.; SEYLER, R. J. Vapor pressure by DSC: extending ASTM E 1782 below 5 kPa. **Thermochimica Acta**, v. 402, n. 1–2, 3 p. 145-152, 2003.

CABALLERO, V.; BAUTISTA, F.M.; CAMPELO, J.M.; LUNA, D.. MARINAS J.M.; ROMERO, A.A. HIDALGO, J.M.; LUQUE, R.; MACARIO, A.; GIORDANO, G. Sustainable preparation of a novel glycerol-free biofuel by using pig pancreatic lipase: Partial 1.3-regiospecific alcoholysis of sunflower oil. **Process Biochemistry**, v. 44, p. 44:334–342, 2009.

CALERO, J.; LUNA, D.; SANCHO, E.D.; LUNA, C.; BAUTISTA, F. M.; ROMERO, A. A.; POSADILLO, A.; BERBEL, J.; VERDUGO-ESCAMILLA, C. An overview on glycerol-free processes for the production of renewable liquid biofuels. applicable in diesel engines. **Renewable and Sustainable Energy Reviews**, v. 42, p.1437-1452, 2015

CAHOON, E. B.; SCHMID, K. M. Metabolic engineering of the content and fatty acid composition of vegetable oils, In: BOHNERT, H. J.; NGUYEN, H.; LEWIS, N. G. (Eds).

Advances in Plant Biochemistry and Molecular Biology, Pergamon, v. 1, Elsevier Ltd, p. 161-200, 2008.

CASSERINO, M.; BLEVINS, D. R.; SANDERS, R. N. An improved method for measuring vapor pressure by DSC with automated pressure control I. **Thermochimica Acta**, v. 284, p. 145-152, 1996.

CARARETO, N. D. D.; COSTA, M. C.; ROLEMBERG, M. P.; KRÄHENBÜHL, M. A.;. MEIRELLES, A. J. A. The solid–liquid phase diagrams of binary mixtures of even saturated fatty alcohols. **Fluid Phase Equilibria**, v. 303, n. 2, p. 191.e1-191.e8, 2011.

CERIANI, R.; GANI, R.; LIU, Y.A. Prediction of vapor pressure and heats of vaporization of edible oil/fat compounds by group contribution. **Fluid Phase Equilibria**, v. 337, p. 53-59, 2013.

CERIANI, R.; GONÇALVES, C.; COUTINHO, J. Prediction of viscosities of fatty compounds and biodiesel by group contribution. **Energy and Fuels**, v. 25, p. 3712-3717, 2011.

COELHO, R. A. Equilíbrio líquido-vapor de sistemas binários envolvendo ésteres etílicos do biodiesel (glicerol ou água) + etanol: dados experimentais e modelagem termodinâmica. 2011. Tese de doutorado. Paraná. Dissertação de mestrado – UFP. 2011.

COMPTON, D. L.; VERMILLION, K. E.; LASZLO, J. A. Acyl migration kinetics of 2-monoacylglycerols from soybean oil via 1h nmr. **Journal of the American Oil Chemists Society**, v. 84, p.343-348, 2007.

CONTRERAS, M. D.; GIRELA, F.; PARERA, A. The perfection of a method for the determination of the temperature/vapour-pressure function of liquids by differential scanning calorimetry. **Thermochimica Acta**, v. 219, n. 27, p. 167-172, 1993.

CORRÊA, L. F. F.; RIBEIRO, L. F. J.; CERIANI, R. Levantamento de dados experimentais de equilíbrio líquido-vapor e líquido-líquido de sistemas graxos e biodiesel. Congresso Brasileiro de Engenharia Química XX. 2014. Florianópolis. **Anais**... COBEQ, 2014.

COSTA, M. C.; ROLEMBERG, M. P.; SANTOS, A. O.; CARDOSO, L. P.; KRÄHENBÜHL, M. A.; Meirelles, A. J. A. Solid−liquid equilibrium of tristearin with refined rice bran and palm oils. **Journal of Chemical and Engineering Data** , v.55, n. 11, p. 5078-5082, 2010.

CUNICO, L.P.; HUKKERIKAR, A.S.; CERIANI, R.; SARUP, B.; GANI, R. Molecular structure-based methods of property prediction in application to lipids: A review and refinement. **Fluid Phase Equilibria**, v. 357, p. 2– 18, 2013.

CUNICO, L. P.; DAMACENO, D.S.; MATRICARDE FALLEIRO, R.M.; SARUP, B.; ABILDSKOV, J.; CERIANI, R.; GANI, R. Vapour liquid equilibria of monocaprylin plus palmitic acid or methyl stearate at P = (1.20 and 2.50) kPa by using DSC technique, **Journal of Chemical Thermodynamics**, v. 91 p. 108 – 115, 2015.

DAMACENO, S. D. Determinação de dados de temperatura de ebulição de acilgliceróis parciais e tocoferol por calorimetria diferencial exploratória. 2014. Dissertação de mestrado. Faculdade de Engenharia Química – UNICAMP. 2014.

DAMACENO, S. D.; MATRICARDE FALLEIRO, R. M.; KRÄHENBÜHL, M. A; MEIRELLES, A. J. A.; CERIANI. R. Boiling Points of Short-Chain Partial Acylglycerols and Tocopherols at Low Pressures by the Differential Scanning Calorimetry Technique. **Journal of Chemical and Engineering Data**, v. 59, n. 5, p. 1515-1520, 2014.

DE GREYT, W. D., KELLENS, M. Deodorization In: SHAHIDI, F. (Org.) **Bailey's Industrial Oil & Fat Products**, 6 ed., v.5, New York, John Wiley & Son, p.341-383, 2005.

DEVI, P.; ZHANG, H.; DAMSTRUP, M. L.; GUO, Z.; ZHANG, L.; LUE, B. M.; XU, X. Enzymatic synthesis of designer lipids. **Oleagineux - Corps Gras - Lipides**, v. 15, n. 3, p. 189–195, 2008.

FREDENSLUND, A., JONES, R. L.; PRAUSNITZ, J. M. Group-contribution estimation of activity coefficients in nonideal liquid mixtures. **American Institute of Chemical Engineers Journal**, v. 21, p. 1086–1099, 1975.

GOODRUM, J. W. e GELLER, D. P. Rapid thermogravimetric measurements of boiling points and vapor pressure of satured medium- and long-chain triglycerides. **Bioresource Technology**, v. 84, p.75-80, 2002.

GHOSH, S.; REDDY, B. P.; NAGARAJAN, K.; KUMAR, K. C. H. Experimental investigations and thermodynamic modelling of KCl–LiCl–UCl3 system. **Calphad**, v. 45, p. 11-26, 2014.

GUNSTONE, F. D. Enzymes as biocatalysts in the modification of natural lipids: Review. **Journal of the Science of Food and Agriculture**, v. 79, n.12, p. 1535–1549, 1999.

GUNSTONE, F. D.; HARWOOD, J. L.; PADLEY, F. B. **The Lipid Handbook**. 2. ed. London: Chapman & Hall, 1994. 316p.

GUNSTONE, F. D.; HERSLÖF, B. G. **Lipid Glossary 2**. 12. ed. Bridgewater, United Kingdom: The Oily Press, 2000, 247p.

GUNSTONE, F. D. Vegetable Oils. In: SHAHIDI, F. (Org.). **Bailey's Industrial Oil & Fat Products**, 6ª ed. v.1, John Wiley & Son, New York, p. 213-267, 2005.

GOODRUM, J.W.; E.M. SIESEL. Thermogravimetric analysis for boiling points and vapour pressure. **The Journal of Thermal Analysis and Calorimetry**, v. 46, p. 1251-1258, 1996.

HALA, E.; PICK, J.; FRIED, V.; VILIM, O. Vapour-liquid equilibrium, 1 ed, Standart, Pergamon press, New York, 1958.

HANSEN, H. K.; COTO, B.;KUHLMANN, B. UNIFAC with linearly temperature-dependent group-interaction parameters. Internal report. 1992.

HIRATA, G. F.; ABREU, C. R. A.; BESSA, L. C. B. A.; FERREIRA, M. C; BATISTA, E. A. C.; MEIRELLES, A. J. A. Liquid–liquid equilibrium of fatty systems: A new approach for adjusting UNIFAC interaction parameters. **Fluid Phase Equilibria**. v. 360, p. 379-391, 2013.

KANG, J. W.; DIKY, V.; CHIRICO, R. D.; MAGEE, J. W.; MUZNY, C. D.; ABDULAGATOV, I.; KAZAKOV, A.F.; FRENKEL, M. Quality Assessment Algorithm for Vapor−Liquid Equilibrium Data. **Journal of Chemical and Engineering Data**, v. 55, p. 3631−3640, 2010.

KANG, J. W.; DIKY, V.; J.W.; FRENKEL, M. New modified UNIFAC parameters using critically evaluated phase equilibrium data**. Fluid Phase Equilibria.** v. 388, p. 128–141, 2015.

KITTS, D. Toxicity and Safety of Fats and Oils In: HUI, Y.H. (Org.) **Bailey's Industrial Oil & Fat Products**, 5 ed., v.1, New York, John Wiley & Son, p.215-280, 1996.

KIKIC, I., ALESSI, P., RASMUSSEN, P., REDENSLUND, A. On the combinatorial part of the UNIFAC and UNIQUAC models. **The Canadian Journal of Chemical Engineering.** v.58, p.253-258, 1980.

KNOTHE, G.; GERPEN, J. V.; KRAHL, J. **The Biodiesel Handbook**. 1 ed. Champaign, AOCS Publishing, 2005.

KNOTHE, G.; STEIDLEY, K. Lubricity of components of biodiesel and petrodiesel: the origin of biodiesel lubricity. **Energy and Fuels**, v. 19, p. 1192–1200, 2005.

KROG N. **Lipid Technologies and Applications**. In: Food Emulsifiers. New York: Marcel Dekker Inc., 1997: 521-34.

KROG, N.; SPARSO, F. V. **Food emulsifiers and their chemical and physical properties**. In: Food Emulsions. ed. S. E. Friberg. Marcel Dekker Inc.. New York. 1990. p. 127–180.

LARSEN, B.; RASMUSSEN, P.; FREDENSLUND, A. **A modified UNIFAC group-contribution model for prediction of phase equilibria and heats of mixing. Ind.** Eng. Chem. Res.. v. 26, p. 2274 – 2286, 1987.

MATRICARDE FALLEIRO, R. M.; MEIRELLES, A. J. A.; KRÄHENBÜHL, Experimental determination of the (vapor-liquid) equilibrium data of binary mixtures of fatty acids by

differential scanning calorimetry. **The Journal of Chemical Thermodynamics**, v. 42, n. 1, p. 70-77, 2010.

MATRICARDE FALLEIRO, R. M. Determinação experimental de dados de equilíbrio líquido-vapor de misturas binárias de componentes de ésteres graxos etílicos e ácidos graxos através da Calorimetria Exploratória Diferencial. Campinas, 2012. Tese de doutorado – FEQ UNICAMP. 2012.

MATRICARDE FALLEIRO, R. M. Determinação experimental de dados de equilíbrio líquido-vapor de misturas binárias de componentes de óleos vegetais através da Calorimetria Diferencial Exploratória. Campinas, 2009. Dissertação de mestrado – FEQ UNICAMP. 2009.

MATRICARDE FALLEIRO, R. M.; SILVA, L. Y. A.; MEIRELLES, A. J. A.; KRÄHENBÜHL, M. A. Vapor pressure data for fatty acids obtained using an adaptation of the DSC technique. **Thermochimica Acta**, v. 547, n. 10, p. 6-12, 2012.

MATRICARDE FALLEIRO, R. M.; SILVA, L. Y. A.; MEIRELLES, A. J. A.; KRÄHENBÜHL, M. A. A influência da taxa de aquecimento na determinação de dados de equilíbrio líquido-vapor pela calorimetria exploratória diferencial. In: Congresso Brasileiro de Termodinâmica Aplicada VI. 2011. Salvador. **Anais**... CBtermo, 2011.

MATSUOKA, M.; OZAWA, R. Determination of solid-liquid phase equilibria of binary organic systems by differential scanning calorimetry. **Journal of crystal growth**, v. 96, n. 3, p. 596-604, 1989.

MARRERO, J.; GANI, R. Group-contribution based estimation of pure component properties. **Fluid Phase Equilibria**, v. 183-184, p. 183-208, 2001.

MIRANDA, J. Criação do banco de dados, simulação e análise energética do processo de produção do biodiesel de soja, mamona e pinhão manso, Campinas, 2011. Dissertação de mestrado - FEQ UNICAMP. 2011.

NDIAYE, P. M. Equilíbrio de fases de óleos vegetais e de biodiesel em co2, propano e n-butano. 2004. Rio de Janeiro. Tese de Doutorado - Tecnologia de Processos Químicos e Bioquímicos da Escola de Química, UFRJ. 2004.

O'BRIEN, R.D. **Fats and Oils: Formulating and Processing for Applications**. Technomic, 1998.

OLIVEIRA, M. Óleo para o biodiesel. Pesquisa Fapesp, 2016.

PARENTE, E. J. S. **Biodiesel: Uma aventura tecnológica num país engraçado**. Fortaleza: Unigráfica, 2003.

POLING, B.E.; PRAUSNITZ, J.M.; O'CONNELL, J.P. **The properties of gases and liquids**. 5. ed., McGraw-Hill, 2004.

PRAUSNITZ, J. M.; LINCHTENTHALER, N. L. e GOMES DE AZEVEDO, E. **Molecular thermodynamics of fluid-phase equilibria**. 3 ed. Upper Saddle River: Prentice Hall, 1999.

RASLAVIČIUS, L.; STRIŪGAS, N.; FELNERIS, M.; SKVORČINSKIENĖ, R.; MIKNIUS. L. Thermal characterization of P. moriformis oil and biodiesel. **Fuel**, v. 220, p. 140-150, 2018

REDDY, K. R.; KUMAR, D. B. K.; RAO, G. S.; SRI, P. B. S.; BEGUM, Z.; RAMBABU, C. Ebulliometric determination of vapor–liquid equilibria for binary mixtures of NMP with some cyclic compounds. **Journal of Molecular Liquids**, v. 193, p. 220-225, 2014.

RENON, H.; PRAUSNITZ, J. M. Local compositions in thermodynamic excess functions for liquid mixtures. **American Institute of Chemical Engineers Journal**,v. 14, p. 135–144, 1968.

SANTANDER, C.M.G.; RUEDA, S.M.G.R.; DA SILVA, N.L.; DE CAMARGO, C.L.; THEO, G.; KIECKBUSCH, T.G.; MACIEL. M.R.W. Measurements of normal boiling points of fatty acid ethyl esters and triacylglycerols by thermogravimetric analysis. **Fuel**, v. 92, p. 158-161, 2012.

SEYLER, R.J. Parameters affecting the determination of vapor pressure by differential thermal methods. **Thermochimica Acta**, v. 17, n. 2, p. 129-136, 1976.

SILVA, L. Y. A. Determinação Experimental de Dados de Pressão de Vapor e de Equilíbrio Líquido-Vapor de Componentes do Biodiesel Através da Calorimetria Exploratória Diferencial. Campinas, 2012. Tese de Doutorado - Faculdade de Engenharia Química, UNICAMP. 2010.

SILVA, L. Y. A.; FALLEIRO, R. M. M.; MEIRELLES, A. J. A.; KRÄHENBÜHL, M. A. Vapor–liquid equilibrium of fatty acid ethyl esters determined using DSC. **Thermochimica Acta**, v. 512, n.1–2, p. 178-182, 2011.

SIITSMAN, C.; KAMENEV, I.; OJA, V. Vapor pressure data of nicotine, anabasine and cotinine using differential scanning calorimetry, **Thermochimica Acta**, v. 595, p. 35 –42, 2014.

SIITSMAN, C.; OJA, V. Extension of the DSC method to measuring vapor pressures of narrow boiling range oil cuts, **Thermochimica Acta**, v. 622, p. 31 – 37, 2015.

SIITSMAN, C.; OJA, V. Application of a DSC based vapor pressure method for examining the extent of ideality in associating binary mixtures with narrow boiling range oil cuts as a mixture component, **Thermochimica Acta**, v. 637, p. 24 – 30, 2016.

SMITH, J. M.; VAN NESS, H. C.; ABBOTT, M. M. **Introdução à termodinâmica da engenharia química**. 7 ed. Rio de Janeiro: LTC, 2007.

SKOOG, D. A.; HOLLER, F. J.; NIEMAN, T. A. **Principles of Instrumental Analysis**. Saunders Brace College Publishers, 1992.

TA. Termo Analysis Instrumental. 2000. Disponível em: <http://www1.chm.colostate.edu/Files/CIFDSC/dsc2000.pdf>. Acesso em: 16 jan. 2017.

TANG, G.; DING, H.; HOU, J.; XU, S. Isobaric vapor–liquid equilibrium for binary system of ethyl myristate+ethyl palmitate at 0.5, 1.0 and 1.5kPa. **Fluid Phase Equilibria**, v. 347, p. 8-14, 2013.

TRONI, K.L Aprimoramento da técnica da calorimetria exploratória diferencial na determinação de dados de temperatura de ebulição de compostos puros e misturas binárias. Tese de doutorado. UNICAMP. Campinas. 2016.

TRONI. K. L.; DAMACENO. D. S.; CERIANI. R. Improving a variation of the DSC technique for measuring the boiling points of pure compounds at low pressures. **Journal of Chemical Thermodynamics**. v. 100, p. 191-197, 2016.

ULTCHAK, F. S. Equilíbrio líquido-v apor dos sistemas n-butanol *i* dimetilmalonato ou dietilmalonato às pressões de 100 e 200 mmhg. 2000. Campinas. Dissertação de mestrado. FEQ – UNICAMP. 2000.

UNITED STATES DEPARTMENT OF AGRICULTURE (USDA). Disponível em http://www.fas.usda.gov/commodities/oilseeds, Acesso em: jan. 2018.

VERDUGO, C.; LUQUE, R.; LUNA, D. J.; HIDALGO, M.; POSADILLO, A.; SANCHO, E.; RODRÍGUEZ, S.; FERREIRA-DÍAS, S.; BAUTISTA, F. M.; ROMERO, A. A. A comprehensive study of reaction parameters in the enzymatic production of novel biofuels integrating glycerol into their composition. **Bioresource Technology**, v. 101, p. 657–6662, 2010.

WEIDLICH, U.; GMEHLING, J. A modified UNIFAC model. 1. Prediction of VLE, hE, and .gamma..infin. **Industrial & Engineering Chemistry Research,** v. 26, p. 1372–1381, 1987.

WILSON, G. M. Vapor-Liquid Equilibrium. XI. A New Expression for the Excess Free Energy of Mixing. **Journal of the American Chemical Society**, v. 86, n. 2, p. 127-130, 1964.

YOUNG, P. H.; SCHALL, C. A. Cycloalkane solubility determination through differential scanning calorimetry. **Thermochimica Acta**, v. 367–368, p. 387-392, 2001.

CAPÍTULO 3

EFFECT OF HEATING RATES ON THE ACCURACY OF DSC TECHNIQUE FOR DETERMINING BOILING POINTS AT SUBATMOSPHERICAL PRESSURE

Daniela S. Damaceno, Roberta Ceriani

Publicado no CBTermo 2015 – Congresso Brasileiro de Termodinâmica Aplicada

Abstract: Differential Scanning Calorimetry (DSC) technique is extensively used to determine physical properties of a variety of materials. Over the years, such technique has been spread due to its potential of obtaining boiling point data of both pure compounds and mixtures accurately. As any other analytical method, this technique has also been related to several constraints, such as pressure/temperature range, sample size and purity, vessel configuration, and heating rate that must be optimized. To achieve a better understanding of the effect of heating rates on the accuracy of the DSC technique for measuring boiling points at subatmospheric pressure (4.85 ± 0.05) kPa, a reasonable range of heating rates was selected in this work (5 to 25 K/min in a 5 K/min interval). Sample size was fixed at $4 – 5$ mg and sample vessel was a hermetic aluminum crucible (pan + lid) with a pinhole of 0.8 mm on the lid and a tungsten carbide ball with 1.0 mm placed over it. Three different classes of compounds were considered in this study: n-paraffin (n-eicosane), fatty alcohol (1-octadecanol) and fatty acid (palmitic acid). The results showed that the optimum heating rate, i.e., the one that provided the best agreement with boiling points in the literature was 25 K/min for all compounds.

Keywords: boiling point, vapor pressure, DSC technique, heating rate.

3.1 INTRODUCTION

Physical properties of chemical compounds are essential for the design and analysis of processes in the chemical, pharmaceutical, food and related industries. In order to meet the growing demand for accuracy in the description of the behavior of a wide range of chemical structures of complex molecules and mixtures, to determine novel experimental data of some physical properties becomes crucial. Vapor pressures (boiling points) figure among the most relevant thermophysical properties involved in modeling and simulation of separation processes, such as distillation and stripping. The ebulliometer method is widely used for determining vapor pressure or vapor-liquid equilibrium data, mainly because of its reliability. In the meantime, this technique requires at least 30 mL to operate, which is an unfordable amount for costly compounds. In this context, Differential Scanning Calorimetry (DSC) technique has been used for determining thermophysical properties of pure compounds and their mixtures, especially for expensive and low-volatile substances (Matricarde Faleiro et al., 2010; Damaceno et al., 2014), as fatty compounds and vitamins. However, as pointed out in the literature (Seyler, 1979; Contreras et al., 1993; Brozena, 2013; Siitsman et al., 2014), several parameters, such as pressure/temperature range, sample size, purity and vessel, and heating rate, affect its accuracy.

Since the introduction of DSC in the early 1960s the scan rate used for most DSC measurements has been 10 K/min. This rate has provided good data for many applications, though sometimes slower rates have been employed to give improved resolution of events, e.g. polymorphism, or time for a reaction to occur (Gabbott, 2008). In 1996, the first ASTM to vapor pressure data was stablished, whose data suggests a heating rate of 5 K/min (ASTM E1782, 2008). Seyler (1979) recommended a heating rate between 10 – 20 K/min, based on the results obtained for the boiling point of water (18 g/mol) at ambient pressure, and Contreras et al. (1993) suggested a heating rate between 10 – 15 K/min for determining boiling points of isopropyl palmitate (298.5 g/mol) at 0.7 – 3.2 kPa. Occasionally, faster rates of 20 K/min may have been used, but occasionally anything faster than this may have caused inaccuracy of temperature measurement or thermal gradients across a sample that would make the data meaningless. However, this has been proved not to be the case (Gabbott, 2008; Matricarde Faleiro et al., 2010; Matricarde Faleiro et al., 2012; Damaceno et al., 2014). The use of a heating rate of 25 K/min has been reported in several successful studies (Matricarde Faleiro et al., 2011; Silva et al., 2011; Matricarde Faleiro et al., 2012; Damaceno et al., 2014). Siistman and Oja

(2015) affirm that the standardized method has rarely been fully applied and works were concerned in the optimization of operating conditions for a chosen application. In this context, this work aims at evaluating the effect of different heating rates on the accuracy of the DSC technique in the determination of the boiling point of n-eicosane (282.55 g/mol), a n-paraffin, and 1-octadecanol (270.49 g/mol), a fatty alcohol, at a selected subatmospheric pressure (4.85 $\pm$ 0.05) kPa. The heating rates tested in this study were 5, 10, 15, 20 and 25 K/min, taking into account data from previous works (Seyler, 1979; Contreras et al., 1993; Matricarde Faleiro et al., 2011) and the standardized method (ASTM E1782, 2008). As an additional evaluation, the optimal heating rate of a fatty acid (palmitic acid – 256.42 g/mol) was also tested.

3.2 METHODOLOGY

3.2.1 Materials

All the reagents used in this study are listed in Table 3.1, as well as their corresponding names, molecular weights (MW), CAS numbers, purity and manufacturer. All chemicals were used without any further purification step.

Table 3. 1. List of reagents

Compound	MW (g/mol)	CAS number	Purity (%)	Manufacturer
n-tetradecane	198.39	629-59-4	>99	Sigma-Aldrich
n-eicosane	282.55	112-95-8	>99	Sigma-Aldrich
1-octadecanol	270.49	112-92-5	>99	Sigma-Aldrich
n-hexadecanoic acid (palmitic acid)	256.42	57-10-3	>99	Nu-chek prep.

Hermetic aluminum crucibles (pans + lids) for DSC were purchased from TA Instruments. A pinhole (diameter of 0.8 mm) was made on each lid using a system consisting of a fixed assembly, mandrel and drills. A small tungsten carbide ball with a diameter of 1.0 mm was placed over the pinhole (Matricarde Faleiro et al., 2012; Damaceno et al., 2014).

3.2.2 Apparatus

The apparatus consists of a differential scanning calorimeter (DSC) Model Q20 - TA Instruments connected to a vacuum system as follows: a trap to pressurize the vacuum line, a ballast tank to avoid pressure oscillations, a micrometer valve to adjust the pressure, a digital

pressure gauge (Model Rücken RMD) with 0.25 % full scale accuracy, and a vacuum pump (Model RV5 – Edwards). Computer software was used to prompt the DSC and record data of each run. A microbalance (Model C-33 - Thermo Scientific), micropipettes of 0.5 – 10 µL (Model Research – Eppendorf), and a press (Model Tzero press - TA Instruments) were used for sample preparation.

3.2.3   Calibration

It was executed following ASTM E967 (2008) guidelines for calibrate baseline, cell constant, and temperature with indium and zinc as standard materials (TA Instruments). Indium and zinc fusion points were in accordance with the International Temperature Scale (1990): (429.7 and 692.7) K, respectively.

3.2.4   Experimental Procedure

The experimental procedure was based on ASTM E1782 (2008) guidelines. Each run was obtained using a pair of hermetic sealed crucibles, one empty (reference) and the other with a sample of 4 – 5 milligrams of reagent. The absolute pressure inside the cell was measured by a digital pressure gauge, calibrated with n-tetradecane. At the end of the procedure, the pressure cell was restored to ambient conditions. A pressure of (4.85 ± 0.05) kPa was established for all runs. The heating rates tested were 5, 10, 15, 20 and 25 K/min with n-eicosane and 1-octadecanol. After determining the optimal heating rate, the palmitic acid was used to re-check the accuracy of the optimal point. The experimental boiling point was determined according to the extrapolated onset temperature calculated from the thermal curves generated by the DSC technique.

3.2.5   Analysis

The boiling point of each compound can be determined by the onset temperature that is an intersection of the tangents of the baseline and with the endothermic peak (Figure 3.1). The mean value of triplicates of the extrapolated onset temperature measured at each heating rate was compared to the calculated boiling point for n-eicosane (503.26 K), 1-octadecanol (510.69 K) and palmitic acid (514.47 K) at 4.85 kPa by using the NIST ThermoData Engine (version 5.0). The signal change (peak size in W/g) (Figure 3.1) was also

determined, which is a variable that depends on the heating rate and other factors, like sample size and chemical properties, but mostly by heating rate.

Figure 3. 1. DSC endotherm: red line (—) to indicate the onset point (●) and blue lines (—) to indicate the signal change
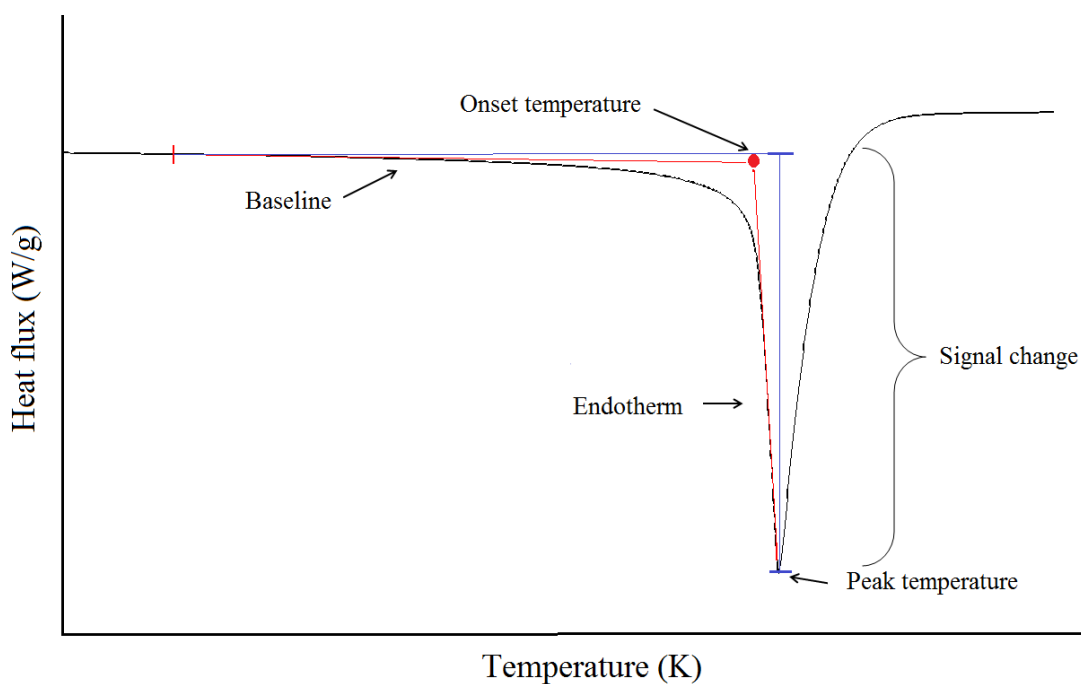
3.3 RESULTS AND DISCUSSION

Figure 3.2 and Figure 3.3 show the endotherms of n-eicosane and 1-octadecanol, respectively, obtained at (4.85 ± 0.05) kPa considering different heating rates. As one can see, despite the peak size (signal change), which is directly related to the heat flow rates to the sample, there is no effect on the smoothness of the baseline prior and after the vaporization event.
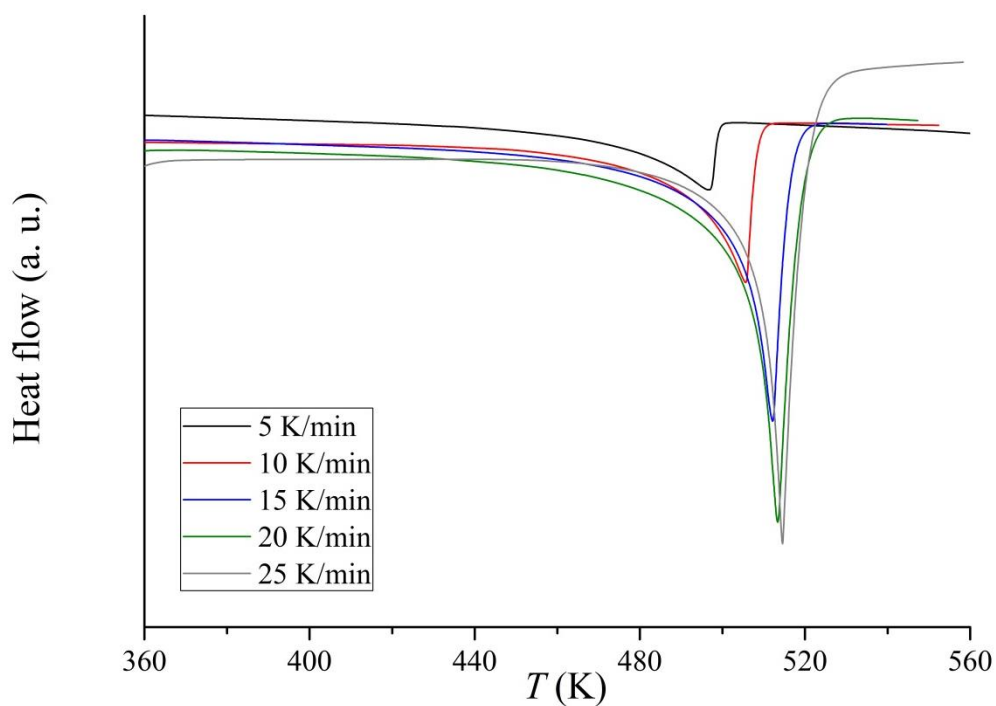
Table 3. 2 Boiling points (T as temperature in K) of each heating rate (K/min) with their respective deviation, uncertainty and signal change (W/g)

Heating rate (K/min)	Compound	Signal Change (W/g)	T (K)	u (K)	[a]D (K)	[b]RD (%)
5		1.0	487.16	0.58	-16.11	-3.31
10		4.0	498.27	0.46	-5.00	-1.00
15	n-eicosane	5.2	500.72	0.42	-2.55	-0.51
20		7.4	501.23	0.36	-2.03	-0.40
25		8.3	504.24	0.10	0.98	0.19
5		1.4	477.42	0.70	-33.27	-6.97
10		2.8	492.13	0.38	-18.56	-3.77
15	1-octadecanol	5.4	504.36	0.50	-6.33	-1.25
20		7.4	506.21	0.37	-4.48	-0.88
25		8.8	509.11	0.37	-1.58	-0.31

[a] D (deviation) = T_{exp}-T_{calc}
[b] RD (relative deviation) = 100.(T_{exp}-T_{calc})/T_{exp}
[*]Standard uncertainty is u (p) = 0.05 kPa

Clearly, the more suitable heating rates for n-eicosane and 1-octadecanol were between 20 and 25 K/min. For n-eicosane the experimental boiling point was higher than the calculated value at the heating rate of 25 K/min while for 1-octadecanol, the experimental boiling point was always lower than the calculated temperature, and the lowest deviation was given at 25 K/min. Average relative deviations for both compounds at 25K/min were around 0.25 %, which is relatively small considering other heating rates and similar works (Matricarde Falleiro et al. 2011). In general, the results showed that the best heating rate was 25 K/min, for which the absolute deviations were not higher than 1.6 K, which is a very reasonable deviation for such experimental procedure (Damaceno et al., 2014), confirming other findings (Matricarde Falleiro et al., 2011).

Another parameter that is directly affected by the heating rate is the signal change (W/g). As Figures 3.2 and 3.3, and Table 3.2 show lower heating rates cause events of pre-vaporization that make the results (boiling points) unclear and affect both the signal change and the baseline rectilinearity prior to endothermic peak, as revealed in this work.

For further comparisons, palmitic acid (n-hexadecanoid acid) was used as a reagent at the optimum heating rate (25 K/min). The deviation (T_{exp}-T_{calc}) in the boiling point temperature was found to be -1.73 K, for T_{exp} = (512.74 ± 0.19) K, which is very similar to the range of deviations (in absolute values) found in the experiments with n-eicosane and 1-octadodecanol. To illustrate the use of the optimum heating rate of 25 K/min, Figure 3.4. show

a comparison among the endotherms obtained for n-eicosane, 1-octadecanol and palmitic acid at (4.85 ± 0.05) kPa, which have pursued characteristics.

Figure 3. 4. Endotherms at 25 K/min for n-eicosane, 1-octadecanol and palmitic acid.
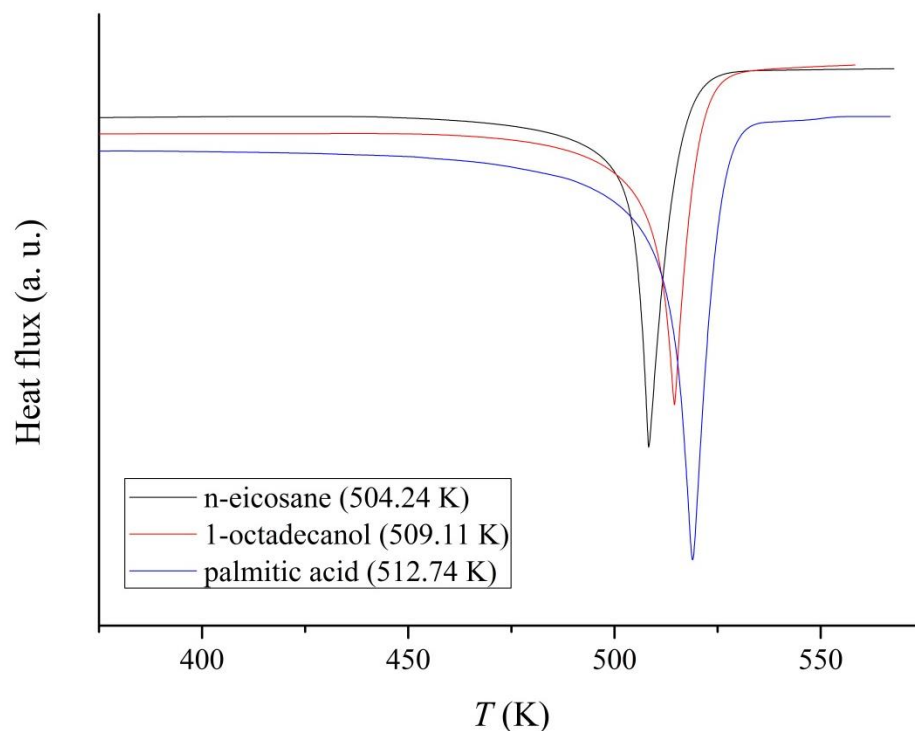
3.4 CONCLUSIONS

In this study, DSC technique proved to be a very useful technique to determine boiling points of selected pure compounds (n-eicosane, 1-octadecanol and palmitic acid) with high accuracy.

The main results of this study indicate that the optimal heating rate is around 25 K/min for all the compounds, and most likely, for all the classes of compounds considered.

3.5 ACKNOWLEDGMENTS

3.6 REFERENCES

ASTM E967. Standard practice for temperature calibration of differential scanning calorimeters and differential thermal analyzers. *Annual Book of ASTM Standards*, v. 1402, 2008.

ASTM E1782. Standard test method for determining vapor pressure by thermal analysis. *Annual Book of ASTM Standards*, v. 1402, 2008.

Brozena, A. Vapor pressure of 1-octanol below 5kPa using DSC. Thermochim. Acta, 561(2013),72-76.

Contreras, M.D.; Girela, F.; Parera, A. The perfection of a method for the determination of the temperature/vapour-pressure function of liquids by differential scanning calorimetry. *Thermochim. Acta*, 219 (1993), 167-172.

Damaceno, D.S.; Matricarde Falleiro, R.M.; Krähenbühl, M.A; Meirelles, A.J.A.; Ceriani. R. Boiling points of short-chain partial acylglycerols and tocopherols at low pressures by the differential scanning calorimetry technique. *J. Chem. Eng. Data*, 59 (2014), 1515-1520.

Gabbott, P. *Principles and Applications of Thermal Analysis.* Blackwell Publishing Ltd, New Delhi, 2008.

Matricarde Falleiro, R.M.; Meirelles, A.J.A.; Krähenbühl, M.A. Experimental determination of the (vapor+liquid) equilibrium data of binary mixtures of fatty acids by differential scanning calorimetry. *J.Chem. Thermodynam.*, 42(2010), 70-77.

Matricarde Falleiro, R.M.; Silva, L.Y.A.; Meirelles, A.J.A.; Krähenbühl, M. A. A influência da taxa de aquecimento na determinação de dados de equilíbrio líquido-vapor pela calorimetria exploratória diferencial. *VI Congresso Brasileiro de Termodinâmica Aplicada*, CBTERMO 2011, BA, Salvador, 2011.

Matricarde Falleiro, R.M.; Silva, L.Y.A.; Meirelles, A.J.A.; Krähenbühl, M.A. Vapor pressure data for fatty acids obtained using an adaptation of the DSC technique. *Thermochim. Acta*, 547 (2012), 6-12.

Preston-Thomas, H. *The International Temperature Scale of 1990 (ITS-90)*. 1990

Seyler, R.J. Parameters affecting the determination of vapor pressure by differential thermal methods. *Thermochim. Acta*, 17 (1976), 129-136.

Siitsman, C.; Kamenev, I.; Oja, V. Vapor pressure data of nicotine, anabasine and cotinine using differential scanning calorimetry. *Thermochim. Acta*, 595(2014), 35-42.

Siitsman, C; Oja, V. (in press). Extension of the DSC method to measuring vapor pressures of narrow boiling range oil cuts. *Thermochim. Acta*, 2015

.

Silva, L.Y.A.; Matricarde Falleiro, R.M.; Meirelles, A.J.A.; Krähenbühl, M.A. Vapor–liquid equilibrium of fatty acid ethyl esters determined using DSC. *Thermochim. Acta*, 512 (2011), 178-182.

CAPÍTULO 4

VAPOR-LIQUID EQUILIBRIA OF MONOACYLGLYCEROL + MONOACYLGLYCEROL OR ALCOHOL OR FATTY ACID AT SUBATMOSPHERIC PRESSURES

Daniela S. Damaceno and Roberta Ceriani

Abstract: Partial acylglycerols are relevant minor compounds in the oil/fat industry. They represent important role to the food industry, as surface-active agents and emulsifiers. Also, they are present in the biodiesel production and its separation steps. Therefore, knowledge of their thermophysical properties are critical to product and process design. Considering that, this study aims at determining by the DSC technique novel boiling point data for two monoacylglycerols, namely, monononanoin and monolaurin at subatmospheric pressures, and for four binary fatty mixtures at selected pressures (PTx data), i.e. lauric acid + monocaprylin (3.42 kPa), monononanoin + monolaurin (2.06 kPa), monononanoin + hexadecanol (2.02 kPa), and monolaurin + octadecanol (2.05 kPa). As expected, the system with two monoacylglycerols (monononanoin + monolaurin) showed an ideal behavior. On the other hand, the other systems presented non-ideal behavior. Experimental data were successfully regressed by the Wilson, the NRTL and the UNIQUAC models. Predictive capacity of the UNIFAC method and its different versions was tested, and results indicated that improvements concerning lipid systems are still necessary. These improvements must be based on diverse and qualified experimental data.

Keywords: monoacylglycerols, oils/fats, biodiesel, boiling points, vapor-liquid equilibrium, DSC technique

4.1 INTRODUCTION

Monoacylglycerols (MAGs) are important amphiphilic compounds frequently found in food, drugs, cosmetics and biofuel industries [1-3]. In the food industry, MAGs are used as surface-active agents and emulsifiers [4]. For instance, monoolein has become one of the most important lipid for drug delivery, emulsion stabilization and protein crystallization [5]. In the biofuel industry, MAGs are intermediate products of biodiesel production in the transesterification reaction, and are related to its technical quality. Technical standard for biodiesel called total glycerin (up to 0.25 %) comprise glycerol, MAGs, di-, and triacylglycerols, which should be removed in the purification steps of biodiesel production. Nevertheless, investigations have shown that MAGs enhance biodiesel lubricity [6-7], and play a significant effect on its cold flow properties, as cloud point, freezing point and cold filter plugging point [8]. More recently [8-10], glycerin-free biofuels, such as Ecodiesel®, have been reported in the literature, in which glycerol remains in the form of MAGs avoiding production of bioglycerol (waste). It is important to highlight that MAGs are normally a mixture of their isomers (1-MAG or 2-MAG) and ratio between isomers may vary depending on temperature, fatty acid composition, crystal form and time of storage [11-13]. In this way, knowledge of thermophysical properties and phase equilibria of such compounds is essential for both deacidification/deodorization of oil/fats, and purification of biodiesel and bioglycerin, in order to avoid neutral oil loss and improve quality of products.

Searching in the recent literature (2014 – 2017) for vapor-liquid equilibrium data of fatty systems, i.e., binary, ternary and quaternary mixtures in which, at least, one compound is a fatty compound (for example, fatty acid, acylglycerol, fatty alcohol, or fatty ester), or can be represented by a pseudo fatty compound (for example, oil/fat, biodiesel), 1,522 experimental data points were found. These data represent almost one-third of all experimental data published from 1900 to 2013 for VLE of fatty systems [14], and highlight an increasing interest of scientific community in biofuel and oil/fat industry related materials. It was only in 2015 [15] that a set of binary VLE data of a fatty system containing a MAG was reported in the literature. The authors used the differential scanning calorimetry (DSC) technique, which was very advantageous in this case, mainly due to the use of very small samples (4 – 5) mg (cost-effective). Prior to that, Damaceno et al. [1] reported boiling points for four partial acylglycerols, monocaprylin (MW = 218.2 g·mol^{-1}), monocaprin (MW = 246.3 g·mol^{-1}),

dicaprylin (MW = 344.5 g·mol^{-1}), and dicaprin (MW = 400.6 g·mol^{-1}), at selected pressures (1.0 kPa up to 13.2 kPa) using also the DSC technique.

Taking into account that oils/fats, biodiesel and bioglycerol are, intrinsically, multicomponent mixtures, the use of group contribution concept for their thermodynamic modeling is very suitable for computer simulation and optimization. However, as pointed out by Kang et al. [16], insufficient (or inconsistent) sets of experimental data represent a major drawback for improving predictive capacity of group contribution methods. In fact, they require large amounts of experimental data for adjusting group-interaction parameters, and frequently incoherent predictions are generated for molecules with large number or diversity of functional groups, and for those in which functional groups appear in unusual ways. Note that MAG molecule is a very good example of both situations. It has –OH and –COO– groups, and it is not linear. In fact, it has the same bone structure of glycerol (–CH$_2$–CH–CH$_2$–), which characterizes acylglycerols.

Following directions of previous works [1, 15, 17], this work contributes with novel boiling point data for two MAGs, monononanoin (MW = 232.3 g·mol^{-1}) and monolaurin (MW = 274.4 g·mol^{-1}) at five different pressures, and for four binary mixtures at selected pressures (PTx data), i.e., lauric acid (MW = 200.3 g·mol^{-1}) + monocaprylin (MW = 218.3 g·mol^{-1}), monononanoin (MW = 232.3 g·mol^{-1}) + monolaurin (MW = 200.3 g·mol^{-1}), monononanoin (MW = 232.3 g·mol^{-1}) + hexadecanol (MW = 242.4 g·mol^{-1}), and monolaurin (MW = 200.3 g·mol^{-1}) + octadecanol (MW = 270.5 g·mol^{-1}), measured with the DSC technique. Vapor pressure data were correlated with Antoine equation. The Wilson [18], the NRTL [19] and the UNIQUAC [20] models together with the ideal model (Raoult's law) were applied for correlating experimental PTx data after checking their thermodynamic consistency using the pure component consistency test [21]. In addition, the original UNIFAC [22], the Lyngby UNIFAC [23], the Dortmund UNIFAC [24], the UNIFAC modified by Cunico et al. [15], and the NIST modified UNIFAC [16] methods were applied and their predictive capacities were compared.

4.2 METHODOLOGY

4.2.1 Materials

Table 4.1 lists all the reagents used in this study (CAS Registry numbers, solubility, purities in mass fraction, IUPAC names and suppliers). All chemicals were used without any further purification step. Water contents to n-tetradecane, lauric acid, hexadecanol and octadecanol are reported in the literature [25]. To the best of our knowledge, none experimental data of water content is available for monoacylglycerols in the open literature. Therefore, monocaprylin and monononanoin were analyzed by using the Karl Fischer Coulometric (Metrohm – model 831) titration method [26] for obtaining water content. Water content is not reported for monolaurin, which is solid at analytical conditions.

Table 4.1. List of compounds with their respective IUPAC name, CAS Registry No., water content, supplier and purity

Compound	IUPAC name	CAS Registry No.	Supplier	Water content	Purity (mass fraction)
n-tetradecane	Tetradecane	629-59-4	Sigma-Aldrich	6.944×10^{-6} g.L^{-1} at 25 ºC [25]	0.99
monocaprylin[a]	2,3-dihydroxypropyl octanoate	502-54-5	Nu-Chek Prep, Inc.	0.26 % (w/w)[b]	0.99
monononanoin[a]	2,3-dihydroxypropyl nonanoate	3065-51-8	Nu-Chek Prep, Inc.	0.16 % (w/w)[c]	0.99
monolaurin[a]	2,3-dihydroxypropyl dodecanoate	142-18-7	Nu-Chek Prep, Inc.	-	0.99
lauric acid	dodecanoic acid	143-07-7	Sigma-Aldrich	1.700×10^{-3} g.L^{-1} at 25 ºC [25]	0.99
hexadecanol	hexadecan-1-ol	36653-82-4	Sigma-Aldrich	8.001×10^{-6} g.L^{-1} at 34 ºC [25]	0.99
octadecanol	octadecan-1-ol	112-92-5	Sigma-Aldrich	1.082×10^{-6} g.L^{-1} at 34 ºC [25]	0.99

[a] Thin layer chromatography showed only the monoacylglycerol moiety present according to the certificate of analysis provided by Nu-Chek Prep, Inc. [b,c] Experimental data given by the Karl Fischer Coulometric titration method [26]. Standard uncertainties are 0.01% (w/w) for monocaprylin and 0.02 % (w/w) for monononanoin.

4.2.2 Experimental procedure

Apparatus and experimental procedure used in this work can be reached referring to Troni et al. [17]. In general, it consists of a variation of the DSC technique based on ASTM E1782-14 guidelines [27]. Therefore, each assay was obtained using a pair of hermetic sealed crucibles, one empty (reference) and the other with a sample of 4 – 5 mg of reagent, with a pinhole on the lid, and a tungsten carbide ball over it (acting as a pressure relief valve). Pressure cell was subjected to a heating rate of 25 K min^{-1}, from 300 to 700 K at constant pressure. It

should be highlighted that the heating rate and sample mass were selected based on Troni et al. [17], and are within their reported optimal conditions. Absolute pressure inside the cell was measured by a pressure gauge calibrated with n-tetradecane. After each run, pressure cell was restored to ambient conditions. For each pressure, boiling point was determined from the extrapolated onset temperature calculated from the thermal curves generated by the DSC software. Previous works used the same methodology to collect experimental data for pure compounds and binary mixtures [1, 15, 17, 28-30].

4.2.3 Boiling points of pure compounds

For the six fatty compounds listed in Table 4.1, regressed coefficients for the Wagner equation (Eq. S1) (Supplementary material – Table 4S.1) were obtained for lauric acid, hexadecanol and octadecanol in the NIST Thermo Data Engine v. 5.0 – Aspen Plus v. 8.4, while regressed coefficients of the Antoine equation (Eq. 1) are reported for monocaprylin by Damaceno et al. [1]. To the best of our knowledge none experimental data of boiling points are reported for monononanoin or monolaurin in the open literature. So, five novel boiling points for both MAGs at subatmospherical pressure range are provided in this work. For describing the relation between vapor pressure p (kPa) and temperature T (K), the Antoine equation was (Eq. 1) selected:

$$\ln p = A + \frac{B}{T + C} \tag{1}$$

where p is the vapor pressure in kPa, T is the boiling point in K, and A, B and C are parameters fitted by least-squares regression using the Curve Fitting Toolbox 3.5.1 in MatLab R2015a (The MathWorks Inc.).

4.2.4 Sample preparation of binary mixtures

It followed the procedure described by Cunico et al. [15]. In brief, known amounts (g) of pure components were mixed in an analytical balance (Model AS220 – Radwag) comprising 0.2 g of the binary mixture, approximately. After that, samples were mixed in a vortex shaker (Marconi MA 162) for a few minutes to ensure they were completely homogenous. Eleven molar fractions of the more volatile compound (x_1) ranging from 0 to 1 in

0.1 intervals were prepared. Then, microsamples of 4 mg to 5 mg were obtained from each binary mixture using micropipettes of 0.5 – 10 µL (Model Research – Eppendorf), and weighted in a microanalytical balance (Model C-33 – Thermo Scientific).

4.2.5 Thermodynamic consistency test for isobaric PTx data

Following Cunico et al. [15], thermodynamic consistency of measure VLE data was achieved using the pure component consistency test described by Kang et al. [21] (Eq. 2). It is carried out between the end points of the VLE curve, i.e., molar fractions of 0 and 1. Data validation is conducted by comparing the experimental boiling points of the pure compounds with data in the literature. Thus, for isobaric PTx data (Eq. 2 and Eq. 3):

$$p_{bubble}\left(x_1 \to 1\right) = p_1, p_{buble}\left(x_1 \to 0\right) = p_2 \tag{2}$$

$$\Delta p_1 = \left| \frac{p_{bubble}\left(x_1 \to 1\right) - p_1}{p_1} \right|, \Delta p_2 = \left| \frac{p_{bubble}\left(x_1 \to 0\right) - p_2}{p_2} \right| \tag{3}$$

where p_{bubble} is the pressure of the bubble point of the mixture, p_1 and p_2 are the pure component vapor pressures, and Δp_1 and Δp_2 must have lower limits of 1.

The variation of Van Ness consistency test ($Q_{test,1}$) was also applied to check the quality of the PTx data [15,21]. This Van Ness test is not based on the Gibbs-Duhem equation, because PTxy data are required. Bubble-point is calculated by molecular models, as Wilson, NRTL or UNIQUAC. In this work, the UNIQUAC model was used. The quality factor of Van Ness was carried out by Eq. 4.

$$Q_{test,1} = \frac{1}{1 + ARD\left(\%\right)} \tag{4}$$

where ARD (%) is the average relative deviation between the measured boiling point and the estimated boiling point by the thermodynamic molecular model, UNIQUAC.

4.3 RESULTS AND DISCUSSION

4.3.1 Vapor pressure of pure components

Experimental boiling points of monononanoin (1.26 – 6.87) kPa and monolaurin (0.69 – 2.77) kPa are listed in Table 4.2., with their respective standard uncertainties. Regressed values for constants *A*, *B* and *C* (Eq. 1) are listed in Table 4.3. Average absolute deviations (AAD), average relative deviations (ARD) and coefficients of determination (R^2) are also given. In general, very suitable values were found for these statistical tests.

Table 4.2. Experimental data for boiling points *T* (K) at the selected pressures *p* (kPa) for monononanoin and monolaurin, with their respective standard uncertainties u(*T*)

Monononanoin			Monolaurin		
p (kPa)[a]	*T* (K)	*u* (*T*) (K)	*p* (kPa)[b]	*T* (K)	*u* (*T*) (K)
1.26	471.02	0.47	0.69	482.77	0.49
2.39	486.08	0.36	1.15	493.97	0.26
3.01	492.07	0.65	2.07	505.19	0.44
4.74	502.29	0.70	2.41	509.07	0.06
6.87	509.88	0.46	2.77	510.94	0.69

[a] Standard uncertainty $u(p) \leq 0.04$ kPa; [b] Standard uncertainty $u(p) \leq 0.03$ kPa.

Table 4.3. Regressed constants for Antoine equation

Compounds	*A*	*B*	*C*	[a]AAD (K)	[b]ARD (%)	[c]R²
Monononanoin	67.86	-98500	983.8	0.666	0.136	0.9983
Monolaurin	42.39	-35300	342.0	0.436	0.088	0.9969

[a] $AAD = \sum_{i=1}^{n} \frac{1}{n} \cdot \left| T_{exp} - T_{calc} \right|_i$, [b] $ARD = \sum_{i=1}^{n} \frac{1}{n} \cdot \left[100 \cdot \frac{\left| T_{exp} - T_{calc} \right|}{T_{exp}} \right]$, where T_{exp} is experimental temperature in K and T_{calc} is calculated temperature in K, [c]R² = Coefficient of determination (*R – square*)

For comparison purposes, Figure 4.1. shows linearized relations of vapor pressures *p* (kPa) as a function of temperature *T* (K) for a homologous series of MAGs: monocaprylin (MAG of octanoic acid [1]), monononanoin (MAG of nonanoic acid), monocaprin (MAG of decanoic acid [1]) and monolaurin (MAG of dodecanoic acid). As expected, at the same pressure, monocaprylin, the lightest compound (218.2 g·mol⁻¹), boils at the lowest temperature, followed by monononanoin (232.3 g·mol⁻¹), monocaprin (246.3 g·mol⁻¹) and monolaurin (274.4 g·mol⁻¹) which presents the highest molecular weight in this series.

Figure 4.1. Linearized relation for vapor pressure ln (p) in kPa as function of temperature T^{-1} (K^{-1}) for monoacylglycerols. This work: monononanoin ($\triangle$) and monolaurin ($\diamondsuit$). Damaceno et al. [1]: monocaprylin (■) and monocaprin (●)
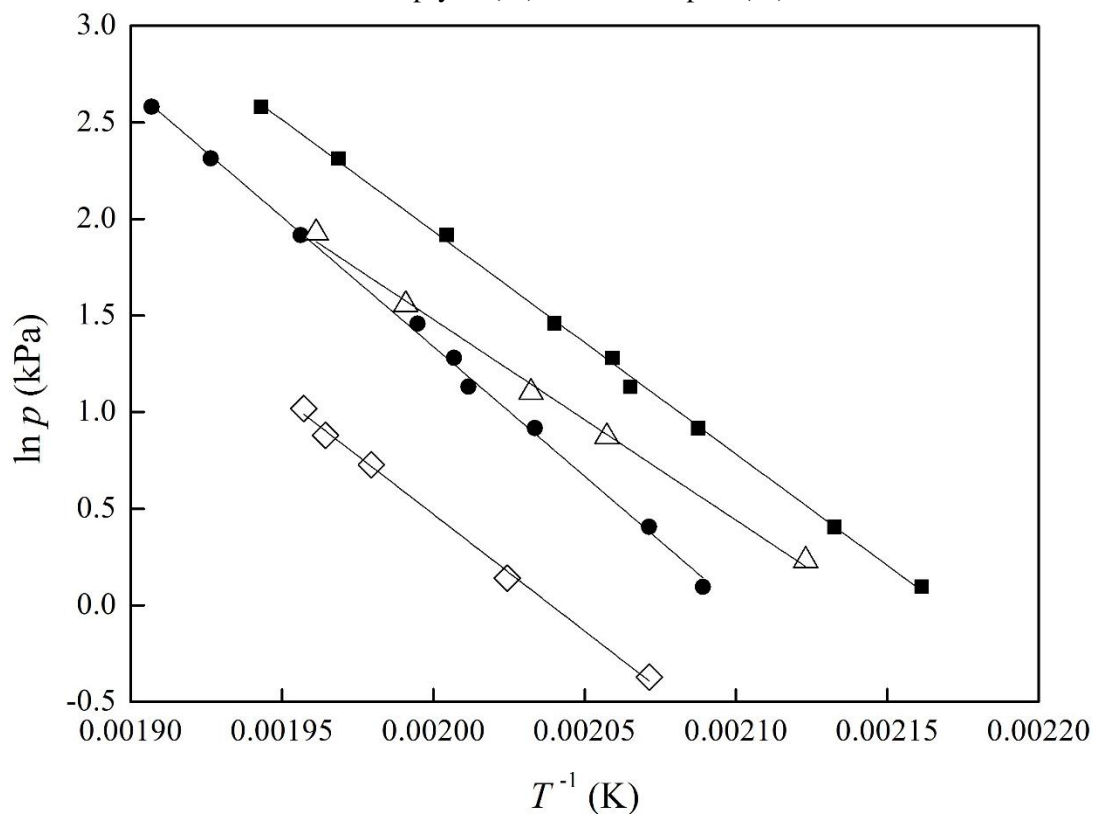
4.3.2 VLE of binary systems

Novel VLE data were obtained in this work for four fatty binary systems: lauric acid + monocaprylin (system 1) at p = 3.42 kPa with $u(p)$ = 0.06 kPa, monononanoin + monolaurin (system 2) at p = 2.06 kPa with $u(p)$ = 0.04 kPa , hexadecanol + monononanoin (system 3) at p = 2.02 kPa with $u(p)$ = 0.06 kPa, and octadecanol + monolaurin (system 4) p = 2.05 kPa with $u(p)$ = 0.04 kPa). Table 4.4. presents molar fractions of the more volatile compound (x_1), boiling points (T), and pressures (p) for each of the four binary systems considered. Before performing regression of binary parameters of molecular models for activity coefficients, the pure component consistency test was applied, and results are presented in Table 4.5. This test evaluated the end point of the mixture, and the results must be lower than 1. As one can see in Table 4.5, none of the end points present higher values than 0.03 kPa, which shows a satisfactory result to the consistency test applied. The variation of Van Ness consistency test ($Q_{test,1}$) results are is Table 6. The quality factor for all investigated systems

were higher than $Q_{test,1} \geq 0.911$, which indicates a high quality factor for our experimental values.

Experimental PTx data (T, p and x_1) were regressed using the Wilson [18], the NRTL [19] and the UNIQUAC [20] models with software *Aspen Plus* V8.4 for activity coefficients, considering modified Raoult's law (ideal vapor phase). Vapor pressures of lauric acid, hexadecanol and octadecanol were calculated with the Wagner equation. Regressed coefficients for the Antoine equation (Eq. 1) are available for monocaprylin in Damaceno et al. [1], and for monononanoin and monolaurin in Table 4.3. Binary interaction parameters of each model are given in Table 4.8a. and Table 4.8b.

In Figure 4.2. – 4.7., experimental data and estimated values using the UNIQUAC model, which provided lowest deviations in terms of AAD and ARD (see Table 4.8), can be observed. Very similar VLE curves were found for the Wilson and NRTL models (not shown). In general, very good correlations were achieved for all three models tested. Table 4.7 also presents values for activity coefficients γ_1 and γ_2 calculated with molecular models. Binary systems 1 (Figure 4.2.), 3 (Figure 4.5.) and 4 (Figure 4.6.) presented non-ideal behaviors and an azeotrope ($x_1 \approx 0.9$), corroborating with previous works. In fact, Cunico et al. [15] observed azeotropes for monocaprylin + palmitic acid and methyl stearate at 1.20 kPa and 2.50 kPa, respectively. In addition, Constantinescu and Wichterle [31] found azeotropes for the binary systems ethanol + methyl propanoate and ethanol + methyl butanoate at 326.30 K and 346.30 K, and Ortega et al. [32] for methyl butanoate + ethanol or 1-propanol at 101.32 kPa. On the other hand, system 2 showed an ideal behavior, as expected for binary mixtures of homologous series compounds [33].

Predicted values of boiling points obtained using different versions of the UNIFAC method, original UNIFAC [22], Lyngby [23], Dortmund [24], original UNIFAC modified by Cunico et al. [15] and NIST modified [16], are represented in Table 4.9a and Table4.9b, with their respective deviations (AAD and ARD). In general, original UNIFAC [22] and UNIFAC modified by Cunico et al. [15] presented similar results for all systems. However, original UNIFAC showed lower deviations. Both the UNIFAC Lyngby and UNIFAC Dortmund always overestimated boiling points, i.e., they underestimated nonidealities of liquid mixtures (calculated activity coefficients were lower than experimental ones). The NIST modified UNIFAC presented a better prediction when compared with the other modified UNIFACs (Dortmund and Lyngby). With no exception, the original UNIFAC showed the lowest deviations for all fatty systems studied.

For comparison purposes, Figure 4.3 brings VLE of palmitic acid + monocaprylin at 2.50 kPa given by Cunico et al. [15] together with experimental data for system 1 (lauric acid + monocaprylin). Lauric acid is a fatty acid more volatile (MW = 200.3 g·mol^{-1}) than palmitic acid (MW = 256.4 g·mol^{-1}). Figure 4.3 clearly shows non-ideal behavior with negative deviation of Raoult's law for both systems. Comparing predictions given by original UNIFAC and UNIFAC modified by Cunico et al. [15], both overestimated expected temperatures for the majority of molar fractions for the more volatile system (system 1). Though, the original UNIFAC underestimates temperatures for palmitic acid + monocaprylin. This variance of results could be associated to the length of carbons of lauric acid and palmitic acid, also, the difference in the pressure. It is of note that experimental data for palmitic acid + monocaprylin were used in the regression of UNIFAC binary group interaction parameters given by Cunico et al. [15]. In this sense, a high-quality experimental data are still necessary for VLE of partial acylglycerols.

Table 4.4. Experimental PTx data for binary systems: lauric acid (x_1) + monocaprylin, monononanoin (x_1) + monolaurin, hexadecanol (x_1) + monononanoin and octadecanol (x_1) + monolaurin.

lauric acid + monocaprylin (system 1)			monononanoin + monolaurin (system 2)			hexadecanol + monononanoin (system 3)			octadecanol + monolaurin (system 4)		
x_1	T (K)	u (T) (K)	x_1	T (K)	u (T) (K)	x_1	T (K)	u (T) (K)	x_1	T (K)	u (T) (K)
1.0000	465.77	0.43	1.0000	483.61	0.24	1.0000	465.70	0.46	1.0000	487.25	0.65
0.9009	464.91	0.85	0.9090	484.01	0.22	0.8769	466.61	0.41	0.9008	486.77	0.16
0.8002	464.73	0.51	0.8011	484.90	0.41	0.7862	466.08	0.76	0.7995	488.16	0.46
0.7019	464.69	0.35	0.7019	486.89	0.33	0.6848	466.73	0.50	0.7015	489.10	0.51
0.5974	465.19	0.71	0.5924	488.11	0.45	0.5762	467.90	0.27	0.6056	490.03	0.46
0.5054	466.19	0.56	0.4976	490.51	0.60	0.4936	468.38	0.76	0.5050	491.13	0.47
0.4015	468.21	0.59	0.3986	493.63	0.47	0.3872	469.74	0.81	0.4000	491.39	0.41
0.3018	471.25	0.66	0.3014	496.04	0.63	0.2814	471.42	0.63	0.3151	494.24	0.47
0.2021	476.19	0.42	0.2005	498.88	0.65	0.1993	475.78	0.54	0.2062	496.87	0.34
0.1008	480.43	0.69	0.1002	501.14	0.12	0.0992	479.76	0.49	0.1110	501.35	0.08
0.0000	484.73	0.18	0.0000	505.19	0.44	0.0000	483.61	0.24	0.0000	505.19	0.44
p (kPa)	3.42			2.06			2.02			2.05	
u (p) (kPa)	0.06			0.04			0.06			0.04	

Standard uncertainty u(x_1) = 0.0005, calculated by error propagation.

Table 4.5. Experimental data points ($x_1 = 1$ and $x_1 = 0$) and the calculated variables to apply the pure component consistency test

Compounds	T (K)	Measured values	p (kPa)	Reference	p (kPa)	Δp_1^0, Δp_2^0
lauric acid	465.77	$x_1 = 1$	3.42	NIST TDE Aspen plus v. 8.4	3.51	0.03
hexadecanol	465.70	$x_1 = 1$	2.02	NIST TDE Aspen plus v. 8.4	1.96	0.03
octadecanol	487.25	$x_1 = 1$	2.05	NIST TDE Aspen plus v. 8.4	2.00	0.02
monocaprylin	484.73	$x_1 = 0$	3.42	[1]	3.35	0.02
monononanoin	483.61	$x_1 = 0$	2.02	This work	2.09	0.03
monononanoin	483.61	$x_1 = 1$	2.06	This work	2.09	0.01
monolaurin	505.19	$x_1 = 0$	2.05	This work	2.06	0.00
monolaurin	505.19	$x_1 = 0$	2.06	This work	2.06	0.00

Δp_1^0, Δp_2^0: for calculation to these variables refer to Eq. 3

Table 4.6. Quality factor ($Q_{test,1}$) calculated by the variation of the Van Ness consistency test

Binary system	p (kPa)	$Q_{test,1}$
lauric acid + monocaprylin	3.42	0.921
monononanoin + monolaurin	2.06	0.959
hexadecanol + monononanoin	2.02	0.911
octadecanol + monolaurin	2.05	0.923

Table 4.7. Binary interaction parameters for the Wilson, NRTL and UNIQUAC models

Binary system	Wilson[a]		NRTL[a]			UNIQUAC[a]	
	b_{12} (J·mol^{-1})	b_{21}(J·mol^{-1})	b_{12} (J·mol^{-1})	b_{21} (J·mol^{-1})	α_{12}	b_{12} (J·mol^{-1})	b_{21} (J·mol^{-1})
lauric acid + monocaprylin	1281.89	-10935.49	11124.64	-2812.47	0.3	-4282.35	2348.76
monononanoin + monolaurin	3755.37	-10763.73	10053.02	-5042.23	0.3	-3739.51	2469.20
hexadecanol + monononanoin	1042.31	-6267.64	7714.72	-2407.93	0.3	-3319.09	2054.48
octadecanol + monolaurin	1128.77	-6496.92	7538.77	-2347.62	0.3	-2989.57	1943.42

[a] Equations for the activity coefficient models Wilson (S3 – S4), NRTL (S7 – S12) and UNIQUAC (S13 – S16) are in Supplementary material.

Table 4.8a. Estimated VLE data of four binary systems lauric acid + monocaprylin (1), monononanoin + monolaurin (2), hexadecanol + monononanoin (3), octadecanol + monolaurin (4) using the Wilson, NRTL and UNIQUAC models with their respective deviations

lauric acid + monocaprylin						monononanoin + monolaurin					
Molar fraction (x_1)	Wilson	NRTL	UNIQUAC	γ_1	γ_2	Molar fraction (x_1)	Wilson	NRTL	UNIQUAC	γ_1	γ_2
	T (K)	T (K)	T (K)				T (K)	T (K)	T (K)		
1.0000	465.17	465.17	465.17			1.000	483.36	483.36	483.36		
0.9009	464.03	464.14	464.13	1.04	3.04	0.9090	483.87	484.12	484.05	1.02	1.37
0.8002	463.99	464.12	464.08	1.14	1.83	0.8011	485.05	485.21	485.13	1.05	1.10
0.7019	464.59	464.49	464.47	1.24	1.39	0.7019	486.69	486.65	486.63	1.09	1.00
0.5974	465.50	465.31	465.33	1.35	1.19	0.5924	488.36	488.28	488.30	1.11	0.97
0.5054	466.70	466.49	466.52	1.44	1.09	0.4976	490.63	490.53	490.57	1.11	0.96
0.4015	468.73	468.58	468.61	1.53	1.04	0.3986	493.42	493.35	493.39	1.10	0.97
0.3018	471.54	471.54	471.56	1.59	1.01	0.3014	495.88	495.87	495.89	1.08	0.98
0.2021	475.55	475.77	475.74	1.64	1.00	0.2005	498.71	498.81	498.78	1.05	0.99
0.1008	479.73	480.06	479.98	1.66	1.00	0.1002	501.69	501.85	501.78	1.01	1.00
0.000	485.12	485.12	485.12			0.000	505.19	505.19	505.19		
AAD (K)	0.52	0.40	0.43				0.20	0.21	0.20		
ARD (%)	0.110	0.086	0.091				0.041	0.043	0.040		

$$AAD = \sum_{i=1}^{n} \frac{1}{n} \cdot \left| T_{exp} - T_{calc} \right|_i . \quad ARD = \sum_{i=1}^{n} \frac{1}{n} \cdot \left[100 \cdot \frac{\left| T_{exp} - T_{calc} \right|}{T_{exp}} \right]$$. where T_{exp} is experimental temperature in K and T_{calc} is calculated temperature in K. γ_1 and γ_2 are calculated by NRTL model.

Table 4.8b. Estimated VLE data of four binary systems lauric acid + monocaprylin (1), monononanoin + monolaurin (2), hexadecanol + monononanoin (3), octadecanol + monolaurin (4) using the Wilson, NRTL and UNIQUAC models with their respective deviations

hexadecanol + monononanoin						octadecanol + monolaurin					
Molar fraction (x_1)	Wilson T (K)	NRTL T (K)	UNIQUAC T (K)	γ_1	γ_2	Molar fraction (x_1)	Wilson T (K)	NRTL T (K)	UNIQUAC T (K)	γ_1	γ_2
1	466.34	466.34	466.34			1.0000	487.87	487.87	487.87		
0.8769	465.88	465.87	465.87	1.03	2.05	0.9008	487.55	487.63	487.63	1.04	2.13
0.7862	466.12	466.10	466.10	1.09	1.60	0.7995	488.27	488.31	488.30	1.12	1.40
0.6848	466.72	466.70	466.69	1.16	1.32	0.7015	488.97	488.98	488.98	1.20	1.13
0.5762	467.77	467.78	467.77	1.25	1.16	0.6056	489.90	489.87	489.87	1.26	1.03
0.4936	468.61	468.66	468.65	1.31	1.10	0.5050	491.12	491.08	491.09	1.30	0.99
0.3872	470.20	470.35	470.34	1.39	1.05	0.4000	492.12	492.06	492.07	1.31	0.98
0.2814	472.29	472.29	472.30	1.46	1.02	0.3151	494.46	494.43	494.44	1.31	0.98
0.1993	475.23	475.67	475.69	1.53	1.01	0.2062	497.25	497.26	497.27	1.29	0.99
0.0992	478.69	479.13	479.16	1.58	1.00	0.1110	500.67	500.72	500.72	1.25	1.00
0.000	482.95	482.95	482.95			0.0000	505.09	505.09	505.09		
AAD (K)	0.49	0.43	0.43				0.35	0.36	0.36		
ARD (%)	0.103	0.091	0.090				0.072	0.073	0.073		

$$AAD = \sum_{i=1}^{n} \frac{1}{n} \cdot \left| T_{exp} - T_{calc} \right|_i . \quad ARD = \sum_{i=1}^{n} \frac{1}{n} \cdot \left[100 \cdot \frac{\left| T_{exp} - T_{calc} \right|}{T_{exp}} \right]$$. where T_{exp} is experimental temperature in K and T_{calc} is calculated temperature in K. γ_1 and γ_2 are calculated by NRTL model.

Table 4.9a. Predicted VLE data for the follow binary systems: lauric acid + monocaprylin. monononanoin + monolaurin. hexadecanol + monononanoin. octadecanol + monolaurin using UNIFAC methods (Original. Lyngby. Dortmund and modified by Cunico et al. [15]) with thei

	lauric acid + monocaprylin						monononanoin + monolaurin				
	UNIFAC methods						UNIFAC methods				
Mole fraction (x_1)	Original [22]	Lyngby [23]	Dortmund [24]	Modified by Cunico et al [15]	NIST-modified [16]	Mole fraction (x_1)	Original [22]	Lyngby [23]	Dortmund [24]	Modified by Cunico et al [15]	NIST-modified [16]
	T (K)	T (K)	T (K)	T (K)	T (K)		T (K)	T (K)	T (K)	T (K)	T (K)
1.0000	465.14	465.14	465.14	465.14	465.14	1.0000	483.34	483.34	483.34	483.34	483.34
0.9009	465.71	466.99	467.38	465.95	465.89	0.9090	484.68	484.71	484.71	484.70	484.69
0.8002	466.46	469.15	470.18	466.87	466.73	0.8011	486.37	486.45	486.44	486.41	486.39
0.7019	467.31	471.52	473.38	467.87	467.64	0.7019	488.03	488.16	488.15	488.10	488.06
0.5974	468.39	474.26	477.11	469.07	468.73	0.5924	490.01	490.20	490.18	490.11	490.05
0.5054	469.55	476.72	480.35	470.31	469.83	0.4976	491.87	492.10	492.08	491.99	491.93
0.4015	471.18	479.35	483.39	471.98	471.33	0.3986	493.99	494.26	494.23	494.13	494.05
0.3018	473.22	481.52	485.23	474.00	473.17	0.3014	496.27	496.55	496.53	496.41	496.34
0.2021	475.95	483.19	485.93	476.62	475.64	0.2005	498.91	499.17	499.14	499.03	498.96
0.1008	479.76	484.39	485.76	480.19	479.30	0.1002	501.74	501.92	501.90	501.93	501.89
0.0000	485.13	485.13	485.13	485.13	485.13	0.0000	505.19	505.19	505.19	505.19	505.19
AAD (K)	1.69	6.03	8.0	2.06	1.90		0.73	0.88	0.87	0.82	0.77
ARD (%)	0.361	1.286	1.705	0.439	0.405		0.150	0.182	0.177	0.166	0.160

$$AAD = \sum_{i=1}^{n} \frac{1}{n} \cdot |T_{exp} - T_{calc}|_i \cdot ARD = \sum_{i=1}^{n} \frac{1}{n} \cdot \left[100 \cdot \frac{|T_{exp} - T_{calc}|}{T_{exp}} \right]$$. where T_{exp} is experimental temperature in K

Table 4.9b. Predicted VLE data for the follow binary systems: lauric acid + monocaprylin. monononanoin + monolaurin. hexadecanol + monononanoin. octadecanol + monolaurin using UNIFAC methods (Original. Lyngby. Dortmund and modified by Cunico et al. [15]) with the

	hexadecanol + monononanoin						octadecanol + monolaurin				
	UNIFAC methods						UNIFAC methods				
Mole fraction (x_1)	Original [22]	Lyngby [23]	Dortmund [24]	Modified by Cunico et al [15]	NIST-modified [16]	Mole fraction (x_1)	Original [22]	Lyngby [23]	Dortmund [24]	Modified by Cunico et al [15]	NIST-modified [16]
	T (K)	T (K)	T (K)	T (K)	T (K)		T (K)	T (K)	T (K)	T (K)	T (K)
1.0000	466.37	466.37	466.37	466.37	466.37	1.0000	487.91	487.91	487.91	487.91	487.92
0.8769	466.14	467.40	467.31	466.94	466.76	0.9008	488.22	489.19	489.06	488.73	488.65
0.7862	466.33	468.27	468.11	467.50	467.23	0.7995	488.76	490.59	490.31	489.65	489.51
0.6848	466.76	469.39	469.14	468.26	467.92	0.7015	489.45	492.04	491.62	490.64	490.44
0.5762	467.44	470.77	470.41	469.24	468.84	0.6056	490.26	493.59	493.00	491.72	491.48
0.4936	468.11	471.98	471.53	470.14	469.69	0.5050	491.30	495.33	494.60	493.00	492.74
0.3872	469.27	473.79	473.23	471.56	471.07	0.4000	492.67	497.29	496.44	494.57	494.30
0.2814	470.96	475.89	475.26	473.40	472.91	0.3151	494.11	498.95	498.06	496.08	495.82
0.1993	472.90	477.75	477.13	475.28	474.83	0.2062	496.60	501.12	500.34	498.45	498.24
0.0992	476.59	480.25	479.81	478.40	478.08	0.1110	499.71	503.00	502.47	501.09	500.95
0.0000	482.91	482.91	482.91	482.91	482.91	0.0000	505.09	505.09	505.09	505.09	505.09
AAD (K)	0.89	2.22	1.90	1.22	1.05		0.63	2.98	2.51	1.47	1.33
ARD (%)	0.188	0.472	0.403	0.259	0.222		0.127	0.608	0.512	0.299	0.273

$$AAD = \sum_{i=1}^{n} \frac{1}{n} \cdot \left| T_{exp} - T_{calc} \right|_i . \quad ARD = \sum_{i=1}^{n} \frac{1}{n} \cdot \left[100 \cdot \frac{\left| T_{exp} - T_{calc} \right|}{T_{exp}} \right]$$. where T_{exp} is experimental temperature in K

Figure 4.2. Vapor-liquid equilibria of lauric acid + monocaprylin. Experimental data from this work
(●). The UNIQUAC model for liquid phase (-○-) and vapor phase (○). Predictions for liquid phase
of different versions of the UNIFAC method: Original (--), Lyngby (-·-), Dortmund (···), modified by
Cunico et al. [15] (-··-) and NIST modified (—).
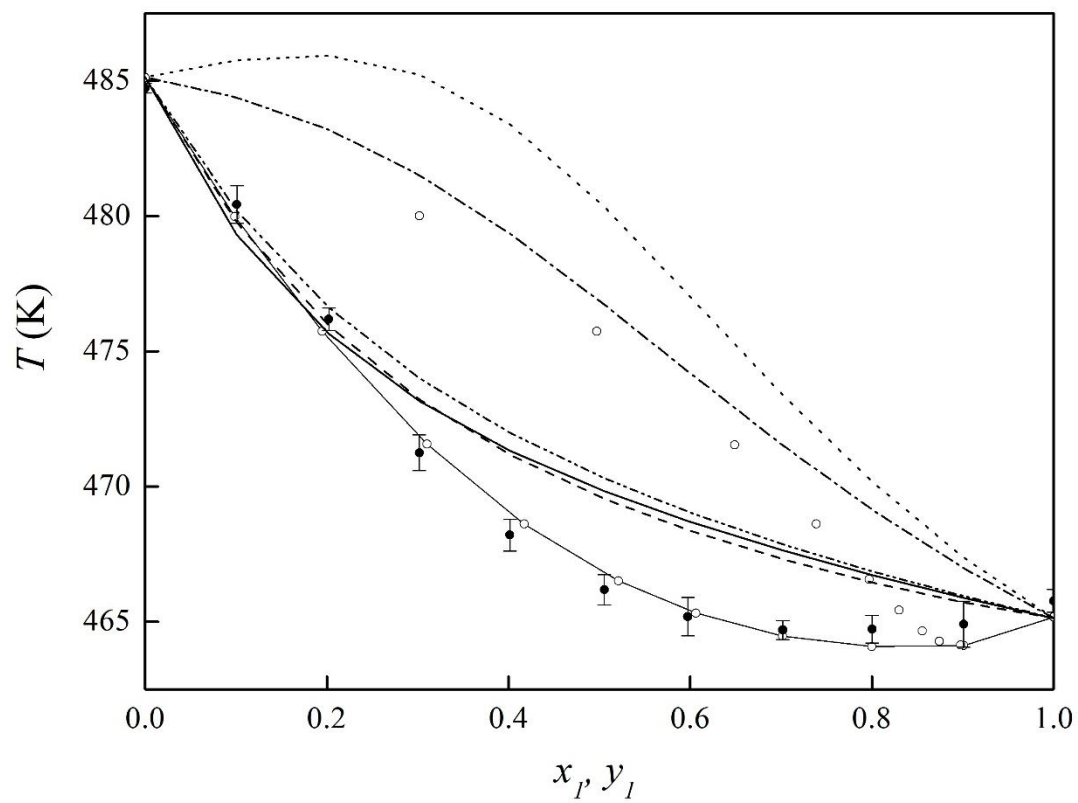
Figure 4.3. Liquid phase data of lauric acid + monocaprylin at 3.42 kPa and palmitic acid + monocaprylin at 3.50 kPa. Experimental data (●). Ideal behavior (--). Original UNIFAC (—) and modified UNIFAC by Cunico et al. [15] (⋯).
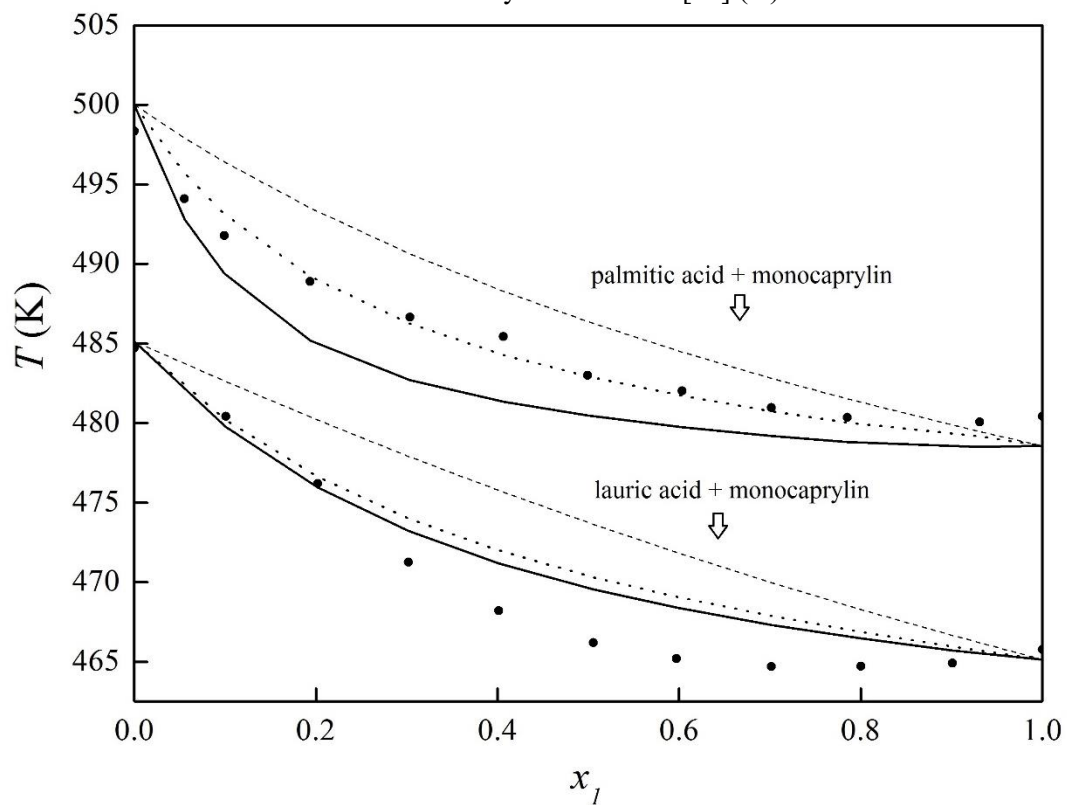
Figure 4.4. Vapor-liquid equilibria of monononanoin + monolaurin. Experimental data from this work (●). The UNIQUAC model for liquid phase (-○-) and vapor phase (○). Predictions for liquid phase of different versions of the UNIFAC method: Original (--), Lyngby (-··-), Dortmund (···), modified by Cunico et al. [15] (-···-) and NIST modified (—).

Figure 4.5. Vapor-liquid equilibria of hexadecanol + monononanoin. Experimental data from this work (●). The UNIQUAC model for liquid phase (-○-) and vapor phase (○). Predictions for liquid phase of different versions of the UNIFAC method: Original (--), Lyngby (-··-), Dortmund (···), modified by Cunico et al. [15] (-···-) and NIST modified (—).
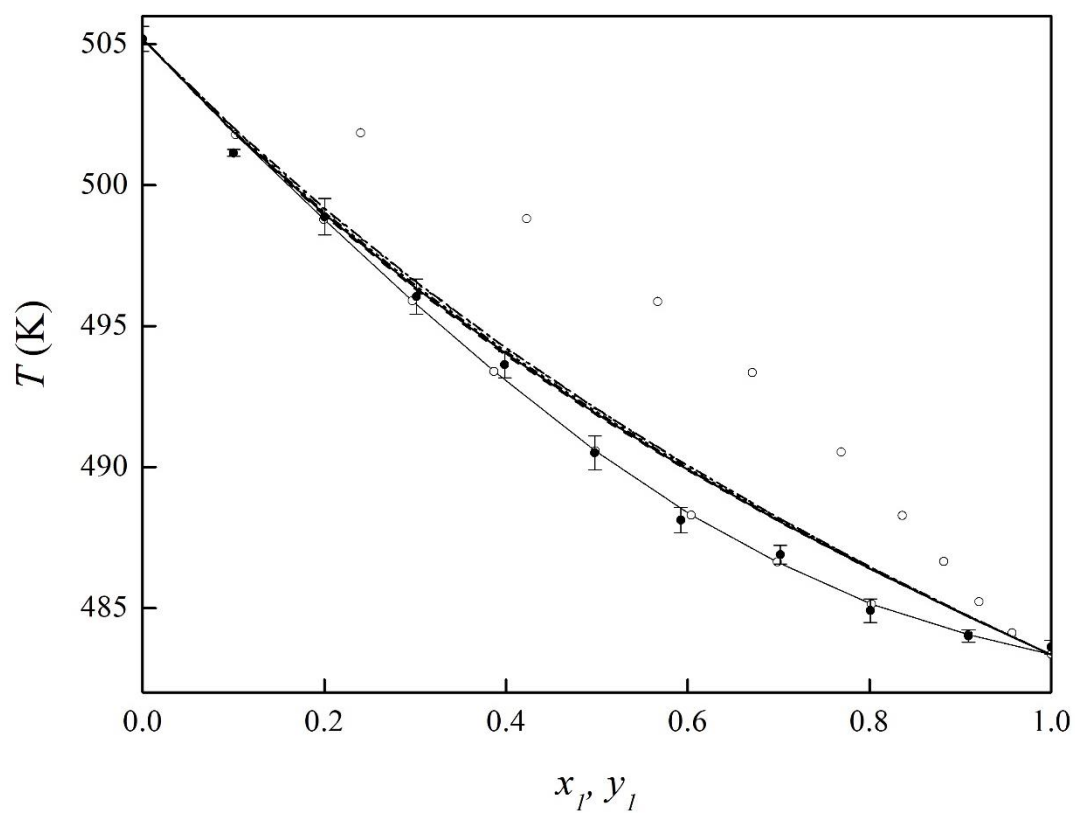
Figure 4.6. Vapor-liquid equilibria of octadecanol + monolaurin. Experimental data from this work (●). The UNIQUAC model for liquid phase (-○-) and vapor phase (○). Predictions for liquid phase of different versions of the UNIFAC method: Original (--), Lyngby (-··-), Dortmund (···), modified by Cunico et al. [15] (-···-) and NIST modified (—).
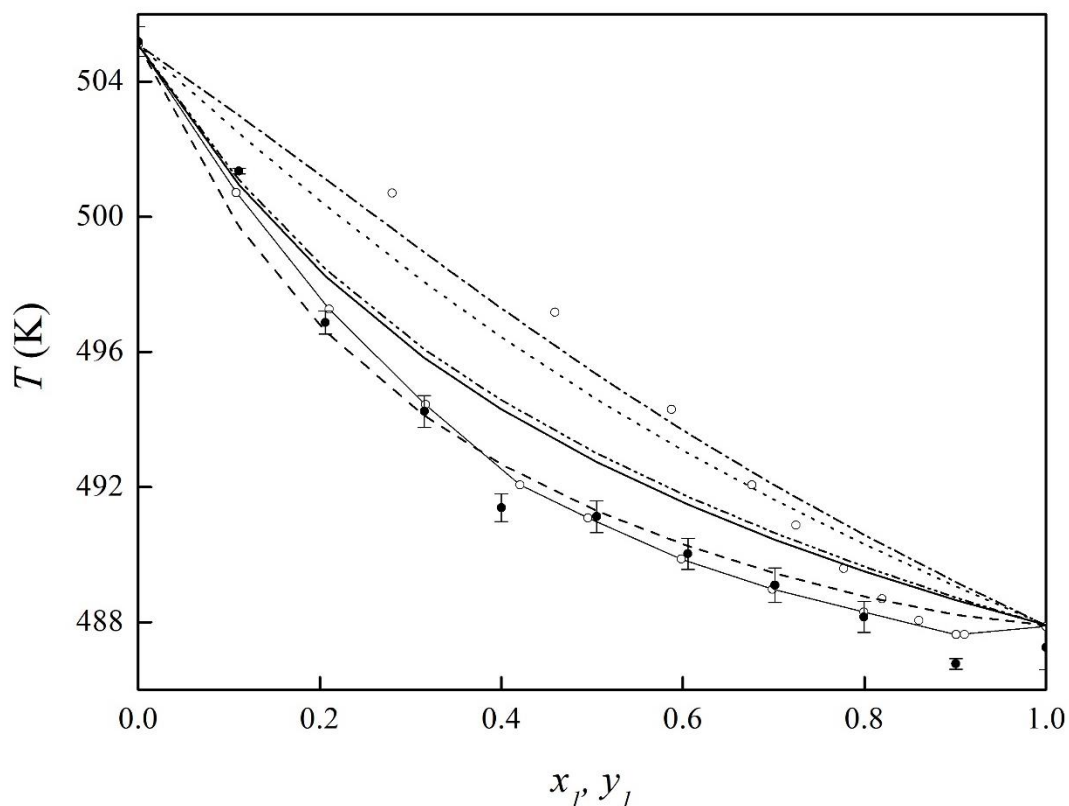
4.4 CONCLUSION

Novel boiling points for monononanoin and monolaurin were obtained at subatmospheric pressure. They showed suitable behavior when compared to other MAGs. and were correlated by the Antoine equation. VLE data were acquired for lauric acid + monocaprylin (3.42 kPa). monononanoin + monolaurin (2.06 kPa). monononanoin + hexadecanol (2.02 kPa). and monolaurin + octadecanol (2.05 kPa). Except for monononanoin + monolaurin (ideal behavior), all other systems presented positive deviation of Raoult's law (non-ideal). PTx data satisfied the pure thermodynamic consistency test. The Wilson, NRTL and UNIQUAC successfully correlated experimental data. The UNIFAC method in different versions: original, Lyngby, Dortmund, original modified by Cunico et al [15] and NIST modified were evaluated. Results showed that it presents shortcomings for predicting VLE of lipid compounds. and are an indication of necessity of more qualified and diverse experimental data in order to improve its predictive capacity.

4.5 ACKNOWLEDGEMENTS

4.6 LITERATURE CITED

[1]   D.S. Damaceno. R.M. Matricarde Falleiro. M.A. Krähenhühl. A.J.A. Meirelles. R. Ceriani. **Boiling points of short-chain partial acylglycerols and tocopherols at low pressures by the differential scanning calorimetry technique**. J. Chem. Eng. Data. 59 (2014). pp. 1515–1520

[2]   A. Watanabe**. On the sub-α-form and the α-form in monoacylglycerols**. J. Am. Oil Chem. Soc.. 74 (1997). pp. 1569-1573.

[3]   M. M. C. Feltes. D. Oliveira. J. M. Block. J. L. Ninow. **The production. benefits. and applications of monoacylglycerols and diacylglycerols of nutritional interest**. Food Bioprocess Technol.. 6 (2013). pp. 17–35

[4]   Casimir C. Akoh. David B. **Food lipids: chemistry. nutrition. and biotechnology**. 3ed. CRC Press. 2008

[5]   A. Ganem-Quintanar. D. Quintanar-Guerrero. P. Buri. **Monoolein: a review of the pharmaceutical applications**. Drug Dev Ind. Pharm.. 26 (2000). pp. 809-820.

[6]   J. Hu. Z. Du. C. Li. E. Min. **Study on the lubrication properties of biodiesel as fuel lubricity enhancers**. Fuel. 84 (2005). pp. 1601-1606.

[7]   KNOTHE. G.; STEIDLEY. K. Lubricity of components of biodiesel and petrodiesel: the origin of biodiesel lubricity. **Energy and Fuels**. 19 (2005). pp. 1192–1200.

[8]   J. Calero. D. Luna. E.D. Sancho. C. Luna. F. M. Bautista. A. A. Romero. A. Posadillo. J. Berbel. C.Verdugo-Escamilla. **An overview on glycerol-free processes for the production of renewable liquid biofuels. applicable in diesel engines**. Renew. Sustainable Energy Rev.. 42 (2015). pp.1437-1452.

[9]   Caballero V.. Bautista F.M.. Campelo J.M.. Luna D.. Marinas J.M.. Romero A.A.. Hidalgo J.M.. Luque R.. Macario A.. Giordano G. **Sustainable preparation of a novel**

glycerol-free biofuel by using pig pancreatic lipase: Partial 1.3-regiospecific alcoholysis of sunflower oil. Process Biochem.. 44 (2009). pp. 44:334–342.

[10]   C. Verdugo. R. Luque. D. Luna. J.M. Hidalgo. A. Posadillo. E. Sancho. S. Rodríguez. S. Ferreira-Días. F. M. Bautista. A. A Romero. **A comprehensive study of reaction parameters in the enzymatic production of novel biofuels integrating glycerol into their composition**. Bioresour. Technol.. 101 (2010). pp. 657–6662.

[11]   D. L. Compton. K. E. Vermillion. J. A. Laszlo. **Acyl migration kinetics of 2-monoacylglycerols from soybean oil via 1h nmr**. J Am. Oil Chem Soc. 84 (2007). pp.343-348.

[12]   N. Krog. F. V. Sparso. **Food emulsifiers and their chemical and physical properties**. In: Food Emulsions. ed. S. E. Friberg. Marcel Dekker Inc.. New York. 1990. p. 127–180.

[13]   J. A Laszlo. D. L. Compton. K. E. Vermillion. **Acyl migration kinetics of vegetable oil 1.2-diacylglycerols**. J Am Oil Chem Soc.. 85 (2008). pp. 307-312.

[14]   L.F.F.Corrêa; L.F.J. Ribeiro; R. Ceriani. XX Congresso Brasileiro de Engenharia Química. Florianopolis. 2014.

[15]   L.P. Cunico. D.S. Damaceno. R.M. Matricarde Falleiro. B. Sarup. J. Abildskov. R. Ceriani. R. Gani. **Vapour liquid equilibria of monocaprylin plus palmitic acid or methyl stearate at P = (1.20 and 2.50) kPa by using DSC technique.** J. Chem. Thermodyn.. 91 (2015). pp. 108–115

[16]   J.W. Kang. V. Diky. M. Frenkel. **New modified UNIFAC parameters using critically evaluated phase equilibrium data.** Fluid Phase Equilib.. 388 (2015). pp. 128–141

[17]   Troni. K. L.; Damaceno. D. S.; Ceriani. R. **Improving a variation of the DSC technique for measuring the boiling points of pure compounds at low pressures**. J. Chem. Thermodyn. 100 (2016). pp. 191-197.

[18]   G.M. Wilson. Vapor-Liquid Equilibrium. XI**. A new expression for the excess free energy of mixing**. J. Am. Chem. Soc.. 86 (1964). pp. 127–130

[19]   H. Renon. J.M. Prausnitz. **Local compositions in thermodynamic excess functions for liquid mixtures.** AIChE J.. 14 (1968). pp. 135–144

[20]   D.S. Abrams. J.M. Prausnitz. **Statistical thermodynamics of liquid mixtures: a new expression for the Excess Gibbs energy of partly or completely miscible systems.** AIChE J.. 21 (1975). pp. 116–128

[21]   J.W. Kang. V. Diky. R. D. Chirico. J. W. Magee. C. D. Muzny. I. Abdulagatov. **A. F. Kazakov. M. Frenkel. Quality assessment algorithm for vapor−liquid equilibrium data**. J. Chem. Eng. Data.55 (2010). pp. 3631−3640.

[22]   A. Fredenslund. R. Jones. J.M. Prausnitz. **Group-contribution estimation of activity coefficients in nonideal liquid mixtures.** AIChE J.. 21 (1975). pp. 1086–1099.

[23]   B. Larsen. P. Rasmussen. A. Fredenslund. **A modified UNIFAC group-contribution model for prediction of phase equilibria and heats of mixing. Ind.** Eng. Chem. Res.. 26 (1987). pp. 2274–2286.

[24]   J. Gmehling. J. Li. M. Schiller. **A modified UNIFAC model. 2. Present parameter matrix and results for different thermodynamic properties.** Ind. Eng. Chem. Res.. 32 (1993). pp. 178–193.

[25]   S. H. Yalkowsky. Y. He. P. Jain. **Handbook of aqueous solubility data.** 2ed. CRC Pressed: Boca Raton. 2010.

[26]   Metrohm Application Bulletin 137/4. Coulometric water content determination according to Karl Fischer.

[27]   ASTM E1782-14. 2014. Standard Test Method for Determining Vapour Pressure by Thermal Analysis 1405.

[28]   R. M. Matricarde Falleiro. A. J. A. Meirelles. M. A. Krähenbühl. **Experimental determination of the (vapor-liquid) equilibrium data of binary mixtures of fatty acids by differential scanning calorimetry**. J. Chem. Thermodyn.. 42 (2010). pp. 70-77.

[29]   L. Y. A. Silva. R. M. Matricarde Falleiro. A. J. A. Meirelles. M. A. Krähenbühl. **Vapor–liquid equilibrium of fatty acid ethyl esters determined using DSC**. Thermochimica Acta. 512 (2011). pp. 178-182.

[30]   R.M. Matricarde Falleiro. L.Y.A. Silva. A.J.A. Meirelles. M.A. Krähenbühl. **Vapor pressure data for fatty acids obtained using an adaptation of the DSC Technique**. Thermochim. Acta. 547 (2012). pp. 6-12.

[31]   D. Constantinescu. I. Wichterle. **Isothermal vapour–liquid equilibria and excess molar volume in the binary ethanol + methyl propanoate or methyl butanoate systems**. Fluid Phase Equilib.. 203(2002). pp.71-82

[32]   Juan Ortega. Pedro Susial. Casiano De Alfonso. **Isobaric vapor-liquid equilibrium of methyl butanoate with ethanol and 1-propanol binary systems**. Chem. Eng. Data. 1990. 35 (2). pp 216–219

[33]   A. Dejoz. V. González-Alfaro. P. J. Miguel. M. I. Vázquez. **Isobaric vapor−liquid equilibria for binary systems composed of octane**. **decane. and dodecane at 20 kpa.** J. Chem. Eng. Data. 41 (1996). pp 93–96.

CAPÍTULO 5

VAPOR-LIQUID EQUILIBRIA OF BINARY SYSTEMS WITH LONG-CHAIN ORGANIC COMPOUNDS (FATTY ALCOHOL, FATTY ESTER, ACYLGLYCEROL AND N-PARAFFIN) AT SUBATMOSPHERIC PRESSURES

Daniela S. Damaceno, Roberta Ceriani

Publicado na Journal of Chemical Engineering and Data

Abstract: In the past years, the oil and fat industry has been growing on a large scale, mostly due to the need of biodiesel production. Considering this fact, the understanding of thermophysical properties and phase equilibrium of the compounds found in this industry became crucial, i.e., acylglycerols, fatty esters, alcohols. Therefore, this work aims to obtain liquid-vapor equilibrium data of the following mixtures: hexadecanol + octadecanol (1.73 kPa), hexadecanol + methyl myristate (1.72 kPa) monononanin + tributyrin (1.69 kPa), dinonanoin + octacosane (1.70 kPa), by the differential scanning calorimetry (DSC) technique. As expected, the system with two long-chain alcohols (hexadecanol + octadecanol) showed an ideal behavior. In contrast, the other systems presented non-ideal behavior. Experimental data were effectively regressed by the UNIQUAC model. The pure component consistency test and the variation of Van Ness consistency test were applied to all systems. Activity coefficients were modeled using the Linear UNIFAC, the Modified UNIFAC and the Dortmund UNIFAC with both their original parameters (a_{mn}) and the lipid-based parameters regressed by Damaceno et al. 2017, and also the NIST modified UNIFAC. Predictive capacity of all these methods were tested, and no single method showed to be the best for all systems.

5.1 INTRODUCTION

Sustainable fuels as biodiesel are a great alternative to unrenewable fuels. According to ANP (Agência Nacional do Petróleo, Gás Natural e Biocombustíveis), in Brazil biodiesel is added at 9% in diesel, and this percentage will increase to 10% in 2019 [1]. Due to increase in biodiesel production, knowledge of thermophysical properties of related compounds, and phase equilibria among them, has become crucial to better predict and optimize separations and purification processes of biodiesel and bioglycerol (by-product) [2].

Recent works from Damaceno and Ceriani [2], Damaceno et al. [3], Troni et al [4], Kang et al. [5], Bessa et al. [6], Cunico et al [7] and Belting et al. [8] evidenced concerns towards relevance of improving predictive capacity of group contribution methods, as the UNIFAC method (UNIQUAC Functional-group Activity Coefficients) related to fatty compounds. In fact, a diverse databank is substantial for mapping interactions among different functional groups of complex compounds. Recently, Damaceno and Ceriani [2] performed a search in the Web of Science from 2014 up to 2016 looking for experimental data points of vapor-liquid equilibria with at least one lipid compound, and as a result, they found 1,522 data points, which is a clear indication of the interest of the scientific community on this subject. Of course, non-ideal systems give a more substantial analysis of predictive capacity of the UNIFAC method. Partial acylglycerols, as monoacylglycerols and diacylglycerols, are formed during the transesterification reaction to produce biodiesel [2,3,7], and they are emulsifiers largely used in food industry. In terms of functional groups, combinations of CCOO and OH groups, which are of special interest in lipid technology, are present. However, the open literature presents only very few works reporting vapor-liquid equilibria of systems including monoacylglycerols [2,7]

More recently, Damaceno et al. [9] improved predictive tools for vapor-liquid equilibria based on group contribution methods (UNIFAC) involving lipid compounds. New matrixes for the Linear UNIFAC [10], Modified UNIFAC [11] and Dortmund UNIFAC [12] were presented, and their performances in prediction were compared with the original parameters.

As an effort to contribute to phase equilibria understanding of fatty compounds, this work provides novel boiling point data of dinonanoin (MW = 372.5 $g \cdot mol^{-1}$) at five different pressures, and vapor-liquid equilibria data of four fatty binary mixtures at selected pressures

(TPx data), i.e.: hexadecanol (MW = 242.4 g·mol^{-1}) + octadecanol (MW = 270.5 g·mol^{-1}), hexadecanol (MW = 242.4 g·mol^{-1}) + methyl myristate (MW = 242.4 g·mol^{-1}), monononanoin (MW = 232.3 g·mol^{-1}) + tributyrin (MW = 302.4 g·mol^{-1}), and dinonanoin (MW = 372.5 g·mol^{-1}) + octacosane (MW = 394.8 g·mol^{-1}) measured with the DSC technique. Considering its adequacy to high cost and thermal sensitive compounds, the DSC technique was selected. [2-4]. Vapor pressure data for dinonanoin was modeled using the Antoine equation. TPx data were correlated using the *gamma-phi* approach (considering vapor phase as ideal) after checking their thermodynamic consistency using the pure component consistency test [2,5,7]. Activity coefficients were modeled using the UNIFAC method [13], and different versions of the UNIFAC method: the Linear UNIFAC [10], the Modified UNIFAC [11] and the Dortmund UNIFAC [12] with both their original parameters (a_{mn}) and the lipid-based parameters regressed by Damaceno et al. [9], and also with the NIST modified UNIFAC [5]. For comparison purposes, Raoult's law was also applied.

5.2 METHODOLOGY

5.2.1 Materials

Table 5.1 lists all the reagents used in this study (CAS Registry numbers, purities in mass fraction, IUPAC names and suppliers). All chemicals were used without any further purification step. Monononanoin and dinonanoin are respectively, a monoacylglycerol and a diacylglycerol of nonanoic acid ($C_9H_{18}O_2$), while tributyrin is a triacylglycerol of butyric acid ($C_4H_8O_2$) and methyl myristate is a methyl ester of tetradecanoic acid ($C_{14}H_{28}O_2$)

Table 5.1 List of compounds with their respective IUPAC name, CAS Registry No., supplier and purity

Compound	IUPAC name	CAS Registry No.	Supplier	Purity (mass fraction)
n-tetradecane	Tetradecane	629-59-4	Sigma-Aldrich	0.99
n-octacosane	Octacosane	630-02-4	Sigma-Aldrich	0.99
monononanoin [a]	2,3-dihydroxypropyl nonanoate	3065-51-8	Nu-Chek Prep, Inc.	0.99
dinonanoin [a]	(2-decanoyloxy-3-hydroxypropyl) nonanoate	-	Nu-Chek Prep, Inc.	0.99
trybutyrin	2,3-di(butanoyloxy)propyl butanoate	60-01-5	Sigma-Aldrich	0.99
methyl myristate	methyl tetradecanoate	124-10-7	Sigma-Aldrich	0.99
hexadecanol	hexadecan-1-ol	36653-82-4	Sigma-Aldrich	0.99
octadecanol	octadecan-1-ol	112-92-5	Sigma-Aldrich	0.99

[a] Thin layer chromatography showed only the monoacylglycerol moiety present according to the certificate of analysis provided by Nu-Chek Prep, Inc.

5.2.2 Experimental procedure

Apparatus and experimental procedure used in this work can be reached in details referring to Troni et al. [4] and Damaceno and Ceriani [2]. It consists of a variation of the DSC technique based on the ASTM E1782-14 guidelines [14]. Briefly, boiling point was obtained using a pair of hermetic sealed crucibles, one empty (reference) and the other with a sample (4 – 5) mg, with a pinhole on the lid, and a tungsten carbide ball placed over it. The heating rate used was 25 K min^{-1}, at constant pressure [4]. Absolute pressure inside the cell was measured by a pressure gauge calibrated with n-tetradecane. After each procedure, pressure cell was restored to ambient conditions. All boiling points were determined from the extrapolated onset temperature calculated from the thermal curves generated by the TA instruments software.

5.2.3 Boiling points of pure compounds

Five novel boiling points for dinonanoin at subatmospherical pressure range were measured in this work. For describing the relation between vapor pressure p/kPa and temperature T/K, the Antoine equation was (Eq. 1) selected:

$$\ln p = A + \frac{B}{T + C} \tag{1}$$

where p is the vapor pressure in kPa, T is the boiling point in K, and A, B and C are parameters fitted by least-squares regression using the Curve Fitting Toolbox 3.5.1 in MatLab R2015a (The MathWorks Inc.). The boiling points of hexadecanol, octadecanol, octacosane and methyl myristate were obtain from data of NIST TDE Aspen Plus 8.4v. For monononanoin [2] and tributyrin [4] it was used data from literature.

5.2.4 Sample preparation of binary mixtures

Sample preparation followed the procedure described by Damaceno and Ceriani [2] and Cunico et al. [7]. In general, known amounts (g) of pure components were mixed in an analytical balance (Model AS220 – Radwag) containing around 0.2 g of the binary mixture. Subsequently, the samples were mixed in a vortex shaker (Marconi MA 162) for few minutes to ensure homogeneity. A total of 11 molar fractions of the more volatile compound (x_1) ranging from 0 to 1 in 0.1 interval were prepared. Then, microsamples of (4 – 5) mg were gained from each binary mixture using micropipettes of 0.5 – 10 μL (Model Research – Eppendorf), and weighted in a microanalytical balance (Model C-33 – Thermo Scientific).

5.2.5 Thermodynamic consistency test for isobaric TPx data

Considering Damaceno and Ceriani [2] and Cunico et al. [7], the pure component consistency test for TPx data described by Kang et al. [15] (Eq. 2) were calculated. It is calculated with the endpoints of the VLE curve (x1 = 0.0 and x1 = 1.0). In this way, the validation is conducted by comparing the experimental boiling points of the pure compounds with data in the literature. Thus, for isobaric TPx data (Eq. 2 and Eq. 3):

$$p_{bubble}\left(x_1 \rightarrow 1\right) = p_1, \, p_{buble}\left(x_1 \rightarrow 0\right) = p_2 \tag{2}$$

$$\Delta p_1 = \left| \frac{p_{bubble}\left(x_1 \to 1\right) - p_1}{p_1} \right|, \Delta p_2 = \left| \frac{p_{bubble}\left(x_1 \to 0\right) - p_2}{p_2} \right| \tag{3}$$

where p_{bubble} is the pressure of the bubble point of the mixture, p_1 and p_2 are the pure component vapor pressures.

According to Damaceno and Ceriani [2], the variation of Van Ness consistency test ($Q_{test,1}$) can be also applied to check the quality of the TPx data [7,15]. This Van Ness test is not based on the Gibbs-Duhem equation, due the fact that TPxy data are required in this case. The quality factor of Van Ness was calculated by Eq. 4.

$$Q_{test,1} = \frac{1}{1 + ARD\left(\%\right)} \tag{4}$$

where ARD (%) is the average relative deviation between the measured boiling point and the estimated boiling point calculated with a molecular model, such as the UNIQUAC model.

5.3 RESULTS AND DISCUSSION

5.3.1 Vapor pressure of dinonanoin

Experimental boiling points of dinonanoin (0.54 – 2.63) kPa are listed in Table 5.2, with their respective standard uncertainties. Regressed values for constants *A*, *B* and *C* (Eq. 1) are listed in Table 5.3. Average absolute deviations (AAD), average relative deviations (ARD) and coefficients of determination (R^2) are also given. Suitable values were found for all statistical tests applied.

Table 5.2 Experimental data for boiling points T/K at the selected pressures p/kPa for dinonanoin, with its respective standard uncertainties u(T) in/K

	Dinonanoin	
p/kPa[a]	T/K	u (T)/K
0.54	504.22	0.23
1.42	526.20	0.26
1.74	531.55	0.43
2.14	537.01	0.70
2.63	543.12	0.54

[a] Standard uncertainty $u(p) \leq 0.03$ kPa.

Table 5.3 Regressed constants for the Antoine equation (Eq.1).

Compound	A	B	C	[a]AAD /K	[b]ARD (%)	[c]R²
Dinonanoin	8.594	-1726.0	-316.8	0.056	0.008	0.9999

[a] $AAD = \sum_{i=1}^{n} \frac{1}{n} \cdot \left| T_{exp} - T_{calc} \right|_i$, [b] $ARD = \sum_{i=1}^{n} \frac{1}{n} \cdot \left[100 \cdot \frac{\left| T_{exp} - T_{calc} \right|}{T_{exp}} \right]$, where T_{exp} is experimental temperature in K and

T_{calc} is calculated temperature in K, [c]R² = Coefficient of determination ($R - square$)

For comparison purposes, Figure 5.1 shows linearized relations of vapor pressures p/kPa versus temperature T/K for a homologous series of diacylglycerols and one monoacylgycerol: dicaprylin [3], dinonanoin (this work), dicaprin [3] and monononanoin [2]. At a given pressure, dicaprin, the heaviest compound (400.6 g·mol^{-1}), boils at higher temperatures, followed by dinonanoin (372.5 g·mol^{-1}), dicaprylin (344.5 g·mol^{-1}), and finally monononanoin (232.3 g·mol^{-1}) which is the lightest compound in this sequence of partial acylglycerols.

Figure 5.1 Linearized relation for vapor pressure ln (p) in kPa as function of temperature T^{-1} (K^{-1}) for a homologous series of diacylglycerols and for mononononanoin. This work: dinonanoin (●). Literature: monononanoin [2] (×), dicaprylin [3] (□) and dicaprin [3] (Δ)
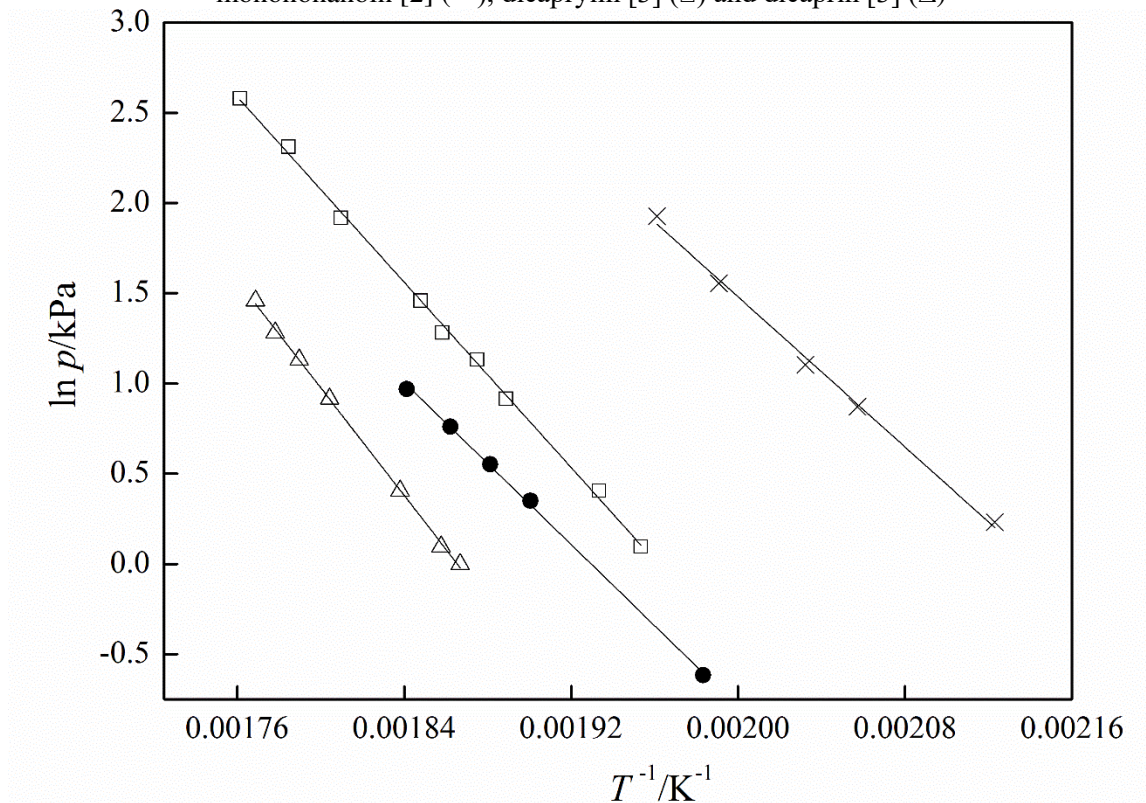
5.3.2   VLE of binary systems

Four binary systems (TPx data) were measured in this work at selected pressures: System 1 - hexadecanol (*1*) + octadecanol (2) at $p = 1.73$ kPa with $u(p) = 0.04$ kPa, System 2 - methyl myristate (1) + hexadecanol (2) at $p = 1.72$ kPa with $u(p) = 0.04$ kPa, System 3 - tributyrin (1) + monononanoin (2) at $p = 1.69$ kPa with $u(p) = 0.04$ kPa, and System 4 - dinonanoin (1) + octacosane (2) at $p = 1.70$ kPa with $u(p) = 0.04$ kPa. Table 5.4 presents molar fractions of the more volatile compound (x_1), boiling points (*T*), and pressures (*p*) for each of the four binary systems considered.

The pure component consistency test was applied to all systems, and results are presented in Table 5.5. It is possible to observe in Table 5.5 that none of the endpoints (Δp_1^0, Δp_2^0) presented higher values than 0.04, and comparing those values (Table 5.5) with other works that used the same consistency test to TPx data [2,7], it is possible to verify satisfactory and reliable results. The variation of Van Ness consistency test ($Q_{test,1}$) results are given in Table

6. The quality factor, $Q_{test,1}$, for all investigated systems were higher than 0.862, and 75% of the results for the $Q_{test,1}$ were above 0.921, which indicate high quality factors for our experimental values [2].

Experimental TPx data (*T, p* and x_1) were regressed using the UNIQUAC [16] model with software *Aspen Plus* v8.4 for activity coefficients, considering modified Raoult's law (ideal vapor phase). The software Aspen Plus 8.4v used the Maximum Likelihood as objective function and Britt-Luecke as the main algorithm to regress the activity coefficients [17-18]. Vapor pressures of hexadecanol, octadecanol, octacosane and methyl myristate were calculated with the Antoine equation (Supporting Information Available – Table 5.S1). Regressed coefficients for the Antoine equation (Eq. 1) are available for all compounds in Table 5.S1 (Supporting Information), except for dinonanoin that is in Table 5.3 (this work). Binary interaction parameters are given in Table 5.7.

In Figure 5.2 – 5.5, experimental data and regressed values using the UNIQUAC model are presented. In general, very good correlations were achieved, as in previous works [2]. Table 5.8 brings estimated VLE data of the binary systems studied together with their respective deviations. It also gives calculated values for activity coefficients (γ_1 and γ_2) using the UNIQUAC model to account for nonidealities in the liquid phase, and in Table 5.9 activity coefficients at infinite dilution (γ_1^∞ and γ_2^∞) were provided.

Binary system 1 (Figure 5.2) showed behavior analogous to ideal, as expected for binary mixtures of compounds of a homologous series with γ close to unity (Table 5.8). System 2 (Figure 5.3) presented non-ideal behavior (γ = 0.80 – 1.19, see Table 5.8) and an azeotrope ($x_1 \approx 0.95$), corroborating with previous works. In fact, considering binary systems of alcohol + methyl ester, several studies shows the presence of an azeotropic behavior. For example, the binary systems ethanol + methyl propanoate at 326.30 K, or ethanol + methyl butanoate at 346.30 K [19], or for methyl butanoate + ethanol at 101.32 kPa or 1-propanol at 101.32 kPa. [20]. System 3 (Figure 5.4) also presented non-ideal behavior with activity coefficients varying from 0.96 – 1.51 (Table 5.8). As well, system dinonanoin + octacosane (system 4) showed non-ideal behavior (γ = 0.95 – 1.99, see Table 5.8) and an azeotrope ($x_1 \approx 0.90$). In general, our results for systems 3 and 4 corroborated with others for systems composed by partial acylglycerols. For example, Damaceno and Ceriani [2] and Cunico et al. [7] reported non-ideal behavior and an azeotrope for systems monocaprylin + palmitic acid or methyl stearate [7], monocaprylin + lauric acid, monononanoin + hexadecanol and monolaurin + octadecanol [2] at subatmospheric pressures. It is important to highlight that, from the best of our knowledge,

none previous experimental data are available in the open literature for binary systems of monoacylglycerol + triacylglycerol and of diacylglycerol + n-paraffin.

Predictive capacity of the Linear, Modified and Dortmund UNIFAC methods with their original parameters [10-12] and with the lipid-based parameters [9], and of the NIST modified UNIFAC [5] were evaluated. Predicted values of boiling temperatures with their respective deviations (AAD and ARD) are given in Supporting Information Available – Tables 5.S2 and 5.S3. Equations of the models are presented in Supporting Information Available – Tables 5.S4 and Table 5.S5 and Eq. 5.S.5 to Eq. S13, the parameters of area Q_k and volume R_k for the functional groups of all the four UNIFACs methods are in Table 5.S6, and Table 5.S7 contains the interaction parameters $a_{mn,0}$, $a_{mn,1}$ and $a_{mn,2}$ to all the UNIFAC methods versions considered in this work. Table 5.S8 presents the molecular structure of the compounds used in this work to better comprehend the functional groups of the selected compounds. In general, all the UNIFAC methods (Linear, Modified and Dortmund) with their original parameters and the NIST modified UNIFAC overestimated boiling points of the four binary systems studied (Tables 5.S2 and 5.S3). On the other hand, the Linear, Modified and Dortmund UNIFAC methods with the lipid-based parameters [9] showed different behaviors for each system. In Figures 5.2 – 5.5 results for selected UNIFAC methods (lowest deviations for each binary system among results presented in Tables 5.S2 and 5.S23 were plotted for comparison purposes together with predictions given by the Raoult's law and by the NIST UNIFAC method. Results are discussed as follows. For System 1 (Figure 5.2) all curves overlapped as a consequence of its ideality. In fact, for a similar binary system of medium chain alcohols, as the system decanol + dodecanol [21] at 13.33 kPa, experimental data almost equal the ideal behavior curve (Figure 5.6), and curves calculated with the Raoult's law and with the Modified UNIFAC overlapped. For system 2 the best performance was presented by the Modified UNIFAC method with its original parameters. Figure 5.3 shows that as mole fraction of the more volatile compound (methyl myristate) increases from $x_1 = 0$ to 0.5, boiling points are underestimated while from $x_1 = 0.5$ to 1 they are overestimated. It is interesting to note that as x_1 increases from 0 to 0.5, contributions of the functional group CCOO in calculated values of γ are also decreasing in relevance while contributions of the functional group OH are increasing instead. On the other hand, as x_1 increases from 0.5 to 1, the opposite behavior is verified.

For System 3, the Linear UNIFAC method with its original parameters showed lower deviations. It can be observed in Figure 5.4 (system 3) that boiling points for mixtures richer (x_1 up to 0.6) in the less volatile compound (monononanoin), in which contributions of

the functional group CCOO are decreasing, are overestimated. For $x_1 > 0.6$, predicted values are lower than experimental boiling points. Note that for system 3, tributyrin has 3 functional groups CCOO while monononanoin has 1 CCOO and 2 OH. Somehow, similar behaviors of predicted values of boiling points were found with the NIST modified UNIFAC for the system hexadecanol + monononanoin at $p = 2.02$ kPa with $u(p) = 0.06$ kPa [2], i.e., for x_1 up to 0.3, in which contributions of CCOO are stronger (due to monononanoin), boiling points are underestimated. On the contrary, for $x_1 > 0.3$ when the contribution of OH increases due to the presence of hexadecanol which is summed to the OH present in monononanoin, boiling points are overestimated. In general, it was found that the predictions of boiling points using the UNIFAC methods for VLE of fatty binary systems [2,7], excluding the above-mentioned cases, were overestimated.

For system 4 (Figure 5.5), the Modified UNIFAC model with lipid-based parameters provided best predictive capacity. It is of note that higher disparities among predicted values of the UNIFAC methods were found for this system, also the predicted values are higher than the experimental boiling points for the evaluated UNIFAC models.

In general, predicted results revealed that there is not a single best model, which is suitable for all cases. For systems 1 and 4, the UNIFAC methods with the lipid-based parameters presented the lowest deviations, while for systems 2 and 3 the UNIFAC methods with their original parameters had better predictive capacities. Compounds in systems 1 to 4 were selected in a way that interactions among functional groups relevant in lipid technology (CCOO, OH and CH_2) were present, considering compounds of different classes and different numbers of these functional groups within these compounds, and also different proportions among them). In fact, efforts toward improvements in predictive capacity of group contribution methods as the UNIFAC method for compounds of lipid technology necessarily go through expanding related experimental databank.

Table 5.4 Experimental TPx data for binary systems: hexadecanol (x_1) + octadecanol, methyl myristate (x_1) + hexadecanol, tributyrin (x_1) + monononanoin and dinonanoin (x_1) + octacosane.

hexadecanol (1) + octadecanol (2) (system 1)			methyl myristate (1) + hexadecanol (2) (system 2)			tributyrin (1) + monononanoin (2) (system 3)			dinonanoin (1) + octacosane (2) (system 4)		
x_1	T/K	u (T)/K	x_1	T/K	u (T)/K	x_1	T/K	u (T)/K	x_1	T/K	u (T)/K
1.0000	462.29	0.53	1.000	437.72	0.69	1.0000	459.56	0.75	1.0000	532.03	0.69
0.8997	462.6	0.39	0.9014	439.44	0.68	0.9020	461.71	0.62	0.8944	532.30	0.28
0.8026	464.37	0.31	0.8000	440.40	0.41	0.8058	462.19	0.53	0.7889	532.40	0.21
0.7016	466.09	0.30	0.7005	442.09	0.30	0.7035	463.05	0.67	0.6824	532.18	0.76
0.6084	467.19	0.52	0.6001	443.46	0.44	0.6087	462.93	0.46	0.5973	531.96	0.28
0.5008	469.18	0.58	0.5032	445.99	0.30	0.5066	464.52	0.48	0.5006	532.08	0.09
0.4011	471.43	0.60	0.3979	450.59	0.67	0.4001	466.19	0.39	0.4068	533.08	0.45
0.3003	475.27	0.76	0.3049	453.64	0.19	0.3107	467.45	0.55	0.2974	536.05	0.38
0.2017	478.24	1.20	0.1980	457.41	0.74	0.2041	471.09	0.20	0.2024	541.31	0.44
0.0932	480.93	0.47	0.1017	460.26	0.43	0.0999	475.43	0.56	0.0984	545.15	0.74
0.0000	483.46	0.66	0.0000	462.29	0.53	0.0000	478.88	0.75	0.0000	550.62	0.55
p/kPa	1.73			1.72			1.69			1.70	
u (p)/kPa	0.04			0.04			0.04			0.04	

Standard uncertainty u(x_1) = 0.0005, calculated by error propagation.

Table 5.5 Experimental data points ($x_1 = 1$ and $x_1 = 0$) and the calculated variables to apply the pure component consistency test

Compounds	T/K	Measured values	p_{exp}/kPa	Reference	p_{calc}/kPa	Δp_1^0, Δp_2^0
hexadecanol	462.29	$x_1 = 1$	1.73	NIST TDE Aspen plus v. 8.4	1.70	0.02
hexadecanol	462.29	$x_1 = 0$	1.72	NIST TDE Aspen plus v. 8.4	1.70	0.01
octadecanol	483.46	$x_1 = 0$	1.73	NIST TDE Aspen plus v. 8.4	1.72	0.01
methyl myristate	437.72	$x_1 = 1$	1.72	NIST TDE Aspen plus v. 8.4	1.66	0.04
tributyrin	459.56	$x_1 = 1$	1.69	[4]	1.66	0.02
monononanoin	478.88	$x_1 = 0$	1.69	[2]	1.68	0.01
dinonanoin	532.03	$x_1 = 1$	1.70	This work	1.78	0.04
octacosane	550.62	$x_1 = 0$	1.70	NIST TDE Aspen plus v. 8.4	1.66	0.02

Δp_1^0, Δp_2^0: for calculation to these variables refer to Eq. 3.

Table 5.6 Quality factor ($Q_{test,1}$) calculated by the variation of the Van Ness consistency test

Binary system	p/kPa	$Q_{test,1}$
hexadecanol (1) + octadecanol (2)	1.73	0.948
methyl myristate (1) + hexadecanol (2)	1.72	0.942
tributyrin (1) + monononanoin (2)	1.69	0.912
dinonanoin (1) + octacosane (2)	1.70	0.864

Table 5.7 Binary interaction parameters for the UNIQUAC model

Binary system	p/kPa	b_{12} (J·mol^{-1})	b_{21} (J·mol^{-1})
hexadecanol (1) + octadecanol (2)	1.73	-3692.67	2441.75
methyl myristate (1) + hexadecanol (2)	1.72	-4574.00	2779.31
tributyrin (1) + monononanoin (2)	1.69	-1403.89	980.58
dinonanoin (1) + octacosane (2)	1.70	-536.38	243.03

[a] Equations for the activity coefficient of the UNIQUAC model (S1 – S4) are in the Supporting Information Available. .

Table 5.8 Estimated VLE data of four binary systems hexadecanol + octadecanol (1), methyl myristate + hexadecanol (2), tributyrin + monononanoin (3) and dinonanoin + octacosane (4) by the UNIQUAC model with their respective deviations.

Hexadecanol (1) + octadecanol (2) (system 1) at 1.73 kPa				methyl myristate (1) + hexadecanol (2) (system 2) at 1.72 kPa				Tributyrin (1) + monononanoin (2) (system 3) at 1.69 kPa				Dinonanoin (1) + octacosane (2) (system 4) at 1.70 kPa			
Molar fraction	UNIQUAC	γ_1	γ_2	Molar fraction	UNIQUAC	γ_1	γ_2	Molar fraction	UNIQUAC	γ_1	γ_2	Molar fraction	UNIQUAC	γ_1	γ_2
(x_1)	T/K			(x_1)	T/K			(x_1)	T/K			(x_1)	T/K		
1.0000	462.70			1.000	438.46			1.0000	459.95			1.0000	530.93		
0.8997	463.24	1.03	1.31	0.9014	439.10	1.04	1.21	0.9020	460.74	0.96	1.51	0.8944	530.77	1.02	2.17
0.8026	464.29	1.07	1.02	0.8000	440.14	1.10	0.87	0.8058	461.54	0.99	1.38	0.7889	531.11	1.06	1.73
0.7016	465.76	1.11	0.93	0.7005	441.91	1.13	0.81	0.7035	462.55	1.03	1.27	0.6824	531.70	1.13	1.46
0.6084	467.29	1.12	0.91	0.6001	443.84	1.13	0.82	0.6087	463.40	1.13	1.21	0.5973	532.24	1.20	1.31
0.5008	469.40	1.12	0.92	0.5032	446.32	1.10	0.86	0.5066	464.74	1.17	1.13	0.5006	533.00	1.29	1.19
0.4011	471.80	1.09	0.95	0.3979	450.57	1.05	0.91	0.4001	466.43	1.25	1.08	0.4068	534.20	1.40	1.11
0.3003	475.10	1.06	0.97	0.3049	453.64	0.99	0.95	0.3107	468.03	1.36	1.06	0.2974	536.66	1.55	1.05
0.2017	477.92	1.02	0.99	0.1980	457.18	0.92	0.98	0.2041	471.04	1.38	1.02	0.2024	540.44	1.69	1.02
0.0932	480.95	0.97	1.00	0.1017	459.97	0.85	0.99	0.1008	479.98	1.41	0.97	0.0984	544.72	1.86	1.01
0.0000	483.64			0.0000	462.58			0.000	485.12			0.0000	551.26		
AAD/K	0.26			AAD/K	0.28			AAD/K	0.45			AAD/K	0.84		
ARD (%)	0.055			ARD (%)	0.062			ARD (%)	0.097			ARD (%)	0.157		

$$AAD = \sum_{i=1}^{n} \frac{1}{n} \cdot \left| T_{exp} - T_{calc} \right|_i . \quad ARD = \sum_{i=1}^{n} \frac{1}{n} \cdot \left[100 \cdot \frac{\left| T_{exp} - T_{calc} \right|}{T_{exp}} \right]$$ where T_{exp} is experimental temperature in K and T_{calc} is calculated temperature in K. γ_1 and γ_2 are calculated by UNIQUAC model.

Table 5.9. Estimated activity coefficient at infinite dilution of four binary systems hexadecanol (1) + octadecanol (2), methyl myristate (1) + hexadecanol (2), tributyrin (1) + mononanoin (2) and dinonanoin (1) + octacosane (2) by the UNIQUAC model at γ_i^∞

Binary system	γ_1^∞	γ_2^∞
hexadecanol (1) + octadecanol (2)	0.70	1.41
methyl myristate (1) + hexadecanol (2)	0.52	1.57
tributyrin (1) + mononononanoin (2)	1.56	1.83
dinonanoin (1) + octacosane (2)	2.25	2.68

Figure 5.2 Vapor-liquid equilibria of hexadecanol (1) + octadecanol (2) at p = 1.73 kPa with $u(p)$ = 0.04 kPa. Experimental data from this work (■). Ideal behavior for liquid phase (--). The UNIQUAC model for liquid phase (—) and vapor phase (-··-). Predictions for liquid phase of the Modified UNIFAC with its lipid-based parameters [9] (···), and of the NIST modified UNIFAC (-···-).
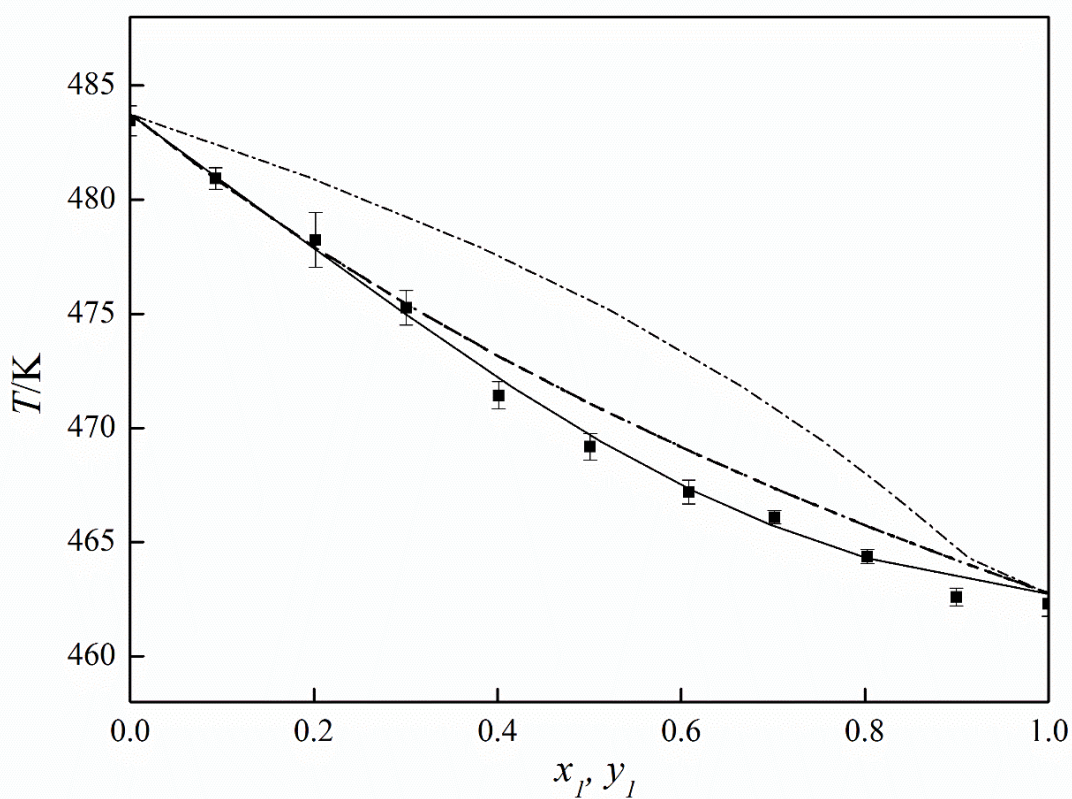
Figure 5.3 Vapor-liquid equilibria of methyl myristate (1) + hexadecanol (2) at p = 1.72 kPa with $u(p)$ = 0.04 kPa. Experimental data from this work (■). Ideal behavior for liquid phase (--). The UNIQUAC model for liquid phase (—) and vapor phase (-··-). Predictions for liquid phase of the Modified UNIFAC with its original parameters (···), and of the NIST modified UNIFAC (-···-).
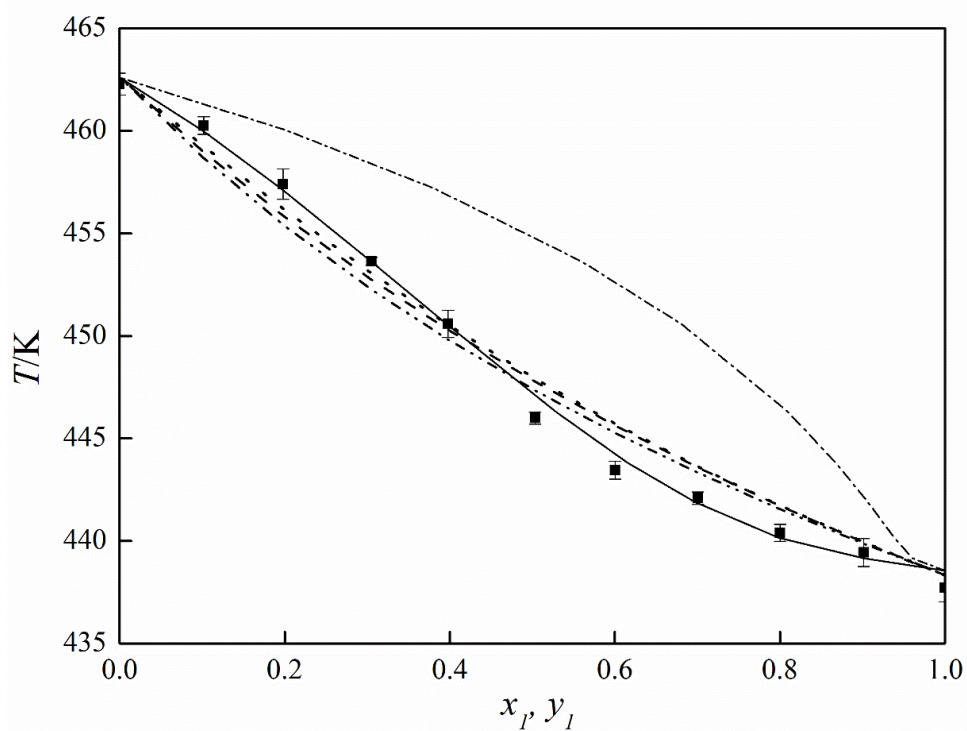
Figure 5.4 Vapor-liquid equilibria of tributyrin (1) + monononanoin (2) at p = 1.69 kPa with $u(p)$ = 0.04 kPa. Experimental data from this work (■). Ideal behavior for liquid phase (--). The UNIQUAC model for liquid phase (—) and vapor phase (-·-). Predictions for liquid phase of the Linear UNIFAC with its original parameters (···), and of the NIST modified UNIFAC (-···-).
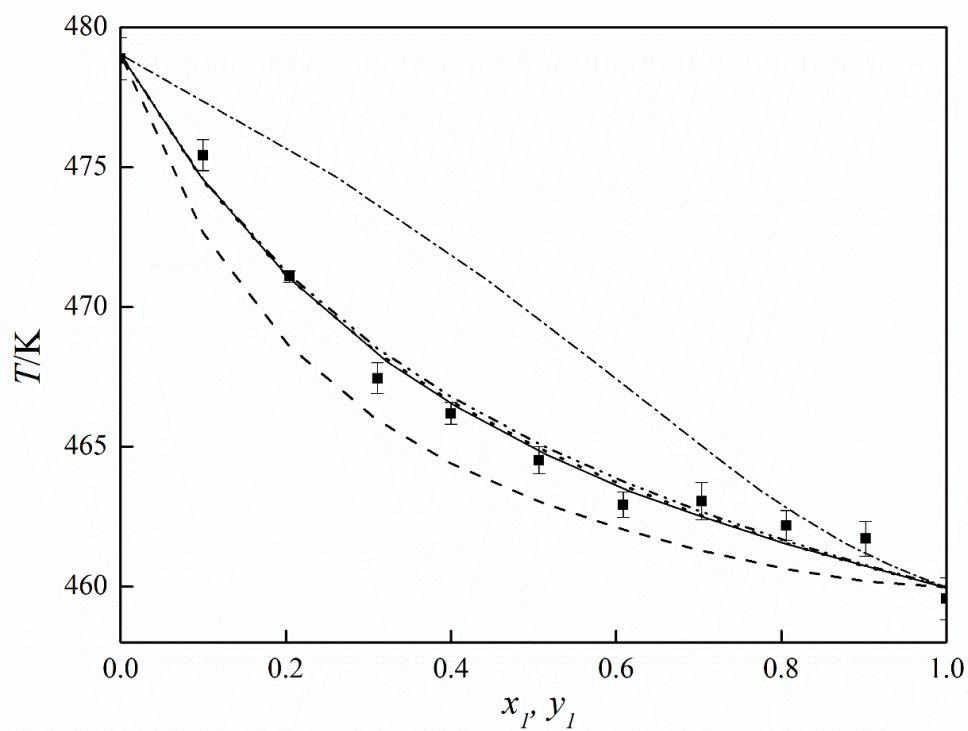
Figure 5.5 Vapor-liquid equilibria of dinonanoin (1) + octacosane (2) at p = 1.70 kPa with $u(p)$ = 0.04 kPa. Experimental data from this work (■). Ideal behavior for liquid phase (--). The UNIQUAC model for liquid phase (—) and vapor phase (-·-).Predictions for liquid phase of the Modified UNIFAC with its lipid-based parameters [9] (···), and of the NIST modified UNIFAC (-··-).
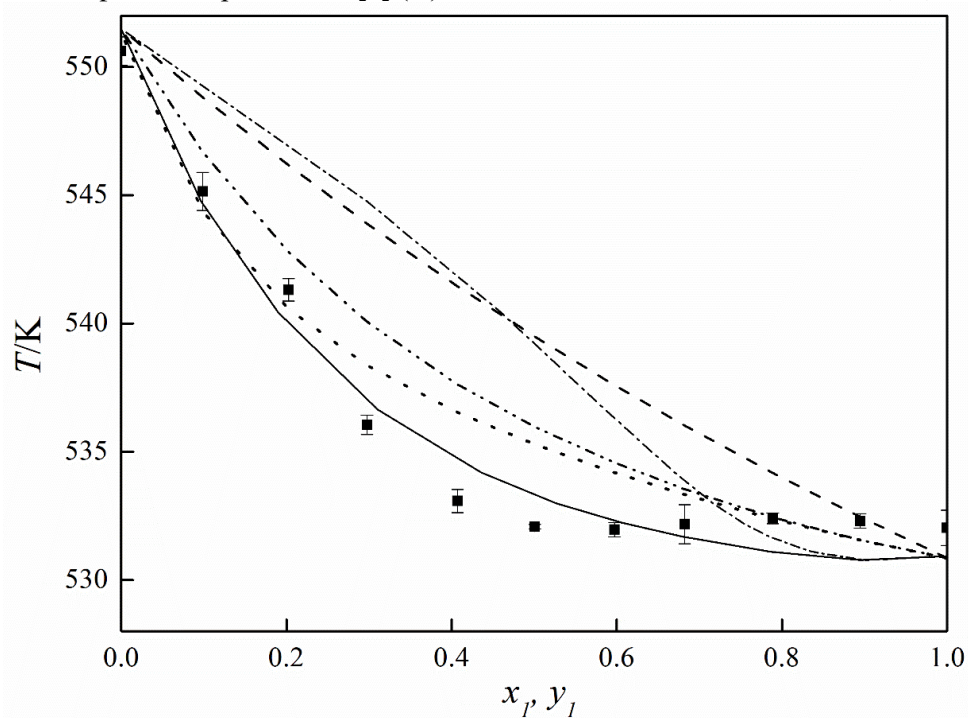
Figure 5.6 Liquid phase of the vapor-liquid equilibria of hexadecanol (1) + octadecanol (2) at $p = 1.73$ kPa with $u(p) = 0.04$ kPa from this work (■) and of decanol (1) + dodecanol (2) from literature at at $p = 13.33$ kPa [18] (▲) Ideal behavior for liquid phase (—). Predictions for liquid phase of the Modified UNIFAC with its original parameters (--).
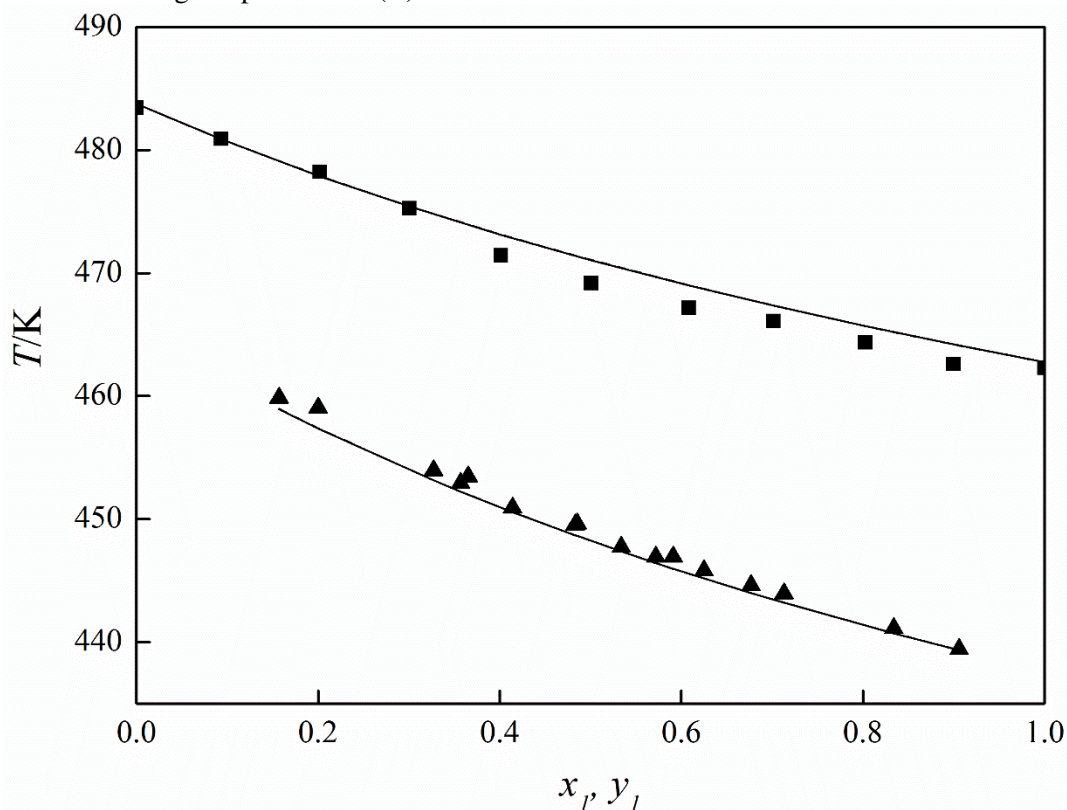
5.4 CONCLUSION

Novel boiling points for dinonanoin were obtained at subatmospheric pressures. Results were suitable when compared to other available data for di- and monoacylglycerols. VLE data were measured for hexadecanol + octadecanol at $p = 1.73$ kPa, methyl myristate + hexadecanol at $p = 1.72$ kPa, tributyrin + monononanoin at $p = 1.69$ kPa, and dinonanoin + octacosane at $p = 1.70$ kPa. Hexadecanol + octadecanol system presented an ideal behavior, differently from the others, in which azeotropes were found. The UNIQUAC model successfully correlated experimental data. The UNIFAC method in different versions: Linear [9,10], Modified [9,11], Dortmund [9,12], and the NIST modified [5] were evaluated as predictive tools. Results showed that there was not a single best model for all systems and besides some improvements in predictive capacity of these methods, there is a lack of qualified and diverse experimental data in order to develop better predictive tools based on the group contribution concept.

5.5 ACKNOWLEDGEMENTS

5.6 LITERATURE CITED

[1]   Agência Nacional do Petróleo, Gás Natural e Biocombustíveis. Biodiesel. **2017**.

[2]   Damaceno, D.S.; Ceriani. R. Vapor-liquid equilibria of monoacylglicerol + monoacylglicerol or alcohol or fatty acid at subatmospheric pressures. Fluid Phase Equilib. **2017**, 452, 135-142.

[3]   Damaceno, D.S.; Matricarde Falleiro, R.M.; Krähenhühl, M.A.; Meirelles, A.J.A.; Ceriani. R. Boiling points of short-chain partial acylglycerols and tocopherols at low pressures by the differential scanning calorimetry technique. J. Chem. Eng. Data **2014**, 59, 1515–1520.

[4]   Troni. K. L.; Damaceno. D.S.; Ceriani. R. Improving a variation of the DSC technique for measuring the boiling points of pure compounds at low pressures. J. Chem. Thermodyn. **2016**, 100, 191-197.

[5]   Kang, J.W.; Diky, V.; Frenkel, M. New modified UNIFAC parameters using critically evaluated phase equilibrium data. Fluid Phase Equilib. **2015**, 388, 128–141.

[6]   Bessa, L.C.B.A.; Ferreira, M.C.; Abreu, C.R.A.; Batista, E.A.C.; Meirelles, A.J.A. A new UNIFAC parameterization for the prediction of liquid-liquid equilibrium of biodiesel systems. Fluid Phase Equilib. **2016**, 425, 98–107.

[7]   Cunico, L.P.; Damaceno, D.S.; Matricarde Falleiro, R.M.; Sarup, B.; Abildskov, J.; Ceriani, R. Gani, R. Vapour liquid equilibria of monocaprylin plus palmitic acid or methyl stearate at P = (1.20 and 2.50) kPa by using DSC technique. J. Chem. Thermodyn. **2015**, 91, 108–115.

[8]   Belting, P.C.; Rarey, J.; Gmehling, J.; R. Ceriani. Chiavone-Filho, O.; Meirelles, A.J.A. Measurements of activity coefficients at infinite dilution in vegetable oils and capric acid using the dilutor technique. Fluid Phase Equilib. **2014**, 361, 215-222.

[9]   Damaceno, D.S.; Perederic, O.A.; Ceriani, R.; Kontogeorgi, G.M.; Gani. R. Improvement of predictive tools for vapor-liquid equilibrium based on group contribution methods applied to lipid technology. Fluid Phase Equilibria. **2017**, DOI: 10.1016/j.fluid.2017.12.009.

[10]   Hansen, H. K.; Coto, B.; Kuhlmann, B. UNIFAC with linearly temperature-dependent group-interaction parameters. Internal report. **1992**.

[11]   Larsen, B.; Rasmussen, P.; Fredenslund. A. A modified UNIFAC group-contribution model for prediction of phase equilibria and heats of mixing. Ind. Eng. Chem. Res. **1987**, 26, 2274–2286.

[12]   Gmehling, J.; Li, J.; Schiller, M. A modified UNIFAC model. 2. Present parameter matrix and results for different thermodynamic properties. Ind. Eng. Chem. Res. **1993**, 32, 178–193.

[13]   Fredenslund. A.; Jones, R., Prausnitz, J.M. Group-contribution estimation of activity coefficients in nonideal liquid mixtures. AIChE J. **1975**, 21, 1086–1099.

[14]   ASTM E1782-14. Standard Test Method for Determining Vapour Pressure by Thermal Analysis 1405. **2014.**

[15]   Kang, J.W.; Diky, V.; Chirico, R. D.; Magee, J. W.; Muzny, C. D.; Abdulagatov, I. A. F. Kazakov. M. Frenkel. Quality assessment algorithm for vapor−liquid equilibrium data. J. Chem. Eng. Data **2010**, 55, 3631−3640.

[16]   Abrams, D.S.; Prausnitz, J.M. Statistical thermodynamics of liquid mixtures: a new expression for the Excess Gibbs energy of partly or completely miscible systems. AIChE J. **1975**, 21, 116–128.

[17]   Gay, D. Algorithm 717. Subroutines for Maximum Likelihood and Quasi-Likelihood Estimation of Parameters in Nonlinear Regression Models. ACM Trans. on Math Software. **1993**, 19, 109-130.

[18]   Luecke, R.; Britt, H. The Estimation of Parameters in a Non-linear, Implicit Model. Technometrics. **1973**, 15.

[19]   Constantinescu, D.; Wichterle, I. Isothermal vapour–liquid equilibria and excess molar volume in the binary ethanol + methyl propanoate or methyl butanoate systems. Fluid Phase Equilib. **2002**, 203, 71-82.

[20]   Ortega, J.; Susial, P.; Alfonso, C. Isobaric vapor-liquid equilibrium of methyl butanoate with ethanol and 1-propanol binary systems. Chem. Eng. Data **1990**, 35, 216–219.

[21]   Rose, A.; Papahronis; B.T.; Williams, E.T. Experimental Measurement of Vapor-Liquid Equilibrium for Octanol- Decanol and Decanol-Dodecanol Binaries. Chem. Eng. Data Ser. **1958**, 3, 216-219.

CAPÍTULO 6

IMPROVEMENT OF PREDICTIVE TOOLS FOR VAPOR-LIQUID EQUILIBRIUM BASED ON GROUP CONTRIBUTION METHODS APPLIED TO LIPID TECHNOLOGY

Daniela S. Damaceno, Olivia A. Perederic, Roberta Ceriani, Georgios M. Kontogeorgis, Rafiqul Gani

Abstract: Predictive methodologies based on group contribution methods, such as UNIFAC, play a very important role in the design, analysis and optimization of separation processes found in oils, fats and biodiesel industries. However, the UNIFAC model has well-known limitations for complex molecular structures that the first-order functional groups are unable to handle. In the particular case of fatty systems these models are not able to adequately predict the non-ideality in the liquid phase. Consequently, a new set of functional groups is proposed to represent the lipid compounds, requiring thereby, new group interaction parameters. In this work, the performance of several UNIFAC variants, the Original-UNIFAC, the Linear-UNIFAC, Modified-UNIFAC and the Dortmund-UNIFAC is compared. The same set of experimental data and the parameter estimation method developed by Perederic et al. (2017) have been used. The database of measured data comes from a special lipids database developed in-house (SPEED Lipids database at KT-consortium, DTU, Denmark). All UNIFAC models using the new lipid-based parameters show, on average, improvements compared to the same models with their published parameters. There are rather small differences between the models and no single model is the best in all cases.

6.1 INTRODUCTION

In the recent years, the oil and fat industry has grown significantly, mainly as a result of increased production of biofuels, such as biodiesel. Among the unit operations required for biodiesel/biofuels production, those involving mass transfer, such as distillation and stripping, are among the most important steps in the separation and purification process. In these cases, the vapor-liquid equilibrium (VLE) description of the multicomponent mixture is essential to map the behavior of the different compounds under process conditions. As a consequence, the availability of predictive tools with acceptable accuracy and wide application for engineering design of oil/fat and biodiesel processes is underlined.

Predictive tools based on the group contribution method consider a mixture or any substance as an aggregate of functional groups present in the molecules that constitute it. Therefore, the mixture properties are the result of the sum of contributions of each of these groups, which are predicted through adjustable group interaction parameters. These group interaction-parameters are estimated through regression with carefully selected experimentally measured data. In the case of pure component properties, the contributions of the groups representing the compounds are used to estimate the corresponding property. Like the mixture properties, measured pure component property data are used to estimate the group parameters. The advantage of this type of property estimation method is to allow the calculation of thermophysical properties (e.g. boiling points, heat capacity, critical point, densities) of pure compounds or multicomponent mixtures, for example, phase equilibria (activity coefficients of compounds in liquid phase in equilibrium with a vapor phase) of oil and fats. Thus, the use of predictive models based on group contribution methods in design, analysis and optimization of separation processes of oils, fats and biodiesel industries is very important. In particular, those group contribution methods associated with phase equilibrium are among the most important. Group contribution methods for activity coefficients are a valuable tool for process design in the absence of data or when insufficient or inaccurate data are available [1].

Original UNIFAC (UNIQUAC Functional-group Activity Coefficients) [2] and its variants [3-9] has limitations that are intrinsic to their generality, especially the so-called proximity effects. Other methods based on the group contribution approach share this limitation [10]. These proximity effects are particularly important when two or more functional groups are situated at equal or adjacent positions of the carbon atom. Recent works have indicated that these limitations of the UNIFAC method also affect the predictions involving fatty systems.

Cunico et al. [11] and Belting et al. [12], evaluating the Original-UNIFAC and UNIFAC-Dortmund, observed that they were not able to adequately predict the non-ideality of the liquid phase of fatty systems, and they proposed changes in the division and/or interaction parameters of the functional groups.

Considering the limitations due to proximity effects and trying to enhance the accuracy of group contribution methods for estimation of activity coefficients related to applications in lipids technology, this work presents a new matrix of Linear-UNIFAC [5], Modified-UNIFAC [3] and Dortmund-UNIFAC [4] models, especially suited for the estimation of VLE of mixture with lipids compounds, as well as an evaluation of the performance of the published [3-5] and the new lipid-based model-parameters. For purposes of completion purposes, the performance of the Original-UNIFAC model with its published and lipid-based parameters [13] is also included in the study. The same database and parameter estimation method developed [13] are applied to all UNIFAC-based models.

6.2 MODELS DESCRIPTION

In group contribution methods, the activity coefficient of compound i in liquid solution is calculated from the sum of the entropic contributions, related to the size and shape differences between molecules, and the residual contribution, which accounts for the intermolecular interactions of functional groups of multicomponent mixtures, as represented by Eq. 1 [10].

$$\ln \gamma_i = \ln \gamma_i^C + \ln \gamma_i^R \tag{1}$$

The general form of the combinatorial-term equation applied to all the UNIFAC models studied in this manuscript is described by Eq. 2. Original-UNIFAC and Linear-UNIFAC models have the same form for the combinatorial part. Modified-UNIFAC and Dortmund-UNIFAC models on the other hand have different volume fractions terms within the combinatorial part, as listed in Table 6.1. The Modified-UNIFAC [3] model uses a modified volume fraction of $r^{2/3}$, as suggested by Kikic et al. [14], while the Dortmund-UNIFAC model is based on volume fraction of $r^{3/4}$. Both modified volume fractions are of semi-empirical basis and they are shown to work well for mixtures of compounds with very different sizes [4] but

they nevertheless fail for polymer solutions. The Modified-UNIFAC model is the only model that does not have the Staverman-Guggenheim correction term in the combinatorial part [3]. The surface and volume parameters used for the Original-, Linear- and Modified-UNIFAC models are determined through Bondi's method [15], while for the Dortmund-UNIFAC model they are fitted from experimental data together with group interaction-parameters [4]. This poses a problem for extension of the Dortmund-UNIFAC model for the lipid-compounds and regression of the group-interaction parameters.

The residual term of Eq. 1 has the same expression for all models (Eq. 3). The difference between the models is represented by the group-group interaction parameter expression (a_{mn}), as represented by Eq.6 and given in Table 6.2. For Original-UNIFAC model the binary group-interaction parameters are temperature independent. In Linear- and Modified-UNIFAC models the group-interaction parameters are temperature dependent. In Dortmund-UNIFAC model the group-interaction parameters are temperature dependent but a different function is employed.

$$\ln \gamma_i^C = \ln \frac{r_i^{C_0}}{\sum_j x_j r_j^{C_0}} + 1 - \frac{r_i^{C_0}}{\sum_j x_j r_j^{C_0}} - C_1 \left(\ln \left(\frac{\Phi_i}{\theta_i} \right) + 1 - \frac{\Phi_i}{\theta_i} \right) \tag{2}$$

$$\Phi_i = \frac{r_i}{\sum_j x_j r_j} \tag{3}$$

$$\theta_i = \frac{q_i}{\sum_j x_j q_j} \tag{4}$$

Table 6.1 C_0 and C_1 of Eq. 2

Model	C_0	C_1
Original-UNIFAC	1	$5q_i$
Linear-UNIFAC	1	$5\ q_i$
Modified-UNIFAC	$2/3$	0
Dortmund-UNIFAC	$\frac{3}{4}$	$5\ q_i$

$$\ln \gamma_i^R = \sum_K^{groups} v_k^{(i)} \left[\ln \Gamma_k - \ln \Gamma_k^{(i)} \right] \tag{3}$$

$$ln\Gamma_k = Q_k \cdot \left[1 - ln \left(\sum_m \Theta_m \Psi_{mk} \right) - \sum_m \left(\theta_m \Psi_{mk} \Big/ \sum_n \Theta_n \Psi_{nm} \right) \right] \tag{4}$$

$$\Theta_m = \frac{Q_m X_m}{\sum_n Q_n X_n} \tag{5}$$

$$X_m = \frac{\sum_i^M v_m^{(i)} x_i}{\sum_i^M \sum_j^N v_j^{(i)} x_i} \tag{6}$$

$$\Psi_{mn} = \exp\left(\frac{-a_{m,n}}{T}\right) \tag{7}$$

$$a_{m,n} = A_0 a_{mn,0} + A_1 a_{mn,1} + A_2 a_{mn,2} \tag{8}$$

Table 6. 2 A_0, A_1 and A_2 of Eq. 6

Model	A_0	A_1	A_2
Original-UNIFAC	1	0	0
Linear-UNIFAC	1	T-T_0	0
Modified-UNIFAC	1	T-T_0	$T\ln(T_0/T) + T - T_0$
Dortmund-UNIFAC	1	T	T^2

T_0 is reference temperature ($T_0 = 298.15$ K)

6.3 PARAMETER ESTIMATION METHOD

The estimation of a new set of group-interaction parameters for Linear-UNIFAC, Modified-UNIFAC and Dortmund-UNIFAC models dedicated to systems with lipid compounds was performed using the systematic parameter estimation method of Perederic et al. [13] and employing an in-house database, SPEED Lipids Database, also used by Perederic et al. [13]. The method is divided into three hierarchical parts: a) data collection and analysis; b) data organization and selection; and finally c) parameter estimation according to an estimation order and validation. All parts are hereafter briefly described.

6.3.1 Data Collection and Analysis

Considering the SPEED Lipids Database [13] is already available, according to the employed method [13], the next step is to analyze the collected experimental data. Thus, pure compound data availability (e.g.: vapor pressure) and transcript errors (outlier points) are checked. Also, thermodynamic consistency tests [16] are applied to all collected data sets. The TDE (ThermoData Engine) software from NIST is used to calculate the quality factor (Q_{VLE})

for all binary systems. Note that the same data and analysis are also used by Perederic et al. [13].

6.3.2 Data Organization and Selection

The first step of the data organization and selection is the compound group definition and assignment. In this step the main groups and subgroups of the mixtures are defined and identified (see Table 6.3). The main groups and subgroups of the UNIFAC models are listed and assigned to represent the compounds found in the VLE datasets, in this case the SPEED Lipids database. The group selection was based on Original-UNIFAC model division/assignment [13]. All the compounds found in this database are represented by the selected model groups and subgroups. Also, the two new functional groups proposed by Perederic et al [13] to better describe systems containing glycerol [13,17-18] and acylglycerols [13,17], are used in this work, which are GLY and OH_{acyl} groups. In this work, all UNIFAC models have the same groups division, however, to the subgroups of Dortmund-UNIFAC has an exceptional [6], this UNIFAC-based model has two OH subgroups divisions for R_k and Q_k parameters (see Table 6.3), the OH primary (OH_p) and secondary (OH_s). It is important to underline that, the same OH_p and OH_s division was applied to the OH_{acyl} group to Dortmund-UNIFAC (see Table 6.3). For this case, the monoacylglycerols, which have two OH_{acyl} groups, where described with one $OH_{acyl,p}$ and one $OH_{acyl,s}$. For example, the system oleic acid + ethanol is represented by the following main groups: CH_2, CH=CH, OH and COOH. In this example, the OH subgroup is OH for Linear- and Modified-UNIFACs, and OHp (primary) for Dortmund-UNIFAC. The surface and volume parameters for the functional groups used are given in Table 6.3.

Table 6.3 Area (Q_k) and volume (R_k) parameters for the groups used for the UNIFAC models.

Main Group	Sub group	Original-, Linear- and Modified-UNIFAC [10]		Dortmund-UNIFAC [6]	
		R_k	Q_k	R_k	Q_k
	CH3	0.9011	0.8480	0.6325	1.0608
CH_2	CH2	0.6744	0.5400	0.6325	0.7081
	CH	0.4469	0.2280	0.6325	0.3554
C=C	CH=CH	1.1167	0.8670	1.2832	1.2489
	OH	1.0000	1.2000	-	-
OH	OHp[*a]	-	-	1.2302	0.8927
	OHs[*a]	-	-	1.0630	0.8663
CH_3OH	CH3OH	1.4311	1.4320	0.8585	0.9938
H_2O	H2O	0.9200	1.4000	1.7334	2.4561
CH_3CO	CH3CO	1.6724	1.4880	1.7048	1.6700
CCOO	CH2COO	1.6764	1.4200	1.2700	1.4228
COOH	COOH	1.3013	1.2240	0.8000	0.9215
	OH$_{acyl}$	1.0000	1.2000	-	-
OH_{acyl}[*b]	OH$_{acylp}$[*c]	-	-	1.2302	0.8927
	OH$_{acyls}$[*c]	-	-	1.0630	0.8663
GLY[*d]	GLY[*e]	4.7957	4.9080	-	-
	GLY[*f]	-	-	5.4209	4.4233

[*a] OHp and OHs subgroups are used only for Dortmund UNIFAC
[*b] OHacyl describes mono- and diacylglycerols molecules and uses same R and Q as OH group
[*c] For Dortmund UNIFAC monoacylglycerols are described with one OH$_{acylp}$ and one OH$_{acyls}$, while diacyglycerols are described with one OH$_{acylp}$
[*d] GLY represents the glycerol molecule. R and Q parameters are calculated from contribution of constitutive groups
[*e] For all UNIFAC models except Dortmund GLY is considered as 2 CH_2, 1 CH, 3 OH
[*f] For Dortmund UNIFAC GLY is considered as 2 CH_2, 1 CH, 2 OHp, 1 OHs

The second step of the data organization and selection is data category assignment and quality sorting. The data organization algorithm of Perederic et al. [13] is used to assign the data in different category-groups according to binary-interaction provided. A category-group contains VLE data sets that involve the same binary group interaction parameters. The Algorithm A provides the following notation for the category-groups: X.M.N, where: X is the number of group-interaction parameters involved within a category-group, M is the number of binary pairs that need to be estimated, and N is the type of involved pairs of the mixture (the user can select the order of parameter estimation and this will not affect the final result). Examples are presented in Table 6.4. The Algorithm A and more details of the method are presented by Perederic et al. [13].

Table 6.4 Data organization through Algorithm A

Binary systems	Interaction pars	X	M	N	Category-groups: X.M.N
octanoic acid + hexanoic acid	CH_2-COOH	X=1, one pair of interaction parameter	M=1, one pair of interaction parameter to be estimated	M=1, the user can select the order to estimate, this order will not affect the next step.	1.1.1
ethyl myristate + ethyl palmitate	CH2-CCOO	X=1, one pair of interaction parameter	M=1, one pair of interaction parameter to be estimated	M=2, the user can select the order to estimate, this order will not affect the next step.	1.1.2
methyl dodecanoate + methanol	CH_2-CCOO; CH_2-CH_3OH; CCOO-CH_3OH	X=3, three pairs of interaction parameters	M=2, two pairs of interaction parameter to be estimated, because CH2-CCOO was estimated in step 1.1.2	M=1, the user can select the order to estimate, this order will not affect the next step.	3.2.1
methyl dodecanoate + ethanol	CH_2-CCOO; CH_2-OH; CCOO-OH	X=3, three pairs of interaction parameters	M=2, two pairs of interaction parameter to be estimated, because CH2-CCOO was estimated in step 1.1.2	M=2, the user can select the order to estimate, this order will not affect the next step	3.2.2

The third step of data organization and selection is the data selection. The best data is chosen by using a selection algorithm, Algorithm B. The foundation of this step is the quality factor and the data availability. Each category-group is independently evaluated with this algorithm. If there are data sets with quality value equal or higher than 0.5 those come first in the evaluation list (descending order). Then, if a binary system has quality factor below 0.5, the next step is to evaluate if, in this category-groups, there are other systems with quality factor above 0.5. If there are indeed other systems, the data set is not selected, but if there are no other systems available, the data set is selected. For example: the system octanoic acid + hexanoic acid, from the category-group: 1.1.1, has a quality factor equal to 0.650, which means, that this system will be used for parameter estimation. Another example, the system methyl dodecanoate + ethanol, from the category-group 3.2.2, has quality factor equal to 0.250, and the only other available system in this category-group has also quality factor equal to 0.250. According to the algorithm, both systems will be used for the estimation. The Algorithm B and more details are given in Ref. [13].

Table 6.5 gives the results of organization and selection part of the method. The same datasets are selected/used for parameter estimation as in Perederic et al. [13], ensuring thus a fair comparison between all UNIFAC-based models. Table 6.5 lists the order in which the data and corresponding groups are to be estimated, the number of available systems and the number of selected systems used for estimation of the interaction parameters in each category-group.

Table 6.5. gives the results of organization and selection part of the method. The same datasets are selected/used for parameter estimation as in Perederic et al. [13], ensuring thus a fair comparison between all UNIFAC-based models. Table 6.5 lists the order in which the data and corresponding groups are to be estimated, the number of available systems and the number of selected systems used for estimation of the interaction parameters in each category-group.

Table 6.5 Data organization and selection of binary mixtures database used for parameter estimation [13]

Category-group [a]	Binary system type		Available systems	Selected systems
	Compound I	Compound II		
1.1.1.	Saturated Fatty Acids	Saturated Fatty Acids	23	4
1.1.2.	Saturated Ester	Saturated Ester or Hydrocarbon	26	9
1.1.3.	Glycerol	Methanol	20	9
1.1.4.	Glycerol	Water	44	14
3.1.1.	Saturated Fatty Acids	Saturated Ester	1	1
3.2.1.	Saturated Ester	Methanol	5	5
3.2.2.	Saturated. Ester	Ethanol	2	2
3.2.3.	Saturated Monoacylglycerol	Saturated Ester	2	2
3.2.4.	Glycerol	Saturated Alcohol	34	11
3.2.5.	Unsaturated Fatty Acids	Saturated Fatty Acid or Hydrocarbon	3	1
3.2.6.	Unsaturated Ester or Triacylglycerol	Saturated Ester or Hydrocarbon	3	2
6.1.1.	Saturated Monoacylglycerol	Saturated Fatty Acids	2	2
6.1.2.	Unsaturated. Ester	Methanol	2	1
6.1.3.	Unsaturated Ester	Ethanol	2	2
6.1.4.	Unsaturated Fatty Acids	Methanol	1	1
6.1.5.	Saturated Fatty Acids	Saturated Alcohol	2	2
6.3.1.	Unsaturated Triacylglycerol	Acetone	1	1
6.3.2.	Saturated Fatty Acids	Acetone	1	1

[a] The category-group is described in Data Organization and Selection section [13]

6.3.3   Parameter Estimation and Validation

The parameter estimation task is performed by minimization of the summation of least squares of the pressure, as the objective function (Eq. 9) shows. The optimization problem is solved with the Harwell subroutine VA07AD [19], in this way, the full set of parameters can be regressed efficiently and quickly [13].

$$F_{obj} = \sum_i \left(\frac{P^{experimental} - P^{calculated}}{P^{experimental}} \right)_i^2 + \frac{1}{\beta} \sum_m \sum_n \left(a_{mn} - a_{mn}^0 \right)^2 \tag{9}$$

where, F_{obj} is the objective function, $P^{experimental}$ is the experimental pressure, and $P^{calculated}$ is the calculated pressure, a_{mn} is the estimated binary interaction parameter, and a^0_{mn} is the initial value of the binary interaction parameter. The initial values are in this work the Linear- [5], Modified- [3] and Dortmund- [4] UNIFAC model group-interaction parameter values, or zero for the GLY and OH$_{acyl}$ interactions. β is an empirical term, that it can range from 10^3 up to 10^5, in this work was set equal to 10^5 [13], based on trial and error from several regressions, and monitoring the first and second parts of Eq 9 [11,17,20]. So, the first part of Eq. 9 represents the residual pressure, and the second part is the regularization term, which only the most sensitive parameters are allowed to deviate from their nominal values (a^0_{mn}), avoiding unreliable values to the estimated parameters (a_{mn}) [11,17,20].

Finally, to evaluate the performance of the models, all data sets from the SPEED Lipids database are employed to compare them with those predicted with the new parameters and the published parameters. For this purpose, the average relative deviation (ARD, %), Eq. 10, is used.

$$ARD(\%) = \frac{1}{N} \sum_{i=1}^{N} \left| \frac{P^{experimental} - P^{calculated}}{P^{experimental}} \right| . 100 \tag{10}$$

where, ARD is the average relative deviation in %, $P^{experimental}$ is the experimentally measured pressure, and $P^{calculated}$ is the calculated pressure.

6.4 RESULTS AND DISCUSSION

New binary interaction parameters for lipids systems were regressed for the Linear-, Modified- and Dortmund-UNIFAC models. All the new, lipids-based group-interaction parameters are given in Table 6.6, along with the parameters for Original-UNIFAC model [13]. The temperature ranges for the VLE data for each binary system is also given in Table 6.6.

Table 6.7 lists the ARD (%) for all VLE binary datasets retrieved from the SPEED lipids database in terms of category-group of the dataset for all the UNIFAC-based models with their published parameters and with the lipids-based group interaction parameters from this work. Furthermore, Table 6.7 gives the consistency test scores (Q_{VLE}) for each data-type (category-group) of the mixtures from the database, indicating the quality of the data.

In general, the Linear-UNIFAC model with lipids-based group-interaction parameters show the best performance as it has the lowest overall deviation of about 8.9%. This is about 1% better than the Dortmund-UNIFAC model, which is the second best model (also with lipids-based group-interaction parameters). The Modified-UNIFAC using lipids-based group interaction parameters show the lowest deviation for the category-group of saturated fatty acid + saturated ester mixtures (ARD = 1.5%). Also, lipids-based Dortmund-UNIFAC model gives the best performance for the category-group of saturated ester + saturated ester or hydrocarbon mixtures with ARD = 4.8%. Still, the general conclusion is that differences between the UNIFAC-based models with the lipids-based group-interaction parameters is rather small as all four models have deviations are around 8–14%. All four models perform far better than when the published parameters are used where the deviations are about or above 20%.

Figure 6.1 shows the performance of all models (using published and lipids-based group-interaction parameters) for the system dodecanoic acid + methyl dodecanoate at 0.5 kPa [21]. All models show similar behavior, and better prediction is achieved with the lipids-based group-interaction parameters (given in Table 6.6).

Figure 6.1 Binary system methyl dodecanoate (x_1) + dodecanoic acid (x_2) at 0.5 kPa. Experimental data [18] (●). Published parameters models: Original- (--), Linear- (--) Modified- (--) and Dortmund-UNIFAC (--). Lipids-based group interaction parameters models: Original- (—), Linear- (—), Modified- (—) and Dortmund-UNIFAC (—)
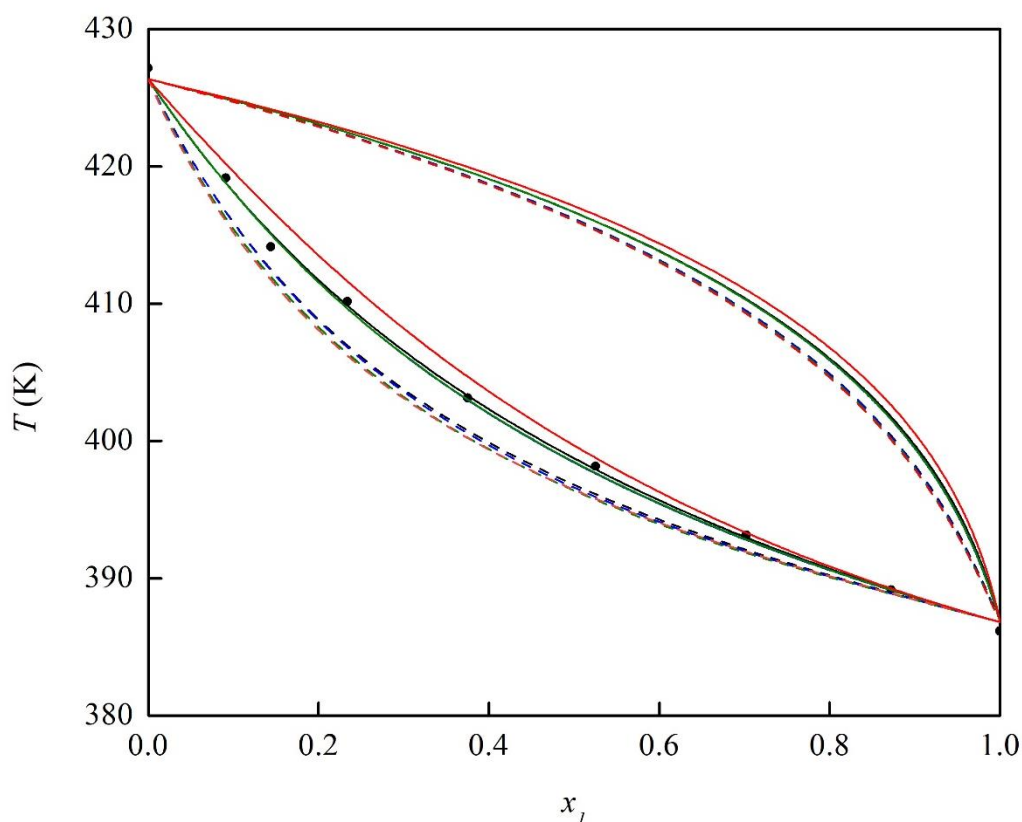
Figure 6.2 shows the performance of the new group GLY (glycerol group) for the binary system glycerol + water at 14.19 kPa [22]. The Linear- and Modified-UNIFAC models with lipids-based group-interaction parameters have the best predictions for this system, which is the most complex among all systems considered (with deviations around 50% for the best performing models). The ARD (%) for the group-categories: glycerol + methanol, glycerol + water and glycerol + alcohols, show that all UNIFAC-based models with lipids-based group-interaction parameters have similar performances, and lower deviations when compared with UNIFAC-based models with published parameters (given in Table 6.7). The Dortmund-UNIFAC model with published parameters give the highest deviation for the group-category glycerol + water, while with the lipids-based group-interaction parameters the same model showed a significant improvement, a reduction from an ARD of 198% [4] to 56% (this work). It is important to highlight that for the calculations with the published UNIFAC parameters the glycerol compound is considered as 2 CH_2, 1 CH and 3 OH, except for Dortmund-UNIFAC, where glycerol is considered as 2 CH_2, 1 CH, 2 OH_p and 1 OH_s. The deviations for all glycerol-containing mixtures (with water, methanol or other alcohols) are the highest among all systems

considered. These are cross-associating systems with very strong hydrogen bonding both self and cross-assosciations. The UNIFAC-models account for such effects only indirectly (interaction parameters and local composition concept) and better performance for such complex mixtures can be obtained with association equations of state like CPA [23] and SAFT [24], as shown in literature by Tsivintzelis et al. [25]

Figure 6.2 Binary system water (x_1) + glycerol (x_2) at 14.19 kPa. Experimental data [19] (●). Published parameters models: Original- (--), Linear- (--) Modified- (--) and Dortmund-UNIFAC (--). Lipids-based group interaction parameters models: Original- (—), Linear- (—), Modified- (—) and Dortmund-UNIFAC (—)
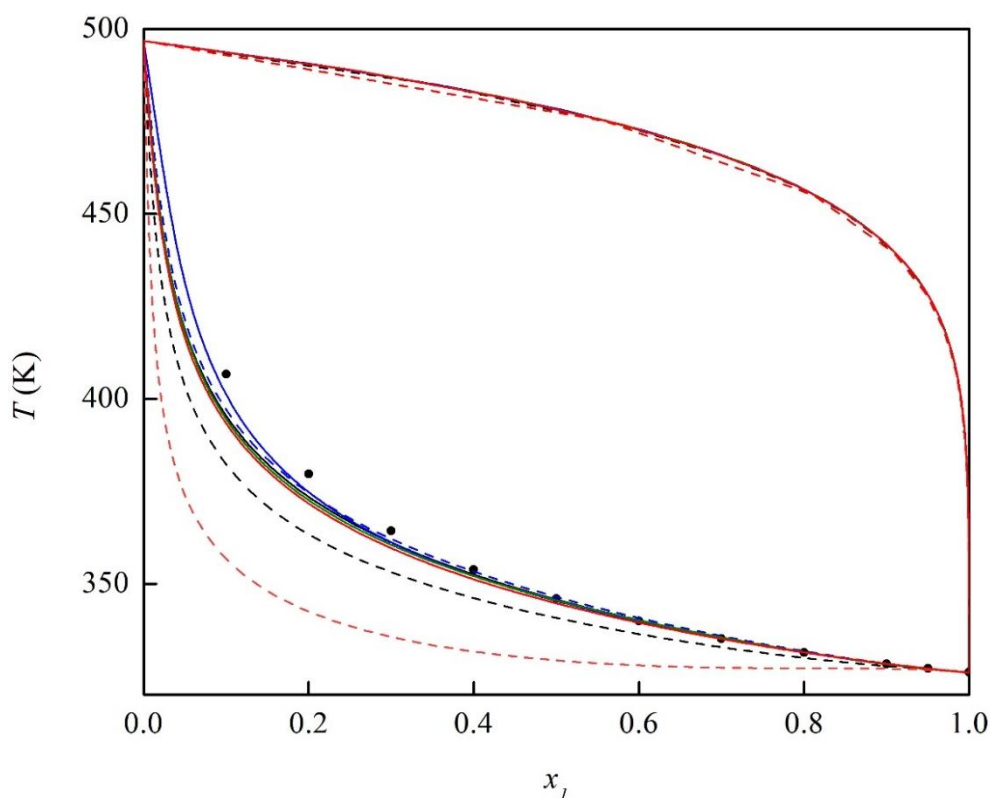
The new group OH_{acyl} introduced for the UNIFAC-based models with lipids-based group-interaction parameters, demonstrated improved predictions for mixtures with acylglycerols, such as monoacylglycerols, when compared with the UNIFAC-based models using the published parameters. Figure 6.3 shows a poor prediction of the Modified- and Dortmund-UNIFAC models using the published parameters. Both models with published parameters overestimate the temperature of monoacylglycerols + fatty acids systems.

Figure 6.3 Binary system monocaprylin (x_1) + palmitic acid (x_2) at 1.20 kPa. Experimental data [11] (●). Published parameters models: Original- (--), Linear- (--) Modified- (--) and Dortmund-UNIFAC (--). Lipids-based group interaction parameters models: Original- (—), Linear- (—), Modified- (—) and Dortmund-UNIFAC (—)
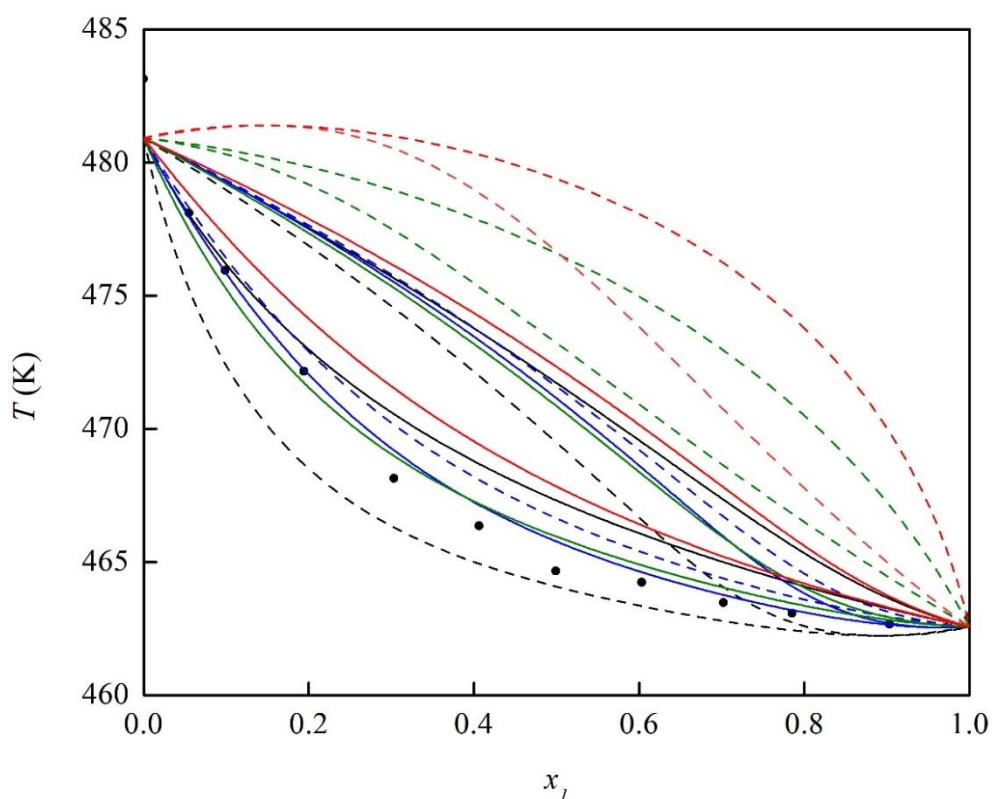
Figure 6.4 shows the total value of ARD (%) versus number of data points for the UNIFAC-based models with lipids group-interaction parameters. It is possible to observe that the model with the lowest deviation is the Linear-UNIFAC model, while Original-UNIFAC has the highest deviation. Among all models, Original-UNIFAC is the only one with temperature-independent parameters, and has thus fewer adjustable parameters compared to the other three UNIFAC variant models. Figure 6.5 presents the total ARD (%) versus the number of data points for the Linear-UNIFAC model with published and lipids group-interaction parameters, which shows an improvement for the lipids-based model.

Figure 6.4 Total ARD (%) for the Original- (—), Linear- (—), Modified- (—) and Dortmund-UNIFAC (—) using the lipids-based group interaction parameters for the UNIFAC models versus the total number of data points
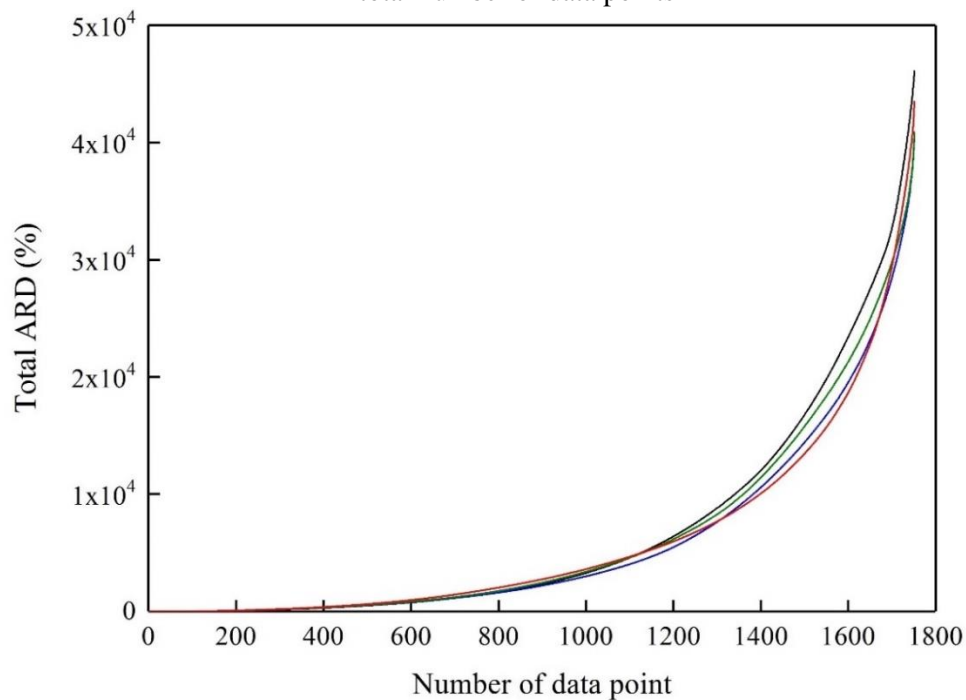
Figure 6. 5 Total ARD (%) for the published parameters of the Original-UNIFAC (--), and the lipids group-interaction parameters for the Linear-UNIFAC (—) versus the total number of data points
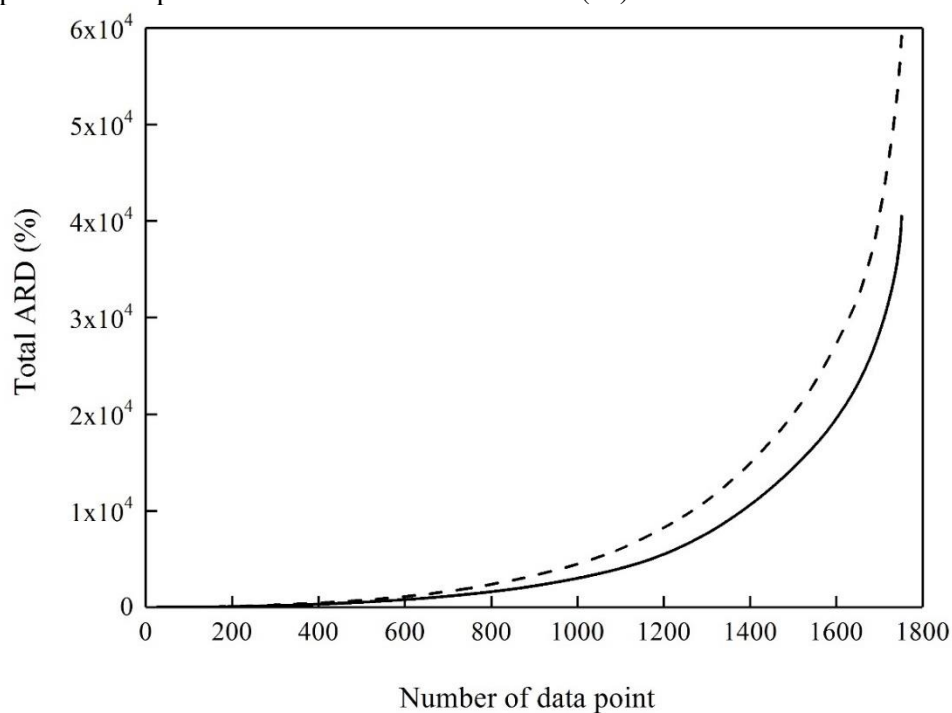
The parity plots, experimental vs. calculated pressure for all data points, varying from sub-atmospheric pressure to ≈ 101 kPa (except for the glycerol systems), and for all UNIFAC-based models with published and lipids group-interaction parameters are presented in Figure 6.6. The glycerol systems were not included due to the large deviations for both sets of parameter values. Figure 6.6 (a) and (b) shows that Original- and Linear-UNIFAC models with published and lipids-based group-interaction parameters underestimate the pressure values for lipids systems. On the other hand, Figure 6.6 (c) for the Modified-UNIFAC model with both sets of parameters shows that this model tends to overestimate the pressure of the lipids systems. The Dortmund-UNIFAC model with published parameters underestimates the pressure, while using the lipids group-interaction parameters, an overestimation of the pressure is observed. For all models, published and lipids UNIFAC, a high deviation is observed, around 100 kPa, when compared with data at lower pressures (e.g.: systems with alcohol compounds), though, with the lipids-based group-interaction parameters it is possible to observe a lower deviation.

Figure 6. 6 Experimental pressure (P_{exp}) versus calculate pressure (P_{calc}) of all data points (except for glycerol mixtures) using published parameters Original-UNIFAC (●), lipids group-interaction parameters Original-UNIFAC (○), published parameters Linear-UNIFAC (●), lipids group-interaction parameters Linear-UNIFAC (○), published parameters Modified-UNIFAC (●), lipids group-interaction parameters Modified-UNIFAC (○) and published parameters Dortmund-UNIFAC (●), lipids group-interaction parameters Dortmund-UNIFAC (○)

Table 6.6a Group-interaction parameters a_{mn0}, a_{mn1} and a_{mn2} for the Original-, Linear-, Modified- and Dortmund-UNIFAC models fitted to lipid data

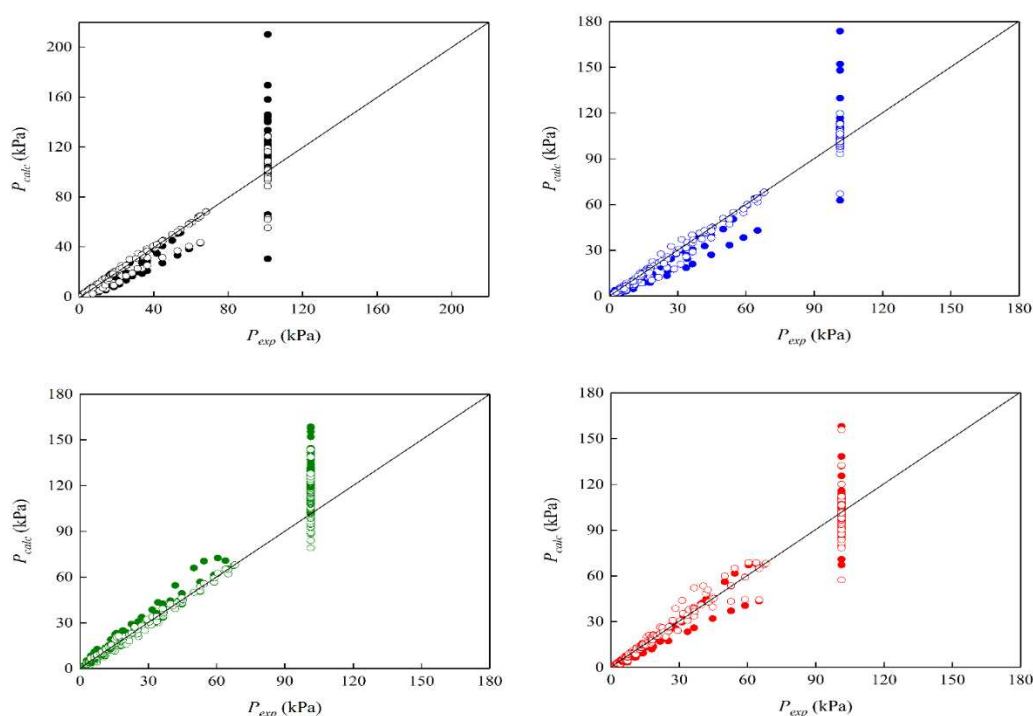| Groups (mn)	Original Lipids	Linear Lipids		Modified Lipids			Dortmund Lipids			Temperature range	
	a_{mn0}	a_{mn0}	a_{mn1}	a_{mn0}	a_{mn1}	a_{mn2}	a_{mn0}	a_{mn1}	a_{mn2}	T_{min} (K)	T_{max} (K)
CH$_2$/COOH	320.95	685.10	-2.0030	614.54	1.3170	-7.3900	1315.00	-5.0072	0.0088	371.65	524.25
COOH/CH$_2$	1337.28	64.02	-2.4591	151.63	-1.7430	4.0193	1970.40	-9.2756	0.0098		
CH$_2$/CCOO	459.02	277.81	0.0905	253.66	-0.0909	-3.7850	65.65	2.6493	-0.0008	327.37	535.50
CCOO/CH$_2$	395.55	76.42	-0.9890	149.49	-0.9999	0.5518	348.47	-2.2544	0.0011		
GLY/CH$_3$OH	159.54	86.31	0.0600	191.55	-1.5700	-8.3300	-96.34	0.0726	0.0005	282.55	561.18
CH$_3$OH/GLY	-7.25	49.44	0.0700	-53.90	0.0220	0.2500	-73.29	0.6586	0.0001		
GLY/H$_2$O	138.70	258.23	-1.8800	-268.78	1.1600	-6.8700	-12.62	-0.5880	-0.0001	153.15	563.18
H$_2$O/GLY	140.77	-232.25	1.3010	491.57	-5.1800	-5.2400	-15.60	-0.0260	0.0001		
COOH/CCOO	-256.39	-280.38	0.0599	-211.13	-0.5032	-1.1867	18.58	-0.7700	0.0003	386.15	427.15
CCOO/COOH	660.60	610.73	-2.0130	244.68	0.0180	3.6303	57.89	0.6900	-0.0005		
CH$_2$/CH$_3$OH	515.53	757.92	0.3612	1321.00	-0.0126	9.0000	2791.12	-2.0988	-0.0013	337.63	617.50
CH$_3$OH/CH$_2$	41.86	21.55	-0.4125	15.50	-0.7456	0.6924	82.61	-0.4901	-0.0002		
CCOO/CH$_3$OH	421.58	369.86	0.1220	395.10	-0.5610	-0.1005	294.76	0.2493	0.0010		
CH$_3$OH/CCOO	229.89	5.45	-3.6900	-49.46	-0.7764	0.4687	299.76	-1.2700	-0.0001		
CH$_2$/OH	613.72	874.14	-0.8130	629.70	0.5774	8.7730	2159.41	-4.4226	0.0005	351.46	617.50
OH/CH$_2$	35.84	35.59	-1.4292	405.36	-3.4830	-2.7090	1946.97	-3.2692	0.0001		
CCOO/OH	406.11	427.70	-0.8859	266.90	-0.9990	0.6670	788.63	3.5416	-0.0002		
OH/CCOO	555.63	212.89	-0.0080	169.10	0.3607	0.1110	1176.55	-5.2856	0.0080		
CH$_2$/OH$_{acyl}$	50.30	1264.6	-6.6027	645.14	0.6569	8.4845	2252.43	-4.3074	0.0007	461.24	493.38
OH$_{acyl}$/CH$_2$	499.23	297.02	0.5200	418.85	-3.4137	-2.9607	1860.42	-3.6451	-0.0008		
CCOO/OH$_{acyl}$	253.23	242.30	-0.4278	-632.85	3.3000	7.2200	788.73	9.4865	0.0384		
OH$_{acyl}$/CCOO	124.02	104.60	-0.7800	83.48	-0.0870	1.3875	799.93	-4.8488	0.0080		
GLY/OH	120.90	41.27	-1.1890	478.60	-1.3700	-8.4900	327.01	0.2139	0.0006	232.15	561.18
OH/GLY	128.76	-18.85	-1.5900	-217.53	-2.411	-2.1300	-287.98	-0.0030	-0.0001		
GLY/CH$_2$	45.83	198.50	0.8480	86.36	2.3100	1.9990	18.58	0.2598	0.0006		
CH$_2$/GLY	137.56	232.00	1.2269	966.13	-3.5631	5.9958	525.55	-0.4333	-0.0018		

Table 6.6b (continuation.). Group-interaction parameters a_{mn0}, a_{mn1} and a_{mn2} for the Original-, Linear-, Modified- and Dortmund-UNIFAC models fitted to lipid data

Groups (mn)	Original Lipids	Linear Lipids		Modified Lipids			Dortmund Lipids			Temperature range	
	a_{mn0}	$a_{mn\,0}$	$a_{mn\,1}$	$a_{mn\,0}$	$a_{mn\,1}$	$a_{mn\,2}$	$a_{mn\,0}$	$a_{mn\,1}$	$a_{mn\,2}$	T_{min} (K)	T_{max} (K)
COOH/CH=CH	1318.50	-647.09	-5.0780	227.30	-9.1300	7.2000	-347.50	0.4466	-0.0026		
CH=CH/COOH	998.50	4334.00	0.1008	143.39	-0.8700	-0.1777	-2026.10	6.7093	-0.0046	318.14	481.08
CH₂/CH=CH	125.74	-102.30	0.1679	245.29	-0.1834	-0.3660	518.75	-0.2723	0.0033		
CH=CH/CH₂	555.93	144.80	-0.2720	-46.45	-0.1817	-1.4700	-29.00	0.0803	0.0004		
CCOO/CH=CH	135.28	200.62	7.0201	524.35	1.2210	4.7700	-546.07	-0.7768	-0.0011	318.14	514.61
CH=CH/CCOO	54.61	-153.14	4.7899	-24.00	0.6530	0.0700	981.10	-0.9514	-0.0015		
COOH/OH_acyl	-129.89	-39.43	2.5500	-15.76	-1.0721	0.3364	2654.44	-4.8021	0.0004	462.67	498.35
OH_acyl/COOH	222.89	872.19	-5.7000	213.59	0.6206	-0.9373	918.67	4.9300	-0.0008		
CH=CH/CH₃OH	1424.55	875.80	-7.5100	3056.13	3.0000	1.9600	-726.27	9.6322	-0.0163	338.28	387.11
CH₃OH/CH=CH	64.65	-110.20	2.9200	-102.00	0.2710	0.8500	-103.71	0.6024	-0.0019		
CH=CH/OH	384.72	984.73	-4.1293	1192.06	3.4403	-1.4330	2903.73	-5.9300	0.0048	318.15	617.42
OH/CH=CH	407.71	215.88	-5.9670	800.02	-8.1016	0.0320	1281.84	-6.5900	0.0052		
COOH/CH₃OH	2981.07	-63.07	9.7476	714.07	9.6100	3.6990	1077.72	-3.4269	0.0001	318.15	
CH₃OH/COOH	-272.84	52.19	-5.7800	-321.10	-7.1201	3.0110	-761.76	2.2449	-0.0003		
COOH/OH	37.73	-267.59	1.8507	-75.83	0.8131	0.6300	1531.83	-4.8965	0.0007	318.15	
OH/COOH	294.83	513.52	-4.9999	35.55	-1.3114	0.3400	-1323.86	4.2727	-0.0002		
CCOO/CH₂CO	778.64	327.78	0.2500	43.65	0.1905	0.0030	113.15	0.4210	-0.0001		
CH₂CO/CCOO	44.62	33.37	-2.4311	-11.93	-0.0406	0.0010	-4.61	-0.2792	0.0001		
CH=CH/CH₂CO	528.31	607.86	7.0965	1217.00	9.7600	1.0080	485.78	0.6991	-0.0001	318.15	
CH₂CO/CH=CH	-153.42	-176.49	-9.6200	-72.75	3.5800	-0.1090	107.82	-1.5500	-0.0001		
CH₂/CH₂CO	529.15	525.94	4.4100	476.78	-5.2902	1.8030	568.85	0.1403	-0.0001		
CH2CO/CH₂	13.51	13.24	-2.8907	71.93	-9.2220	-2.9160	150.59	-0.8800	-0.0001		
COOH/CH₂CO	39.48	-17.25	5.5567	-183.43	9.2540	-6.0396	356.88	-0.8000	0.0001	303.13	318.15
CH₂CO/COOH	247.02	24.81	-0.6438	282.94	0.7244	1.0960	-156.75	0.8200	-0.0001		

Table 6.7 ARD (%) between experimental and predicted bubble-point pressured using UNIFAC models with the published and lipids-based group interaction parameters. The lipids-based group interaction parameters for Linear-, Modified- and Dortmund-UNIFAC are from this work.

Binary system type[a]		Original		Linear		Modified		Dortmund		Consistency score		
		Published [2]	Lipids [13]	Published [5]	Lipids	Published [3]	Lipids	Published [4]	Lipids	(Q_{VLE})		
Compound I	Compound II	ARD %								$Q_{VLE, minimum}$	$Q_{VLE, maximum}$	$Q_{VLE, average}$
Saturated Fatty Acids	Saturated Fatty Acids	2.67	2.63	2.22	2.15	2.27	2.24	2.26	2.20	0.000	0.650	0.137
Saturated Ester	Saturated Ester or Hydrocarbon	6.18	5.71	5.16	5.12	5.00	4.85	5.06	4.84	0.001	0.760	0.258
Glycerol	Methanol	20.76	12.50	19.14	9.31	17.14	11.11	19.39	10.26	0.063	0.500	0.243
Glycerol	Water	91.50	88.50	68.81	48.67	78.87	50.98	198.01	56.83	0.005	0.500	0.172
Saturated Fatty Acids	Saturated Ester	24.39	1.65	8.34	1.58	9.76	1.53	10.06	4.25	0.027	0.027	0.027
Saturated Ester	Methanol	15.14	10.89	9.44	5.05	17.64	14.66	9.04	8.29	0.250	0.500	0.400
Saturated. Ester	Ethanol	11.69	2.58	2.55	2.23	9.63	4.25	6.58	5.27	0.250	0.250	0.250
Saturated Monoacylglycerol	Saturated Ester	11.63	5.45	24.07	3.76	9.17	4.38	3.91	3.84	0.009	0.009	0.009
Glycerol	Saturated Alcohol	27.99	24.63	22.76	21.87	21.90	20.56	17.27	15.91	0.000	0.460	0.188
Unsaturated Fatty Acids	Saturated Fatty Acid or Hydrocarbon	30.76	28.56	23.15	21.78	20.56	19.64	18.41	14.49	0.007	0.500	0.183
Unsaturated Ester or Triacylglycerol	Saturated Ester or Hydrocarbon	17.88	15.48	9.28	9.15	4.58	4.51	7.55	7.48	0.097	0.377	0.248
Saturated Monoacylglycerol	Saturated Fatty Acids	17.26	3.62	3.91	1.40	17.14	1.92	22.21	5.93	0.008	0.011	0.009
Unsaturated Ester	Methanol	22.25	2.94	4.31	4.03	24.66	15.39	9.53	4.94	0.250	0.250	0.250
Unsaturated Ester	Ethanol	33.87	32.07	13.47	6.88	23.77	12.10	10.68	10.55	0.001	0.250	0.125
Unsaturated Fatty Acids	Methanol	10.12	5.91	18.20	8.06	33.94	8.69	8.56	6.28	0.500	0.500	0.500
Saturated Fatty Acids	Saturated Alcohol	4.68	4.07	11.40	6.70	13.19	6.60	7.77	5.31	0.008	0.500	0.254
Unsaturated Triacylglycerol	Acetone	21.30	1.99	21.49	1.19	16.80	11.21	8.72	8.53	0.476	0.476	0.476
Saturated Fatty Acids	Acetone	20.68	2.10	18.68	0.95	4.55	2.97	6.76	2.40	0.500	0.500	0.500
ARD (%) for all model (Published and lipids)		21.71	13.96	15.91	8.88	18.36	10.98	20.65	9.87			

[a] The binary systems tested are from the SPEED Lipids database.

6.5 MODEL EXTRAPOLATION CAPABILITY FOR SLE PREDICTION

The parameters obtained for each UNIFAC model are further validated by checking their prediction capability for lipids SLE data. As mentioned previously, SLE data is not used for the regression of the parameters. The SLE data is extracted from the SPEED Lipids Database [13]. The SLE data is organized in category-groups in the same way as the VLE data, by applying the data organization algorithm (Algorithm A). For consistency, the same name category-groups are used for describing the SLE data sets. A new category-group is defined for SLE, named "Others". This category-group contains unsaturated triacylglycerols – saturated fatty acids and saturated triacylglycerols – unsaturated fatty acids type of systems. Available SLE data used in this study is given in Table 6.8.

All the SLE calculations are performed with ICAS-MoT [26]. SLE is calculated using Eq. 11. The melting temperature (T_m) is taken from literature when data is available; otherwise values from SPEED Lipids Database [13] are used. The heat of fusion (H_f) values are taken from SPEED Lipids Database.

$$\ln(x_i) = \ln \gamma_i + H_f \left(\frac{1}{T_{m,i}} - \frac{1}{T} \right) \tag{11}$$

where x_i is the mole fraction of the compound with higher melting point, γ_i is the activity coefficient of compound i, H_f is the fusion enthalpy of compound i, $T_{m,i}$ is the melting point of compound i, and T is the mixture melting temperature.

The results obtained for each category-group, with all UNIFAC-based models, using both published and lipids-based group-interaction parameters are given in Table 6.9. A slight improvement is noticed for Modified-UNIFAC model using the lipids-based group-interaction parameters compared to the published parameters, except for Linear- and Dortmund-UNIFAC model. This bigger deviation for Dortmund-UNIFAC with lipids group-interaction parameters could be due to the R_k and Q_k parameters, which are not regressed for lipids systems in this work. Also, the extrapolation of the parameters to outside the range of temperatures and phase equilibria type could affect the prediction of this models. From all UNIFAC-based models using published parameters, the best performance is obtained with Dortmund-UNIFAC model (ARD = 1.34%) followed by Linear-UNIFAC model (ARD = 1.35%). Using the lipids

group-interaction parameters, again the best overall results is provided Linear-UNIFAC model (ARD = 1.43%). Analyzing the deviations for each-category group, the best performances are in general when lipids group-interaction parameters are used. It is important to emphasize, that for the SLE prediction, the parameters are not only extrapolated to another type of phase equilibria, but also to another range of temperatures (see also Table 6.6 and Table 6.8), so unexpected behavior may occur.

An example of SLE prediction is presented in Figure 6.7, where the best performances are shown for different UNIFAC-based models (see also Table 6.9). In Figure 6.7, the prediction for system ethyl linoleate + ethyl stearate [27] is presented for Linear, Modified and Dortmund UNIFAC models using lipids-based group-interaction parameters, all models presented analogous behavior.

Figure 6.7 SLE system ethyl linoleate (x_1) + ethyl stearate (x_2). Experimental data [24] (●). Lipids-based group interaction parameters UNIFAC models: Linear (—), Modified (—) and Dortmund (—)
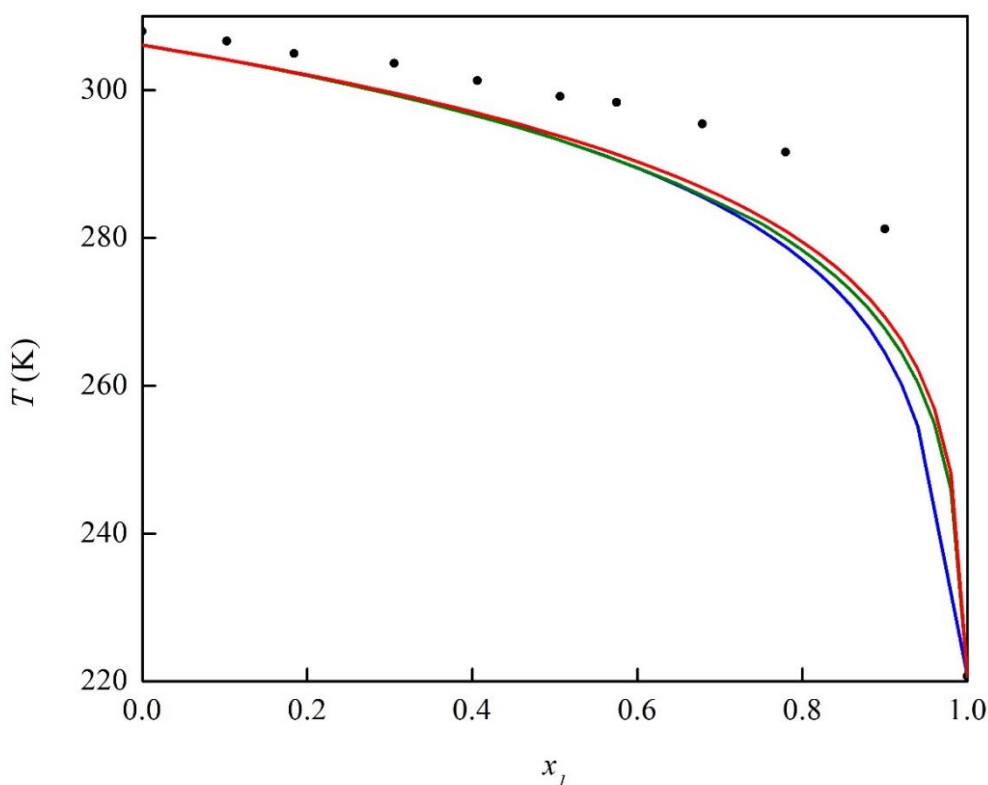
The extrapolation results do show that in general the lipids group-interaction parameters can be used for SLE predictions, nonetheless one should use them with some care since different temperature ranges and behaviors are encountered for this type of systems and

this form of phase equilibria. It cannot be concluded that one model works best for all type of SLE systems, but the selection of a model for performing SLE prediction should be done according to the type of SLE systems involved.

Table 6.8 Database used for the SLE predictions with UNIFAC models.

Category-group	System type		Constitutive groups	SLE datasets	Temperature range	
					$T_{minimum}$ (K)	$T_{maximum}$ (K)
1.1.1.	Saturated Fatty Acids	Saturated Fatty Acids	CH_2 COOH	12	278.36	343.98
1.1.2.	Saturated Ester	Saturated Ester	CH_2 CCOO	9	272.51	314.07
3.2.5.	Unsaturated Fatty Acids	Sat. FA	CH_2 COOH CH=CH	5	264.99	342.25
3.2.6.	Unsaturated Ester Saturated Triacylglycerol	Saturated Ester Unsaturated Triacylglycerol	CH_2 CH=CH CCOO	8	220.68	338.79
6.3.2.	Saturated Fatty Acids	Acetone	CH_2 CH=CH CH_2CO COOH	1	333.71	329.95
Other*	Unsaturated Triacylglycerol Saturated Triacylglycerol	Saturated Fatty Acids Unsaturated Fatty Acids	CH_2 CH=CH CH_2COO COOH	9	258.62	342.25
Total				44	220.68	343.98

*Other category-group contains constitutive groups that were not in any of the VLE identified category-groups

Table 6.9 SLE prediction for Linear, Modified and Dortmund-UNIFAC using published and lipids-based group interaction parameters.

Category-Group	Linear		Modified		Dortmund	
	Published [5]	Lipids	Published [3]	Lipids	Published [5]	Lipids
	ARD (%)					
1.1.1	0.94	0.94	0.92	0.92	0.92	0.92
1.1.2	1.25	1.25	1.15	1.33	1.16	1.15
3.2.5	0.36	1.66	0.38	0.42	0.43	0.56
3.2.6	2.33	2.37	2.35	2.33	2.32	2.32
6.3.2	0.35	0.19	2.21	2.18	1.43	1.43
Other	2.88	2.20	4.76	3.51	1.78	3.77
Total ARD (%)[b]	1.35	1.43	1.96	1.78	1.34	1.69

$$^a\ ARD(\%) = \frac{1}{N} \sum_{i=1}^{N} \left| \frac{T^{experimental} - T^{calculated}}{T^{experimental}} \right| .100, \quad ^b\ Total ARD(\%) = \frac{1}{M} X.M.N$$

6.6 CONCLUSIONS

The method of Perederic et al. [2017] was successfully applied for the binary interaction parameter estimation for three UNIFAC-based models: Linear, Modified and Dortmund. For the estimation of the binary group interaction parameters, the SPEED Lipids Database was used for VLE data collection, and the same data sets were used as in Perederic et al. [2017]. Two new functional groups were added for the description of acylglycerols (OH_{acyl}) and glycerol (GLY) compounds for all models for improving their prediction capabilities for lipids, as was also done for Original-UNIFAC [13].

The estimated group-interaction parameters have been validated by checking their performances on all VLE data sets available in the SPEED Lipids Database. All UNIFAC-based models present better performances with the new sets of binary group-interaction parameters compared to the original published parameters. Among all the models, the Linear-UNIFAC model has been found to give the best overall performance for VLE predictions. Addition of the OH_{acyl} improves qualitatively and quantitatively the VLE prediction of acylglycerol systems. For the glycerol systems, introduction of the GLY group results in a significant improvement in the VLE prediction, but the deviations remain quite high for all models considered. This is a limitation of the group contribution concept for the description of systems containing compounds with many OH groups attached to the adjacent carbon atoms, such as glycerol, that has three OH groups. For strongly hydrogen bonding systems, the group contribution concept does not work very well and more advanced models are needed e.g. association equations of state like CPA [23] and SAFT [24].

The parameters are also tested for SLE predictions for lipids systems. All the SLE datasets are collected from the SPEED Lipids Database. For the UNIFAC with lipids group-interaction parameters, a slight improvement in SLE prediction is observed for Modified-UNIFA model when compared to the published parameters are used.

The main drawback in developing and extending the predictive capabilities of the group contribution concept remains the accuracy and availability of experimental data used for parameter estimation. Attention should be taken when using the parameters for other types of systems and other range of temperatures than the ones used in the parameter estimation as well as for strongly polar and hydrogen bonding systems for which the group contribution and local composition concepts deteriorate.

6.7 REFERENCES

[1]   G. M. Kontogeorgis and G. K. Folas. Thermodynamic models for industrial applications : from classical and advanced mixing rules to association theories. Wiley, 2010.

[2]   A. Fredenslund. R. Jones. J.M. Prausnitz. *AIChE J*. 21 (1975). pp. 1086–1099.

[3]   B. Larsen. P. Rasmussen. A. Fredenslund. *Ind. Eng. Chem. Res*. 26 (1987). pp. 2274–2286.

[4]   U. Weidlich and J. Gmehling. *Ind. Eng. Chem. Res*. 26 (1987). pp. 1372–1381.

[5]   H. K. Hansen, B. Coto, and B. Kuhlmann. UNIFAC with linearly temperature-dependent group-interaction parameters. Internal report. 1992.

[6]   J. Gmehling. J. Li. M. Schiller. *Ind. Eng. Chem. Res*. 32 (1993). pp. 178–193.

[7]   J. Gmehling, J. Lohmann, A. Jakob, J.D. Li, R.A. Joh. *Ind. Eng. Chem. Res*. 37 (1998) 4876–4882.

[8]   J. Gmehling, R. Wittig, J. Lohmann, R.A. Joh. *Ind. Eng. Chem. Res*. 41 (2002) 1678–1688.

[9]   J.W. Kang. V. Diky. M. Frenkel. *Fluid Phase Equilib*. 388 (2015). pp. 128–141

[10]   B. E. Poling, J. M. Prausnitz, J. P. O'Connell. Properties of Gases and Liquids. 5ed. McGraw-Hill Education. 2001.

[11]   L.P. Cunico. D.S. Damaceno. R.M. Matricarde Falleiro. B. Sarup. J. Abildskov. R. Ceriani. R. Gani. *J. Chem. Thermodyn.* 91 (2015). pp. 108–115

[12]   P. C. Belting. J. Rarey. J. Gmehling. R. Ceriani. O. Chiavone-Filho, A.J.A. Meirelles. *Fluid Phase Equilib*. 361 (2014). p. 215-222

[13]   O.A. Perederic, L.P. Cunico, S. Kalakul, B. Sarup, J.M. Woodley, G.M. Kontogeorgis, R. Gani. J. Chem. Thermodyn. (2017).

[14]   I. Kikic. P. Alessi. P. Rasmussen. A. Fredenslund. *Can. J. Chem. Eng*., 58(1980). pp. 253–258.

[15]   Bondi, A., Physical Properties of Molecular Crystans, Liquids and Glasses, Wiley, New York (1968).

[16]   J.W. Kang. V. Diky. R. D. Chirico. J. W. Magee. C. D. Muzny. I. Abdulagatov. *J. Chem. Eng. Data.* 55 (2010). pp. 3631−3640.

[17]   L. P. Cunico. Modelling of Phase Equlibria and Related Properties of Mixtures Involving Lipids. Technical University of Denmark (DTU), 2015.

[18]   L.C.B.A. Bessa, M.C. Ferreira, C.R.A. Abreu, E.A.C. Batista, A.J.A. Meirelles, Fluid Phase Equilib. 425 (2016) 98–107

[19]   M. Sales-Cruz, R. Gani, Comput. Chem. Eng. 16 (2003) 209–249.

[20]   K. Balslev, J. Abildskov, Ind. Eng. Chem. Res. 41 (2002) 2047–2057.

[21]   J.A. Monick. H.D. Allen.C.J. Marlies. Oil Soap, 23:177 (1946). pp 177–182.
[22]   J. Soujanya, B. Satyavathi, and T. E. Vittal Prasad. *J. Chem. Thermodyn.,* 42 (2010). pp. 621–624.
[23]   G.M. Kontogeorgis, M.L. Michelsen, G.K. Folas, S. Derawi, N. von Solms, E.H. Stenby. *Ind. Eng. Chem. Res.* 2006, 45 (14). pp 4855–4868
[24]   W.G. Chapman, K.E. Gubbins, G. Jackson, M. Radosz. *Fluid Phase Equilib.* 52(1989). pp. 31-38J. Gross, G. Sadowski, *Ind. Eng. Chem. Res*. 2002, 41 (22). pp 5510–5515
[25]   I. Tsivintzelis, A. Shahid, G.M. Kontogeorgis. *Fluid Phase Equilib*, 430 (2016). pp. 75-92.
[26]   M. Sales-Cruz. R. Gani. *Comput. Chem. Eng*. 16 (2003). pp. 209–249.
[27]   L. Boros. M. L. S. Batista. Raquel V. Vaz. B. R. Figueiredo. V. F. S. Fernandes. M. C. Costa. M. A. Krahenbuhl. A. J. A. Meirelles. J. A. P. Coutinho. Energy Fuels. 23 (2009). pp. 4625-4629.

CAPÍTULO 7

EXPERIMENTAL DATA AND PREDICTION OF NORMAL BOILING POINT OF PARTIAL ACYLGLYCEROLS

Daniela S. Damaceno, Evandro P. Jesus, Roberta Ceriani

Publicado na Fuel

Abstract: Normal boiling point is an important thermophysical property for quality control of biofuels, as biodiesel, and is related to purification processes as distillation. Monoacylglycerols and diacylglycerols are formed during transesterification reaction of oils, and directly affect quality parameters of biodiesel, as its viscosity. Nevertheless, to the best of our knowledge, normal boiling point data of partial acylglycerols are completely absent in the open literature. This paper goals at providing experimental data of normal boiling points for five monoacylglycerols, monobutyrin, monocaprin, monolaurin, monopalmitin and monoestearin, and three diacylglycerols, dicaprylin, dinonanoin and dicaprin using the thermogravimetric analysis (TGA) technique. Predictive capacities of available methods in the literature were also evaluated.

Key-words: monoacylglycerols, diacylglycerols, biodiesel, normal boiling point, TGA

7.1 INTRODUCTION

Currently, nonrenewable sources of energy are considered as a major threat to the environment, for this reason seek for alternatives forms of energy is an issue of modern society. In this sense, biodiesel figures as an interesting alternative for diesel fuel, particularly in transport sector, considering that it produces a lower global pollution in comparison with a conventional source of fuel [1].

During transesterification reaction, monoacylglycerols (MAG) and diacyglycerols (DAG) are produced together with fatty esters (biodiesel). These compounds directly affect biodiesel quality parameters, as viscosity, and its content is controlled by the standard for total glycerine (0.25 % m/m, max.) [2,3]. In this way, during purification of biodiesel, mono- and diacylglycerols need to be removed. Besides, partial acylglycerols are widely used in food industry, as surface-active agents and emulsifiers [4], and are purified by molecular distillation [5].

Normal boiling point is the basis for estimating critical properties, and temperature-dependent properties such as vapor pressure, density, latent heat of vaporization, viscosity, and surface tension of chemicals [6]. In general, there is a lack of experimental data for thermophysical properties of compounds related to the lipid technology. For normal boiling points of partial acylglycerols, to the best of our knowledge, experimental data are completely absent. In fact, there are only two data for triacylglycerols provided by Santander et al. [7] using the thermogravimetric analysis technique: 692.25 K for triolein (MW = 885.4 g·mol^{-1}) and 690.02 K for tripalmitin (MW = 807.3 g·mol^{-1}). Very few data are still available for boiling points of partial acylglycerols [8-10], and they are concentrated at low pressure values (up to 13.2 kPa).

Normal boiling points can be measured by thermogravimetric analysis (TGA) [11]. This method provides a rapid mean for quantifying boiling points of pure compounds or mixtures, for example: n-paraffins, alcohols, fatty acids, fatty esters, triacylglycerols, biodiesel, and others [7,11-13]. Boiling point is taken from a plot of weight loss versus temperature (thermogram), provided by the TGA equipment. The extrapolated onset point of the thermogram is the boiling point of the sample [11]. As any other analytical technique, the TGA technique can be affected by many factors, as: impurities, heat rate, crucible configuration, amount of mass, among others [7-9,14]. In fact, some of these issues have been addressed when using the DSC technique to determine boiling points of organic compounds. For instance, Troni

et al. [14] developed a systematic study to test the influence of two factors that affect the results of the DSC technique when measuring boiling points of pure compounds at low pressures: sample sizes (mg) and heating rates (K.min^{-1}). Also, the TGA analysis provides important information about thermal stability, oxidation and degradation of pure compounds or mixtures. Further investigations could address similar studies for the TGA technique. Furthermore, one important advantage of the TGA technique is that it requires very low sample mass (7 mg approx.), which is cost-effective for fatty compounds [7,12]. In a recent work, the TGA technique was applied for measuring normal boiling points of pseudobinary mixtures of biodiesel/diesel, biodiesel/oil and diesel/oils [13].

For contributing to the lipid technology field, this work measured novel normal boiling point data for five monoacylglycerols (MAGs) and three diacylglycerols (DAGs), i.e: monobutyrin, monocaprin, monolaurin, monopalmitin, monoesterain, dicaprylin, dinonanoin and dicaprin using the TGA technique. In the case of monocaprin and monolaurin, two different lots were tested. Also, the ^{13}C-Nuclear Magnetic Ressonance (NMR) analysis was used for both lots of monocaprin to qualitatively verify the presence of isomers 1-MAG and 2-MAG [15]. The predictive capacities of the methods of Ceriani et al. [16], Marrero and Gani [17], Joback and Reid [18], and Zong et al. [19] were also evaluated.

7.1 METHODOLOGY

7.1.1 Materials

Table 7.1 lists all the reagents used in this study (CAS Registry numbers, purities in mass fraction, IUPAC names and suppliers). All chemicals were used without any further purification step.

Table 7.1 List of compounds with their respective IUPAC name, CAS Registry No., supplier and purity

Compound	IUPAC name	CAS Registry No.	Supplier	Purity (mass fraction)
n-tetradecane	Tetradecane	629-59-4	Sigma-Aldrich	0.99
n-hexadecane	Hexadecane	544-76-3	Sigma-Aldrich	0.99
Glycerol	Glycerol	56-81-5	Sigma-Aldrich	0.99
Monobutyrin	2,3-dihydroxypropyl butanoate	557-25-5	Sigma-Aldrich	0.99
Monocaprin[a]	2,3-dihydroxypropyl decanoate	2277-23-8	Nu-Chek Prep, Inc.	0.99
Monolaurin[a]	2,3-dihydroxypropyl dodecanoate	142-18-7	Nu-Chek Prep, Inc.	0.99
Monopalmitin[a]	2,3 dihidroxypropyl hexanodecanoate	542-44-9	Nu-Chek Prep, Inc.	0.99
Monoestearin[a]	2,3 dihydroxypropryl stearate	123-94-4	Nu-Chek Prep, Inc.	0.99
Dicaprylin[b]	2 hydroxy-3octanoyloxypropyloctanoate	36354-80-0	Nu-Chek Prep, Inc.	0.99
Dinonanoin[c]	2 hydroxy-3octanoyloxypropylnonanoate	-	Nu-Chek Prep, Inc.	0.99
Dicaprin[b]	3 decanoyloxy 2 hydroxypropyldecanoate	53988-07-01	Nu-Chek Prep, Inc.	0.99

[a]Thin layer chromatography showed only the monoacylglycerol moiety present according to the certificate of analysis provided by Nu-Chek Prep, Inc. [b]Thin layer chromatography showed only the diacylglycerol moiety present (may contain trace amounts of 1,2-DAG) according to the certificate of analysis provided by Nu-Chek Prep, Inc. [c]Thin layer chromatography showed only the diacylglycerol moiety present according to the certificate of analysis provided by Nu-Chek Prep, Inc.

7.1.2 Experimental Procedures

7.1.2.1 The thermogravimetric analysis (TGA) technique

The TGA technique was performed according with Goodrum and Geller [12] and Santander et al. [7]. The equipment used was a TGA/DSC1 – Mettler Toledo. All measurements were conducted at ambient pressure at campus of the State University of Campinas (UNICAMP), in the city of Campinas, São Paulo State, Brazil. Ambient pressure (p) registered by the CEPAGRI (Centro de Pesquisas Meteorológicas e Climáticas Aplicadas à Agricultura) during the days of our analysis was 95.54 kPa with $u(p) = 0.52$ kPa. Nitrogen purge flow through the cell was 50 mL/min and a heating rate of 10 K/min was used. This heating rate value enables to detect whether some irregular situations arise in the experiment [7]. Each assay was obtained using a pair of sealed crucibles (40 μL), one empty (reference) and the other with

a sample of approximately 7 mg (±1 mg) of reagent. To assist for achieving isothermal boiling, 1.0 mg (± 0.2 mg) of α-alumina (standard grade) was added to the sample [12]. Crucibles were sealed with drilled lids using a Mettler Toledo pressing device. Pinhole diameter was within 0.25 – 0.31 mm range. All measurements were conducted in triplicates. Based on Troni et al. [14], we developed a method to select the onset temperatures from the TGA curves, considering the limitations and differences from both thermal analyses, this information is explained in detail in Supplementary material – "Selection of the onset temperatures of TGA".

7.1.2.2 *Nuclear magnetic resonance NMR Spectroscopy*

According to Gunstone [14] and Compton et al. [20], ^{13}C-NRM analysis allows to qualitatively verify the presence of isomers of monoacylglycerols. In fact, the glycerol carbon atoms in each type of isomers of monoacylglycerol give a specific ^{13}C-NMR signal, which it can be used to identify the presence of 1-MAG or 2-MAG [15]. ^{13}C – NMR spectra were obtained on a Bruker Avance 500 MHz spectrometer (125.69 MHz 13C) using a 5 mm BBI probe. All samples were dissolved in $CDCl_3$, and all spectra were acquired at 298.2 K.

7.1.3 Estimation of normal boiling point (T_{nb})

Group contribution methods were used for estimating the normal boiling point (T_{nb}) of mono- and diacylglycerols. The methods applied were Ceriani et al. [16], Marrero and Gani [17], and Joback and Reid [18]. Besides that, the chemical constituent fragment approach for partial acylglycerols developed by Zong et al. [19] was also checked. Table 7.2 lists equations of each method and their description.

Table 7.2 Equations for estimating normal boiling temperature (T_{nb}) and their description

| Method	Equation	Eq. number	Description
Ceriani et al. [16]	$\ln(p) = A + \dfrac{B}{T} + C \cdot \ln(T)$ $A = \sum_k N_k(A_{1k} + M \cdot A_{2k}) + (s_0 + N_{cs} \cdot s_1) + \alpha \cdot (f_0 + N_c \cdot f_1)$ $B = \sum_k N_k(B_{1k} + M \cdot B_{2k}) + \beta \cdot (f_0 + N_c \cdot f_1)$ $C = \sum_k N_k(C_{1k} + M \cdot C_{2k})$	(1) (1a) (1b) (1c)	p = vapor pressure in Pa; T = temperature in K; A, B and C = values of each contribution; N_k = number of groups k in the molecule; M = component molecular weight; N_{cs} = number of carbons of the alcoholic part of esters; N_c = total number of carbon atoms in the molecule; A_{1k}, B_{1k}, C_{1k}, A_{2k}, B_{2k}, C_{2k}, α, β, s_0, s_1, f_0 and f_1 = fitted parameters.
Marrero and Gani [17]	$T_{nb} = 198 + \sum_k N_k(t_{nb}k)$	(2)	T_{nb} = normal boiling point in K; N_k = number of each group k; $t_{nb}k$ = contribution of group k
Joback and Reid [18]	$\exp(T_{nb}/T_{nb0}) = \sum_i N_i T_{nb1i} + \sum_j M_j T_{nb2j} + \sum_k O_k T_{nb3k}$	(3)	T_{nb} = normal boiling point in K; N_i, M_j and O_k = number of each group i; T_{nb1i}, T_{nb2j} e T_{nb3k} = contributions of each group k; T_{nb0} = constant
Zong et al. [19]	$\ln(p) = \dfrac{-\Delta G_\theta^{vap}}{R\theta \ln 10} + \dfrac{\Delta H_\theta^{vap}}{R \ln 10}\left(\dfrac{1}{\theta} - \dfrac{1}{T}\right)$	(4)	p = vapor pressure in Pa; ΔG_θ^{vap} = Gibbs energy of vaporization at a reference temperature θ (298.15 K); ΔH_θ^{vap} = enthalpy of vaporization at a reference temperature θ (298.15 K); T = boiling point in K at pressure p; R = gas constant

Table 7.3 shows the functional groups present in mono- and diacylglycerols according to each group contribution method selected in this work.

Table 7.3 Functional groups of partial acylglycerols for selected methods

Methods	Groups						
	CH$_3$	CH$_2$	CH	OH	CH$_2$COO	COO	CH$_2$CHCH$_2$
Ceriani et al. [16]	X	X		X		X	X
Marrero and Gani [17]	X	X	X	X	X		
Joback and Reid [18]	X	X	X	X		X	

The fragment approach [19] considers a monoacylglycerol component as a compound made up of a backbone monoacylglycerol fragment plus one fatty acid fragment attached. A diacylglycerol component is regarded as a compound made up of a backbone diacyglycerol fragment with two fatty acid fragment attached. Figure 7.1 is an example of the fragment approach division for monolaurin, a monoacylglycerol of lauric acid, a fatty acid of 12 carbons. It is important to highlight that the method of Zong et al. [19] does not consider odd contribution to the fatty acid part, so it was not applied for dinonanoin (fatty acid = nonanoic acid).

Figure 7.1 Monolaurin fragment approach division

fatty acid part

monoacylglycerol part
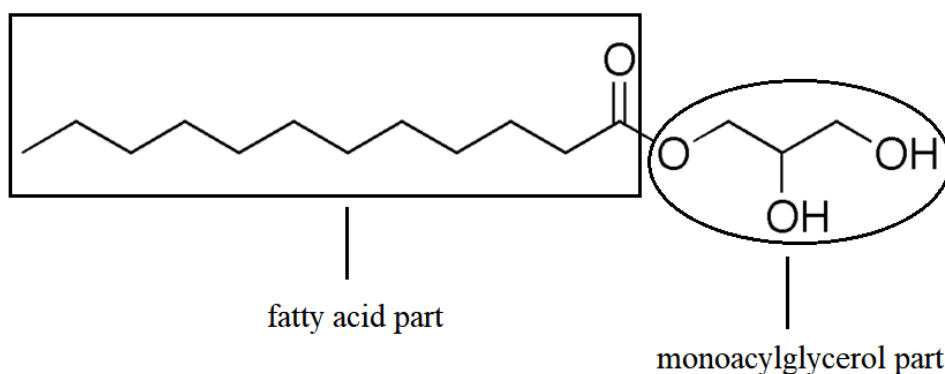
7.2 RESULTS AND DISCUSSION

Primarily, to ensure the accuracy of the boiling points, three well-known compounds with a vast number of experimental data of normal boiling point were measured and compared with experimental literature values. The compounds were tetradecane, hexadecane and glycerol. Table 4 presents the values of the experimental normal boiling points (T_{exp}) of all compounds used in this work at ambient pressure (p) with their respective standard

deviation $u(T)$ in K, and the normal boiling point T_{nb} (K) at 101.3 kPa, calculated with the Sydney-Young equation [21] (Eq. 5). Using the NIST TDE database from Aspen Plus (v.8.4), which provides a vast experimental database with different thermophysical properties, such as T_{nb}. The T_{nb} values are: for glycerol 563.06 K with $u(T) = 4.26$ K [22], for tetradecane 526.67 K with $u(T) = 0.15$ K) [22], and for hexadecane 560.04 K with $u(T) = 0.63$ K [22]. Considering these values, absolute deviations ($T_{nb} - T_{nb\ \text{NIST TDE}}$) of these compounds at 101.3 kPa were as follow: glycerol = 0.83 K, tetradecane = 1.43 K, and hexadecane = 3.80 K. Santander et al. [6] found similar values of absolute deviations by comparing their measured values for T_{nb} of methyl laurate (3.64 K) and for isoamyl alcohol (2.57 K) with values from the literature.

$$\Theta = 0.0009 \cdot (101.3 - p) \cdot (T_{\text{exp}})$$ (5)

where, Θ is the correction in K to be added to the observed boiling point, T_{exp} is the experimental boiling point at ambient pressure in K, and p is the ambient pressure in kPa.

Table 7.4 also contains the T_{exp} (K) monobutyrin, monocaprin, monolaurin, monopalmitin, monoestearin, dicaprylin, dinonanoin and dicaprin at ambient pressure p with their respective standard deviation $u(T)$ in K, and the T_{nb} (K) values at 101.3 kPa (Eq. 5). Values for $u(T)$ presented in this work were lower than the values reported by Santander et al. [6] for ethyl esters and triacylglycerols, which were between 1.92 – 19.13 K.

Table 7.4. Experimental boiling points T_{exp} (K) at ambient pressure[a] with their respective standard deviation u(T) in K, and normal boiling points T_{nb} (K) at 101.3 kPa calculated with Eq. 5.

Compound	MW (g·mol^{-1})	T_{exp} (K)[a]	u(T) in K	T_{nb} (K)
Glycerol	92.1	559.32	0.13	562.23
n-tetradecane	198.4	522.52	1.53	525.24
n-hexadecane	226.4	553.68	2.44	556.24
monobutyrin	162.2	542.57	0.32	545.40
monocaprin – Lot D5X	218.3	602.89	0.98	606.03
monocaprin – Lot D23V	218.3	618.34	1.81	621.56
monolaurin – Lot N19X	274.4	644.72	0.88	648.07
monolaurin – Lot O23Y	274.4	648.04	1.04	651.42
monopalmitin	330.5	668.70	0.26	672.18
monoestearin	358.6	674.20	0.86	677.71
dicaprylin	344.5	595.95	5.40	598.38
dinonanoin	372.5	638.16	0.59	641.48
Dicaprin	400.6	654.04	3.55	657.44

[a]p = 95.54 kPa with $u(p)$ = 0.52 kPa

Figure 7.2 shows T_{nb} (K) of MAGs and DAGs obtained in this work as a function of their molecular weight (MW). As expected, for the same class of compounds, T_{nb} increased with MW. DAGs were more volatile than MAGs of similar MW. For comparison purposes, T_{nb} (K) values for fatty alcohols (1-decanol, 1-dodecanol, 1-tetradecanol, 1-hexadecanol, octadecanol and 1-eicosanol, see Table 7.S1 for T_{nb} and MW) and methyl esters (methyl decanoate, methyl dodecanoate, methyl tetradecanoate, methyl hexadecanoate, methyl octadecanoate and methyl eicosanoate, see Table 7.S1 for T_{nb} and MW) were also included [22]. Same qualitative behavior was found by comparing fatty alcohols and methyl esters of similar MW, i.e., fatty esters were more volatile than fatty alcohols. It also is interesting to observe that experimental data for MAGs were closer to fatty alcohols while for DAGs were closer to methyl esters. In fact, MAGs are diols and monoesters, while DAGs are monols and diesters.

Figure 7.2 MW (g.mol^{-1}) versus T_{nb} (K) of MAGs (this work), DAGs (this work), alcohols (MW = 158.3 g.mol^{-1} up to 298.6 g.mol^{-1}) [22] and methyl esters (MW = 186.3 g.mol^{-1} up to 326.6 g.mol^{-1}) [21]
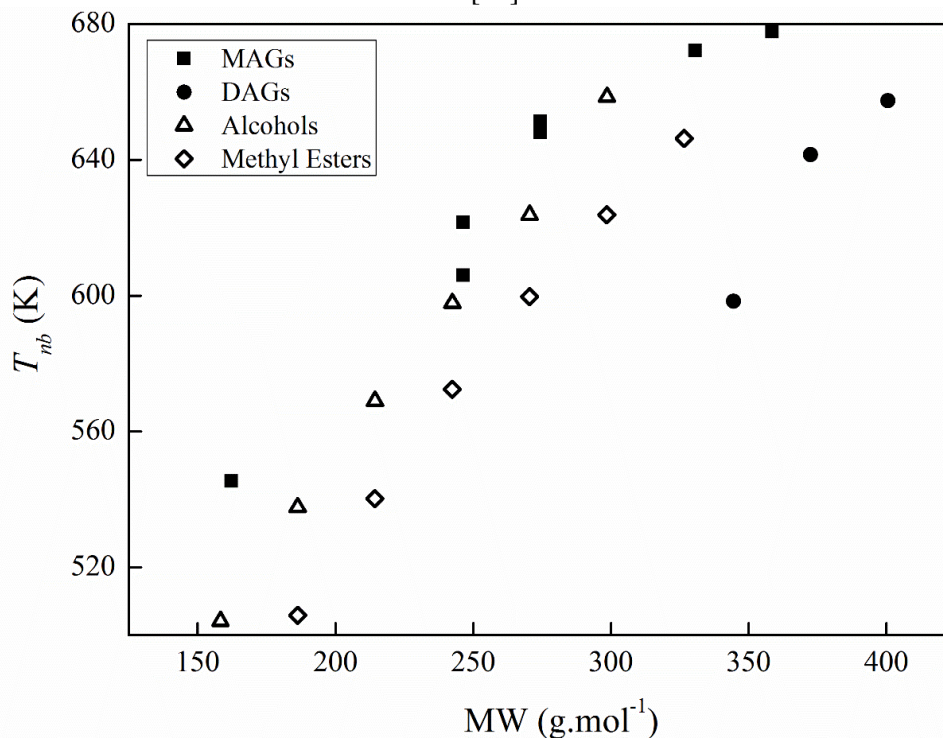
As it was stated before, isomers 1-MAG and 2-MAG may be found in a sample of a given MAG, due to variations in room temperature, fatty acid chain length, crystal form and others [4]. In this work, two lots of monocaprin (Lots: D5X and D23V) and monolaurin (Lots: N19X and O23Y) had their boiling points measured at ambient pressure. Results provided in Table 7.4 were statistically analyzed with the t-test [23]. It was inferred that for monolaurin T_{exp} (K) for both lots were not significantly different at 95% of confidence. On the contrary, for monolaurin T_{exp} (K) for both lots were significantly different at the same level of confidence. Figures 7.3 and 4 depicts the triplicates of the thermograms of both lots of monocaprin (Figure 7.3) and monolaurin (Figure 7.4). First, thermograms show an indication of more than one step, which could be related to the ratios of 1-MAG/2-MAG, and this behavior is analogous to the thermograms of mixtures of biodiesel/diesel, biodiesel/oil and diesel/oils presented by Raslavičius et al. [13]. Besides that, it is possible to see in Figure 7.3 that triplicate of lots D5X and D23V of monocaprin showed a slight gap among curves; the opposite behavior was found between lots N19X and O23Y of monolaurin, in which curves of each triplicate are practically overlapping. To better understand these differences, ^{13}C-NMR spectroscopy was performed to

confirm or not the presence of both 1-MAG and 2-MAG isomers for monocaprin, for which T_{exp} of different lots were statistically different at 95% of confidence. The spectrum and the chemical shifts of the two lots of monocaprin are in Figures 7S1 – 7S2 and Tables 7S1 – 7S2 in the Supplementary Material. According to Gunstone [15], the glycerol carbon atoms in each type of acylglycerol give a specific ^{13}C-NMR signal, which can be used to identify the type of isomers (1-MAG or 2-MAG). Subsequently, ^{13}C-NMR signals around 70.27 ppm or 63.47 ppm are related to 1-MAG and 74.70 ppm or 62.05 ppm are related to 2-MAG, all these chemical shifts were found in both lots of monocaprin (Tables 7S1 – 7S2), which is a clear indication of the presence of 1-monocaprin and 2-monocaprin. Although the ^{13}C-NMR analysis does not specify the ratio of 1-MAG/2-MAG in a sample, differences found in measured values of T_{exp} suggest that different ratios are present in the lots used in this work.

Figures 7S3 – 7S15 (Supplementary material) illustrate the TGA and the DTG curves of glycerol, monobutyrin, monocaprin (two lots), monolaurin (two lots), monopalmitin, monoestearin, dicaprylin, dinonanoin and dicaprin. In the DTG curve, it is possible to observe the presence of water, other compounds or isomers. The DTG of glycerol (Figure 7S4) shows monophasic event, which is expected for standard compounds with 99% of mass purity. Water content for glycerol was also analyzed, and according to previous works, it has more water content than monoacylglycerols, and with an increase of the fatty acid chain length, the water content tends to drop [9]. As reported by Castelló et al. [24], a little mass decrease for glycerol between 303.15 K – 373.15 K was observed, due to water loss. Consequently, water loss of the glycerol was detected around 318.82 K and at 99.27% of weight loss (Figure 7S4), which corroborated with Castelló et al. [24] and the mass purity presented by the manufacturer. Monophasic events were also observed for monobutyrin (Figure 7S6), dicaprylin (Figure 7S7), dinonanoin (Figure 7S8) and dicaprin (Figure 7S9). On the other hand, monopalmitin (Figure 7S10) and monoestearin (Figure 7S11) showed a perturbation in the baseline of the DTG, which is indication of the migration of the acyl group of the monoacylglycerol molecule [4,5,14,20,25,26]. Figures 7S12 – 7S15 of monocaprin (two lots) and monolaurin (two lots) showed in the DTG curves the presence of more than one peak (a deep perturbation in the baseline followed by a peak). In fact, as pointed out by Sanchez-Reinoso and Gutiérrez [25], and Saavedra-Leos et al. [26] these pre-events around 460 K – 615 K for monocaprin (two lots) and monolaurin (two lots), and 460 K – 600 K for monopalmitin and monoestearin are related to long chain compounds and isomerization reactions associated with dehydration of fatty compounds.

Figure 7.3 Thermograms of a tripricate of monocaprin Lot DSX (--) and monocaprin Lot D23V (—)
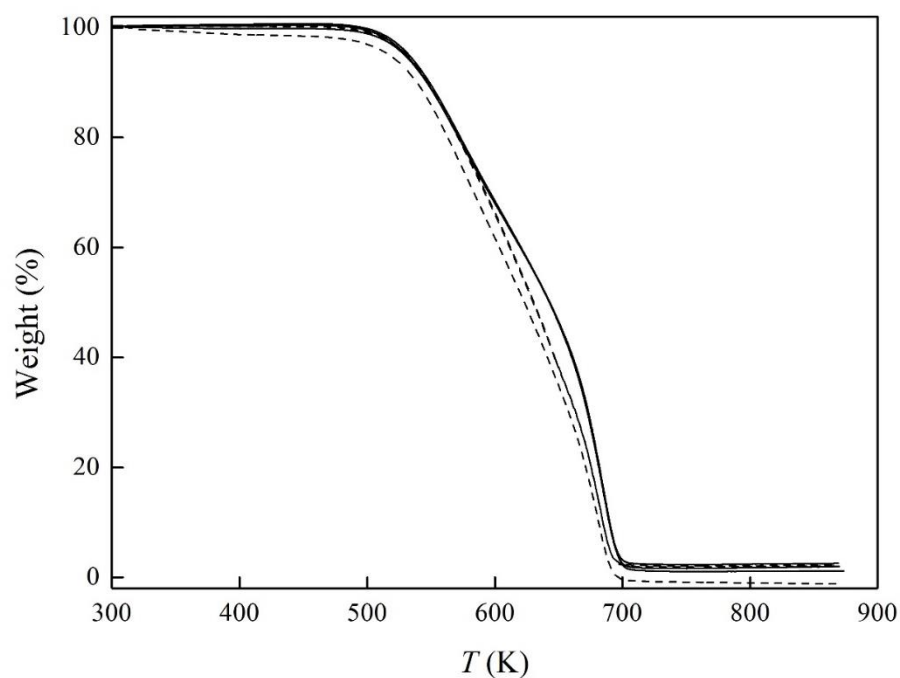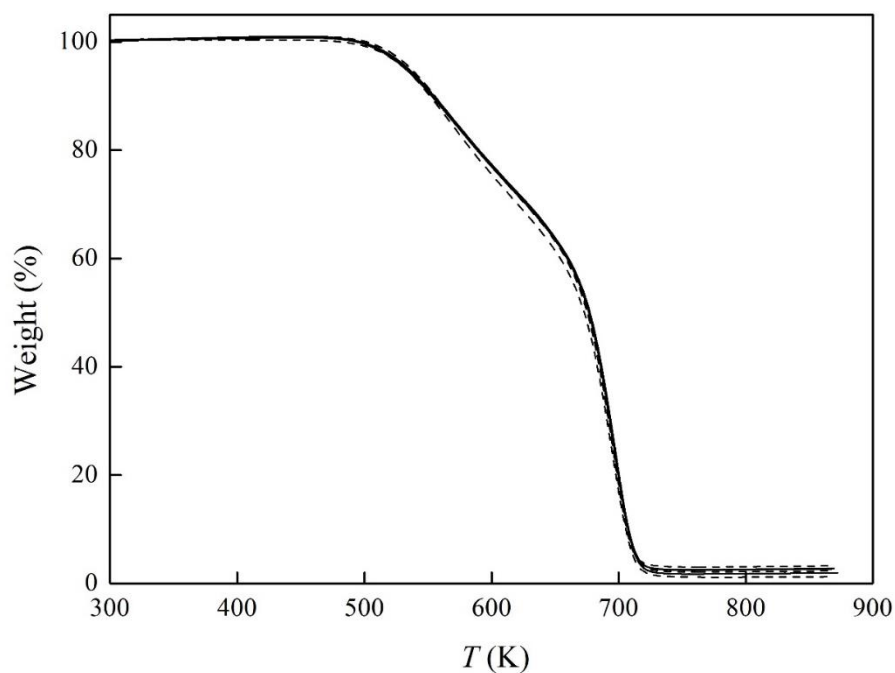

Figure 7.4 Thermograms of a tripricate of monolaurin Lot N19 (--) and monolaurin Lot OS34 (—)

In the view of the relevance of group contribution methods in the lipid technology, predictive capacities of the methods of Ceriani et al. [16], Marrero and Gani [18] and Joback and Reid [17], and also the fragment approach method of Zong et al. [19] were evaluated. Table 7.5 presents the calculated values of T_{nb} (K) and the respective relative deviations (RD) of all

methods studied. Average relative deviations (ARD,%) were similar for all methods, except the Joback and Reid [17] method. In general, Ceriani et al. [16], Marrero and Gani [18], and Zong et al. [19] have a similar values of deviations. However, the method of Zong et al. [19] cannot be applied to compounds with an odd fatty acid, as dinonanoin (C9). Figure 7.5 and 6 illustrates the behavior of the experimental values of T_{nb} of MAGs (Figure 7.5) and DAGs (Figure 7.6) as their number of the fatty acid chain increases, and also the calculated values of T_{nb} for the methods of Ceriani et al. [16], Marrero and Gani [17], and Zong et al. [19]. In general, for the MAGs (Figure 7.5), these methods underestimated the T_{nb}, with few exceptions, for example, the method of Marrero and Gani overestimated the T_{nb} for monoestearin (C18) and monocaprin lot D5X (C10). Observing Figure 7.5 and Table 7.5, the method that presented the lowest deviation for MAGs was the Marrero and Gani method [17]. The T_{nb} predicted by Ceriani et al. [16] and Zong et al. [19] for monolaurin (Figure 7.2) were practically identical. Nevertheless, both method are still underestimating the T_{nb} of monopalmitin (C16) and monoestearin (C18). Monocaprin lot D5X (Figure 7.5) was underestimated by Ceriani et al [16] and Zong et al. [19], and ovestimated by Marrero and Gani [17]. For monocaprin lot D23V, T_{nb} was underestimated by all methods, except Joback and Reid [18] that was overestimated. Predicted value of Marrero and Gani [17] for T_{nb} is in between lots D5X and D23V of monocaprin. For monolaurin in Figure 7.5 lots N19X and O23Y, all methods underestimated their T_{nb}. Differently from MAGs, DAGs (Figure 7.6) had overestimated values for T_{nb} for all methods. Zong et al. [19] was the best method to predict T_{nb} of DAGs, and for dicaprin the values of are practically the same. Ceriani et al. [16], Marrero and Gani [17], and Zong et al. [19] methods showed a good predict capacity to determine T_{nb} of both MAGs and DAGs with ARD (%) around 3%.

Figure 7.5 Normal boiling points T_{nb} (K) at 101.3 kPa for monoacylglycerols: experimental values and predicted values of the methods of Ceriani et al. [16], Marrero and Gani [17] and Zong et al. [19] of monobutyrin (C4), monocaprin (C10 – D5X and C10 – D23V), monolaurin (C12 – N19X and C12 – O23Y), monopalmitin (C16) and monoestearin (C18)
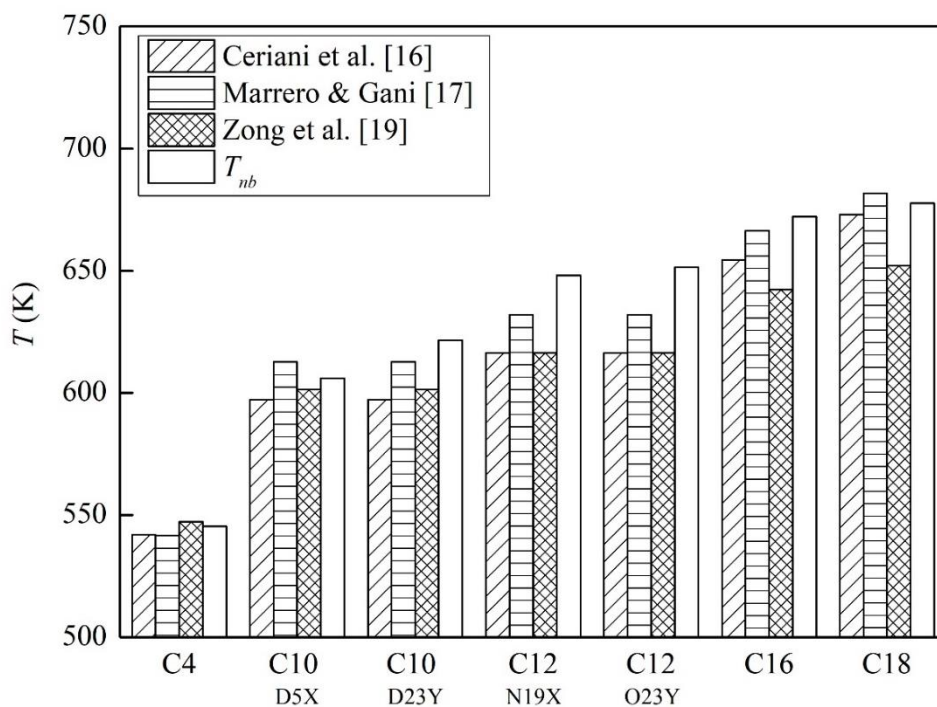

Figure 7.6 Normal boiling points T_{nb} (K) at 101.3 kPa for diacylglycerols: experimental values and predicted values of the methods of Ceriani et al. [16], Marrero and Gani [17] and Zong et al. [19] of dicaprylin (C8), dinonanoin (C9) and dicaprin (C10)
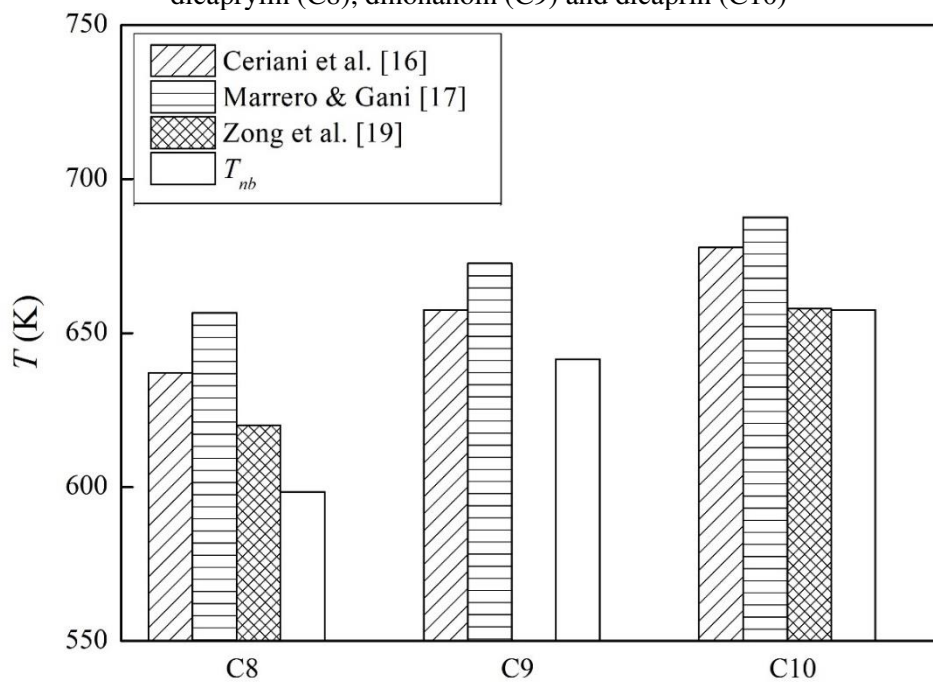
Table 7.5 Normal boiling points Tnb (K) at 101.3 kPa (Eq. 5) and calculated values given by the methods of Ceriani et al. [16], Marrero and Gani [17], Joback and Reid [18] and Zong et al. [19] with their respectives RD (%)[a] and ARD (%)[b]

Compunds	T_{nb} (K)	Ceriani et al. [16]	RD (%) Ceriani et al. [16]	Marrero and Gani [17]	RD (%) Marrero and Gani [17]	Joback and Reid [18]	RD (%) Joback and Reid [18]	Zong et al. [19]	RD (%) Zong et al. [19]
Monobutyrin	545.40	541.91	0.64	541.64	0.69	601.70	10.39	547.24	0.34
Monocaprin – DSX	606.03	597.20	1.46	612.63	1.09	738.98	22.26	601.32	0.78
Monocaprin -D23V	621.56	597.20	3.92	612.63	1.44	738.98	19.66	601.32	3.26
Monolaurin - N19	648.07	616.30	4.90	632.02	2.48	784.74	22.18	616.38	4.89
Monolaurin - 0S34	651.42	616.30	5.39	632.02	2.98	784.74	21.63	616.38	5.38
Monopalmitin	672.18	654.41	2.64	666.37	0.86	876.26	31.18	642.22	4.46
Monoestearin	677.71	672.95	0.70	681.74	0.59	922.02	36.30	652.08	3.78
Dicaprylin	598.38	637.04	6.46	656.58	9.73	842.30	38.29	620.05	3.62
Dinonanoin	641.48	657.48	2.49	672.62	4.85	888.06	37.50	-	-
Dicaprin	657.44	677.76	3.09	687.58	4.58	933.82	40.78	657.89	0.07
ARD (%)			3.17		2.93		28.02		2.95

[a] $RD = 100 \cdot \dfrac{|T_{exp} - T_{calc}|}{T_{exp}}$; [b] $ARD = \sum_{i=1}^{n} \dfrac{1}{n} \cdot \left[100 \cdot \dfrac{|T_{exp} - T_{calc}|}{T_{exp}} \right]$ where T_{exp} is experimental temperature in K and T_{calc} is calculated temperature in K of each method.

7.3 CONCLUSION

A novel series of normal boiling points of partial acylglycerols, monobutyrin, monocaprin, monolaurin, monopalmitin and monoestearin, dicaprylin, dinonanoin and dicaprin was measured by the TGA technique. In general, results presented lower standard deviations. Expected behavior was found for normal boiling points of compounds in homologous series, both for monoacylglycerols and diacylglycerols. Normal boiling points of MAGs were closer to fatty alcohols of comparable molecular weights, while for DAGs, normal boiling points were closer to fatty methyl esters, which is in accordance with their functional groups. The predictive methods of Ceriani et al. [16], Marrero and Gani [17], and Zong et al. [19] presented similar capacities with an ARD around 3%, differently from the method of Joback and Reid [18], which presented an ARD of 28%.

7.4 ACKNOWLEDGEMENTS

7.5 LITERATURE CITED

[1]   S. Thapa, N. Indrawan, P.R. Bhoi. An overview on fuel properties and prospects of Jatropha biodiesel as fuel for engines. Environ. Technol. Innovation,. 9 (2018). pp. 210-219.

[2]   Agência Nacional do Petróleo, Gás Natural e Biocombustíveis. Biodiesel. 2017.

[3]   EN 14105. Fat and oil derivatives - Fatty Acid Methyl Esters (FAME) - Determination of free and total glycerol and mono-, di-, triglyceride contents. 2011.

[4]   N. Krog. F. V. Sparso. Food emulsifiers and their chemical and physical properties. In: Food Emulsions. 4eded. S. E. Friberg. Marcel Dekker Inc. New York. 1990.

[5]   Casimir C.C. Akoh. Food Lipids: Chemistry, Nutrition, and Biotechnology. CRC Press. Boca Raton 4ed. 2017.

[6]   W. Yuan, A.C. Hansen, Q. Zhang, Vapor pressure and normal boiling point predictions for pure methyl esters and biodiesel fuels. Fuel,. 84 (2005). pp. 943-950.

[7]   C.M.G. Santander, S.M.G.R. Rueda, N.L. da Silva, C.L. de Camargo, G. Theo, T.G. Kieckbusch, M.R.W. Maciel. Measurements of normal boiling points of fatty acid ethyl esters and triacylglycerols by thermogravimetric analysis. Fuel,. 92 (2012). pp. 158-161.

[8]   D.S. Damaceno. R.M. Matricarde Falleiro. M.A. Krähenhühl. A.J.A. Meirelles. R. Ceriani. Boiling points of short-chain partial acylglycerols and tocopherols at low pressures by the differential scanning calorimetry technique. J. Chem. Eng. Data. 59 (2014). pp. 1515–1520

[9]   D.S. Damaceno, R. Ceriani. Vapor-liquid equilibria of monoacylglicerol + monoacylglycerol or alcohol or fatty acid at subatmospheric pressures. Fluid Phase Equilib. 452 (2017). pp. 135-142.

[10]   F. Shahidi, in: W. De Greyt; M. Kellens, Bailey's Industrial Oil and Fat Products. Wiley, New York, 2005.

[11]   J.W. Goodrum, E.M. Siesel. Thermogravimetric analysis for boiling points and vapour pressure. J Therm Anal,. 46 (1996). pp. 1251-1258

[12]   J.W. Goodrum, D.P. Geller. Rapid thermogravimetric measurements of boiling points and vapor pressure of saturated medium- and long-chain triglycerides. Bioresour Technol,. 84 (2002). pp. 75-80

[13]   L. Raslavičius, N. Striūgas, M. Felneris, R. Skvorčinskienė, L. Miknius. Thermal characterization of P. moriformis oil and biodiesel. Fuel. 220 (2018). pp. 140-150,.

[14]   K.L. Troni. D.S. Damaceno. R. Ceriani. Improving a variation of the DSC technique for measuring the boiling points of pure compounds at low pressures. J. Chem. Thermodyn. 100 (2016). pp. 191-197.

[15]   F.D. Gunstone. 13C-NMR studies of mono-, di- and tri-acylglycerols leading to qualitative and semiquantitative information about mixtures of these glycerol esters Chemistry and Physics of. Chem. Phys. Lipids,. 58(1991). pp. 219-224

[16]   R. Ceriani, R. Gani, Y. A. Liu. Prediction of vapor pressure and heats of vaporization of edible oil/fat compounds by group contribution. Fluid Phase Equilib. 337 (2013). pp. 53−59.

[17]   J. Marrero, R. Gani, Group-contribution based estimation of pure component properties, Fluid Phase Equilib. 183–184 (2001). pp. 183–208.

[18]   K.G. Joback, R.C. Reid. Estimation of pure-component properties from group-contributions. Chem. Eng. Commun. 57 (1987). pp. 233–243.

[19] L. Zong, S. Ramanathan, C. Chen. Predicting Thermophysical properties of mono- and diglycerides with the chemical constituent fragmentm approach. Ind. Eng. Chem. Res. 49 (2010). pp. 5479−5484.

[20] D. L. Compton. K. E. Vermillion. J. A. Laszlo. Acyl migration kinetics of 2-monoacylglycerols from soybean oil via 1h NMR. J Am. Oil Chem Soc. 84 (2007). pp.343-348.

[21] S. Young. Introduction. In: Distillation principles and processes. Great Britain: Macmillan and Co.; 1922.

[22] Aspen plus v8.4. NIST Thermodata Engine Version 7.1. Burlington, MA: Aspen Technology, Inc.; 2013.

[23] R. W. Murray. Analytical Chemistry. American Chemical Society.ACS. Washington, DC, 2005.M.L.

[24] Castelló. J. Dweck. D.A.G. Aranda. Thermal stability and water content determination of glycerol by thermogravimetry. J Therm Anal Calorim. 97 (2009). pp. 627–630.

[25] Z. Sanchez-Reinoso. L.F. Gutiérrez. Effects of the emulsion composition on the physical properties and oxidative stability of sacha inchi (Plukenetia volubilis l.) oil microcapsules produced by Spray Drying. Food Bioprocess Technol. 10 (2017). pp. 1354–1366.

[26] Z. Saavedra-Leos. C. Leyva-Porras. S.B. Araujo-Díaz. A. Toxqui-Terán. A.J. Borrás-Enríquez. Technological application of maltodextrins according to the degree of polymerization. Molecules. 20(2015). pp. 21067-21081.

CAPÍTULO 8

CONCLUSÕES

O estudo do equilíbrio líquido-vapor de misturas graxas foi determinado e analisado nesta tese de doutorado. De forma geral, a tese foi dividida em três partes, a primeira foi o aprimoramento da técnica do DSC, a segunda foi a determinação e análise experimental de compostos puros e sistemas binários graxos, e a terceira foi a regressão e avaliação de novos parâmetros (a_{mn}) dos métodos UNIFAC Linear, Modificado e Dortmund.

Na primeira parte do trabalho, que consistiu na otimização da taxa de aquecimento utilizada para a técnica do DSC a partir da análise da temperatura de ebulição obtida experimentalmente, observou-se que a melhor taxa de aquecimento foi a de 25 K/min para a classe de compostos testados, os quais são: n-parafinas, álcool e ácido graxos. Esta foi a mesma taxa de aquecimento ótima encontrada por outros trabalhos que utilizaram a técnica do DSC, como Troni et al. (2016). Com a taxa otimizada foi possível prosseguir para a etapa de determinação de dados experimentais de ELV de sistemas graxos pelo DSC.

Foram determinados dados de temperatura de ebulição de três compostos, os quais são: monononanoina, monolaurina e dinonanoina à pressões subatmosféricas. O comportamento esperado para uma serie homóloga de monoacilgliceróis foi obtido, como foi constatado no **Capítulo 4**. Dados de ELV para os seguintes sistemas, monocaprilina + ácido láurico (3,42 kPa), monononanoina + monolaurina (2,06 kPa), monononanoina + hexadecanol (2,02 kPa), monolaurina + octadecanol (2,05 kPa), hexadecanol + octadecanol (1,73 kPa), hexadecanol + metil miristato (1,72 kPa) monononanina + tributirina (1,69 kPa) e dinonanoina + octacosano (1,70 kPa), foram determinados com êxito pela técnica do DSC. Os sistemas monononanoina + monolaurina e hexadecanol + octadecanol apresentaram γ ≈ 1. Já os sistemas monocaprilina + ácido láurico, monononanoina + hexadecanol, monolaurina + octadecanol, hexadecanol + metil miristato, monononanina + tributirina e dinonanoina + octacosano exibiram um comportamento não ideal. A partir destes dados foi possível mapear as interações dos diferentes grupos funcionais e assim testar a capacidade preditiva do UNIFAC, em suas diferentes versões. Nesta análise ficou clara a importância de um banco de dados robusto, pois ainda há uma lacuna a ser explorada referente à aplicação de métodos de contribuição de grupos para a predição do equilíbrio líquido-vapor de compostos lipídicos. O **Capítulo 6** foi feita uma análise ainda mais detalhada do UNIFAC.

A partir do banco de dados *SPEED Lipids Database* (banco de dados desenvolvido pelo grupo SPEED da Denmark Technical University liderado pelo Professor Rafiqul Gani), foi possível realizar a regressão dos parâmetros (a_{mn} e a_{nm}) dos métodos UNIFAC Linear, Modificado e Dortmund para compostos encontrados da tecnologia de lipídios. Foi observado que todos os métodos com os novos valores apresentaram uma melhor predição quando comparado com os mesmos métodos com os seus valores originais para os compostos graxos. De forma geral, todos os métodos com os novos parâmetros apresentaram um desvio relativo global de aproximadamente 10% para compostos graxos.

A temperatura normal de ebulição de acilgliceróis parciais (monobutirina monocaprina, monolaurina, monopalmitina e monoestearina, dicaprilina, dinonanoina e dicaprina) foi medida pela técnica TGA. Os compostos analisados apresentaram o comportamento esperado para séries homólogas de monoacilgliceróis ou diacilgliceróis. Os dados foram comparados com diferentes metodologias preditivas e com dados experimentais de compostos com os mesmos grupos funcionais que os MAGs e DAGs, tanto a comparação preditiva quanto a experimental corroborou com os resultados obtidos. Os métodos preditivos de Ceriani et al. (2013), Marrero e Gani (2001), e Zong et al. (2010) apresentaram capacidades preditivas similares e com desvio relativos global próximo a a 3%, diferentemente do método de Joback e Reid (1987), que apresentou um desvio relativo global em torno de 28%.

De uma forma geral, observou-se que as maiores dificuldades para a obtenção de dados de compostos puros ou de equilíbrio líquido-vapor pela técnica do DSC são: selecionar misturas que sejam possíveis de serem determinadas pela técnica do DSC, dentro das limitações do DSC; considerar o custo das amostras; e encontrar misturas sejam suficientemente não ideais para que o método preditivo seja realmente testado ou aprimorado.

CAPÍTULO 9

TRABALHOS FUTUROS

Ainda há uma grande lacuna na literatura de dados experimentais acurados, então se faz necessária a obtenção de mais dados de pressão de vapor e de equilíbrio liquido-vapor de misturas envolvendo compostos graxos, principalmente os acilgliceróis parciais, considerando outras faixas de pressão, sendo elas binárias ou multicomponentes, envolvendo não idealidades na fase líquida.

Sugere-se, ainda, testar para diversos sistemas graxos a capacidade preditiva dos parâmetros originais (FREDENSLUND et al., 1975; LARSEN et al., 1987; WEIDLICH e GMEHLING, 1987; HANSEN et al., 1992) e dos novos parâmetros desenvolvidos nessa tese a_{mn} dos UNIFACs Linear, Modificado e Dortmund, bem como de outras ferramentas preditivas.

Utilizar os dados experimentais e os novos parâmetros a_{mn} dos UNIFACs Linear, Modificado e Dortmund obtidos neste estudo na simulação de processos envolvidos na tecnologia de lipídeos, tanto na produção de biodiesel como de óleos e gorduras.

9.1 REFERÊNCIAS

FREDENSLUND, A., JONES, R. L.; PRAUSNITZ, J. M. Group-contribution estimation of activity coefficients in nonideal liquid mixtures. **American Institute of Chemical Engineers Journal**, v. 21, p. 1086–1099, 1975.

HANSEN, H. K.; COTO, B.;KUHLMANN, B. UNIFAC with linearly temperature-dependent group-interaction parameters. Internal report. 1992.

LARSEN, B.; RASMUSSEN, P.; FREDENSLUND, A. **A modified UNIFAC group-contribution model for prediction of phase equilibria and heats of mixing. Ind.** Eng. Chem. Res.. v. 26, p. 2274 – 2286, 1987.

WEIDLICH, U.; GMEHLING, J. A modified UNIFAC model. 1. Prediction of VLE, hE, and .gamma..infin. **Industrial & Engineering Chemistry Research,** v. 26, p. 1372–1381, 1987.

APÊNDICES

SUPPLEMENTARY MATERIAL 4 – Capítulo 4

Table 4S.1. Constants for Wagner Equation (S1 and S2) from NIST TDE Aspen Plus 8.4

Constants	lauric acid	hexadecanol	octadecanol
C_{1i}	-15.25105	-10.49475	-9.505732
C_{2i}	17.3757	4.498022	1.172043
C_{3i}	-27.05154	-8.766438	-5.525542
C_{4i}	10.47761	-12.36442	-14.69776
$\ln p_{ci}$ [a]	14.47363	14.21226	14.06551
T_{ci} [b]	743	770	790
T_{lower} (K)	316.9689	318.309	331.15
T_{upper} (K)	743	770	790

[a] p_{ci} is critical pressure of component i; T_{ci} is critical temperature of component i in K.

SUPPLEMENTARY MATERIAL 5 – Capítulo 5

Table 5S2. Constants for Antoine Equation (Eq. 1)

Constants	hexadecanol[a]	octadecanol[a]	methyl myristate[a]	octacosane[a]	tributyrin[b]	monononanoin[c]
A	14.5026	15.3778	16.0648	16.1051	17.9470	67.86
B	-4528.6	-5375.0	-5701.4	-6472.9	-7343.1	-98500
C	-138.2	-121.2	-71.2	-135.7	-38.5	983.8
Lower T	321.98	332.97	340.00	422.00	468.65	471.02
Upper T	530.11	528.85	510.92	588.13	589.30	509.88

[a] NIST TDE Aspen Plus 8.4. [b] Ref. [4]. [c] Ref. [2]

The UNIQUAC (Universal Quasichemical) model for a binary system

$$\ln \gamma_1 = \ln \frac{\Phi_1^*}{x_1} + \frac{z}{2} q_1 \ln \frac{\theta_1}{\Phi_1^*} + \Phi_2^* \left(l_1 - \frac{r_1}{r_2} l_2 \right) - q'_1 \ln(\theta'_1 + \theta'_2 \tau_{21}) + \theta'_2 q'_1 \left(\frac{\tau_{21}}{\theta'_1 + \theta'_2 \tau_{21}} - \frac{\tau_{12}}{\theta'_2 + \theta'_1 \tau_{12}} \right) \quad \text{(S1)}$$

$$\ln \gamma_2 = \ln \frac{\Phi_2^*}{x_2} + \frac{z}{2} q_2 \ln \frac{\theta_2}{\Phi_2^*} + \Phi_2^* \left(l_2 - \frac{r_2}{r_1} l_1 \right) - q'_2 \ln(\theta'_2 + \theta'_2 \tau_{12}) + \theta'_1 q'_2 \left(\frac{\tau_{12}}{\theta'_2 + \theta'_1 \tau_{12}} - \frac{\tau_{21}}{\theta'_1 + \theta'_2 \tau_{21}} \right) \quad \text{(S2)}$$

$$\tau_{12} = \exp\left(\frac{b_{12}}{RT} \right) \quad \text{(S3)}$$

$$\tau_{21} = \exp\left(\frac{b_{21}}{RT} \right) \quad \text{(S4)}$$

Table 5S2. Predicted VLE data for the follow binary systems: hexadecanol + octadecanol (1), methyl myristate + hexadecanol (2), using UNIFAC methods with their original parameters and lipid-based parameters by Damaceno et al. [9] (Linear, Modified and Dortmund), and NIST modified, with their respective deviations (AAD[a] and ARD[b])

| | hexadecanol+octadecanol | | | | | | | methyl myristate + hexadecanol | | | | | | | |
| Molar fraction | Original models | | | | Lipids-based models | | | Molar fraction | Original models | | | | Lipids-based models | | |
(x_1)	Linear [10]	Modified [11]	Dortmund [12]	NIST modified [5]	Linear [9]	Modified [9]	Dortmund [9]	(x_1)	Linear [10]	Modified [11]	Dortmund [12]	NIST modified [5]	Linear [9]	Modified [9]	Dortmund [9]
1.0000	462.73	462.73	462.73	462.73	462.73	462.73	462.73	1.0000	438.4997	438.50	438.50	438.50	438.4997	438.50	438.50
0.8997	464.06	464.17	464.17	464.17	464.06	464.17	464.17	0.9014	440.0282	440.12	440.05	440.05	439.7584	439.91	439.46
0.8026	465.72	465.65	465.66	465.65	465.72	465.65	465.66	0.8000	441.7012	441.92	441.75	441.74	441.1216	441.44	440.53
0.7016	467.34	467.31	467.32	467.31	467.34	467.31	467.32	0.7005	443.4643	443.83	443.55	443.52	442.5538	443.05	441.67
0.6084	469.12	468.95	468.96	468.95	469.13	468.95	468.96	0.6001	445.3929	445.93	445.52	445.47	444.1329	444.81	442.94
0.5008	471.03	471.00	471.01	471.00	471.04	471.00	471.01	0.5032	447.4285	448.12	447.61	447.53	445.8377	446.70	444.35
0.4011	473.27	473.07	473.08	473.07	473.28	473.06	473.08	0.3979	449.8796	450.73	450.13	449.99	447.9802	449.02	446.17
0.3003	475.39	475.35	475.36	475.35	475.40	475.35	475.36	0.3049	452.2981	453.22	452.60	452.42	450.235	451.37	448.18
0.2017	477.90	477.80	477.81	477.80	477.91	477.79	477.81	0.1980	455.4404	456.32	455.75	455.54	453.4534	454.56	451.28
0.0932	480.58	480.79	480.79	480.79	480.59	480.79	480.79	0.1017	458.675	459.30	458.91	458.74	457.2178	458.03	455.39
0.0000	483.65	483.65	483.65	483.65	483.65	483.65	483.65	0.0000	462.5919	462.59	462.59	462.59	462.5919	462.59	462.59
AAD (K)	1.01	0.96	0.97	0.96	1.01	0.96	0.97	AAD (K)	1.21	1.11	1.15	1.20	1.49	1.32	2.24
ARD (%)	0.216	0.207	0.207	0.207	0.218	0.207	0.207	ARD (%)	0.271	0.249	0.249	0.267	0.328	0.293	0.495

[a] $AAD = \sum_{i=1}^{n} \frac{1}{n} \cdot \left| T_{exp} - T_{calc} \right|_i$. [b] $ARD = \sum_{i=1}^{n} \frac{1}{n} \cdot \left[100 \cdot \frac{\left| T_{exp} - T_{calc} \right|}{T_{exp}} \right]$. where T_{exp} is experimental temperature in K

Table 5S3. Predicted VLE data for the follow binary systems: tributyrin + monononanoin (3) and dinonanoin + octacosane (4) using UNIFAC methods with their original parameters and lipids-based parameters by Damaceno et al. [9] (Linear. Modified and Dortmund). and NIST modified. with their respective deviations (AAD[a] and ARD[b])

| | tributyrin + monononanoin | | | | | | | dinonanoin + octacosane | | | | | | | |
| | Original models | | | | Lipids-based models | | | | Original models | | | | Lipids-based models | | |
Molar fraction (x_1)	Linear [10]	Modified [11]	Dortmund [12]	NIST modified [5]	Linear [9]	Modified [9]	Dortmund [9]	Molar fraction (x_1)	Linear [10]	Modified [11]	Dortmund [12]	NIST modified [5]	Linear [9]	Modified [9]	Dortmund [9]
1.0000	459.98	459.98	459.98	459.98	459.98	459.98	459.98	1.000	530.85	530.85	530.85	530.85	530.85	530.85	530.85
0.9020	460.71	461.51	460.91	460.77	461.23	462.07	457.98	0.8944	532.10	532.80	532.19	531.55	531.56	530.33	532.26
0.8058	461.55	463.15	461.91	461.64	462.53	464.44	457.50	0.7889	533.45	535.03	533.65	532.44	532.38	530.39	533.68
0.7035	462.55	465.05	463.08	462.67	464.03	467.23	457.51	0.6824	534.94	537.58	535.25	533.53	533.33	530.79	535.11
0.6087	463.61	466.96	464.30	463.76	465.53	469.97	457.67	0.5973	536.25	539.82	536.65	534.56	534.19	531.27	536.24
0.5066	464.94	469.16	465.79	465.10	467.31	472.87	457.91	0.5006	537.89	542.51	538.39	535.95	535.29	531.99	537.54
0.4001	466.62	471.55	467.63	466.78	469.36	475.58	458.33	0.4068	539.69	545.13	540.24	537.59	536.54	532.94	538.85
0.3107	468.36	473.55	469.47	468.51	471.25	477.36	459.05	0.2974	542.12	547.85	542.68	540.02	538.37	534.60	540.55
0.2041	471.02	475.78	472.13	471.13	473.73	478.71	460.99	0.2024	544.61	549.63	545.07	542.74	540.57	537.02	542.39
0.1008	474.50	477.64	475.33	474.56	476.36	479.19	465.72	0.0984	547.84	550.82	548.06	546.59	544.39	541.90	545.45
0.0000	479.03	479.03	479.03	479.03	479.03	479.03	479.03	0.0000	551.47	551.31	551.31	551.31	551.31	551.31	551.31
AAD (K)	0.56	2.80	0.81	0.58	1.66	4.86	5.68		3.16	6.05	3.43	1.98	1.50	1.56	2.50
ARD (%)	0.12	0.60	0.17	0.12	0.36	1.04	1.22		0.591	1.129	0.41	0.371	0.281	0.291	0.469

[a] $AAD = \sum_{i=1}^{n} \frac{1}{n} \cdot \left| T_{exp} - T_{calc} \right|_i$. [b] $ARD = \sum_{i=1}^{n} \frac{1}{n} \cdot \left[100 \cdot \frac{\left| T_{exp} - T_{calc} \right|}{T_{exp}} \right]$. where T_{exp} is experimental temperature in K

The UNIFAC methods (Linear, Modified, Dortmund and Modified NIST UNIFAC) [5,9-13]

$$\ln \gamma_i^C = \ln \frac{r_i^{C_0}}{\sum_j x_j r_j^{C_0}} + 1 - \frac{r_i^{C_0}}{\sum_j x_j r_j^{C_0}} - C_1 \left(\ln \left(\frac{\Phi_i}{\theta_i} \right) + 1 - \frac{\Phi_i}{\theta_i} \right) \qquad (S5)$$

$$\Phi_i = \frac{r_i}{\sum_j x_j r_j} \qquad (S6)$$

$$\theta_i = \frac{q_i}{\sum_j x_j q_j} \qquad (S7)$$

Table 5S4. C_0 and C_1 of Eq. S5

Model	C_0	C_1
Original-UNIFAC	1	$5q_i$
Linear-UNIFAC	1	$5\ q_i$
Modified-UNIFAC	$^2/_3$	0
Dortmund-UNIFAC and NIST	¾	$5\ q_i$

$$\ln \gamma_i^R = \sum_K^{groups} v_k^{(i)} \left[\ln \Gamma_k - \ln \Gamma_k^{(i)} \right]$$

$$(S8)$$

$$ln\Gamma_k = Q_k \cdot \left[1 - ln \left(\sum_m \Theta_m \Psi_{mk} \right) - \sum_m \left(\theta_m \Psi_{mk} \middle/ \sum_n \Theta_n \Psi_{nm} \right) \right] \qquad (S9)$$

$$\Theta_m = \frac{Q_m X_m}{\sum_n Q_n X_n} \qquad (S10)$$

$$X_m = \frac{\sum_i^M v_m^{(i)} x_i}{\sum_i^M \sum_j^N v_j^{(i)} x_i} \qquad (S11)$$

$$\Psi_{mn} = \exp \left(\frac{-a_{m,n}}{T} \right) \qquad (S12)$$

$$a_{m,n} = A_0 a_{mn,0} + A_1 a_{mn,1} + A_2 a_{mn,2} \qquad (S13)$$

Table S5. A_0, A_1 and A_2 of Eq. S13

Model	A_0	A_1	A_2
Original-UNIFAC	1	0	0
Linear-UNIFAC	1	$T-T_0$	0
Modified-UNIFAC	1	$T-T_0$	$T\ln(T_0/T) + T - T_0$
Dortmund-UNIFAC and NIST	1	T	T^2

T_0 is reference temperature ($T_0 = 298.15$ K)

Table 5S6. Area (Q_k) and volume (R_k) parameters for the groups used for the UNIFAC models.

Main Group	Sub group	Linear- and Modified-UNIFAC [10-11]		Dortmund-UNIFAC and NIST [5,12]	
		R_k	Q_k	R_k	Q_k
CH$_2$	CH3	0.9011	0.8480	0.6325	1.0608
	CH2	0.6744	0.5400	0.6325	0.7081
	CH	0.4469	0.2280	0.6325	0.3554
OH	OH	1.0000	1.2000	-	-
	OHp[*a]	-	-	1.2302	0.8927
	OHs[*a]	-	-	1.0630	0.8663
CCOO	CH2COO	1.6764	1.4200	1.2700	1.4228
OH$_{acyl}$[*b]	OH$_{acyl}$	1.0000	1.2000	-	-
	OH$_{acyl,p}$[*c]	-	-	1.2302	0.8927
	OH$_{acyl,s}$[*c]	-	-	1.0630	0.8663

[*a] OHp and OHs subgroups are used only for Dortmund UNIFAC
[*b] OHacyl describes mono- and diacylglycerols molecules and uses same R and Q as OH group
[*c] For Dortmund UNIFAC monoacylglycerols are described with one OH$_{acyl,p}$ and one OH$_{acyl,s}$, while diacyglycerols are described with one OH$_{acyl,p}$

Table 5S7. Interaction parameters $a_{mn,0}$, $a_{mn,1}$ and $a_{mn,2}$ used in this wok to all the UNIFAC versions.

Parameters		Modified	Dortmund	NIST[a]	Linear[b]	Modified	Dortmund
CH2/OH	$a_{mn,0}$	972.8	2777	3119.2	874.14	629.70	2159.41
	$a_{mn,1}$	0.2687	-4.674	-6.073	-0.8130	0.5774	-44.226
	$a_{mn,2}$	8.773	0.001551	23.986	0	87.730	0.0005
OH/CH2	$a_{mn,0}$	637.5	1606	1857.23	35.59	405.36	1946.97
	$a_{mn,1}$	-5.832	-4.746	-87.982	-14.292	-34.830	-32.692
	$a_{mn,2}$	-0.8703	0.0009181	10.757	0	-27.090	0.0001
CH2/CCOO	$a_{mn,0}$	329.1001	98.656	113.19	277.81	253.66	65.65
	$a_{mn,1}$	-0.1518	1.9294	18.837	0.0905	-0.0909	26.493
	$a_{mn,2}$	-1.824	-3.13E-03	-38.391	0	-37.850	-0.0008
CCOO/CH2	$a_{mn,0}$	44.43	632.22	737.00	76.42	149.49	348.47
	$a_{mn,1}$	-0.9718	-3.3912	-30.713	-0.9890	-0.9999	-22.544
	$a_{mn,2}$	0.5518	3.93E-03	31.041	0	0.5518	0.0011
CCOO/OH	$a_{mn,0}$	266.8999	310.4	252.79	427.70	266.90	788.63
	$a_{mn,1}$	-1.054	1.538	26.565	-0.8859	-0.9990	35.416
	$a_{mn,2}$	3.586	-0.0049	-79.064	0	0.6670	-0.0002
OH/CCOO	$a_{mn,0}$	169.1	973.8	1097.75	212.89	169.10	1176.55
	$a_{mn,1}$	0.1902	-5.633	-78.816	-0.0080	0.3607	-52.856
	$a_{mn,2}$	4.625	0.0077	13.497	0	0.1110	0.0080

[a] $1000a_{mn,2}$. [b] Original values of the Linear UNIFAC are only available by an internal report at Denmark Technical University [10].

Table 4S8. Molecular structure of octacosane, hexadecanol, octadecanol, monononanoin, dinonanoin, tributyrin and methyl myristate.

Compound	Molecular estructure
octacosane	
hexadecanol	
octadecanol	
monononanoin	
dinonanoin	
tributyrin	
Methyl myristate	

SUPPLEMENTARY MATERIAL 7 – Capítulo 7

Table 7S3. T_{nb} of alcohols and methyl esters with their respective standard deviations and MW

Compounds[*]	MW (g.mol^{-1})	T_{nb} (K)	u(T)
1-decanol	158.29	504.18	0.0759
1-tetradecanol	214.39	568.96	0.0539
1-hexadecanol	242.45	597.81	0.7800
1-octadecanol	270.50	623.74	1.5400
1-eicosanol	298.56	658.50	32.6000
methyl decanoate	186.29	505.85	1.4100
methyl dodecanoate	214.35	540.22	2.4200
methyl myristate	242.40	572.41	2.6500
methyl palmitate	270.46	599.70	10.2000
methyl stearate	298.51	623.84	9.4300
methyl eicosanoate	326.57	646.30	15.4000

[*]All data were collected from the NIST TDE database from Aspen Plus v. 8.4.

Table 7S2. Chemical shifts ν (ppm) and intensity (abs) of monocaprin lot D5X

Peak	ν (ppm)	Intensity (abs)
1	174.4214	73525624.00
2	77.3336	136110048.00
3	77.0794	145453986.00
4	76.8247	146779554.00
5	74.8580 [b]	10046079.00
6	70.2759 [a]	172239151.00
7	65.0859	155021614.00
8	63.4184[a]	147428637.00
9	62.0036 [b]	20322544.00
10	34.1765	168614529.00
11	31.8639	155127792.00
12	29.4252	179394634.00
13	29.2671	327658966.00
14	29.1491	142777830.00
15	24.9107	166631811.00
16	22.6703	161027916.00
17	14.1061	184399232.00

[a]Chemical shifts of 1-MAG; [b]Chemical shifts of 2-MAG

190

Figure 7S1. Spectrum of monocaprin lot D5X
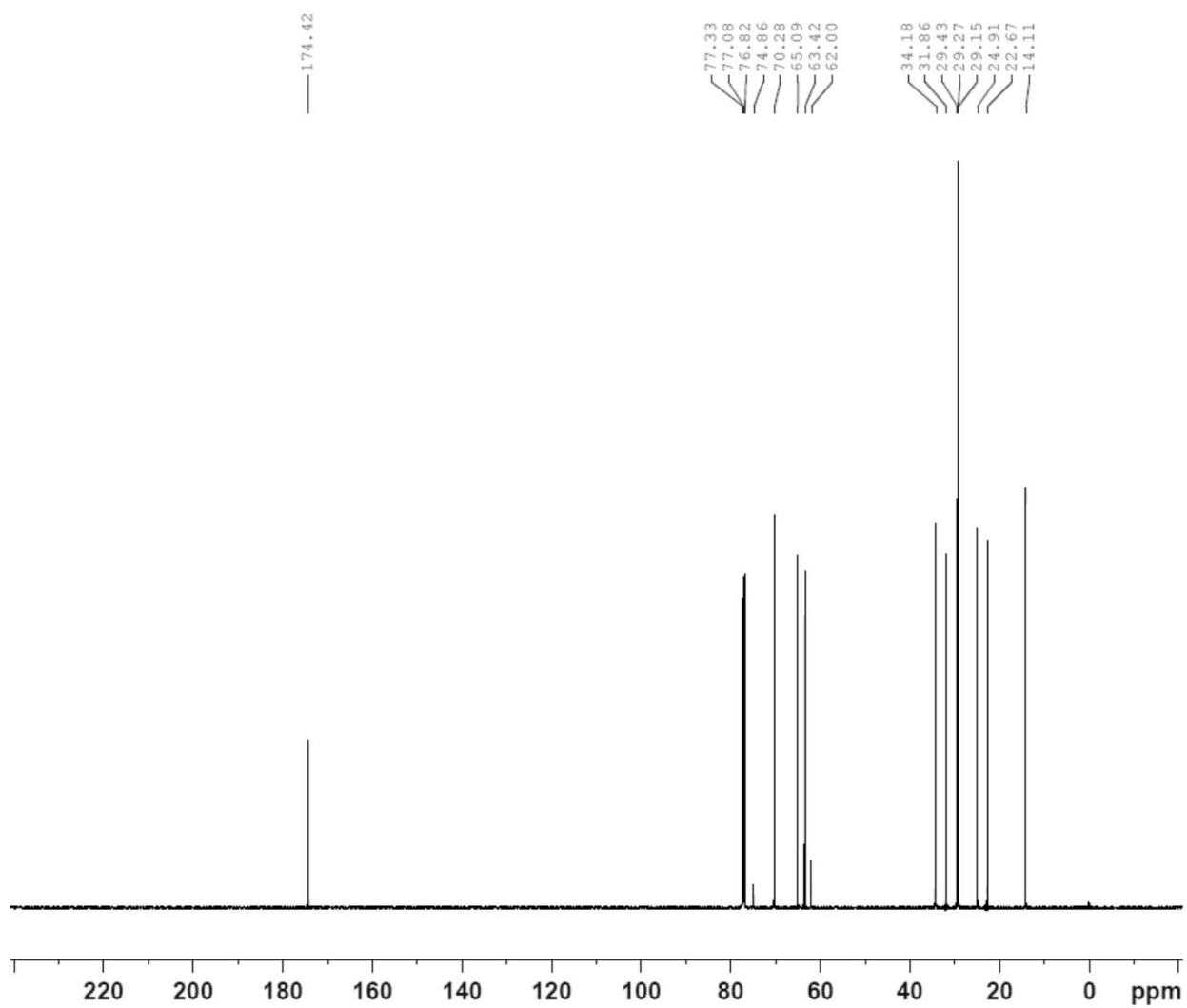
Peak	ν (ppm)	Intensity (abs)
Table 7S3. Chemical shifts ν (ppm) and intensity (abs) of monocaprin lot D23V
1	174.4151	68212966.00
2	77.3303	144694114.00
3	77.0763	151184823.00
4	76.8220	154970327.00
5	74.8668 [b]	8333092.00
6	72.6212	4017406.00
7	70.3299 [a]	3924669.00
8	70.3134 [a]	6891278.00
9	70.2762 [a]	153383476.00
10	70.2442 [a]	6563998.00
11	70.2271 [a]	3767255.00
12	68.9270	4547069.00
13	68.8613	2675897.00
14	65.1456	3586960.00
15	65.0919	154509860.00
16	63.4855 [a]	3048809.00
17	63.4695 [a]	4271804.00
18	63.4526 [a]	7207896.00
19	63.4160 [a]	144150099.00
20	63.3843 [a]	7071597.00
21	63.3667 [a]	3836866.00
22	62.0238 [b]	16490599.00
23	34.1751	161225300.00
24	31.8627	149111467.00
25	29.4230	172140020.00
26	29.2649	325616775.00
27	29.1466	143047301.00
28	24.9099	176361329.00
29	22.6690	152996180.00
30	14.1045	183875206.00

[a]Chemical shifts of 1-MAG; [b]Chemical shifts of 2-MAG

Figure 7S2. Spectrum of monocaprin lot D23V
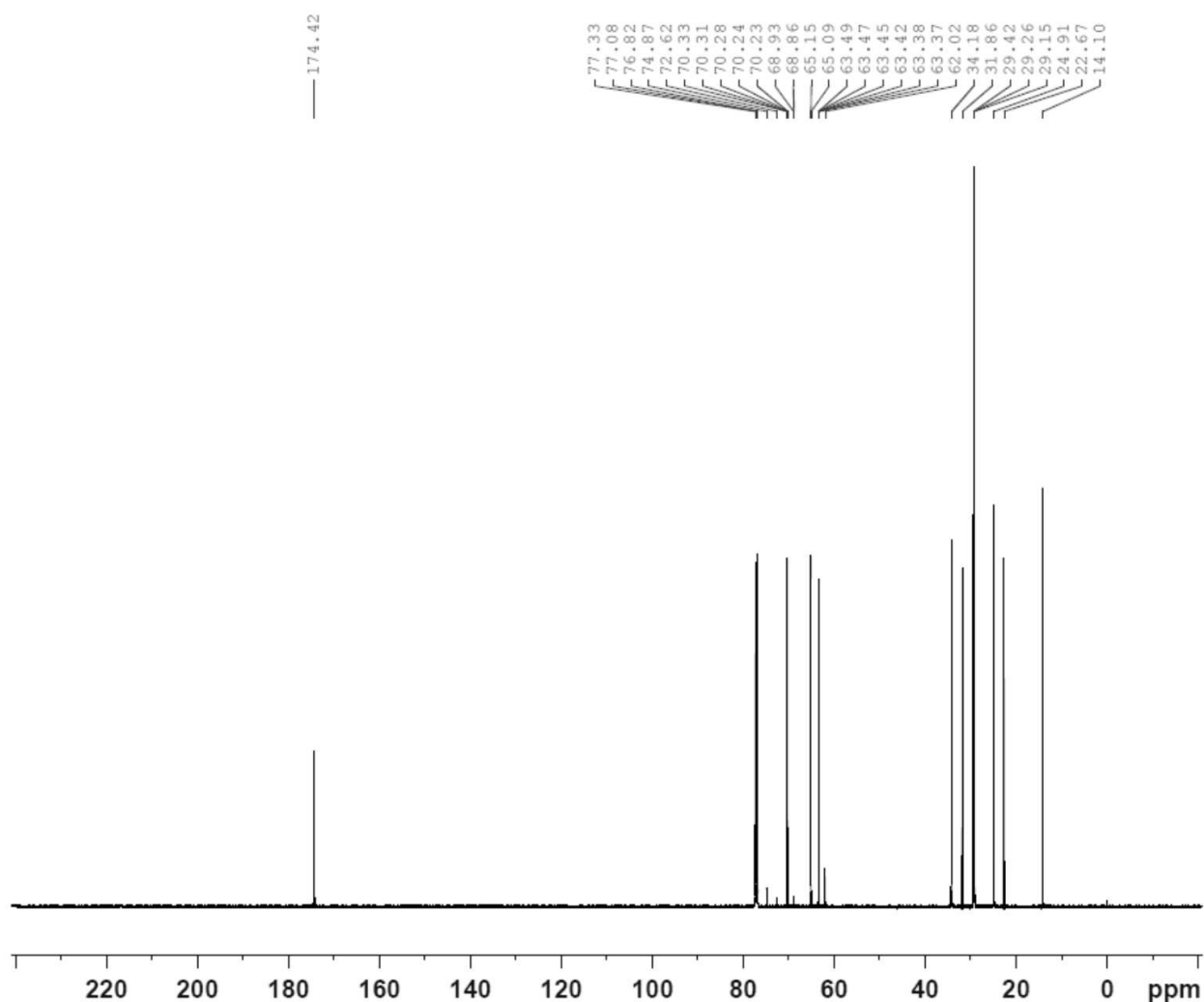
Selection of the onset temperatures of TGA

Based on Troni et al. [14], we developed a method for selecting the onset temperatures from the TGA curves, considering the limitations and differences from both thermal analyses. Figure 2 shows an example of a thermogram obtained from the Mettler Toledo software, in which the experimental procedure was performed and analyzed. The method to acquire the onset temperature data from TGA software was based on the following steps:

1° step   Firstly, based on the TGA step from the thermogram (Figure 7S3), the initial temperature of weight loss was established. Such temperature indicates that the

cumulative mass change reaches a magnitude that the thermobalance detects. In Figure S3, the yellow circle highlights the initial temperature;

2° step   Subsequently, still following the TGA step from the thermogram (Figure 7S3), the final temperature of weight loss was established. Such temperature shows that the cumulative mass change reaches a maximum. In Figure S3, the green circle highlights the final temperature;

3° step   Then, with the temperature range established, the "Horizontal step" function is selected in the Mettler Toledo software, from which it is possible to obtain the weight loss in percentage (%) and the onset temperature of the compound. The onset temperature is calculated from the intersection of the tangent lines from the baselines (blue lines in Figure S3) and the tangent line of the weight loss curve (red line in Figure S3);

4° step For replicates of the same compound, a similar range of temperature was selected to assure accuracy of obtained results. For example: ≈150 K to ≈350 K for glycerol.

Figure 7S3. TGA of glycerol with the onset temperature, tangent of baselines (blue lines), tangent of weight loss curve (red lines), initial temperature (yellow circle) and final temperature (green circle)
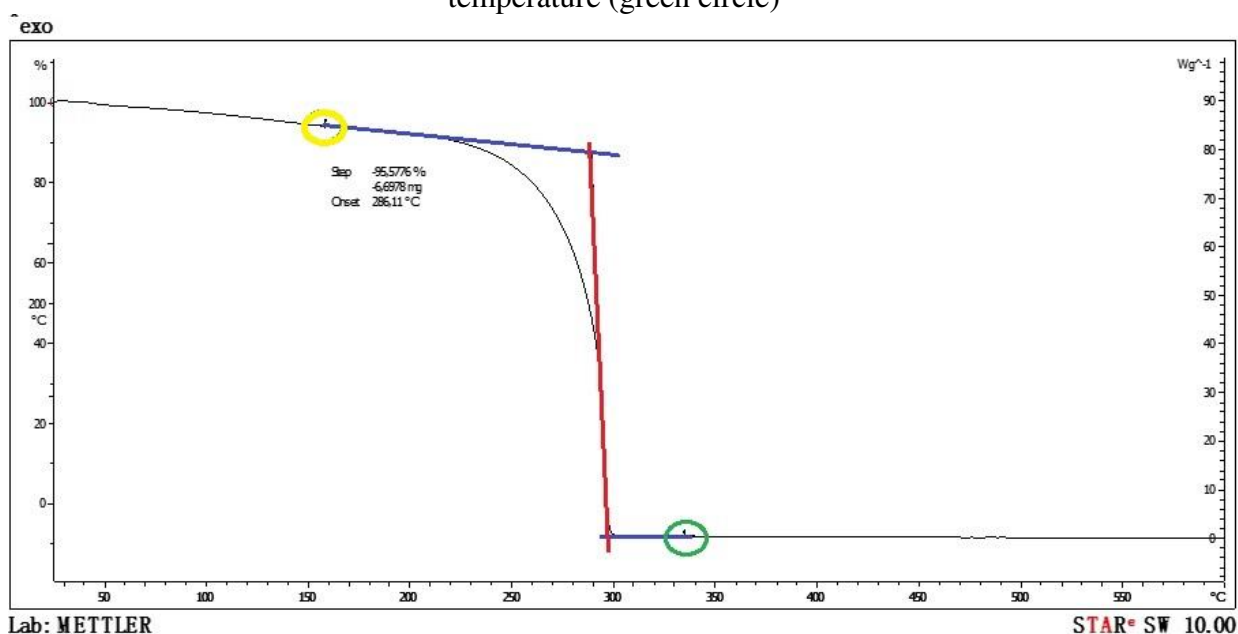
Figure 7S4. TGA and DTG of glycerol
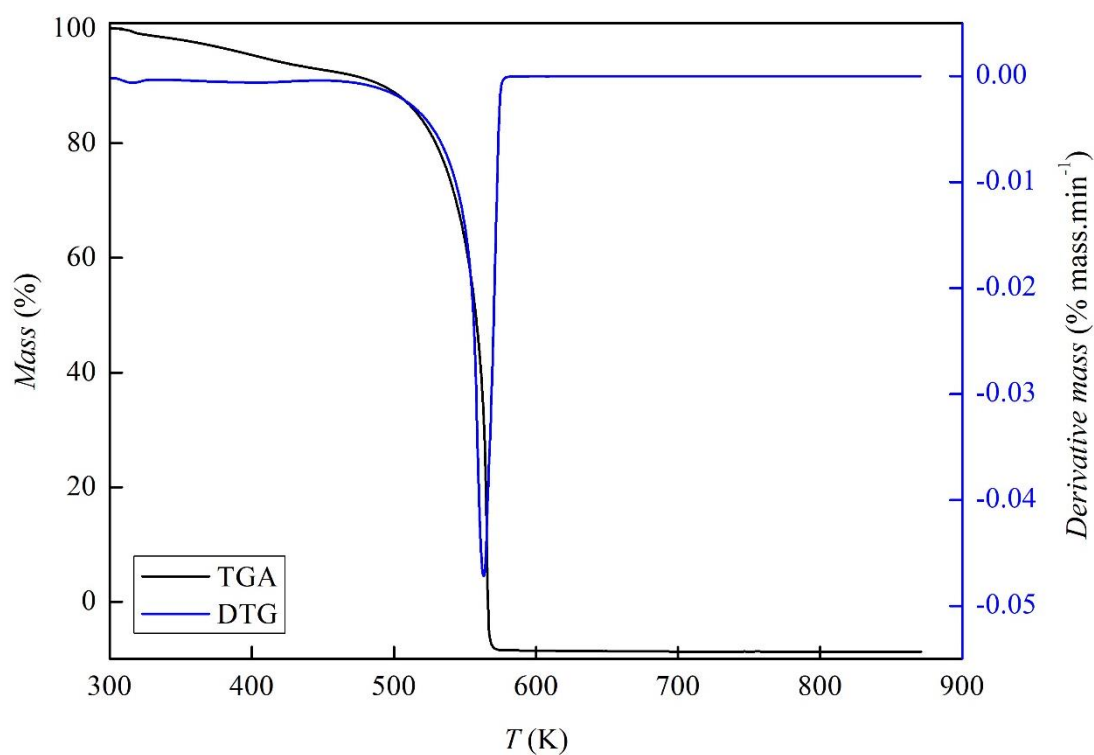
Figure 7S5. TGA and DTG of glycerol focusing on the first event of water loss.
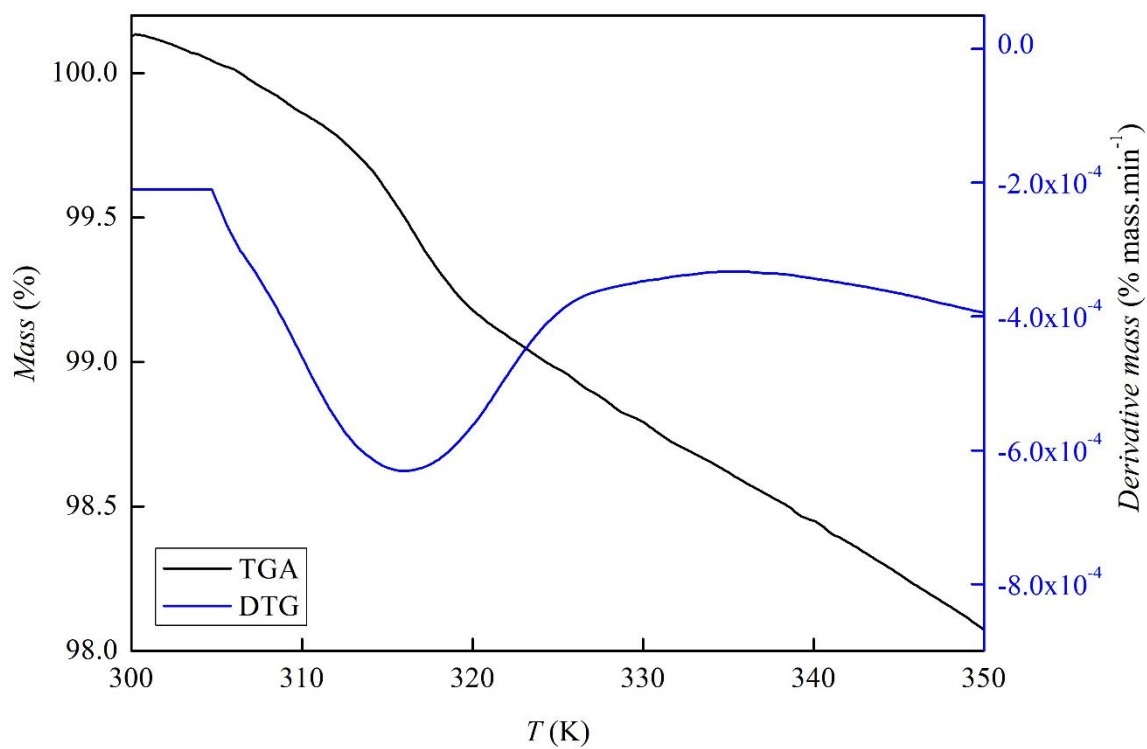
Figure 7S6. TGA and DTG of monobutyrin
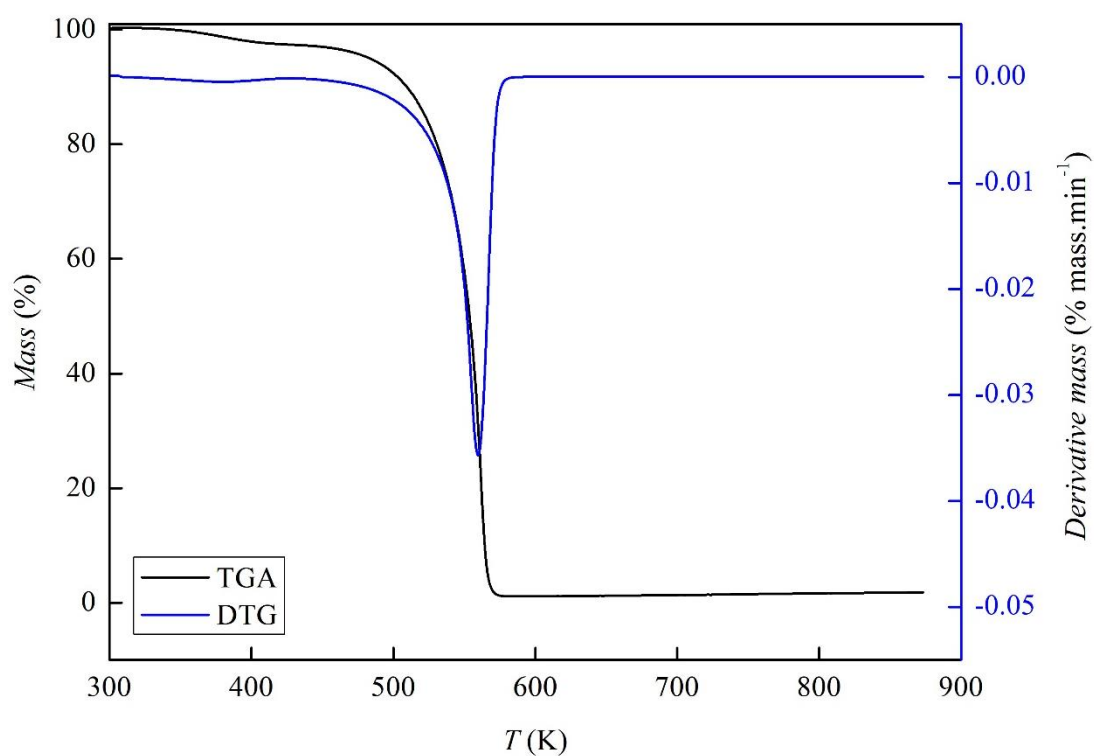
Figure 7S7. TGA and DTG of dicaprylin
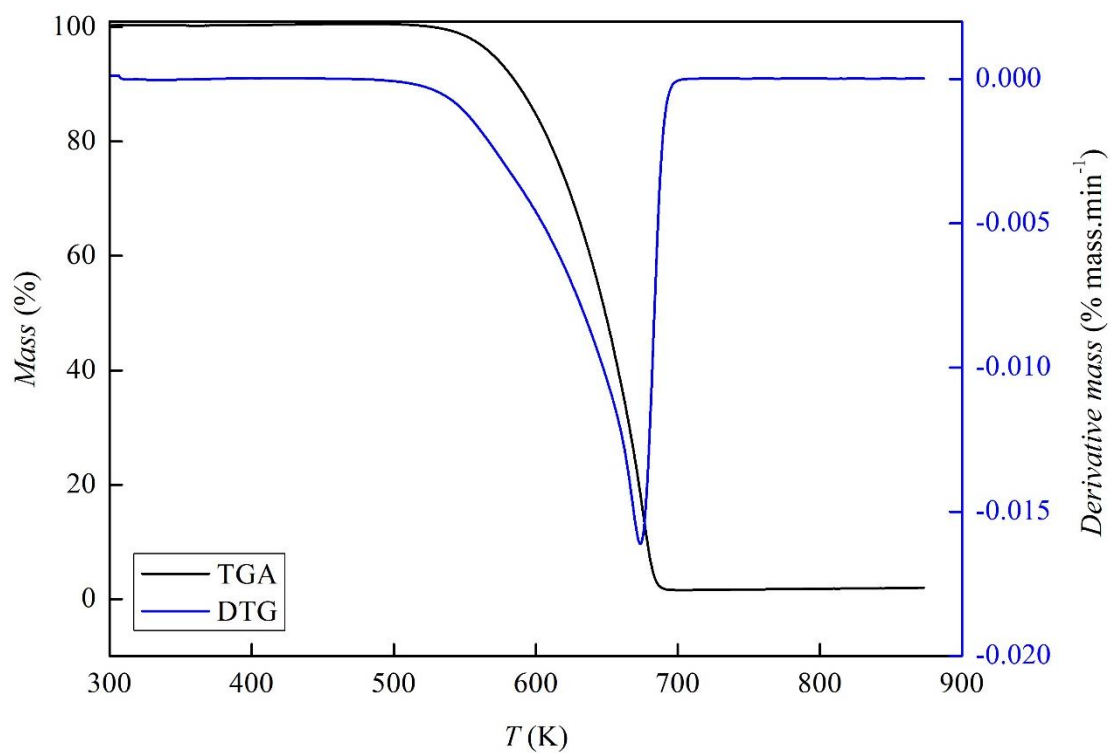
Figure 7S8. TGA and DTG of dinonanoin
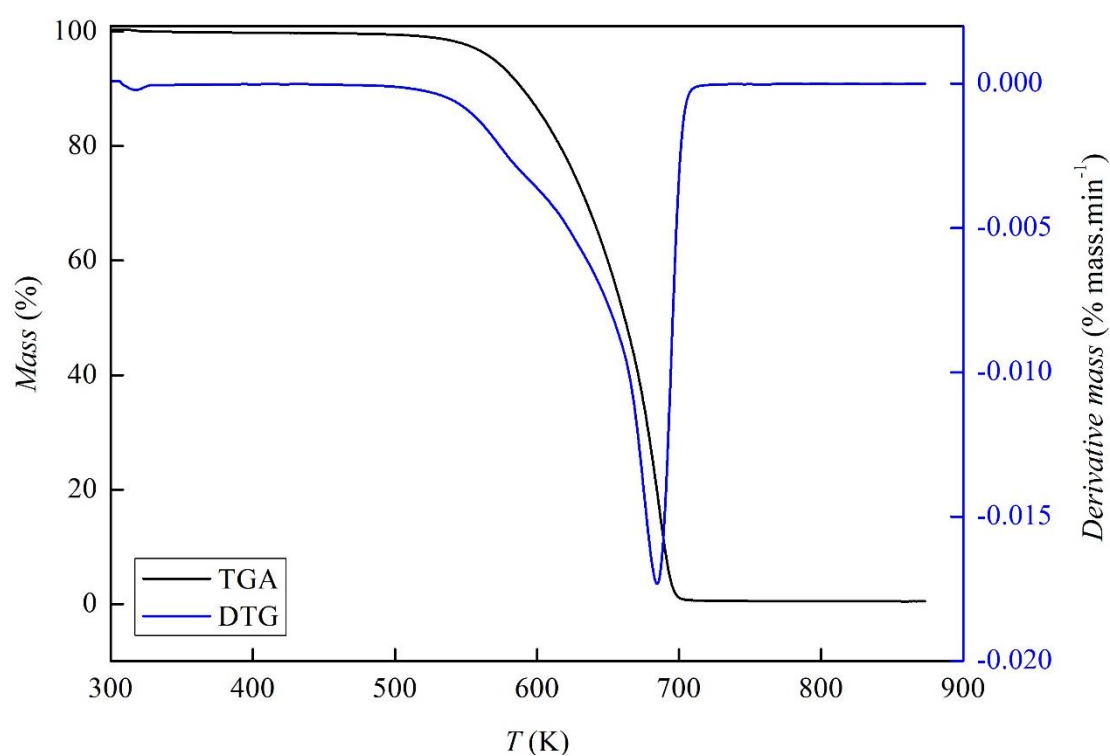
Figure 7S9. TGA and DTG of dicaprin
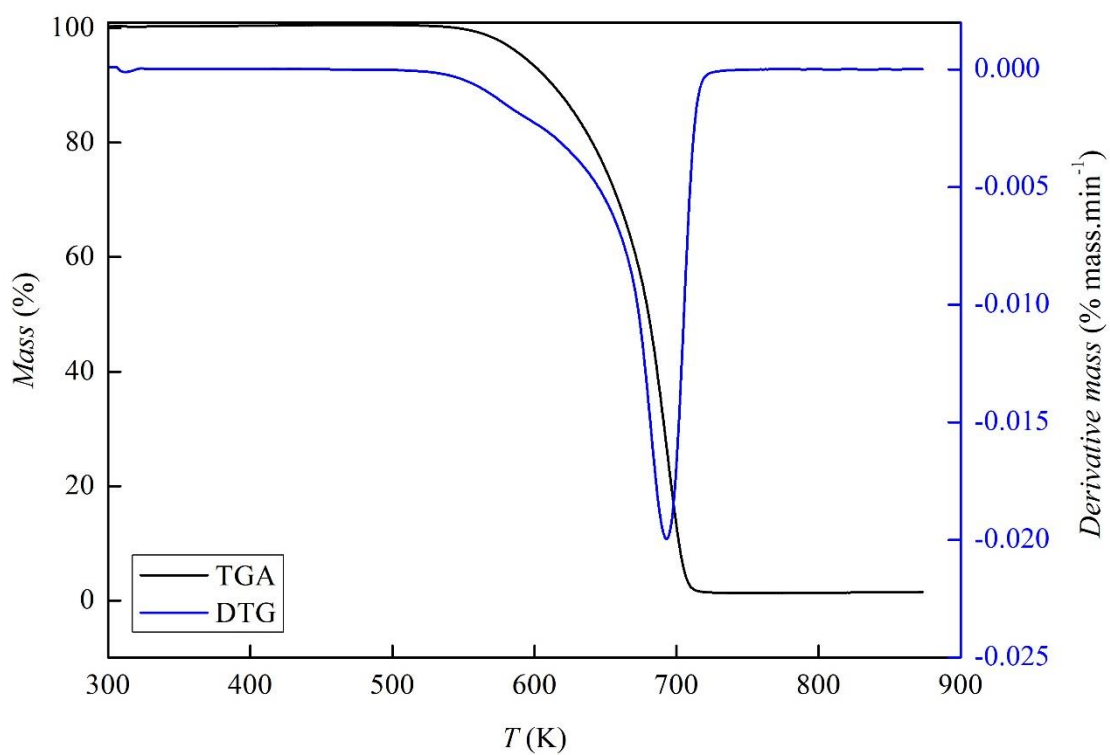
Figure 7S10. TGA and DTG of monopalmitin
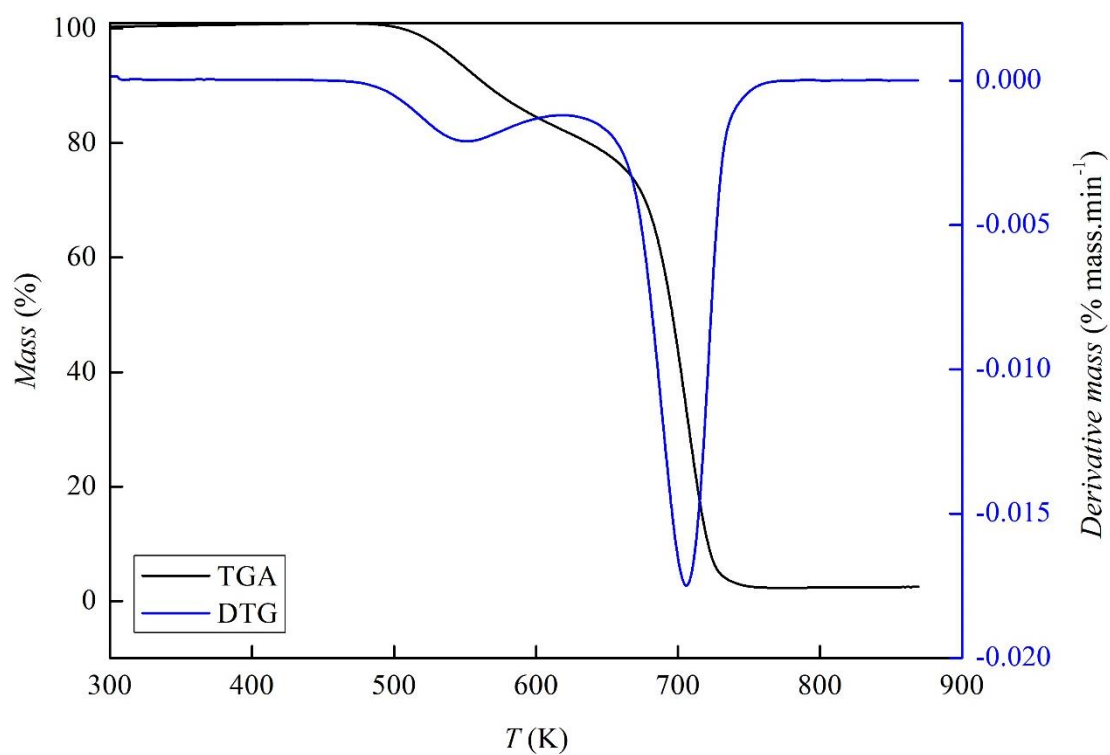
Figure 7S11. TGA and DTG of monoestearin
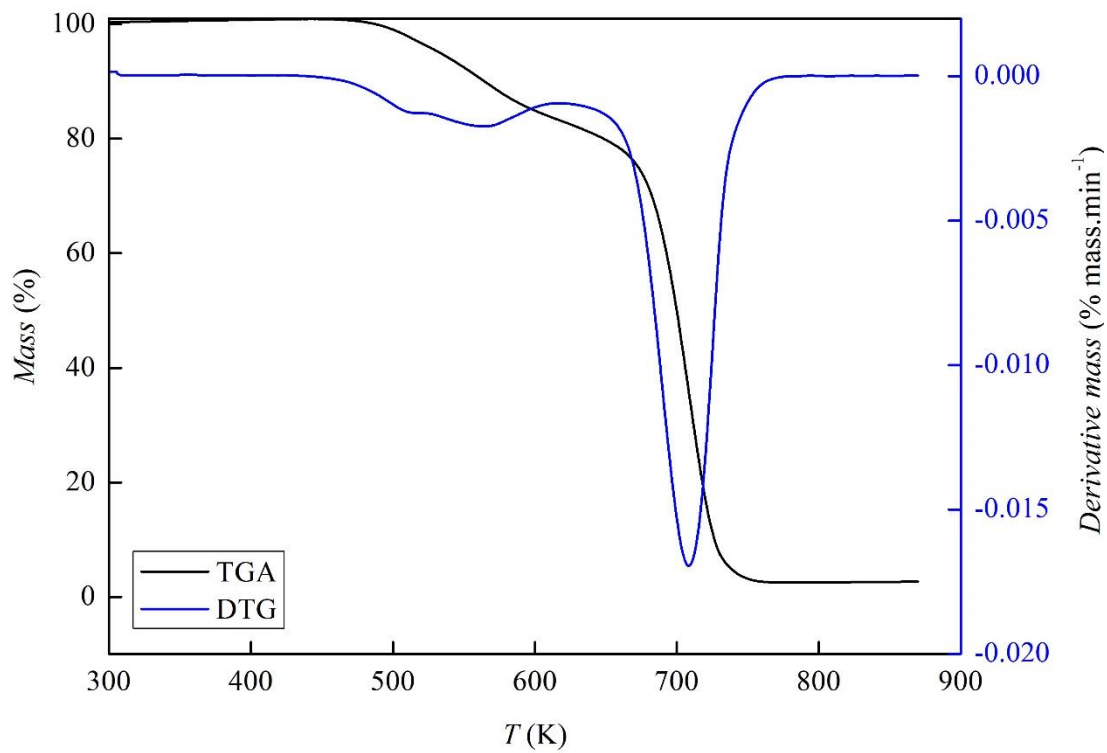
Figure S12. TGA and DTG of monocaprin D5X
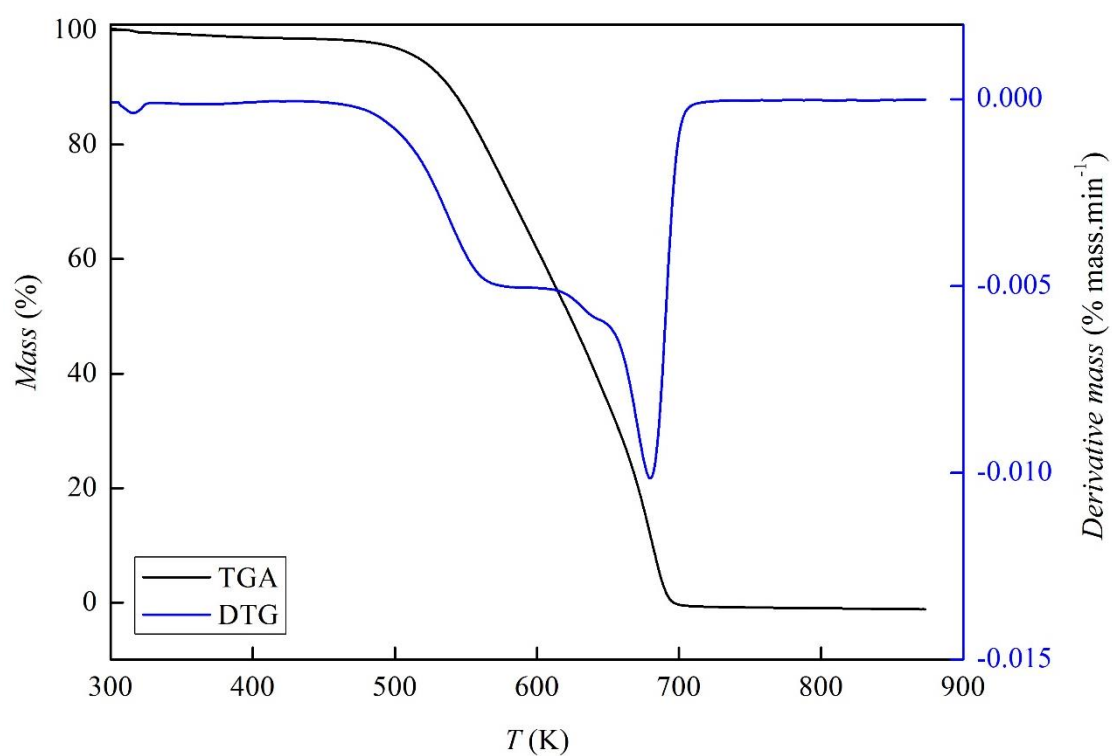
Figure S13. TGA and DTG of monocaprin D23V
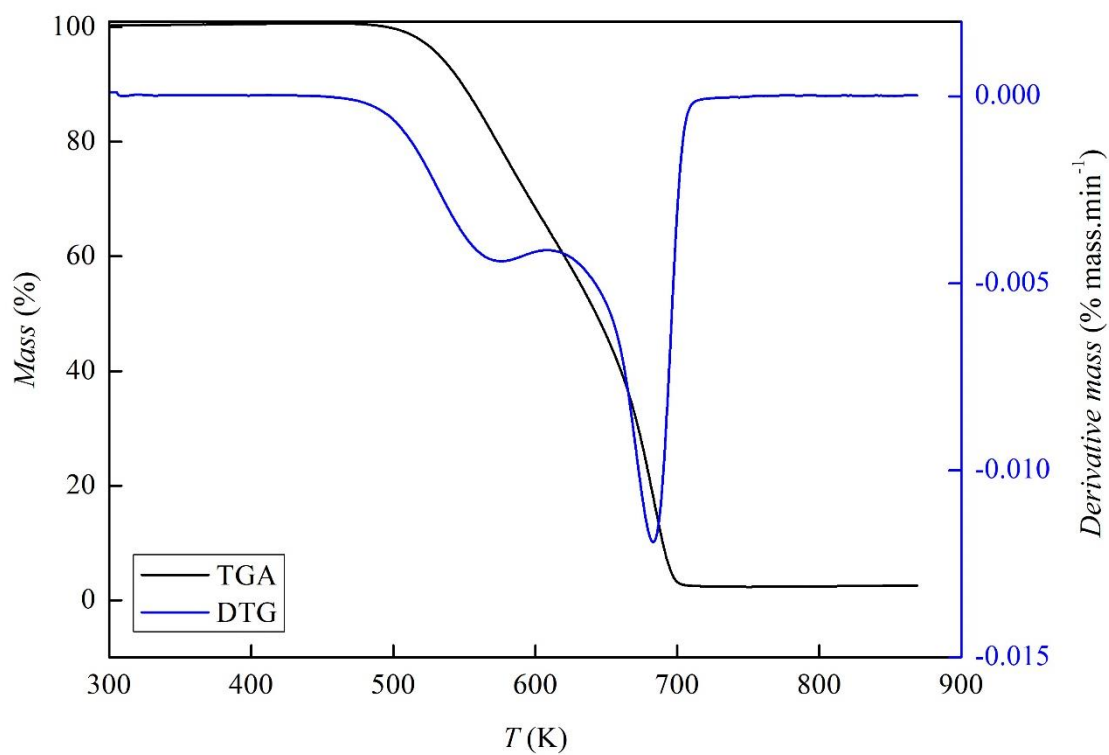
Figure 7S14. TGA and DTG of monolaurin N19X
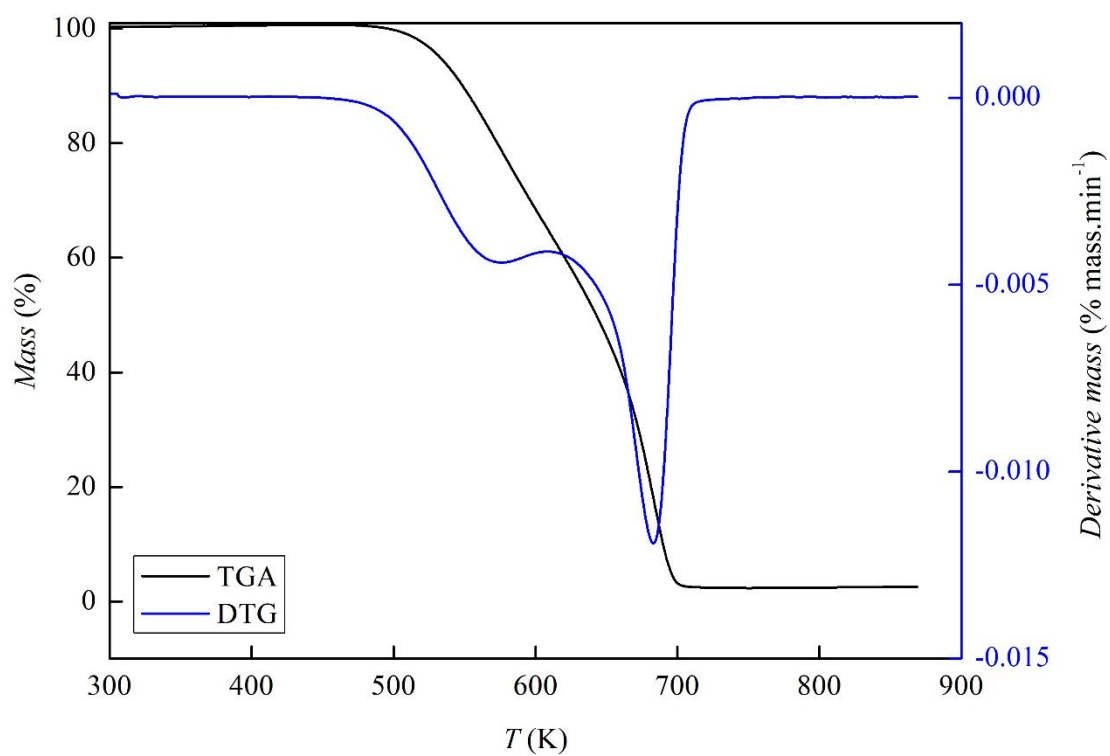
Figure 7S15. TGA and DTG of monolaurin O23Y
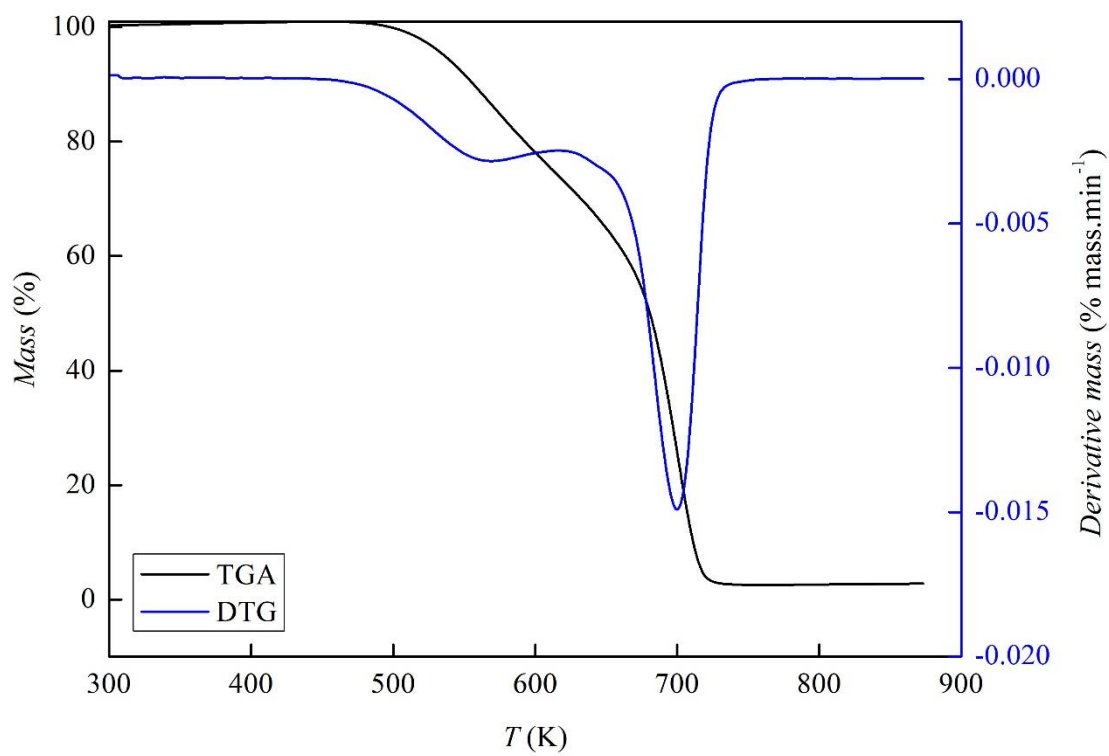
ANEXOS

COPYRIGHT ARTIGO DO CAPÍTULO 4:

VAPOR-LIQUID EQUILIBRIA OF MONOACYLGLICEROL + MONOACYLGLICEROL OR ALCOHOL OR FATTY ACID AT SUBATMOSPHERIC PRESSURES.

14/03/2018   Rightslink® by Copyright Clearance Center

Copyright Clearance Center

RightsLink

Home   Create Account   Help

FLUID PHASE EQUILIBRIA
AN INTERNATIONAL JOURNAL
FLUID PHASE EQUILIBRIA

Title: Vapor-liquid equilibria of monoacylglicerol + monoacylglicerol or alcohol or fatty acid at subatmospheric pressures

Author: Daniela S. Damaceno, Roberta Ceriani

Publication: Fluid Phase Equilibria

Publisher: Elsevier

Date: 25 November 2017

© 2017 Elsevier B.V. All rights reserved.

BACK   CLOSE WINDOW

COPYRIGHT ARTIGO DO CAPÍTULO 5:

VAPOR-LIQUID EQUILIBRIA OF BINARY SYSTEMS WITH LONG-CHAIN ORGANIC COMPOUNDS (FATTY ALCOHOL, FATTY ESTER, ACYLGLYCEROL AND N-PARAFFIN) AT SUBATMOSPHERIC PRESSURES.

Copyright Clearance Center

RightsLink

Home   Create Account   Help

ACS Publications
Most Trusted. Most Cited. Most Read.

Title: Vapor–Liquid Equilibria of Binary Systems with Long-Chain Organic Compounds (Fatty Alcohol, Fatty Ester, Acylglycerol, and n-Paraffin) at Subatmospheric Pressures

Author: Daniela S. Damaceno, Roberta Ceriani

Publication: Journal of Chemical and Engineering Data

Publisher: American Chemical Society

Date: Jun 1, 2018

Copyright © 2018, American Chemical Society

LOGIN

If you're a copyright.com user, you can login to RightsLink using your copyright.com credentials.

Already a RightsLink user or want to learn more?

PERMISSION/LICENSE IS GRANTED FOR YOUR ORDER AT NO CHARGE

This type of permission/license, instead of the standard Terms & Conditions, is sent to you because no fee is being charged for your order. Please note the following:

- Permission is granted for your request in both print and electronic formats, and translations.
- If figures and/or tables were requested, they may be adapted or used in part.
- Please print this page for your records and send a copy of it to your publisher/graduate school.
- Appropriate credit for the requested material should be given as follows: "Reprinted (adapted) with permission from (COMPLETE REFERENCE CITATION). Copyright (YEAR) American Chemical Society." Insert appropriate information in place of the capitalized words.
- One-time permission is granted only for the use specified in your request. No additional uses are granted (such as derivative works or other editions). For any other uses, please submit a new request.

BACK   CLOSE WINDOW

COPYRIGHT ARTIGO DO CAPÍTULO 6:

IMPROVEMENT OF PREDICTIVE TOOLS FOR VAPOR-LIQUID EQUILIBRIUM BASED ON GROUP CONTRIBUTION METHODS APPLIED TO LIPID TECHNOLOGY.

14/03/2018 Rightslink® by Copyright Clearance Center

RightsLink®

Home | Create Account | Help

Title: Improvement of predictive tools for vapor-liquid equilibrium based on group contribution methods applied to lipid technology

Author: Daniela S. Damaceno,Olivia A. Perederic,Roberta Ceriani,Georgios M. Kontogeorgis,Rafiqul Gani

Publication: Fluid Phase Equilibria

Publisher: Elsevier

Date: Available online 6 December 2017

© 2017 Elsevier B.V. All rights reserved.

BACK | CLOSE WINDOW

COPYRIGHT ARTIGO DO CAPÍTULO 7:

EXPERIMENTAL DATA AND PREDICTION OF NORMAL BOILING POINT OF PARTIAL ACYLGLYCEROLS.

Title: Experimental data and prediction of normal boiling points of partial acylglycerols

Author: Daniela S. Damaceno,Evandro P. Jesus,Roberta Ceriani

Publication: Fuel

Publisher: Elsevier

Date: 15 November 2018

BACK | CLOSE WINDOW